



Norwegian University of
Science and Technology

A sedimentological study of the deltaic De Geerdalen Formation in Fulmardalen and of fluvial deposits in the Snadd Formation on the Finnmark Platform

**Cathinka Schaanning
Forsberg**

Geology

Submission date: May 2017

Supervisor: Atle Mørk, IGP

Co-supervisor: Snorre Olausen, UNIS

Norwegian University of Science and Technology
Department of Geoscience and Petroleum

Abstract

In the Late Paleozoic, Svalbard and the Barents Sea were part of a large, shallow embayment located at the north-western corner of the supercontinent Pangea. During the Triassic this embayment was gradually filled with erosional products from the Uralian Mountains located in south-east. A large delta system evolved depositing the upper Triassic De Geerdalen and Snadd formations, on Svalbard and in the Barents Sea, respectively. This study investigates the sedimentology of the two formations, through fieldwork in Fulmardalen on Spitsbergen, and through investigations of a 3D seismic reflection cube and a sediment core from the Finnmark Platform in the south-western Barents Sea. The study aims to complement the understanding of the evolution of the delta system that evolved in the region during the Triassic.

Six sections were measured from different mountains in Fulmardalen. Facies analyses of the outcrops indicate an overall shallowing upwards depositional environment, with open marine shelf and prodelta deposits in the lower part, shallow marine and delta front deposits in the middle part and delta plain deposits in the upper part. This is concordant with previous studies of the formation. Laterally extensive and upwards coarsening sandstone units with sedimentary structures typically associated with wave- and tidal activity, characterize the shallow marine and delta front deposits in Fulmardalen. These units have been interpreted as barrier bars, forming as a result of low accommodation space allowing for basinal processes to rework the sediment.

The seismic investigation of the equivalent Snadd Formation on the Finnmark Platform reveals a much more fluvial dominated depositional environment compared to Fulmardalen. A range of fluvial seismic geomorphological features have been interpreted, such as point-bar deposits from large meandering rivers, braided river morphologies with mid-channel-bars and smaller ribbon shaped channel bodies. The sediment core, retrieved from a large point-bar complex, shows characteristics typical of fluvial deposits. The channels show a general WNW-ESE orientation, reflecting the overall progradation of the delta towards west and north-west. Width-to-thickness plots of selected channels compare well to plots of mainly meandering rivers and distributaries from ancient and modern fluvial systems. Moreover, channel bodies in the lower part appear larger than channels further up in the formation. This trend is thought to be related to tectonic changes in the hinterland.

Sammendrag

I slutten av paleozoikum var Svalbard og Barentshavet en del av en stor grunn bukt ved det nordvestlige hjørnet av superkontinentet, Pangea. Denne bukta ble i løpet av trias gradvis fylt med erosjonsproduktene fra Uralfjellene lokalisert lenger sørøst. Et stort deltasystem utviklet seg og resulterte i avsetninger tilhørende De Geerdals- og Snaddformasjonene, avsatt henholdsvis på Svalbard og i Barentshavet. Dette studiet undersøker sedimentologien i de to formasjonene, gjennom feltarbeid i Fulmardalen på Spitsbergen, og gjennom undersøkelser av en 3D-seismisk refleksjons kube og en sedimentkjerne fra Finnmarksplattformen i den sørvestlige delen av Barentshavet. Studiet tar sikte på å utfylle forståelsen av utviklingen til deltasystemet som bygde seg ut i regionen under trias.

Faciesanalyser fra Fulmardalen indikerer et oppovergrunnende avsetningsmiljø, med åpne marine- og prodelta-avsetninger i nedre del, grunnmarine- og deltafrontavsetninger i midtre del og deltasletteavsetninger i øvre del. Denne oppovergrunnende trenden samsvarer med tidligere studier av formasjonen. De grunnmarine- og deltafrontavsetningene i Fulmardalen kjennetegnes av lateralt utstrakte og oppovergrovende sandsteinsenheter med sedimentære strukturer typisk for bølge- og tidevansaktivitet. Disse enhetene er tolket som barrierebanker som mest sannsynlig ble formet som et resultat av lite akkomodasjonsrom. Bassengprosesser kunne dermed bearbeide sedimentene.

Seismiske undersøkelser av den tilsvarende Snaddformasjonen på Finnmarksplattformen avslører et avsetningsmiljø som i mye høyere grad er dominert av fluviale prosesser sammenliknet med Fulmardalen. En rekke fluviale geomorfologier kan gjenkjennes, slik som pyntbankeavsetninger fra store meandrerende elver, forgreinede elvesystemer med midtbanker og mindre båndformede kanalkropper. Sedimentkjernen, hentet fra et stort pyntbankekompleks, vitner om en typisk fluvial avsetning. Kanalene viser en generell VNV-ØSØ orientering, noe som reflekterer den overordnede prograderingen av deltaet mot vest og nordvest. Bredde-til-tykkelsesforholdet for utvalgte kanaler er hovedsakelig sammenliknbart med meandrerende elver og fordelingskanaler fra både forhistoriske og moderne elvesystemer. Formasjonen viser dessuten en minkende størrelse på kanalkropper fra bunn til topp. Denne trenden antas å være relatert til tektoniske endringer i baklandet.

Preface

The work presented herein is partly written in collaboration with master student Bård Heggem. This was natural as we both were working closely together during fieldwork, investigating the same geological formation. Many of the chapters herein are therefore also included in his thesis ([Chapters 4, 5, 8 and 9](#) except for [Sections 8.1 and 9.4](#)). All of the presented photographs are made by students from NTNU during fieldwork of 2016 unless otherwise stated.

Trondheim, 15-05-2017

Cathinka Schaanning Forsberg

Acknowledgment

First of all I want to thank my main supervisor Atle Mørk, for giving me the opportunity to explore places in the Arctic that most people can only dream of. The three summers I have spent in Svalbard as a part of your team have given me good memories and experiences that will not be easily forgotten. Thank you for great supervision during the process of writing my thesis.

I further extend my thanks to my co-supervisor at the University Centre in Svalbard, Snorre Olaussen and to Bjørn Anders Lundschie and Rune Mattingsdal at the Norwegian Petroleum Directorate (NPD) for their useful help and comments.

NPD is thanked for providing the seismic data and core studied herein, but also for their financial support during fieldwork of 2015, allowing for ship transportation. Cairn Energy (Capricorn Norway), Det Norske Oljeselskap (now Aker BP) and SINTEF are thanked for additional funding during fieldwork. The Svalbard Science Forum is thanked for providing funding through the Arctic Field Grant, making it possible for helicopter transportation during fieldwork 2016. UNIS is thanked for help in organizing the fieldwork and for logistic support.

A special thanks to Bård Heggem, for great collaboration during fieldwork and later during data analysis and the writing process.

I also want to thank Nina Bakke, Sofie Bernhardsen, Jostein Røstad and Martijn Vermeer for excellent assistance during fieldwork in Fulmardalen 2016. Gareth Steven Lord, Turid Haugen, Sondre Krogh Johansen and Simen Jenvin Støen are thanked for nice days in the field on eastern Svalbard during summer 2015. Gareth is also kindly thanked for his useful comments and for always being available for discussions.

Thanks to my fellow master students with whom I have shared an office; "Petroleumsjenta", "Heia Lom", "Bakeriet på Oppdal", "BH'en 92", "v6850" and "Hagelslang", for making the breaks more fun by playing Curve Fever, but also for many memorable years together in Trondheim.

Finally, I want to thank my dear Martijn and parents for great support, help and motivation during the process of writing my thesis.

Contents

Abstract	iii
Sammendrag	v
Preface	vii
Acknowledgments	ix
1 Introduction	1
2 Geological Setting	3
2.1 A large Triassic delta system	4
2.2 Triassic - Middle Jurassic Stratigraphy	7
2.2.1 The Sassendalen Group	8
2.2.2 The Kapp Toscana Group	9
2.3 Structural Geology	10
3 Data and Methods	13
3.1 Fieldwork	13
3.1.1 Methods - Logging Procedure	13
3.1.2 Sources of error	14
3.2 Seismic	15
3.2.1 Dataset	15
3.2.2 Methods	18
3.2.3 Sources of error	19
3.3 Core	20
3.3.1 Gamma-ray log	21
3.3.2 Sources of Error	21
3.4 Laboratory analyses	21
3.4.1 X-ray diffractometer (XRD)	22
3.4.2 Optical microscopy	22

3.4.3	Rock-Eval analysis	22
4	Facies in the De Geerdalen Formation	23
4.1	The meaning of "Facies" and "Facies Analysis"	24
4.2	Facies in Fulmardalen	26
5	Logged sections from Fulmardalen	47
5.1	Wallenbergfjellet	49
5.2	Dyrhø	54
5.3	Ryssen	62
5.4	Milne Edwardsfjellet	70
5.5	Storfjellet	78
5.6	Raggfjellet	87
6	Seismic Results	91
6.1	RMS Amplitude Maps	92
6.1.1	The Guovca sandstone	97
6.2	Seismic Character of Channel Bodies	98
6.3	Channel Measurements	100
6.3.1	Geometries of the Guovca sandstone	101
7	Core Results	105
7.1	Description and Interpretation	107
8	Laboratory Results	119
8.1	XRD	119
8.2	Optical microscopy	121
8.3	Rock-Eval analysis	124
9	Discussion	127
9.1	Delta classification and deltaic sequences	129
9.2	Facies distribution in Fulmardalen	132
9.2.1	The base of the Isfjorden Member	136

9.3 Regional facies distribution	139
9.3.1 Spitsbergen	139
9.3.2 Edgeøya, Barentsøya, Wilhelmøya and Hopen	144
9.4 Channels in the Snadd Formation	146
9.4.1 A change in channel morphology	147
9.4.2 Comparison to ancient and modern fluvial systems	148
10 Conclusions	155
Bibliography	157
A UTM coordinates of measured sections from Fulmardalen	167
B Legend for measured sections	168
C Storfjellet (Knarud, 1980) correlated to Stor 16-1	169
D Thickness map of the Snadd Formation in ST9802	170
E Rock-Eval Analysis	171

1. Introduction

The high arctic archipelago of Svalbard (Figure 1.1), with its impressive landscape and exotic wildlife, has experienced a long and complex geological history which has caught the attention of geoscientists ever since Keilhau lead the first Norwegian geological expedition in 1827 (Sysselmannen, 2012). Svalbard represents an exhumed part of the Barents Sea, hosting rocks free of any dense vegetation, making it a unique place to perform geological studies in order to understand the geological evolution of the entire region, including the subsurface of the Barents Sea (Worsley, 2008). The archipelago has seen an increasing interest from earth scientists during the past thirty years, as it is an analogue for the oil and gas provinces of the Barents Sea (Elvevold et al., 2007; Lundschieen et al., 2014).



Figure 1.1: Map of Svalbard and the Barents Sea, displaying the high latitude position of the area. From Dallmann (2015).

A large delta system prevailed in the region during the Triassic, and the deposits of this system are the focus of this study. The main objective is to investigate the sedimentology of the Upper Triassic De Geerdalen Formation in central to eastern parts of Spitsbergen. Sedimentological data of the formation have been systematically collected over the past years, and the unique part of this study is that it forms the latest piece of the puzzle for the data collection of the Upper Triassic succession on Svalbard. Furthermore, deposits from the equivalent Snadd Formation in the Barents Sea have been investigated, using a 3D seismic reflection cube as well as a sediment core, allowing for spatial comparison to the deposits on Svalbard. The study aims to complement the understanding of the evolution of the delta system that evolved in the region during the Triassic.

2. Geological Setting

The sedimentary record on Svalbard, spanning the Devonian to the Tertiary period, shows that the archipelago has been located in all climate zones through geological time (Elvevold et al., 2007) (Figure 2.1). The conditions were tropical in the transition between Devonian and Carboniferous. Sediments deposited at the transition between Carboniferous and Permian indicate a subtropical arid climate, whereas the conditions must have been temperate to boreal

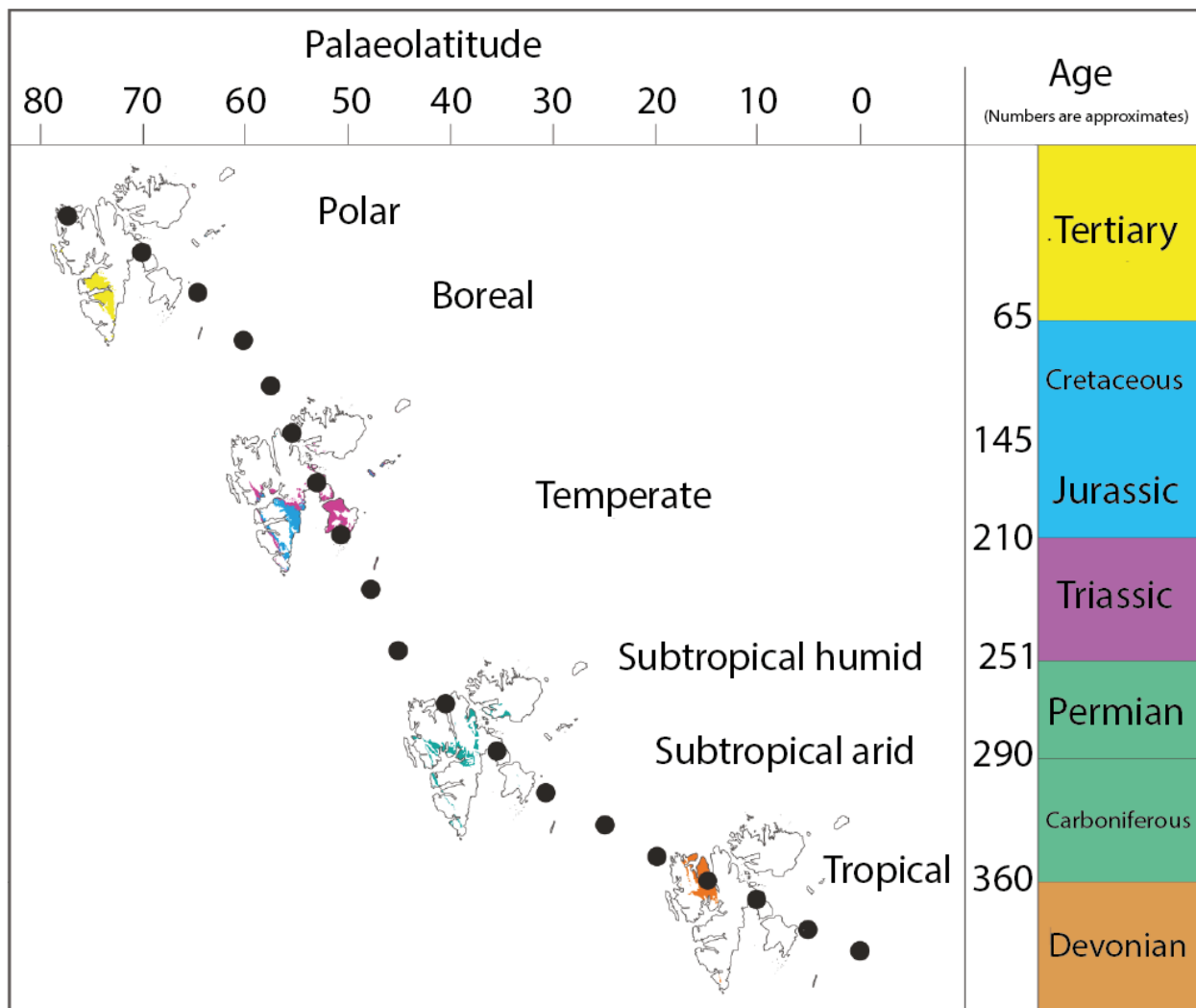


Figure 2.1: The sedimentary record on Svalbard indicates that the archipelago has drifted through all climate zones throughout geological time. Figure retrieved from Elvevold et al. (2007).

during the Mesozoic. These variations are the result of Svalbard and the Barents Sea, located in the north-western corner of the Eurasian plate, drifting from the southern hemisphere, via equatorial latitudes and further northwards to the arctic position we see today (Elvevold et al., 2007). Since Triassic deposits are the main topic of this thesis, a more detailed description of the geological setting during this period will be given in the following [Section 2.1](#).

2.1 A large Triassic delta system

During the Late Paleozoic Svalbard and the Barents Sea were part of a large embayment at the northern margin of the Pangea supercontinent (Buiter and Torsvik, 2007; Riis et al., 2008; Worsley, 2008; Lundschieen et al., 2014; Rød et al., 2014; Blomeier, 2015; Lord et al., 2017a) ([Figure 2.2](#)). With Siberia constantly approaching Euramerica in the Late Permian, the contact with southern areas (Tethys) was sealed off and the Uralian mountain chain was formed (Lundschieen et al., 2014; Blomeier, 2015). This closure resulted in climate changes at northern latitudes, where subtropical conditions and deposition of carbonates in the Permian were replaced by a temperate climate and clastic sedimentation in the Triassic (Elvevold et al., 2007; Worsley, 2008; Lord et al., 2017a).

The erosion of the newly formed Uralian mountain chain in the south-east provided the main source of clastic sediments to the Svalbard-Barents Sea embayment during the Triassic, with the development of a large delta (Lundschieen et al., 2014; Rød et al., 2014; Lord et al., 2017a) ([Figure 2.3](#)). However, important source areas were also located to the west, most likely coming from Greenland (Glørstad-Clark et al., 2010) and to the south, from Norway and the Kola Peninsula (Lundschieen et al., 2014). By the end of the Triassic the basin was completely filled with sediments.

Seismic data from the Barents Sea show clear evidences of a large delta system with clinofolds prograding towards the north and north-east in the early Triassic and later towards the north-west during the Late Triassic when the sediment supply from the Uralides became increasingly important (Glørstad-Clark et al., 2010; Henriksen et al., 2011; Høy and Lundschieen, 2011; Lundschieen et al., 2014). Thickness maps of the Triassic succession in Svalbard and the northern Barents Sea show how the main depo-center changes from north-west to south-east

as a result of an approaching delta coming from the Uralian mountains (e.g., Lord et al., 2017b) (Figure 2.4).

The progradation of clinoforms has resulted in time-transgressive deltaic deposits, where deposition of sediments in the Barents Sea started earlier than equivalent deposits on Svalbard.

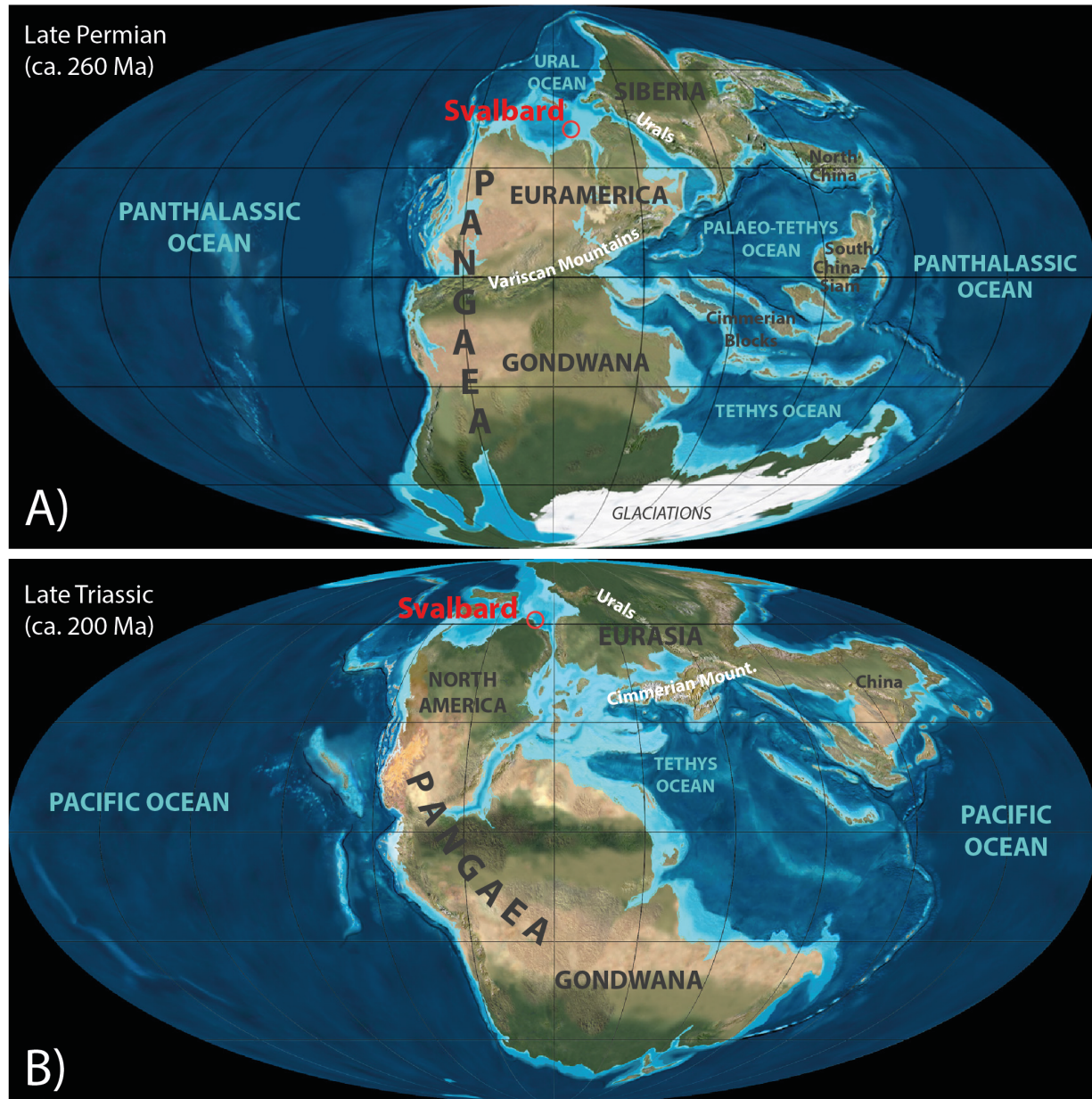


Figure 2.2: (A) Global palaeogeography during Late Permian. Svalbard, forming part of an epicontinental shelf sea at the northern margin of Pangea around 45°N, is encircled. (B) Global palaeogeography during Late Triassic. Svalbard, continuously forming part of an epicontinental shelf sea at the northern margin of Pangea, now located around 55°N, is encircled. Both maps are retrieved from (Dallmann, 2015) and modified from Blakey, R., Colorado Plateau Geosystems Inc. (www.cpgeosystems.com), version accessed 2013.

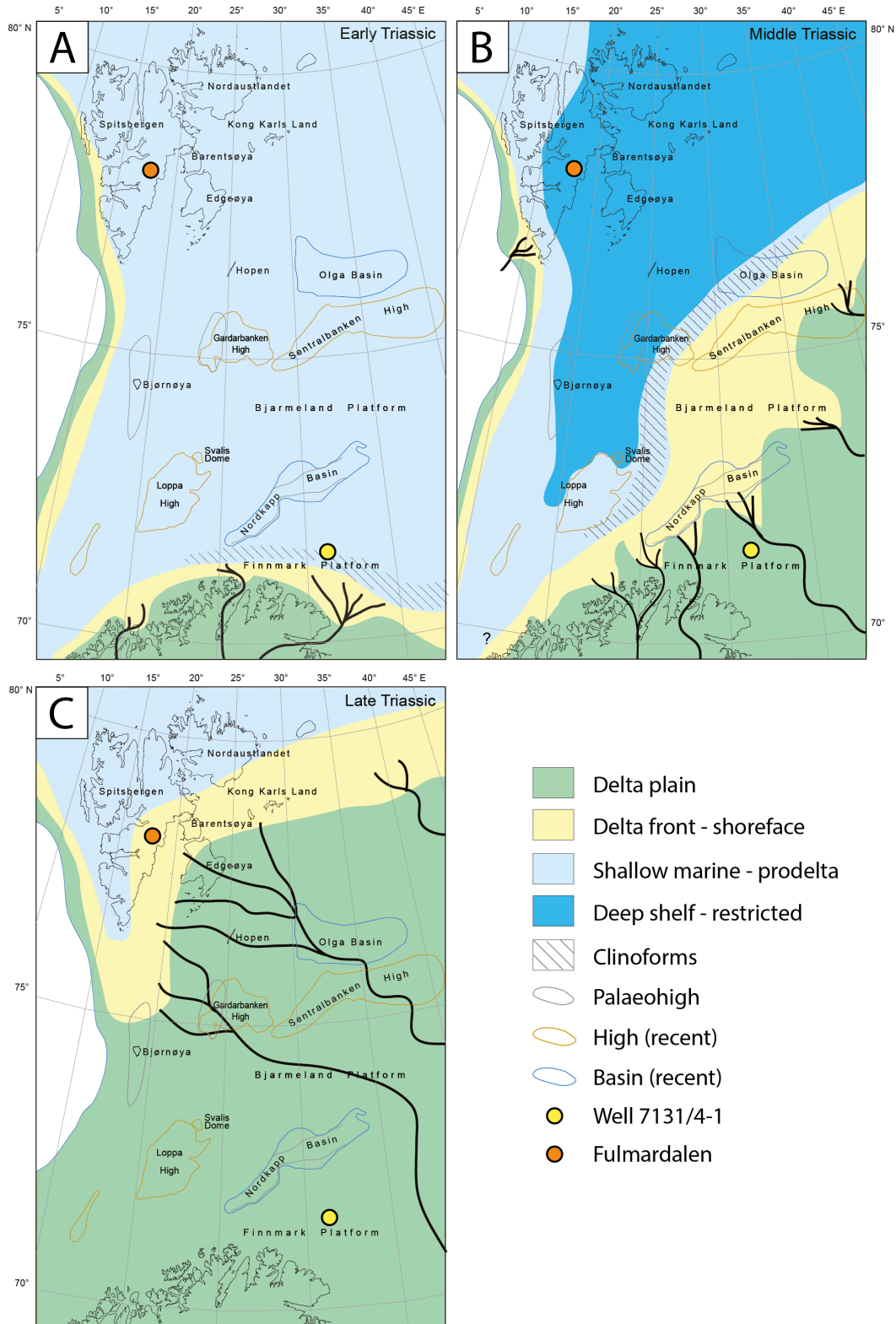


Figure 2.3: Palaeogeographic evolution of the Barents Shelf including Svalbard during the Triassic. The location of the study areas that have been investigated in this thesis are indicated by yellow and orange dots. (A) Early Triassic, (B) Middle Triassic and (C) Late Triassic. From [Lundschieen et al. \(2014\)](#).

In other words, by the time the delta front reached Svalbard in the Late Triassic (Carnian), a delta plain environment dominated the Barents Sea ([Figure 2.3C](#)). Large fluvial channels of Late Triassic age have been observed from attribute analysis of seismic data in the southern Barents Sea with a general orientation towards the north-west ([Klausen et al., 2014](#)). Basin subsidence, sea level fluctuations, erosion and deposition from adjacent land and structural highs of Late Paleozoic age are thought to have been the most important factors controlling the sediment infill patterns of the region ([Riis et al., 2008](#)).

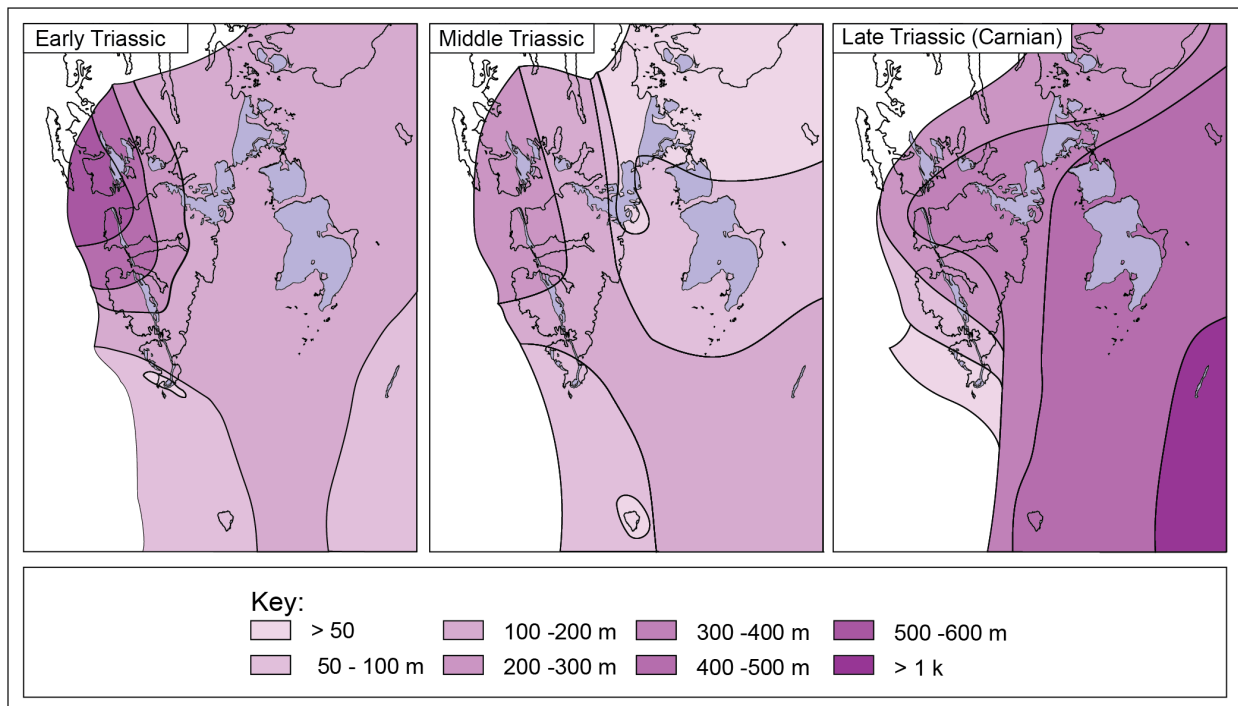


Figure 2.4: Isopach maps of Triassic succession in Svalbard and northern Barents Sea derived from sections measured throughout Svalbard. Note how the main depo-center changes from NW to SE from the Early to Late Triassic. Retrieved from ([Lord et al., 2017b](#)).

2.2 Triassic - Middle Jurassic Stratigraphy

The Triassic to Middle Jurassic succession on Svalbard and in the Barents Sea consists of the Sassendalen Group and the overlying Kapp Toscana Group ([Figure 2.5](#)). The groups reflect two different depositional regimes and a change from a western to a south-eastern sediment source. A brief description of these two groups will be given in this section.

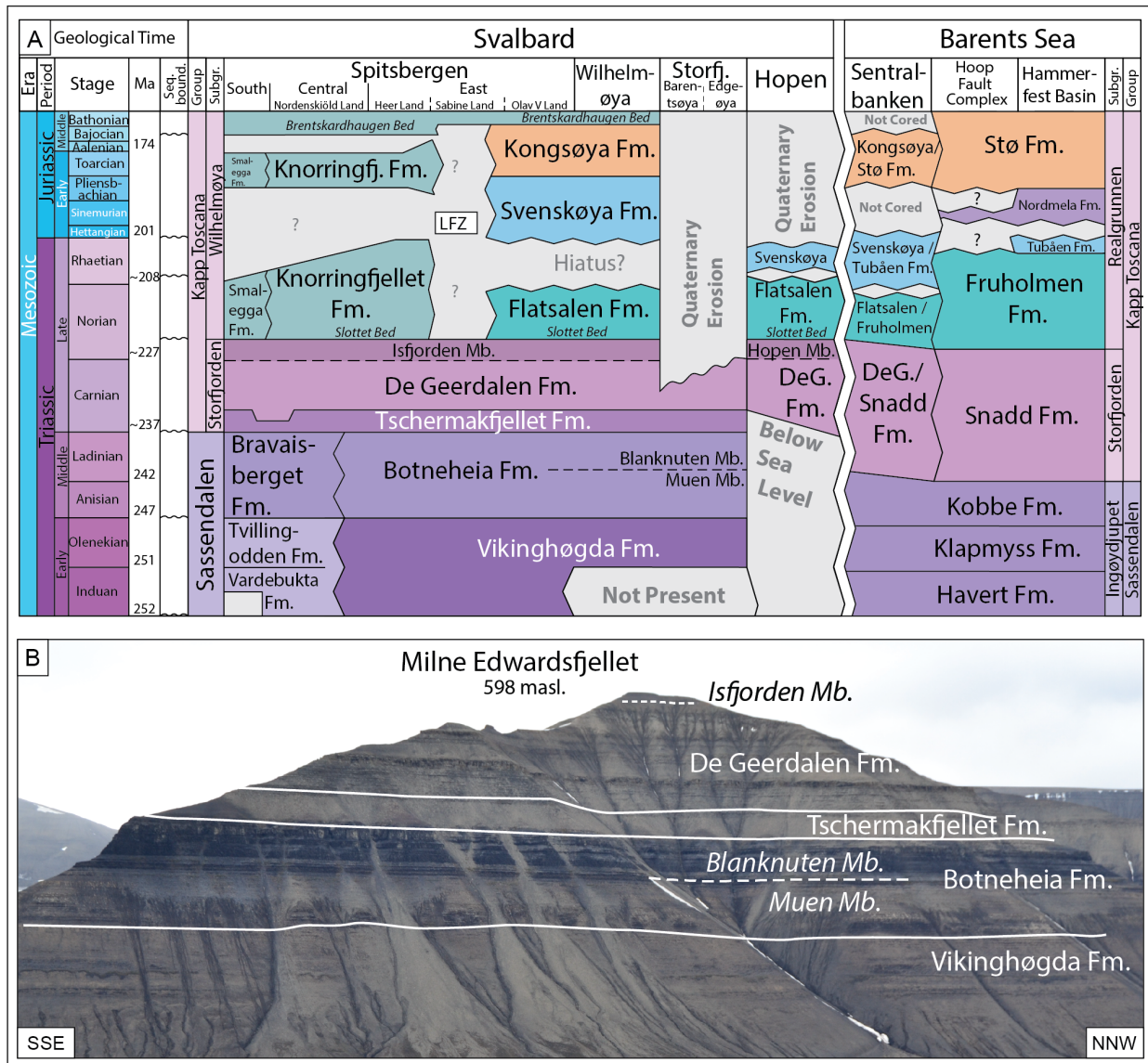


Figure 2.5: (A) Stratigraphic chart showing the relationships between stratigraphic units in Svalbard and the Barents Sea. Modified from [Lord et al. \(2017c\)](#). (B) A photograph of Milne Edwardsfjellet in Fulmardalen, Sabine Land, showing the distribution of stratigraphic units.

2.2.1 The Sassendalen Group

The Sassendalen Group ([Figure 2.5](#)) represents Lower to Middle Triassic fine grained sediments sourced from the west and later from south-east, deposited in an embayment inherited from the Permian ([Buchan et al., 1965](#); [Mørk et al., 1999a,b](#)). The group is subdivided into multiple formations of varying lateral and vertical significance ([Mørk et al., 1999a](#)). In western Spitsbergen the group reflects deposits of coastal to shallow shelf origin (Vardebukta,

Tvillingodden and Bravaisberget Formations) (Mørk et al., 1999a). These coastal sediments grade into shelf mudstones further east and south. In central and eastern Spitsbergen these mudstones comprise the Vinkinghøgda and Botneheia Formations, in which the latter is very organic- and phosphatic-rich, deposited in the central parts of the embayment with periodically anoxic bottom conditions (Mørk and Bjorøy, 1984; Mørk et al., 1999a,b; Mørk and Bromley, 2008; Krajewski, 2008; Vigran et al., 2008, 2014). The Ingøydjupet Subgroup, with the three formations Havert, Klappmyss and Kobbe, is the equivalent in the south-western Barents Sea, reflecting shallow to deep shelf sediments (Mørk et al., 1999a).

2.2.2 The Kapp Toscana Group

The Kapp Toscana Group (Figure 2.5) was deposited in the Late Triassic to Middle Jurassic and reflects the erosional products of the Uralian mountain chain mainly coming from the south-east (Mørk et al., 1999a; Rød et al., 2014; Lundschieen et al., 2014; Lord et al., 2017a). The group consists of the Storfjorden-, Wilhelmøya- and Realgrunnen Subgroup.

The Storfjorden Subgroup

The Storfjorden Subgroup comprises the lower part of the Kapp Toscana Group, and consists of the Early Carnian Tschermakfjellet Formation and the Carnian to Early Norian De Geerdalen Formation on Svalbard, and the equivalent Snadd Formation of Ladinian to Early Norian age in the Barents Sea (Mørk et al., 1999a; Vigran et al., 2014; Paterson et al., 2016b). The base of the subgroup is diachronous, with an earlier onset in the Barents Sea. The Tschermakfjellet Formation and the lower part of the Snadd Formation are dominated by grey pro-delta shales that coarsen upwards into the more sand-rich De Geerdalen Formation and upper Snadd Formation (Mørk et al., 1999a). The base of the De Geerdalen Formation is defined by the first prominent sandstone above the Tschermakfjellet Formation, and the deposits consist of repeated upwards coarsening successions of shale and immature sandstones reflecting a shallow shelf to deltaic environment (Mørk et al., 1999a; Vigran et al., 2014; Rød et al., 2014; Lord et al., 2017a).

The Isfjorden Member of Early Norian age constitutes the upper part of the De Geerdalen Formation and is characterized by alternating red and green mudstones, bivalve coquina beds,

abundant carbonate beds and relatively thin sandstones compared to further down in the formation, and is thought to reflect a shallow marine, coastal to lagoonal environment (Pchelina, 1983; Mørk et al., 1999a; Haugen, 2016).

The Wilhelmøya- and Realgrunnen Subgroups

Overlying the Storfjorden Subgroup is the Upper Triassic to Middle Jurassic Wilhelmøya Subgroup on Svalbard and the offshore Realgrunnen Subgroup in the Barents Sea. The base represents a regional transgressive surface formed as a result of globally rising sea level (Mørk et al., 1999a; Riis et al., 2008; Henriksen et al., 2011; Vigran et al., 2014). The Slottet Bed on Svalbard is a transgressive lag representing this event. The Wilhelmøya Subgroup is the condensed, marine equivalent of the Realgrunnen Subgroup (Mørk et al., 1999a). The Realgrunnen Subgroup consists of mature sandstones that have been reworked and deposited in coastal plain and deltaic to shallow marine environments (Mørk et al., 1999a).

2.3 Structural Geology

During the transition from Paleocene to Eocene the opening of the North-Atlantic Ocean extended northwards (Bergh et al., 1997; Faleide et al., 2008). An associated transpressional movement of Svalbard away from the north-eastern edge of Greenland resulted in the formation of the West Spitsbergen Fold-and-Thrust Belt (Harland et al., 1974; Lyberis and Manby, 1993; Braathen et al., 1999) (Figure 2.6). This event is estimated to have shortened the crust with around 30 km (Worsley, 2008). The deformation along western Spitsbergen is thick-skinned, involving the deformation of metamorphic basement as well as the sedimentary succession. Towards the east it becomes thin-skinned, with the deformation of the sedimentary succession only (Bergh et al., 1997; Braathen et al., 1999; Dallmann, 2015).

Consequently, the Triassic succession on Svalbard is highly deformed to the west (Buchan et al., 1965; Mørk et al., 1982), making sedimentological and stratigraphical investigations in this area challenging. To the east, where this study is conducted, the Mesozoic succession is relatively flat-lying and undeformed (Figure 2.6). However, multiple north-south oriented structural lineaments dissect the strata (Figure 2.6), with the Billefjorden Fault Zone being the

most prominent (Harland et al., 1974; Braathen et al., 2011). The Lomfjorden- and Storfjorden Fault Zone are present further east.

During the Neogene and Quaternary repeated glaciations with associated periods of isostatic subsidence and post-glacial rebound have resulted in the erosion of 2-3 km of sediments in the region (Mangerud et al., 1996; Worsley, 2008; Dallmann, 2015). The present day topography of Svalbard is largely shaped by these glacial processes (Worsley, 2008).

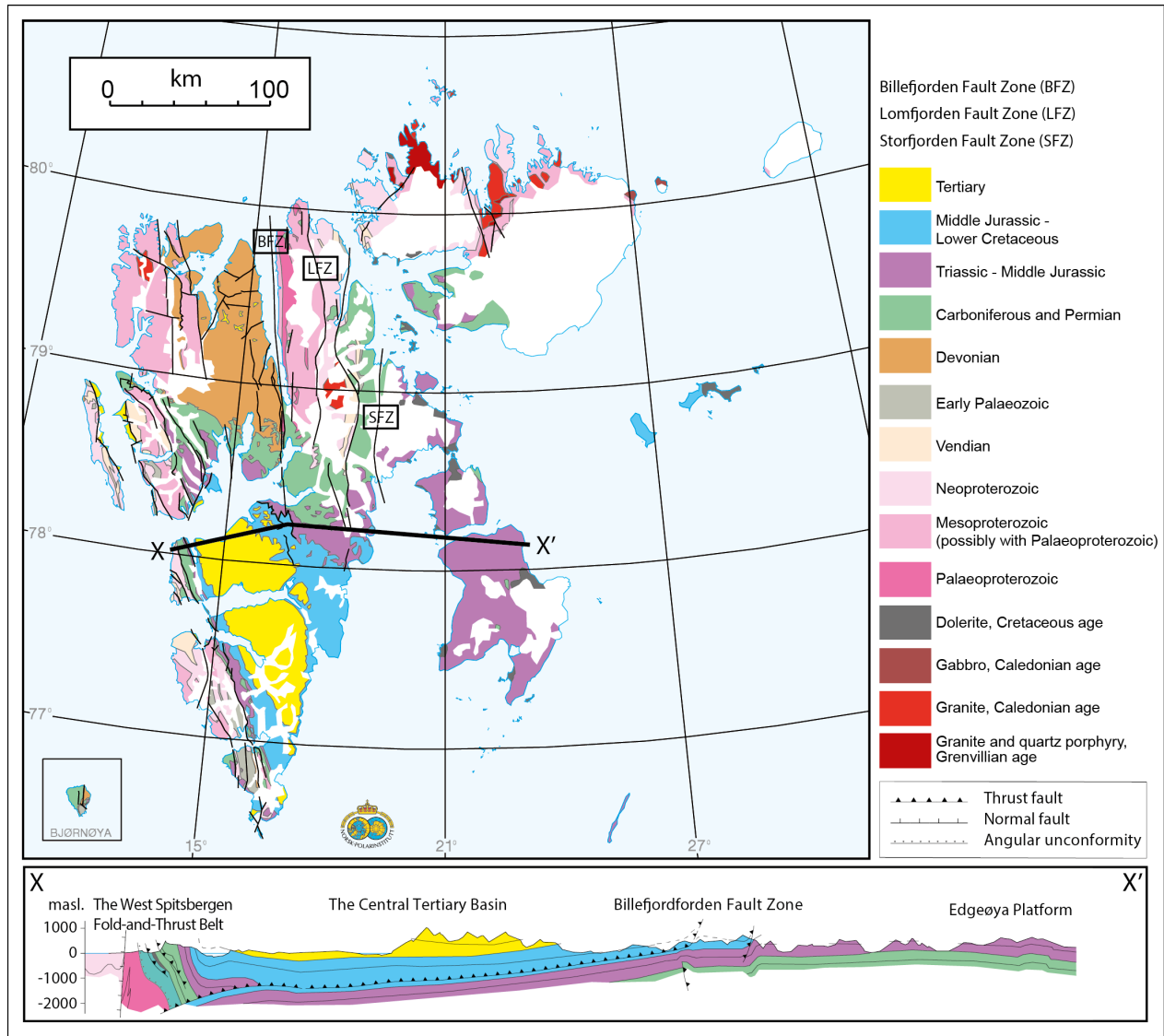


Figure 2.6: Simplified geological map of Svalbard. The stratigraphy is almost vertical in the west and flattens towards the east. Modified from Elvevold et al. (2007).

3. Data and Methods

3.1 Fieldwork

Sedimentological fieldwork has been conducted during two periods. A month long field season took place on eastern Svalbard in August 2015. The second field season took place in Fulmardalen (Figures 2.3 and 5.1) on central/eastern Spitsbergen in August 2016 during a ten days long period. The data collected in 2015 have already been analysed in the master theses of Haugen (2016), Støen (2016) and Johansen (2016) and are summarized in Lord et al. (2017a). This thesis therefore mainly focuses on the data collected in 2016.

The field campaign of 2016 was performed by three master students and three assistants. They were transported by helicopter to the camp site which was located in a flat area at the northern side of Marmorbreen in Fulmardalen. The team was accommodated in tents.

Six mountains, all exposing Triassic outcrops, were visited during the ten days in the field. The field party operated in two teams of three people, one studying the Botneheia Formation (Bakke, In prep) and the other the De Geerdalen Formation, with the latter being part of this thesis and the thesis of Heggem (In prep). A sedimentological log was made of each mountain visited and are further presented in Chapter 5.

3.1.1 Methods - Logging Procedure

GPS was used to record the standard UTM coordinates at the base and top of each log (Appendix A). The logs were drawn at a scale of 1:100. The collected observations were obtained using standard sedimentological field methods in accordance with Tucker (2011). Observations included lithology, sedimentary structures, grain sizes, bed thicknesses, colour, textures, stratigraphic relationships and bed contacts. A standard grain size sheet was used to estimate the grain sizes and a measuring stick was used to measure the sections. Digital cameras were used to document observations of mountains and outcrops. Additionally, samples of both sandstones and shales were collected at different levels in the measured

sections to provide provenance and palynology material for future projects and master theses.

The starts of the logs are normally at the top of the Botneheia Formation or some metres up in the Tschermakfjellet Formation to make sure that the base of the De Geerdalen Formation is included. However, at Raggfjellet the log starts in the upper part of the De Geerdalen Formation due to extensive scree cover over the lower part. The ends of the logs are at or close to the tops of the mountains, when the slope gets too gentle to observe the bedrock under the scree.

3.1.2 Sources of error

The main errors related to the fieldwork are observations, interpretations and measurements of the sections. Some observations and interpretations are subjective and thus vary from individual to individual. Challenges related to steep terrain and scree cover also affect the quality of the data. Steep terrain is more common in sandstone units and may prevent detailed observations. Scree cover is more common in shale dominated intervals (Hynne, 2010), and thin sandstone units or important colour changes may be hidden beneath. The identification of the red and green mudstones of the Isjorden Member and the transition from the Tschermakfjellet Formation to the De Geerdalen Formation is often problematic (Haugen, 2016; Lord et al., 2017a). Good exposures of the mudstones in the Isfjorden Member are mostly obtained by digging through scree, meaning that the amount and thickness of these mudstones may be larger than observed. The challenges related to the lower boundary of the De Geerdalen Formation, on the other hand, are not only related to scree cover, but also to the definition of the base itself. The definition of the base (see Section 2.2.2) is somewhat arbitrary due to extensive thickness variations in the Tschermakfjellet Formation, as well as thickness variations in the basal sandstones (Lord et al., 2017a).

3.2 Seismic

3.2.1 Dataset

The seismic dataset used to study the Snadd Formation in this thesis is the 3D-survey ST9802, located on the Finnmark Platform in the south-western Barents Sea (Figure 6.1). It was gathered and processed by Statoil in 1999. The workflow of the processing has not been provided.

The phase and polarity of the dataset can be found by looking at the seafloor reflector. There is always an increase in acoustic impedance at the interface between water and the seafloor. The variable wiggle display of the seafloor shows a strong peak between two smaller troughs, indicating that the ST9802 dataset has been processed to zero-phase signal with normal polarity (Figure 3.1). Bin size is 12.5 m in both the inline and crossline directions. The sampling interval is 4 ms TWT.

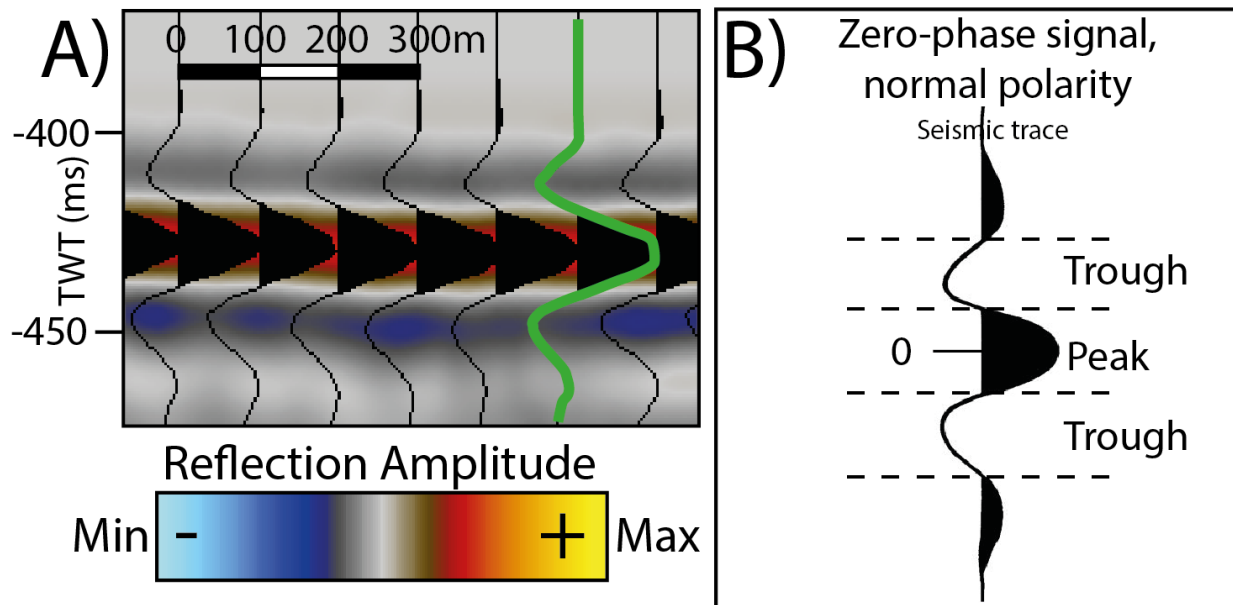


Figure 3.1: (A) Variable wiggle display of the seafloor in the dataset ST9802. The green trace indicates zero-phase signal, normal polarity. (B) Model of a seismic trace showing zero-phase, normal polarity using Society of Exploration Geophysicists (SEG) polarity standard of Sheriff (2006).

Vertical resolution

Vertical resolution is a measure of how thick a layer needs to be in order to be seen in seismic sections. The minimum thickness is dependent on the wavelength (λ), which in turn is a function of seismic velocity (v) and frequency (f) (Brown, 2011) (Table 3.1). Layers can be distinguished from each other when their thickness is more than $\lambda/4$ (Brown, 2011), and is further referred to as the vertical resolution (Table 3.1). However, layers with thickness down to $\lambda/32$ can be detected (Rafaelsen, 2006), and is further referred to as the vertical detectability (Table 3.1).

Table 3.1: The equation for the wavelength (λ) and its relation to the vertical resolution and detectability.
 v = velocity, f = frequency.

Wavelength: $\lambda = v/f$

Vertical Resolution: $\lambda/4$

Vertical Detectability: $\lambda/32$

The vertical resolution of the seismic interval containing the Snadd Formation in the ST9802 dataset was calculated after first obtaining the velocity and dominant frequency. Depth

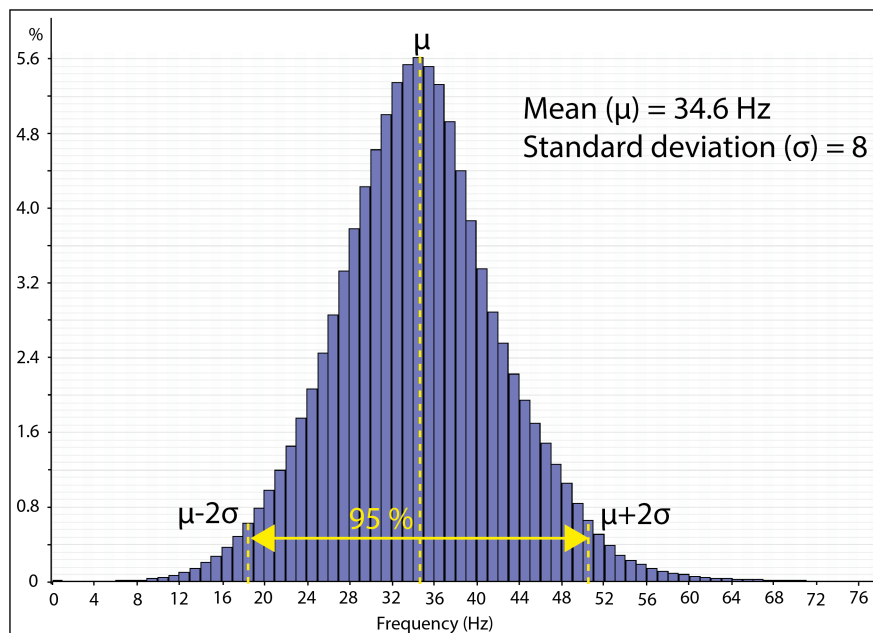


Figure 3.2: Frequency distribution of the Snadd Formation in the dataset ST9802. The graph represents values extracted from a window of 200 ms TWT below the Top Snadd horizon. The distribution is normal with a mean value of 34.6 Hz, and a standard deviation of 8. Ca 95% of the values lie within $\pm 2\sigma$ from the mean.

data from well 7131/4-1 was used to calculate an average velocity of 3000 m/s in the formation. Distribution of the dominant frequencies in the Snadd Formation (Figure 3.2) shows a mean (μ) frequency around 35 Hz. These results give a mean vertical resolution ($\lambda/4$) of approximately 22 m (Table 3.2). The frequency distribution is normal and has a standard deviation (σ) of approximately 8 Hz. Ca 95% of the values in a normal distribution lie within +/- two standard deviations from the mean value ($\mu \pm 2\sigma$). The vertical resolution and detectability have been calculated for the $\mu \pm 2\sigma$ frequency values (Table 3.2).

Table 3.2: The table shows the derived frequencies (f) from the dominant frequency distribution (Figure 3.2) and corresponding wavelengths (λ), vertical resolutions ($\lambda/4$) and detectabilities ($\lambda/32$) using a seismic velocity (v) of 3000 m/s. μ is the mean and σ is the standard deviation.

	μ	$\mu + 2\sigma$	$\mu - 2\sigma$
f [Hz]	34.6	50.6	18.6
λ [m]	86.7	59.3	161.3
$\lambda/4$ [m]	21.7	14.8	40.3
$\lambda/32$ [m]	2.7	1.9	5.0

Horizontal resolution

The horizontal resolution of unmigrated seismic data is defined by the Fresnel zone (Figure 3.3), which is the smallest lateral distance two features must have to appear as two separate reflections in the seismic data. The seismic wave fronts sent out from the source, propagate in spheres, and it is therefore more correct to say that a seismic reflection represents an area rather than a point in the subsurface. The area is dependent on the depth (z) of the seismic reflection in addition to the seismic wavelength (λ). Seismic waves that reach a reflector within a distance smaller than $\lambda/4$, define the geometrical area of the Fresnel zone. After migration, on the other hand, the Fresnel zone can be minimized to $\lambda/4$, which is the same as the vertical resolution.

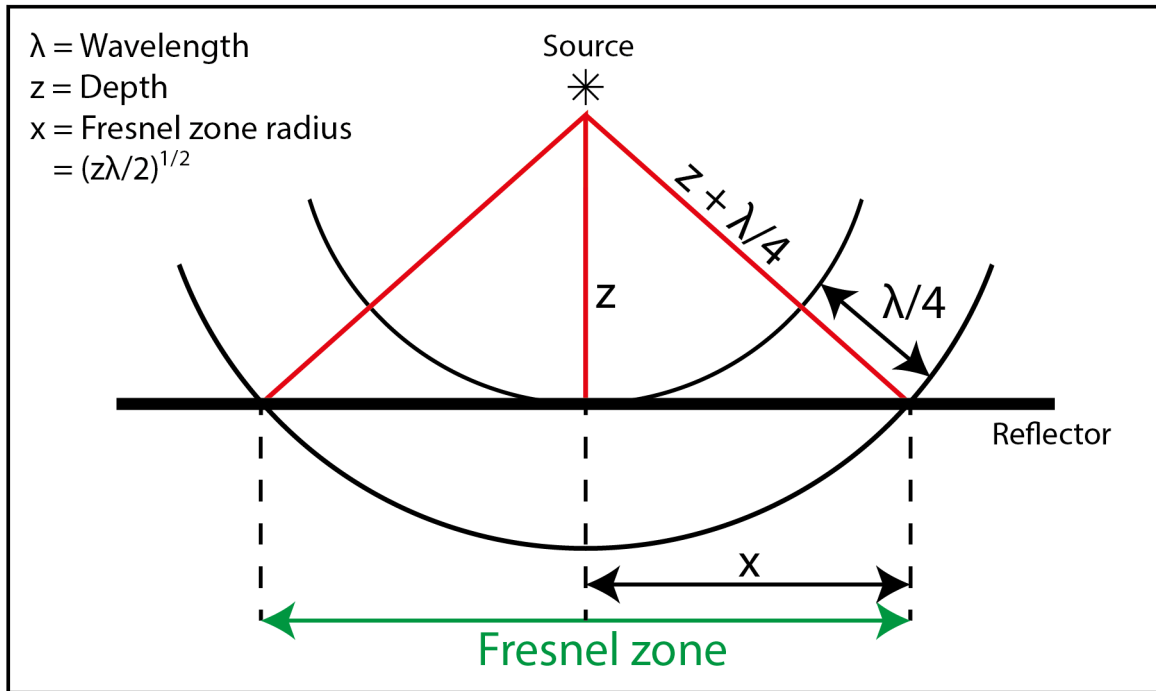


Figure 3.3: Conceptual illustration of the Fresnel zone before migration.

3.2.2 Methods

The Schlumberger software, Petrel 2015, has been used to interpret and visualize the seismic data in this study.

Seismic Interpretation

Formation tops in well 7131/4-1, retrieved from the NPD's FactPages were loaded into the Petrel project. They were correlated to the seismic reflectors representing the top of the Snadd and Kobbe formations, which in turn were laterally traced and interpreted in multiple inline and crossline sections using the "seismic interpretation tool". Subsequently, the "paintbrush tool" was used to fill the areas in between. The interpreted surfaces of the two formation tops were further used to create Root Mean Square (RMS) amplitude maps from different intervals within the Snadd Formation.

RMS amplitude maps

The Root Mean Square is a statistical measure of the magnitude of a dataset's variation. The RMS amplitude attribute extracts a seismic window within which the square root of the sum of squared amplitudes are divided by the number of samples within the specified window used (Daber et al., 2010). The RMS amplitude attribute emphasizes the variations in acoustic impedance in a selected seismic window. Strong amplitudes, both negative and positive, are highlighted and amplitude anomalies within the study area are easily detected. The RMS amplitude attribute in this study was used to detect channels in the Snadd Formation.

The RMS amplitude maps presented in Chapter 6 were created by taking a time window of 15 ms TWT using variable offset values from the interpreted horizons representing the top of the Kobbe Formation or the top of the Snadd Formation.

Channel measurements

Observed channels from RMS amplitude maps and seismic sections were divided into two categories; channel fill or channel belt deposits. Planform and cross-sectional geometries of the channels have been measured (Figure 3.4). The channel width was measured in metres, from planform view at three places perpendicular to the channel direction. The corresponding cross-sectional thickness was measured in ms TWT from the seismic data and translated to metres using a seismic velocity of 3000 m/s. The average width and thickness values for each measured channel were plotted to investigate the width-to-thickness ratios (Figure 6.9). The orientation of the channels were measured and plotted in a rose diagram (Figure 6.8).

3.2.3 Sources of error

Noise (imaging artefact) is an important parameter when it comes to evaluating the quality of seismic data. Processing of seismic data aims to improve the signal to noise ratio, but there will always be some noise left. This is important for the seismic interpreter to be aware of.

The interpretation of the abovementioned formation tops was sometimes challenging as a result of variable quality of the seismic data. It is therefore possible that parts of the horizons have been misinterpreted.

Channel recognition and measurements from seismic sections and RMS amplitude maps are based on subjective observations and interpretations, which in turn may vary from one person to another.

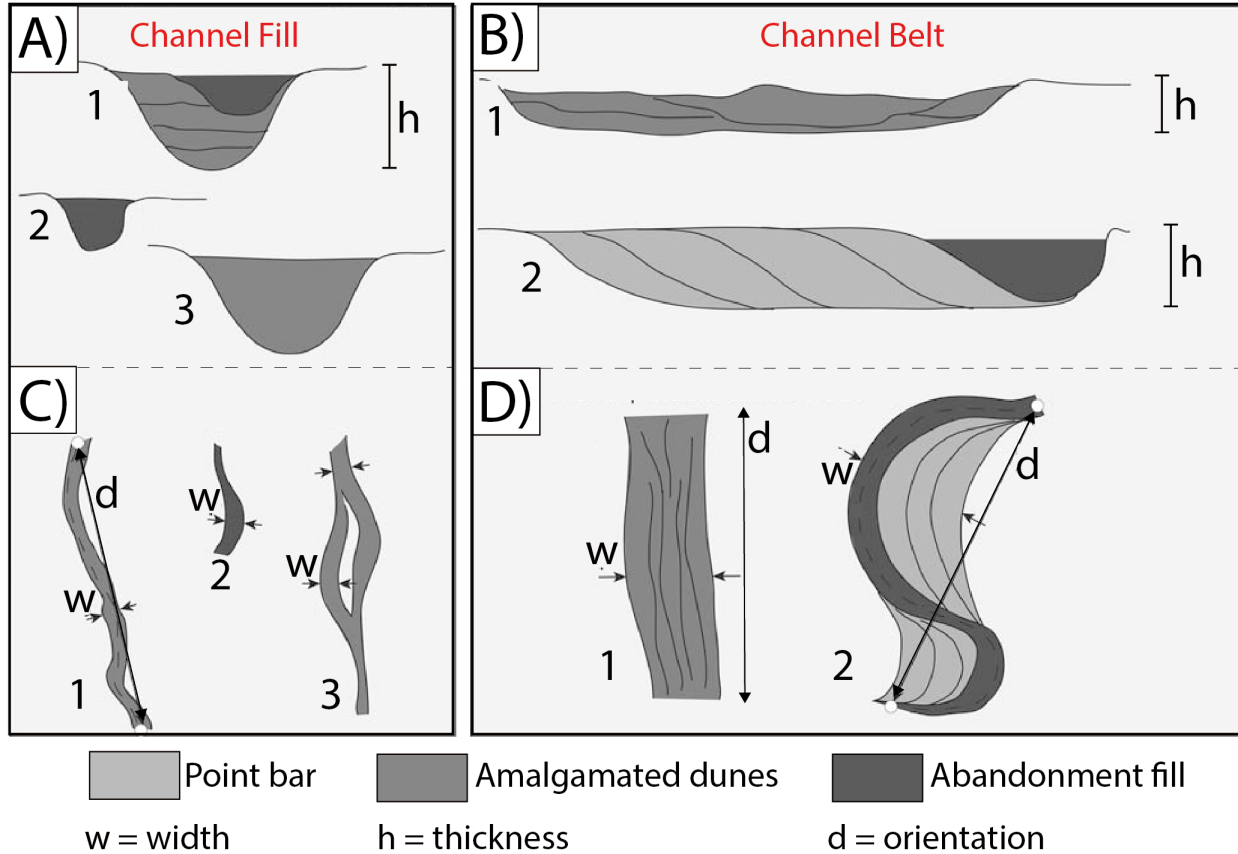


Figure 3.4: Schematic diagram of the measured channel parameters. The figure and figure text are modified from Klausen et al. (2014). **(A)** Perpendicular cross sections of channel-fill deposits: 1, amalgamated beds; 2, abandonment fines; 3, homogeneous sandstone fill. **(B)** Perpendicular cross sections of channel-belt deposits: 1, channel belt with amalgamated internal bedforms; 2, channel-belt with lateral-accretion surfaces. **(C)** A selection of typical planform seismic attribute expressions of the channel-fill sandstone bodies: 1, simple fill, straight to low-sinuosity; 2, abandoned channel plug or solitary low-amplitude channel; 3, channel-fill with anastomosed geometry. **(D)** A selection of typical planform seismic attribute expressions of the channel-belt sandstone bodies: 1, multiple clustered channels; 2, meandering channel, high-sinuosity.

3.3 Core

A core from a channel complex in the Snadd Formation (core 2) recovered from well 7131/4-1 on the Finnmark Platform (Figures 2.3 and 6.1) has been studied and is presented in Chapter 7. The D-cut of the core, which is 1/4 of the cylinder, was provided, and a sedimentological log was made at a scale of 1:100. The methods of the logging procedure are similar to those described in

Section 3.1.1.

3.3.1 Gamma-ray log

The gamma-ray log from well 7131/4-1, retrieved from Statoil's conventional core analysis report, was studied and mainly used for lithological interpretation. The gamma-ray log records the natural gamma radioactivity in the rocks and is a tool commonly used to distinguish mudrocks from sandstone and limestone (Nichols, 2009). Mudrocks typically contain minerals rich in potassium which has a high natural radioactivity and thus a high gamma-ray value.

3.3.2 Sources of Error

The main errors associated with the logging of the core are related to observations and interpretations. The quality of the D-cut was relatively poor resulting in difficulties when attempting to recognize sedimentological structures, textures and grain size variations. Moreover, the limited size of the core, inhibits observations of large scale bedforms.

3.4 Laboratory analyses

XRD-, optical microscopy- and Rock-Eval analysis have been done on selected samples (Table 3.3). The laboratory results are presented in Chapter 8.

Table 3.3: Locality, stratigraphic level and main lithology for the samples selected for laboratory analysis. The performed analysis method is marked with X

Location	Sample name	Metres in log	Lithology	XRD	Thin section	Rock-Eval
Fulmardalen	Stor16-1.17A	163	Sandstone	X		
Fulmardalen	Rys16-1.10A	93	Sandstone	X		
Fulmardalen	Mil16-1.8A	95	Sandstone	X		
Fulmardalen	Mil16-1.14A	217	Calcrete		X	
Fulmardalen	Rys16-1.23A	181	Calcrete		X	
Fulmardalen	Rys16-1.28B	200	Shale			X
Fulmardalen	Dyr16-1.19B	161	Shale			X
Core 2 (7131/4-1)	Sample 1	1102.20	Sandstone	X		
Core 2 (7131/4-1)	Sample 2	1087.30	Sandstone	X		
Core 2 (7131/4-1)	Sample 3	1073.50	Sandstone	X		

3.4.1 X-ray diffractometer (XRD)

Six sandstone samples have been selected for XRD analyses in order to quantify their mineralogy. Three samples are from the De Geerdalen Formation in Fulmardalen and three are from the Snadd Formation from core 2 in well 7131/4-1. The purpose of the XRD analyses is to investigate differences in mineralogy between the two locations.

The XRD analyses were performed by Laurentius Tjihuis at the Chemical/Mineralogical Laboratory at NTNU. The samples were crushed to powder and analysed in the XRD instrument BRUKER D8Advance. The software Diffrac.pluss.EVA was used to identify minerals, whereas the TOPAS software was used to quantify the interpreted minerals according to the Rietveld method.

3.4.2 Optical microscopy

Two petrographic thin sections were made from calcrete samples taken from the De Geerdalen Formation in Fulmardalen. A standard petrographic microscope with plan-polarized and cross-polarized light was used to investigate the mineralogy and texture.

3.4.3 Rock-Eval analysis

Two samples of dark shale were sent to Applied Petroleum Technology AS (APT) at Kjeller for Rock-Eval analysis. The purpose of the analysis was to obtain information on organic matter type and the depositional environment within which the shale was deposited.

4. Facies in the De Geerdalen Formation

The following chapter has been written in collaboration with master student Bård Heggem and is based on fieldwork that was conducted in Fulmardalen on Svalbard during the summer of 2016.

The chapter may be regarded as a continuation of the work that has been presented in the collaboration chapter in the master theses of [Haugen \(2016\)](#), [Johansen \(2016\)](#) and [Støen \(2016\)](#). Their chapter is based on fieldwork that was conducted in areas to the east of Fulmardalen in 2015. Both of the two authors of the facies chapter in this thesis also participated in the fieldwork of 2015, but spent time abroad on exchange studies and were therefore not involved in processing and presenting the data that was collected.

Detailed work on the facies in the De Geerdalen Formation was already presented in [Knarud \(1980\)](#) and laid the foundation for subsequent studies that have been conducted on the formation. The work that will be presented in this chapter is a part of a comprehensive project with an overall aim of extending the understanding of the facies of the Upper Triassic sedimentary succession in Svalbard.

The project was initiated with fieldwork on Hopen, Edgeøya and central Spitsbergen in 2008, 2009 and 2010 and was presented in [Hynne \(2010\)](#), [Rød \(2011\)](#) and [Rød et al. \(2014\)](#). The work was further extended and presented in the master theses of [Enga \(2015\)](#), [Haugen \(2016\)](#), [Johansen \(2016\)](#) and [Støen \(2016\)](#). The work of the latter three theses has been summarized in [Lord et al. \(2017a\)](#). [Figure 4.1](#) displays the location of Fulmardalen in relation to previous studies.

In [Lord et al. \(2017a\)](#), 14 different facies types have been described and interpreted from the De Geerdalen Formation ([Table 4.1](#)). The different facies types are also found to be highly representative for the formation in Fulmardalen. The following chapter will mainly focus on discrepancies between the facies observations from Fulmardalen and those presented in [Table 4.1](#), with the purpose of establishing a representative facies model for the De Geerdalen Formation in Fulmardalen. Hence, facies that have the same appearance in Fulmardalen as

elsewhere on Svalbard will not be described in detail in this chapter. Furthermore, the interpretations of the facies are consistent with those presented in [Table 4.1](#), unless otherwise stated.

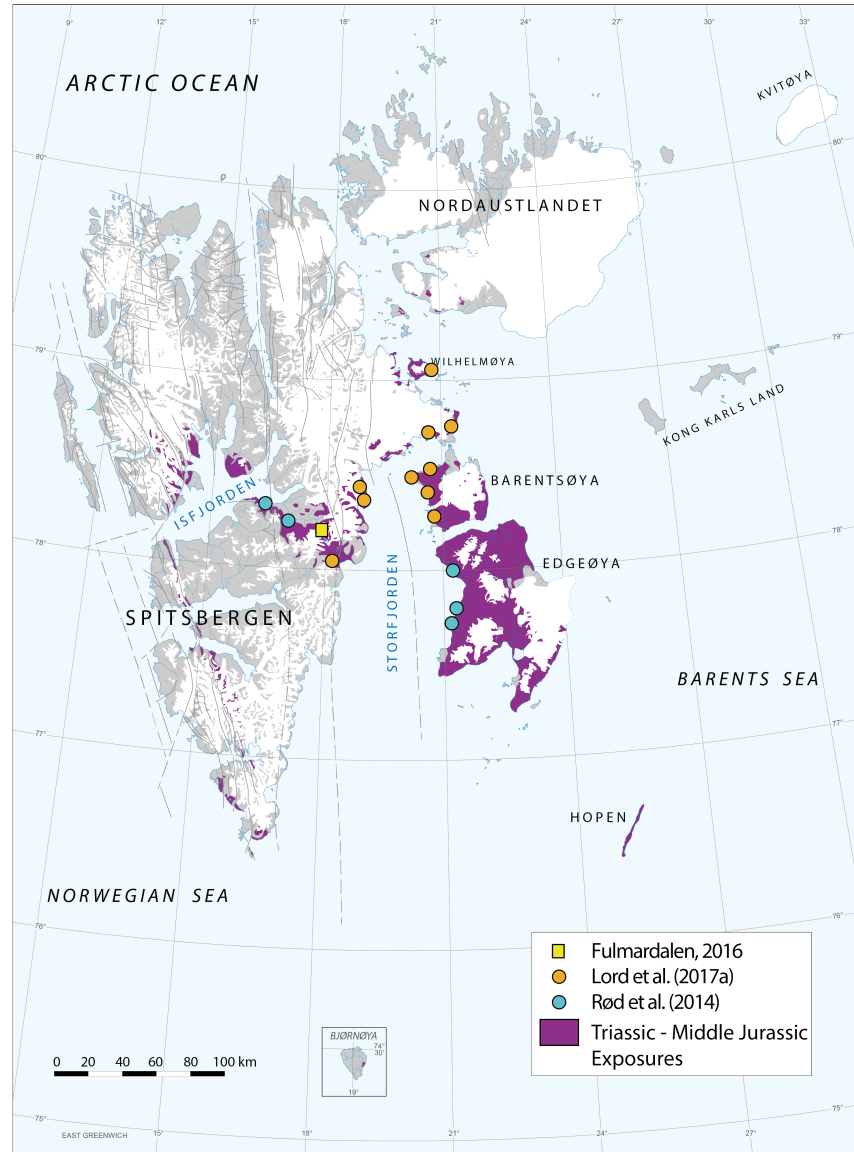


Figure 4.1: Overview map showing Triassic – Middle Jurassic exposures in Svalbard. Fieldwork localities from previous studies ([Rød et al., 2014](#); [Lord et al., 2017a](#)) are indicated. The figure shows how Fulmardalen is located between these localities, linking the previously collected data together.

4.1 The meaning of "Facies" and "Facies Analysis"

The word “facies” comes from the Latin language and means face, figure, appearance, aspect, look and condition ([Miall, 2016](#)), and was first introduced to geological literature by [Steno](#)

(1669). The modern way of understanding the term stems back to a definition that was presented by [Gressly \(1838\)](#). Since then, the usage of the facies term in a geological setting has been much debated (e.g., [Teichert, 1958](#); [Middleton, 1973](#)). In more recent years, publications from [Reading and Levell \(1996\)](#), [Dalrymple \(2010\)](#), [Miall \(2016\)](#) have provided good summaries of how facies is applied in modern day sedimentology.

There are different kinds of facies, depending on which features in a sedimentary rock the observations are focused around. While biofacies mainly consider fossil- and trace fossil components in a rock unit, lithofacies focus on describing rocks based on lithological features such as composition, grains size, stratification characteristics and sedimentary structures ([Miall, 2016](#)). Microfacies is a term typically used when the facies features are identified from thin sections. All of these facies types are classified as descriptive types of facies. However, the facies term can also be used in a more genetic way, emphasising on the depositional processes that were active at the time when the rock was deposited ([Reading and Levell, 1996](#)). "Fluvial facies" and "tidal facies" are examples of such genetic facies types.

Individual facies may be of varying value for interpretation purposes, with some facies (e.g., a coal seam) holding stronger environmental implications than others (e.g., a dark shale). However, all individual facies have their interpretative limitations, and in order to propose environmental interpretations, it is important that the individual facies are seen in relation to the surrounding facies ([Reading and Levell, 1996](#)).

Facies analysis forms a foundation for modern day stratigraphy. The importance of understanding facies sequences was already recognized by [Walther \(1894\)](#) where it was stated that the conformable vertical progression of facies is a result of successive depositional environments that are laterally juxtaposed to each other ([López, 2015](#)). This is a principle that has become so important in sedimentary geology that it often is just referred to as "Walther's Law". By analysing the facies that occur in sedimentary successions one creates a base for correlation between rock units both vertically and horizontally. Observations of spatial and temporal relationships in sedimentary rocks are easiest recognized from outcrops. Facies is therefore best described in a way that makes it possible to correlate it to what can be seen in the field ([Walker, 2006](#)).

4.2 Facies in Fulmardalen

Table 4.1: Overview of the 14 facies defined for the Upper Triassic succession in Eastern Svalbard, retrieved from (Lord et al., 2017a). The table is expanded from the work of Rød et al. (2014) and is also representative for the De Geerdalen Formation in Fulmardalen.

#	Description	Interpretation
A	<p>Mudstone (0.1 - 10's m) Clay and silt, laminated (shale) or non-laminated (mudstone). Thickness varies from a few centimetres to tens of metres. Laminated mudstones are most common and may encase thin beds of silty to very fine sandstone. Colour is dominantly grey or black, but may also be yellow, white or purple colour with weathering of siderite cement.</p> <p>The facies is characterised by horizontal and gently undulating laminae. Load structures and irregular lamination are occasionally observed. Concretions of calcite or siderite are common. Organic content may be high at some intervals. Ammonoids and marine vertebrate fossils are common.</p>	<p>Pelagic shale and mudstone deposited from suspension in low energy environments where clay and silt flocculate and settle on the sea floor (Boggs, 2011; Collinson et al., 2006). Also forms background sedimentation in shallow marine environments closer to the shoreline.</p>
B	<p>Heterolithic Bedding (0.01 - 10's m) Heterolithic bedding is observed as thin beds of very fine to fine sandstone and siltstone alternating with mudstones often forming coarsening upwards units.</p> <p>The thickness of mud and sand layers generally range from 1 mm to a few centimetres, however thicker packages are evident. Units are up to 10-15 m thick. Sedimentary structures preserved in the sandstones of heterolithic successions are commonly hummocky cross-stratification and ripple cross-stratification.</p> <p>Bioturbation is common towards the top of units and <i>Skolithos</i> may be present.</p>	<p>Heterolithic bedding indicates alternating flow regime where sand and mud is available (Davis Jr, 2012). Mud is deposited from suspension, while sand is deposited during current or wave activity (Reineck and Singh, 1980). This facies can form in the transition zone when mud interacts with sand introduced by periods of higher flow and sedimentation.</p>
C	<p>Hummocky Cross-Stratified VF-F Sandstone (0.1 - 1 m) Very fine to fine grained sandstones featuring hummocky and swaley cross-stratification. Consists of 10 cm to 1 m thick sandstone beds and are characterised by cross-laminae in undulating sets. Individual laminae sets are commonly between 5 and 20 cm thick.</p> <p>The sandstones are typically grey to yellow or orange to reddish brown colour. Beds are usually moderately to intensely bioturbated with <i>Skolithos</i> and <i>Diplocraterion</i>. Hummocky cross-stratified sandstones are common in upwards coarsening sequences in the lower part of the De Geerdalen Formation throughout the study area.</p>	<p>Hummocky cross-stratification shows a distinct undulating geometry of lamination formed by the migration of low-relief bed forms in one direction due to wave surge and unidirectional currents (Nottvedt and Kreisa, 1987)</p> <p>This facies is widely recognised as being characteristic of tempestite deposition in shallow marine, storm-dominated inner shelf, to lower shoreface settings (Midtgaard, 1996; Yang et al., 2006). Hummocks form below the fair weather wave base and above, but are most common near storm weather wave base (Dumas and Arnott, 2006).</p>
D	<p>Sandstone with Soft Sediment Deformation (0.3 - 1.5 m) Erosive based, very fine to fine grained sandstones characterised by abundant soft sediment deformation. Units can be laterally restricted but also extensive thickness ranges from 0.3 to 1.5 m. Irregular lamination seen within the sandstone bodies are also present in the upper parts of the underlying, deformed, mudstones.</p> <p>Sandstones are typically green-grey in colour and lack bioturbation. Soft sediment deformed beds are relatively rare throughout the study area, with the most extensive beds occurring at the locality of Mistakodden.</p>	<p>Soft sediment deformation structures typically generate from gravitational processes such as downslope sliding and slumping or rapid loading of sediment (Reineck and Singh, 1980; Bhattacharya and MacEachern, 2009).</p> <p>Likely form the base of distributary mouth bar deposits, where large volumes of sediments are deposited rapidly in front of distributary systems and reworked by wave or fluvial processes.</p>

E	<p>Wave Rippled Sandstone (0.1 - 4 m) Very-fine to fine grained sandstone with symmetrical ripple lamination. Thicknesses range from tens of cm up to ca. 4 m, individual beds can be 10 to 30 cm in thickness. Sandstones have grey, yellow or red weathering colour. Fresh surfaces are light grey. Carbonate cement (calcite/ dolomite) or siderite is common.</p> <p>Sandstone beds of this facies are normally graded and wave ripples are often observed on the upper surfaces in coarsening upwards successions. The crests tend to be continuous and straight. Mud drapes are common and expose ripple foresets. Facies is commonly found interbedded with heterolithic bedding or overlying horizontally bedded sandstone. Moderate bioturbation and <i>Rhizocorallium</i> or <i>Skolithos</i> trace fossils are present.</p>	<p>Wave ripples are commonly found in shallow marine settings. They are formed by the oscillatory movement of currents at normal wave base (upper shoreface) where swash and backwash currents produce symmetrically shaped ripples (Boggs, 2011). Mud drapes on the foresets of ripples indicate a tidal influence.</p>
F	<p>Current Rippled Sandstone (0.1 - 4 m) Very fine to fine grained sandstone with asymmetric ripples forming individual beds or units composed entirely of ripple cross stratification up to 4 m in thickness. Sandstone is yellow, orange and brownish colour.</p> <p>Sandstone beds in this facies are typically normally graded and have sharp lower contacts, whereas contacts to upper facies are gradual. In some instances this facies may fine upwards. Facies is often observed to overlay large-scale cross-bedded and small-scale cross-bedded, normal graded sandstones and itself is overlain by fining upwards beds of horizontally bedded sandstone.</p>	<p>Current ripples occur with the aggradation of ripples under contemporary downstream migration during unidirectional flow. Sets arranged into climbing ripples form under the same regime but with the angle of climb reflecting rate of aggradation (Collinson et al., 2006).</p> <p>Current ripples are commonly found in environments such as fluvial floodplains, with sub-environments such as; crevasse splays and point bars. They are also present in seasonally flooded river deltas (Reading and Collinson, 1996; Boggs, 2011). In marine environments they are usually formed in the shoaling wave zone.</p>
G	<p>Carbonate Cemented Sandstone (0.2 - 2 m) Very fine to fine grained, normally graded, sandstones characterised by structures formed during diagenesis. Sandstone units are commonly hard and heavily cemented with calcite, dolomite or siderite, making observations of primary sedimentary structures difficult, thickness is typically 0.2 – 2 m.</p> <p>Secondary sedimentary structures include cone-in-cone, siderite beds and calcareous concretions. Colour variation between grey, brown and red are observed. Scarce to heavy bioturbation is noticed. Cemented sandstone forms benches in the topography or distinctive layers, that may be laterally continuous for several tens of metres prior to pinching out.</p>	<p>Sources of calcite cement may be dissolved bivalves and coquinas. Recent studies by Tugarova and Fedyaevsky (2014) suggests a genesis driven by micro-organisms and a biochemical precipitation of carbonates during early diagenesis in a shallow marine environment.</p> <p>Siderite occurs in organic-rich brackish to meteoric pore-waters depleted of SO and is commonly found 2 in fine grained deltaic to coastal sediments (Morad, 1998). Siderite concretions and layering might indicate a continental influence on marine sedimentation with organic-rich stagnant waters close to the delta front (Pettijohn et al., 1987).</p>
H	<p>Plane Parallel Laminated Sandstone (0.3 - 2 m) Sandstones with horizontal, plane parallel lamination or plane parallel stratification. Mostly very fine to fine grained sand, but can also be silty and medium grained. Units range between 30 cm and 2 m in thickness, with mm-thin lamina and cm-thick beds. Parting lineation (primary current lineation), is present on bedding surfaces. Stratification varies from lamination to bedding. Colour is grey to pale yellow, but weathers brown to red.</p> <p>Lower boundaries are typically sharp, while the upper are commonly more gradual. Units are often observed towards the top of sandstone benches. Bioturbation is rare in lower parts, but occurs towards the upper part of units. <i>Skolithos</i>, <i>Diplocraterion</i> and <i>Rhizocorallium</i> also observed.</p>	<p>Plane parallel stratification occurs in various environments and is not a unique environmental indicator (Boggs, 2011). The structure form by settling of fine grains from suspension or traction of sand as bed-load in the upper flow regime (Collinson et al., 2006; Boggs, 2011).</p> <p>Laminae are defined by grain size variations or assembling of mica, representing subtle variations in depositional environment (Collinson et al., 2006). It is commonly found in rivers and streams with a high flow (Boggs, 2011), but it can also result from settling of sand grains from suspension.</p>

I	<p>Low Angle Cross-Stratified Sandstone (0.1 - 1.5 m) Very fine to fine grained sand, forming gently inclined sets of planar parallel stratification or lamination, with wedge-shaped set boundaries. The colour is usually grey to red-brown when weathered and grey on fresh surfaces. Unit thickness is usually between tens of cm to 1.5 m, while set thickness range between 5 and 15 cm. Individual sets are composed of both beds and lamina, where the former is the most common.</p> <p>These sandstones are commonly bioturbated and contain plant fragments and rare fish remains. It is frequently found overlying or interbedded with wave rippled sandstones, or heterolithic bedding.</p>	<p>Low angle cross-stratification is not considered a diagnostic sedimentary structure as it can be seen occurring in a range of depositional environments. However, the presence of bioturbation and plant fragments are interpreted as indicators of a proximal position in the shallow marine environment, most likely the upper shoreface or beach foreshore (Reading and Collinson, 1996).</p> <p>Low angle cross-stratified sandstones typically exhibit a gentle dip seawards when found in foreshore and backshore settings (Reading and Collinson, 1996)</p>
J	<p>Tabular Cross-Stratified Sandstone (0.1 - 1.5 m) Very fine to fine grained sandstones with tabular cross-stratification or cross-lamination, arranged in foresets with bedforms of 2 to 10 cm thickness and stacked in units that are up to 1.5 m thick. Calcite cementation is common and varies from vague to pervasive resulting in differences in appearance within facies. Sparse bioturbation is occasionally observed towards the top of units and plant fragments are common. Grey, yellow, brown and reddish colours are observed. Weathering of finer material on sandstone bounding surfaces is interpreted as draping mud or finer sand.</p> <p>Facies J is commonly found overlying large-scale trough cross bedded sandstones in fining upwards units. It is also often found within heterolithic bedded units.</p>	<p>Tabular cross-stratification forms by unidirectional currents of the lower flow regime in shallow waters (Collinson et al., 2006; Boggs, 2011).</p> <p>Environments of formation are fluvial and shallow marine where rip-currents, longshore currents, tidal currents and breaking waves creates unidirectional currents (Reading and Collinson, 1996). Plant fragments, low abundance of trace fossils and close proximity to palaeosols in upper sections indicates that this facies is most likely associated with terrestrial depositional environments.</p>
K	<p>Trough Cross-Stratified Sandstone (0.2 - 4 m) Fine to medium grained trough cross-stratified sandstones with sharp erosive base, displaying a fining upwards trend. Cross set thicknesses range from 20 to 80 cm, whereas stacking of sets results in unit thicknesses of 0.2 to 4 metres.</p> <p>Rip-up clasts and plant fragments are frequent in the basal parts of units and scours. Observed colours are grey, yellow and brown, with reddish and dark colours appearing occasionally on weathered surfaces. Upper parts of sandstones may be sparsely bioturbated, whereas lower parts are essentially free of traces. Trace fossils observed within this facies are <i>Skolithos</i> and <i>Diplocraterion</i>.</p>	<p>Formed by migration of 3D dunes, in unidirectional currents in the lower flow regime (Reading and Collinson, 1996; Boggs, 2011). Complexity of dune morphology is thought to increase at higher current velocities and shallower waters (Collinson et al., 2006; Boggs, 2011) and stacking of co-sets represent superimposed bed-forms (Reineck and Singh, 1980).</p> <p>Facies is interpreted as migrating dunes in a subaqueous environment due to unidirectional current. Mud drapes are attributed to slight changes in current velocity, possibly implemented by tidal activity or seasonal changes in stream discharge.</p>
L	<p>Bioclastic Sandstone and Mudstone (0.1 - 0.5 m) The unit consists mainly of disarticulated and fragmented bivalves (coquina), lacking sedimentary structures. Thickness is from 10 to 50 cm. All the observed units are cemented and display orange and purple weathering colours. Bioclastic beds are found as discrete laterally continuous layers sandwiched between mud and locally as minor shell accumulations within sandstone bodies.</p> <p>Bioclastic beds are typically restricted to the lower parts of the Isfjorden Member, but are also seen at some localities in the lower part of the De Geerdalen Formation.</p>	<p>Fragmented shells indicate a relatively high energy environment. Mass erosion and transportation of shells can lead to concentration of shell fragments in beds where the hydrodynamic energy is low enough for deposition (Reineck and Singh, 1980).</p> <p>The Isfjorden Member is interpreted to be deposited in a shallow marine and lagoonal environment. Based on associated facies, field observations also point towards a proximal shallow marine origin, and coquina beds may represent wave reworked shallow marine shell banks accumulated by currents or waves.</p>

M	<p>Coal and Coal Shale (0.1 - 0.2 m) Units of coal and coal shale are from 1 to 20 cm thick. The units often appear laterally continuous over tens of metres. Coal and coal shales are usually found in close proximity to the top of larger sandstones. Coals are distinguished from coal shales by being more consolidated and vitrinous, reflecting a higher proportion of organic material.</p> <p>Coal and coal shales are commonly associated with underlying paleosols, but coal shale surrounded by grey shale is observed on Wilhelmøya and Hahnfjella. Rhizoliths are also commonly observed in the coals. The facies is found at all localities, but only in the middle and upper parts of the De Geerdalen Formation.</p>	<p>Coal seams found in the De Geerdalen Formation typically overlie paleosols, indicating they are formed in place (histic epipedons) (Retallack, 1991). Coal and coal shale beds found in the De Geerdalen Formation are thin and laterally discontinuous. Coal and coal shales are here interpreted to originate from mires on a dynamic delta plain setting in a humid palaeoclimate with seasonal variations in precipitation, following the conclusions of Enga (2015).</p>
N	<p>Paleosols and Calcrete (0.2 - 1 m) Paleosols are found at all localities. The thickness is in the range of 0.2 to 1.0 metres. Roots and wood fragments up to 20 cm in diameter can be found. The colour varies from brown to reddish brown and yellow. Non-calcareous paleosols are composed of mudstone and weather red or green and are 0.2 to 1 m in thickness. The structure of these mudstones is blocky or gravelly with weathering and mottles being common.</p> <p>Paleosols occur both in grey mudstone and on top of sandstone beds. A gradual contact at the base and sharper contact at the top is typical for paleosols (Boggs, 2011) and is frequently observed in the outcrops. The paleosols are commonly overlain by coal or coal shale.</p>	<p>Paleosols form due to physical, biological and chemical modification of soil during periods of subaerial exposure. Paleosols are continental (Boggs, 2009), but can form in marine strata following sea level fall and sub-aerial exposure (Webb, 1994).</p> <p>Paleosols represent an unconformity, formed in a degrading landscape (Kraus, 1999). Red mudstone beds are interpreted as calcrete horizons formed in a semi-arid environment. Calcretes also imply periods of non-deposition. Red and green colours may result from fluctuations in groundwater and shifts between oxic to anoxic conditions.</p>

Facies A - Mudstone

Mudstones (facies A) in Fulmardalen (Figure 4.2A) fit the description given in Table 4.1. Facies A is interpreted as the most dominant facies in the De Geerdalen Formation in Fulmardalen. Detailed investigations of the facies are, however, challenging due to extensive scree cover and weathering.

Facies B - Heterolithic Bedding

The description of heterolithic bedding (facies B) from previous studies on Svalbard (Table 4.1) is consistent with the observations of this facies in Fulmardalen (Figure 4.2). Intervals of alternating sandstones, siltstones and mudstones occur throughout the formation at all localities. Sedimentary structures preserved in sandstone and siltstone layers are mainly ripples (Figure 4.2D) and hummocky cross-stratification (Figure 4.2E). Erosive-based and deformed sandstone lenses (facies D) are commonly found in these intervals as well.

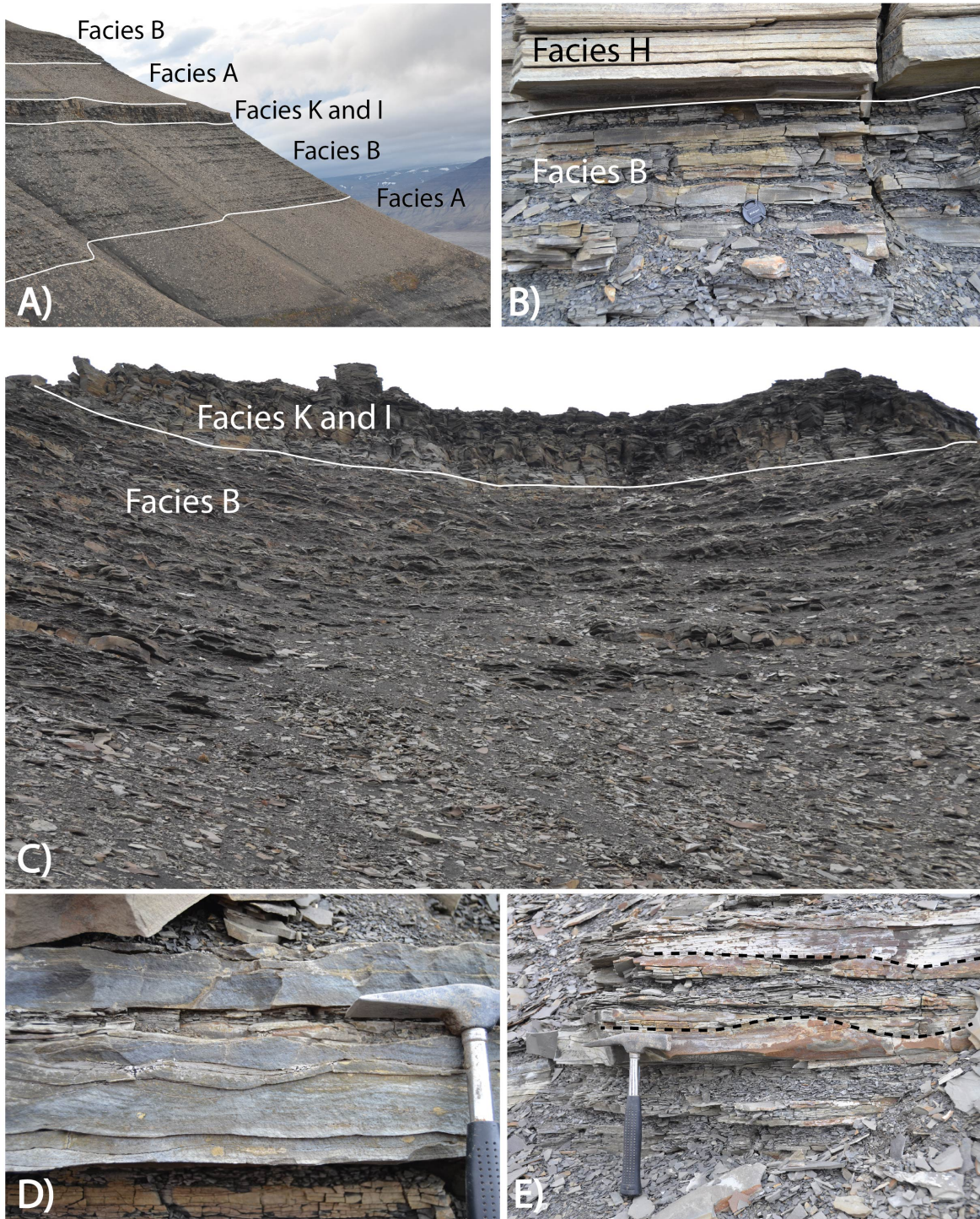


Figure 4.2: (A) Slope of Milne Edwardsfjellet, displaying two repeated upwards coarsening units with mudstones (facies A) in the lower part, heterolithic bedding (facies B) in the middle part and sandstone in the upper part. (B) Outcrop from Dyrhø, displaying the alternating lithological appearance of a heterolithic bedding (facies B) overlain by a planar laminated sandstone (facies H). (C) Slope of Milne Edwardsfjellet, displaying heterolithic bedding (facies B) gradually coarsening upwards into a sandstone dominated unit. (D) Outcrop from Dyrhø, showing climbing ripples in a sandstone within a heterolithic unit. (E) Outcrop from Storfjellet, showing hummocky cross-stratified sandstone (facies C) within a heterolithic unit. Dashed lines indicate the hummocky appearance of the lamination.

Facies C - Hummocky Cross-Stratified Sandstone

Hummocky and swaley cross-stratified sandstones (facies C) in Fulmardalen ([Figure 4.2E](#)) are commonly observed in the lower part of the De Geerdalen Formation. Hummocks and swales are dominating structures in the coarser beds within heterolithic sections, which is consistent with previous description of the facies on Svalbard.

Facies D - Sandstone with Soft Sediment Deformation

Soft sediment deformation in sandstones (facies D) ([Figure 4.3](#)) is commonly observed in the lower part of the formation at multiple locations in Fulmardalen. Following the division from [Oliveira et al. \(2011\)](#), it is possible to distinguish between two different types of soft sediment deformation structures. The first of these two types is called “detached soft sediment deformation structures”, and is the product of lateral movement of slides, slump and debris flow deposits ([Figure 4.3A, B, C, D, H](#)). The other type is called “in situ soft sediment deformation structures”, and is mainly a result of vertical movements forming flame structures, load structures, water-escape structures, convolute bedding etc. ([Figure 4.3E, F, G](#)). In Fulmardalen, detached soft sediment deformation structures often occur as erosive based sandstone lenses within mudstones (facies A) and the heterolithic parts (facies B) of upward coarsening sequences. In situ soft sediment deformation structures are less common than the detached ones, and are only present in the lowermost major sandstone intervals at Storfjellet and Ryssen. Compared to the findings of [Lord et al. \(2017a\)](#), detached soft sediment deformation structures in sandstone bodies capsuled by mudstones appear to be more common in Fulmardalen than in the eastern areas. Especially at Milne Edwardsfjellet, such deformed sandstone lenses are well preserved and exposed in the lowermost part of the De Geerdalen Formation. While in situ soft sediment deformation structures are fairly well described in [Lord et al. \(2017a\)](#), detached soft sediment deformation structures can be more precisely described from the outcrops in Fulmardalen.

All detached soft sediment deformed sandstone outcrops in Fulmardalen appear to be very fine grained. Geometrically, the bodies mainly come in two different shapes, with one type being lense-shaped, ranging from 0.5 m to 3 m in width, while the other type having a more sheet-like geometry, reaches up to 20 m in width. The bodies are between 0.2 and 2 m thick. The intensity of deformation tends to vary locally within the lenses and sheets. Laminations and stratifications within the sandstones are in most cases preserved, displaying complex and laterally elongated folding patterns. Some of the deformed sandstone units may also resemble ball and pillow structures (e.g., [Reineck and Singh, 1980](#)). Plant fragments and mud flakes are commonly observed within the structures, while bioturbation and wave-ripples are present on top of the units. In contrast to what was observed from a similar outcrop at Muen on Edgeøya ([Johansen, 2016](#)) (see [Figure 9.2](#)), carbonate cementation and cone-in-cone structures were not observed in this sub-facies in Fulmardalen.

[Oliveira et al. \(2011\)](#) conclude that the position of the different soft sediment deformation structures can be related to their position on clinoforms. It is suggested that in situ soft sediment deformation structures mainly form due to high sedimentation rates on the relatively stable delta front/clinoform rollover. Detached soft sediment deformation structures require a higher degree of sediment instability, and such conditions are common on the delta slope/clinoform slope. Folding patterns in detached soft sediment deformation structures are mainly a result of "freezing" of slump deposits, and such structures are common in front of migrating sandbars ([Oliveira et al., 2011](#)). This seems to be consistent with the findings from Fulmardalen, where the detached soft sediment deformation structures are interpreted as delta slope deposits, while the in situ soft sediment deformation structures are found in what has been interpreted as delta front barrier sand deposits. The relative content of deformed sandstone bodies observed at the different localities varies, which may be a result of varying proximity to sand distributaries, or due to a varying degree of scree cover.

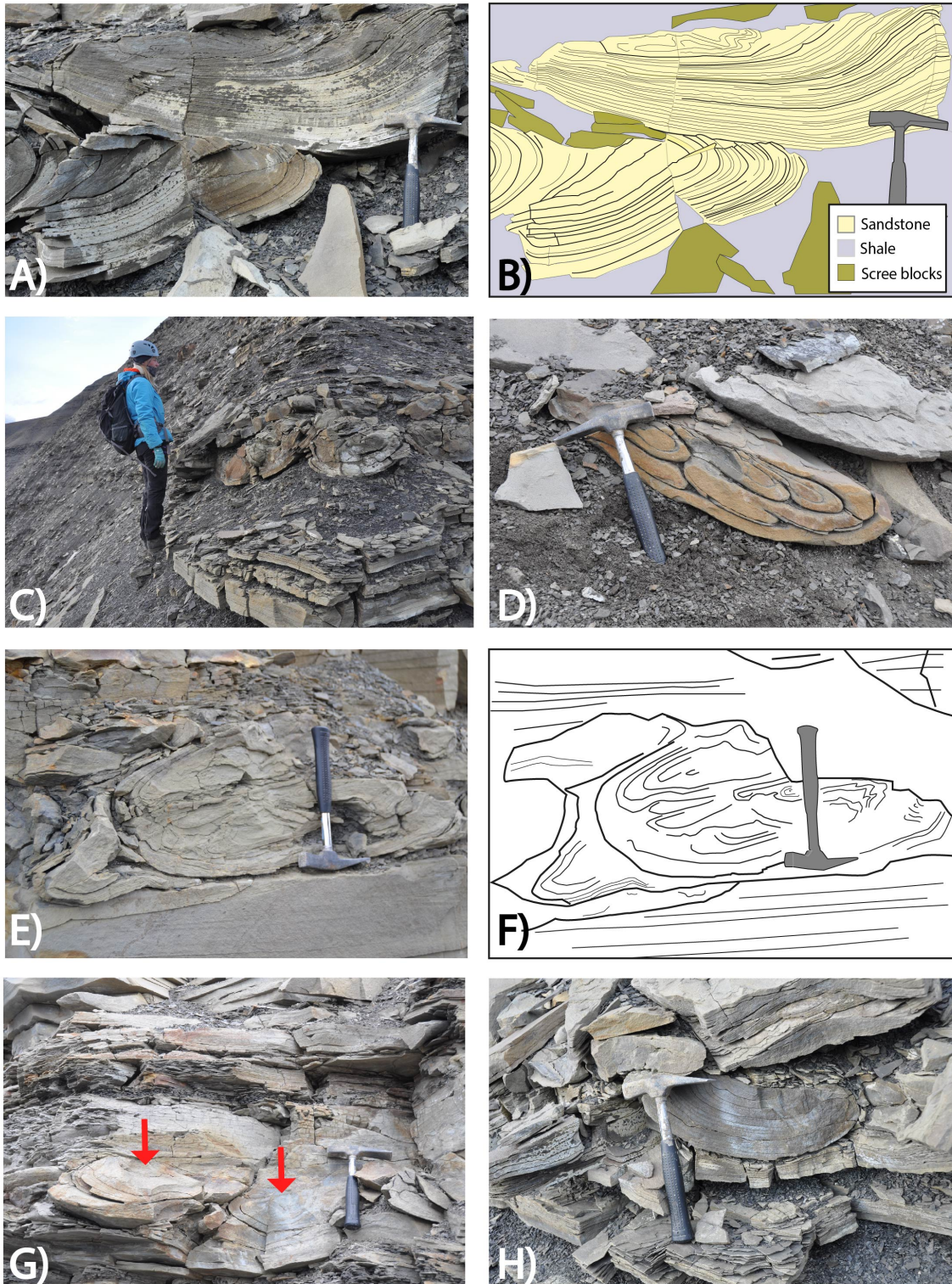


Figure 4.3: Soft sediment deformed sandstones (facies D) in Fulmardalen. Both detached soft sediment deformation structures (DS) and in-situ soft deformation structures (IS) are displayed. **(A)** DS from Milne Edwardsfjellet, resembling ball and pillow structures **(B)** Sketch of the sandstone in A. **(C)** DS in a laterally restricted sandstone at Milne Edwardsfjellet. **(D)** DS from Storfjellet. **(E)** IS from Ryssen. **(F)** Sketch of the sandstone in E. **(G)** IS from Storfjellet. Arrows indicate deformed part. **(H)** DS from Milne Edwardsfjellet.

Facies E - Wave Rippled Sandstone

The wave rippled sandstones (facies E) in Fulmardalen (Figure 4.4) fit well to the description of facies E in Table 4.1. However, the unit thickness appears to be slightly larger in Fulmardalen. *Diplocraterion* is observed in addition to *Skolithos* and *Rhizocorallium*. The facies is found at every location visited and at all stratigraphic levels in the formation.

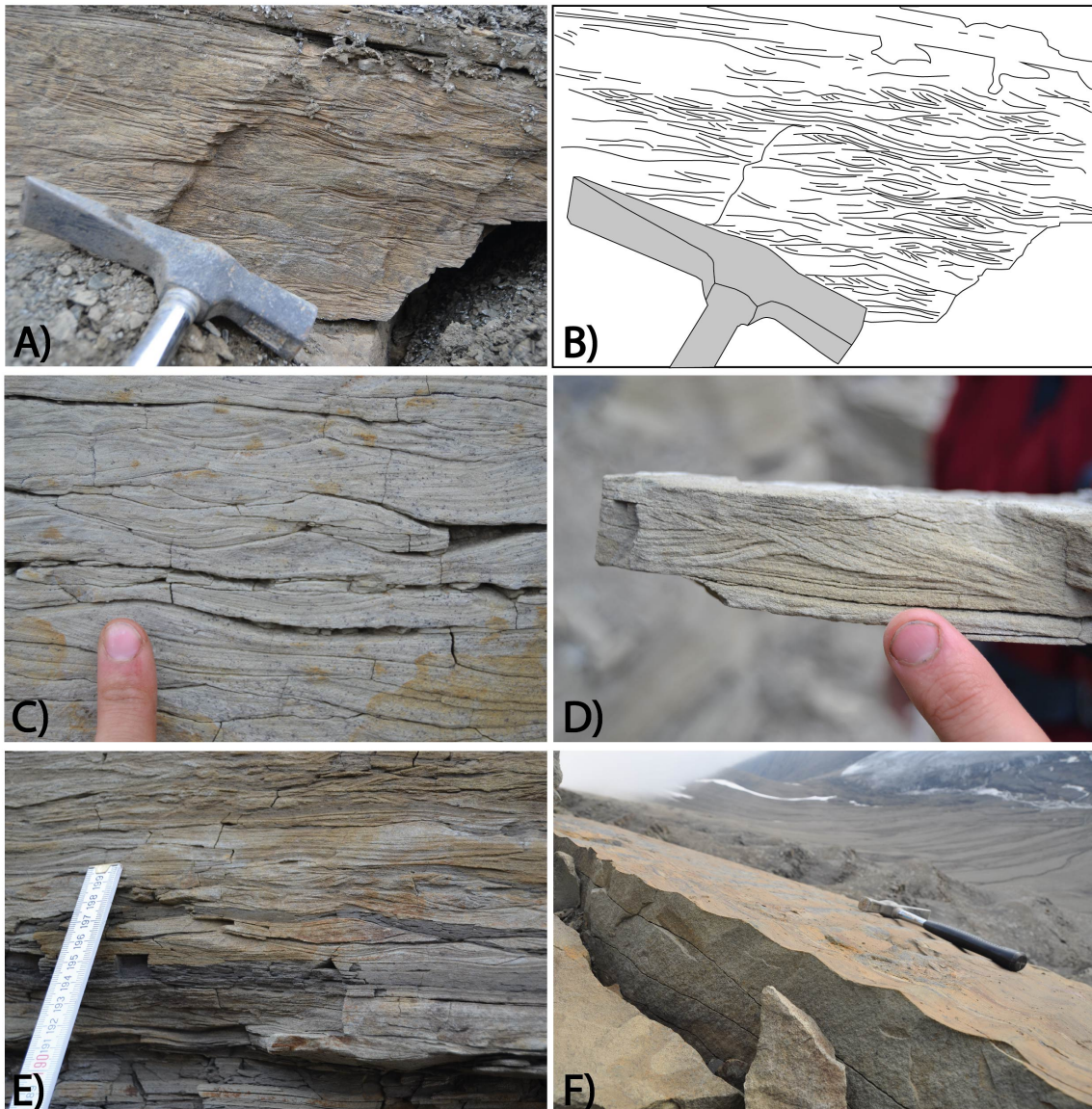


Figure 4.4: Wave rippled sandstones (facies E) in Fulmardalen. (A) Wave rippled sandstone at Ryssen. (B) Sketch of the sandstone in A. (C), (D) Wave rippled sandstone at Ryssen. Notice the well exposed symmetrical shape. (E) Wave rippled sandstone at Dyrhø. Notice mud draping some of the ripple crests. (F) Wave rippled sandstone at Storfjellet, displaying symmetrical ripple crests in 3D.

Facies F - Current Rippled Sandstone

Current rippled sandstones (facies F) are observed in relatively few outcrops in Fulmardalen (Figure 4.5). Where present, the outcrops resemble the facies description from previous studies in having undulating, parallel wavy to straight stratification/set boundaries without apparent cross-stratification (e.g., Johansen, 2016).

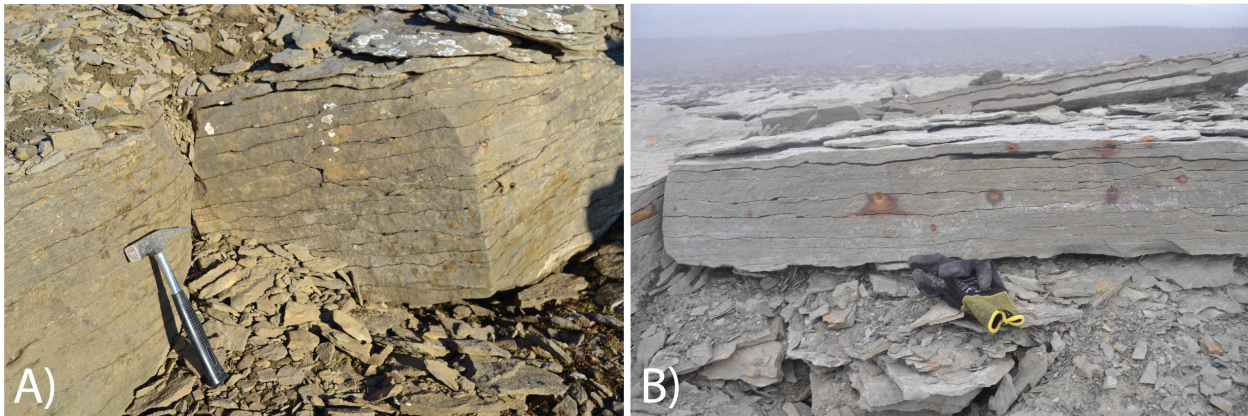


Figure 4.5: Current rippled sandstones in Fulmardalen at (A) Wallenbergfjellet and (B) Storfjellet.

Facies G - Carbonate Cemented Sandstone

Carbonate cemented sandstones (facies G) are observed especially in the middle and upper part of the logged sections in Fulmardalen (Figure 4.6). Cone-in-cone structures (Figure 4.6B), siderite beds and calcareous concretions (Figure 4.6C) are observations similar to the descriptions from Table 4.1. Furthermore, the units are hard and laterally extensive (Figure 4.6A), often with a red to brown weathering colour. Shell fragments which may be assigned to facies L, bioclastic sandstone, occur locally within carbonate cemented sandstones. Additionally, structures interpreted as desiccation cracks are found within facies G in Fulmardalen (Figure 4.7). Such structures are not described from facies G in Table 4.1, and will be described in more detail in the following section.

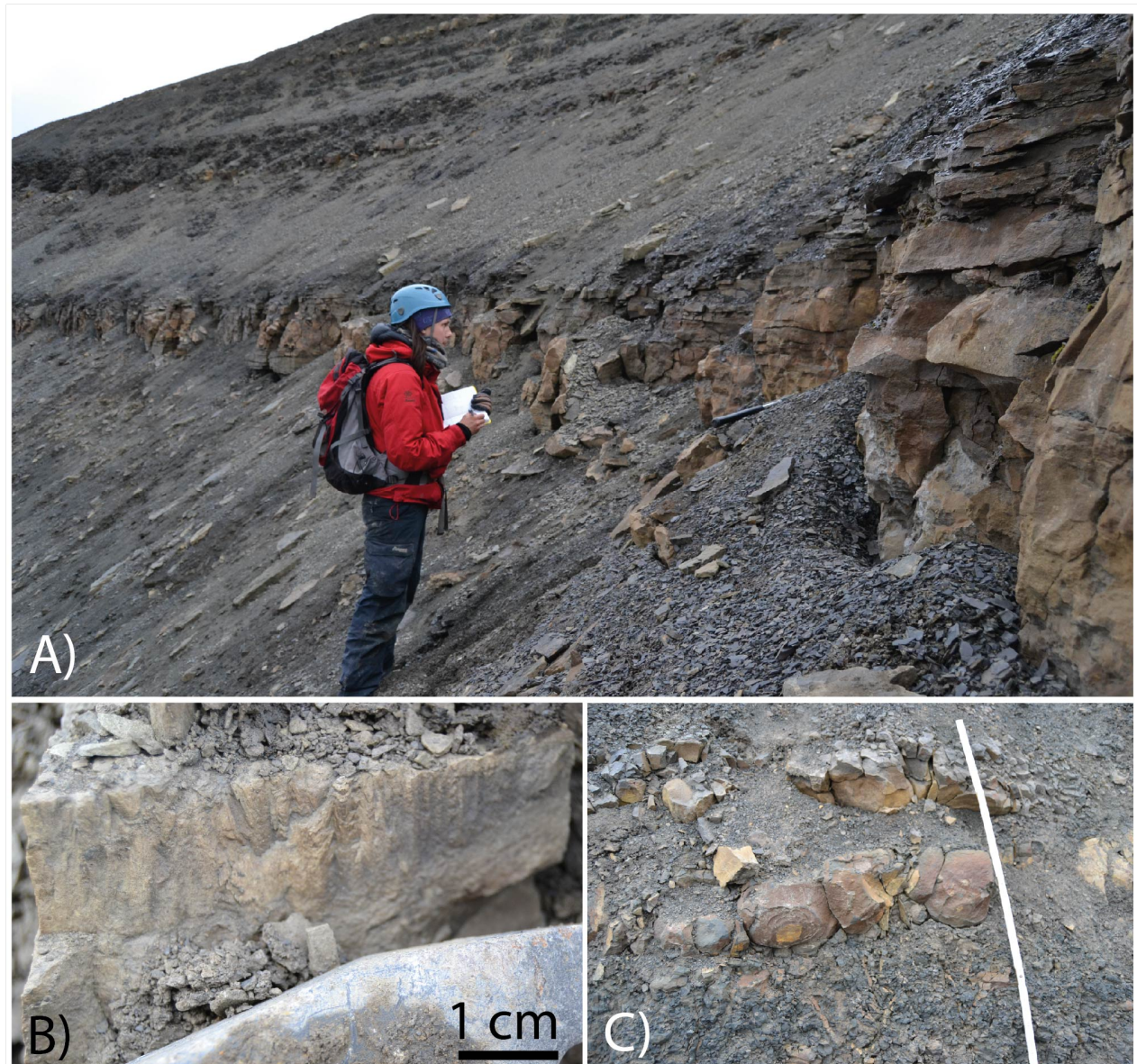


Figure 4.6: Carbonate cemented sandstones (facies G) in Fulmardalen. **(A)** Carbonate cemented sandstone at Dyrhø. Notice its laterally continuous appearance. **(B)** Cone-in-cone structures at Ryssen. **(C)** Siderite concretion layer at Dyrhø.

Potential desiccation cracks in the De Geerdalen Formation

In Fulmardalen, structures resembling desiccation cracks are only found in the upper part of the De Geerdalen Formation within a rusty-red carbonate cemented unit found below a shale unit with a characteristic dark colour. The layer is illustrated with an orange colour in the logs presented in [Chapter 5](#). Desiccation cracks have actually been described from the De Geerdalen

Formation in central and eastern Spitsbergen by [Knarud \(1980\)](#), and are indicative of periodical sub-aerial exposure.

The rusty-red unit in Fulmardalen often shows alternating light and dark coloured laminations representing mud and sand, respectively. At the mountain Ryssen, the mud is interrupted by multiple deformed downward-tapering cracks filled with sand ([Figure 4.7](#)), interpreted as desiccation cracks that have been compacted. The structures often have sharp edges and the mud seems to have been pulled apart which indicates a shrinkage mechanism. Desiccation cracks develop under sub-aerial conditions when muddy sediment dries out ([Nichols, 2009](#)). Desiccation crack patterns are typically polygonal, and are most clearly preserved in sedimentary rocks when filled with sand or silt transported by wind or water ([Nichols, 2009](#)). The sand filled cracks observed at Ryssen are to some extent polygonal ([Figure 4.7E](#)), but are often straight, spindle-shaped or slightly curved tapering cracks ([Figure 4.7F](#)) as well. It is possible that the polygonal crack pattern did not have time to fully develop before a new portion of sand covered the mud. The area between the cracks is sometimes curved upward into a concave shape ([Figure 4.7D](#)), which is typical for desiccation cracks ([Boggs, 2011](#)). However, it is possible that the concave appearance is only a result of mud draping wave ripple crests. An inter-tidal setting is a likely candidate for the depositional environment. The thickness of the mud is relatively thin, and it is reasonable to imagine that it can easily dry out when exposed during low tide.

On the other hand, the observed crack shapes are typical for syneresis cracks ([Nichols, 2009](#); [Boggs, 2011](#)). In contrast to desiccation cracks, syneresis cracks are shrinkage cracks that form under water in clayey sediment when the clay settles and compacts ([Nichols, 2009](#)). They commonly occur in thin mudstones interbedded with sandstones ([Boggs, 2011](#)). The sand-mud ratio in the lamination at Ryssen is high, which could imply that the cracks are syneresis cracks rather than desiccation cracks. Syneresis cracks are typical in carbonate or carbonate cemented sandstones.

The undulating light and dark coloured lamination of the host rock resembles a carbonate

cemented unit that was observed in the upper part of the De Geerdalen Formation during fieldwork in 2015 in eastern Spitsbergen. [Støen \(2016\)](#) presents petrographic data of a sample from this unit from Klementievfjellet in Agardhbukta, located 20 km SE of Ryssen (see [Figure 9.1](#)). Thin-section microscopy reveals that the laminas result from alternating micritic calcite and detrital siliciclastic clasts dispersed in micritic calcite.



Figure 4.7: Structures interpreted as desiccation cracks, or potentially as syneresis cracks, at Ryssen. **(A)** Oblique view. Muddy areas are outlined with dashed lines. **(B)** Side view. Wave ripples are indicated with a dashed line. **(C)** Top view. **(D)** Side view. Notice the concave shape (indicated with dashed lines) and the deformed downward tapering cracks. **(E)** Top view. A partly polygonal pattern can be seen. **(F)** Top view. Notice the straight to spindle-shaped cracks.

Støen (2016) suggests that the laminations could be stromatolitic structures. Such structures form in shallow to marginal marine environments by trapping and binding of sediments as well as chemical action of cyanobacteria (Hofmann, 1973). The laminated organic material and cavities seen in the thin-sections are typical for microbial formation (Boggs, 2009). Støen (2016) states that his findings support the observations by Tugarova and Fedyaevsky (2014). Their study suggests that micro-organisms and biochemical precipitation in connection to cyanobacterial mats are the mechanism for calcite cementation within siliciclastic intervals in the De Geerdalen Formation on Edgeøya.

If the undulating laminations seen in Fulmardalen in the rusty-red layer are stromatolitic structures, the depositional environment must have been shallow to marginal marine, or possibly lacustrine. Modern stromatolites are restricted to shallow subtidal, intertidal and supratidal zones as well as to lacustrine environments where cyanobacteria have sufficient sunlight to carry out photosynthesis (Boggs, 2011). Co-existing shell fragments within the same unit support the interpretation of a shallow marine environment. Wave ripples are observed in the unit too (Figure 4.7B), and may indicate that the undulating lamination is a result of wave activity rather than the formation of stromatolites. The fact that the proportion of mud is low in comparison to sand may imply an environment with relatively high energy level, with occasional calm periods where carbonate mud is deposited from suspension.

In general, all the aforementioned interpretations are consistent with a shallow marine and tidal setting, suggesting that such conditions may have prevailed during the deposition of the respective layer.

Facies H - Plane Parallel Laminated Sandstone

Plane parallel laminated sandstones (facies H) in Fulmardalen (Figure 4.8) share most of the same characteristics as described in Table 4.1. The facies often dominates in relatively thin sandstone units surrounded by mudstones, but also occurs together with facies J, F, E and I in thicker sandstone units. The main difference in how facies H appears in Fulmardalen

compared to elsewhere on Svalbard is related to the level of bioturbation and trace fossils observed. In Fulmardalen the intensity of bioturbation is relatively low, and very few trace fossils are observed, especially when compared to eastern Svalbard.

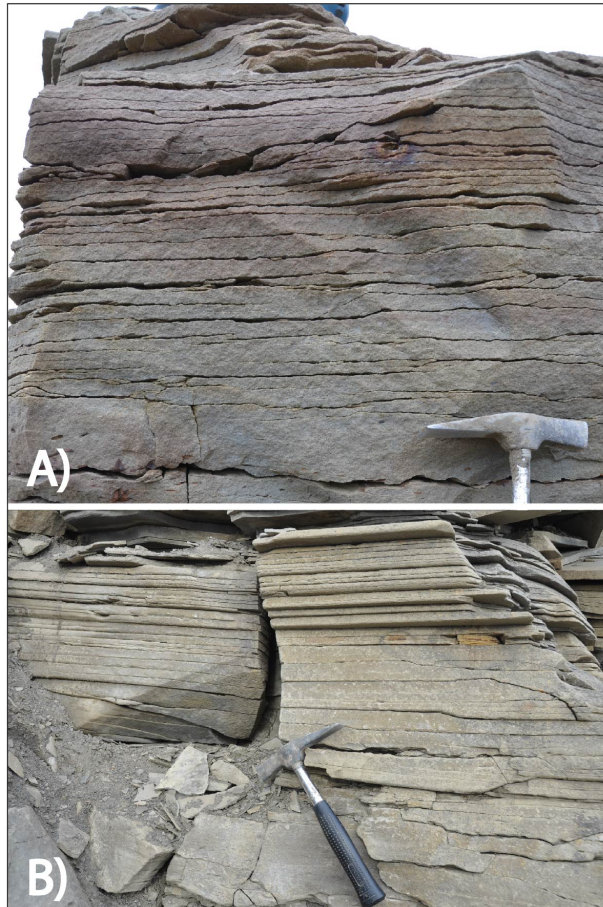


Figure 4.8: Planar parallel stratified sandstone (facies H) in Fulmardalen at (A) Ryssen and (B) Storfjellet.

Facies I - Low Angle Cross-Stratified Sandstone

Low angle cross-bedded sandstones (facies I) in Fulmardalen (Figure 4.9) are frequently observed. The description from Table 4.1 is also representative for Fulmardalen. However, some minor differences are found. Firstly, mud flakes are occasionally observed. Secondly, the units are thicker in Fulmardalen, up to 3 m. Finally, bioturbation is not observed together with low angle cross-stratified sandstone.

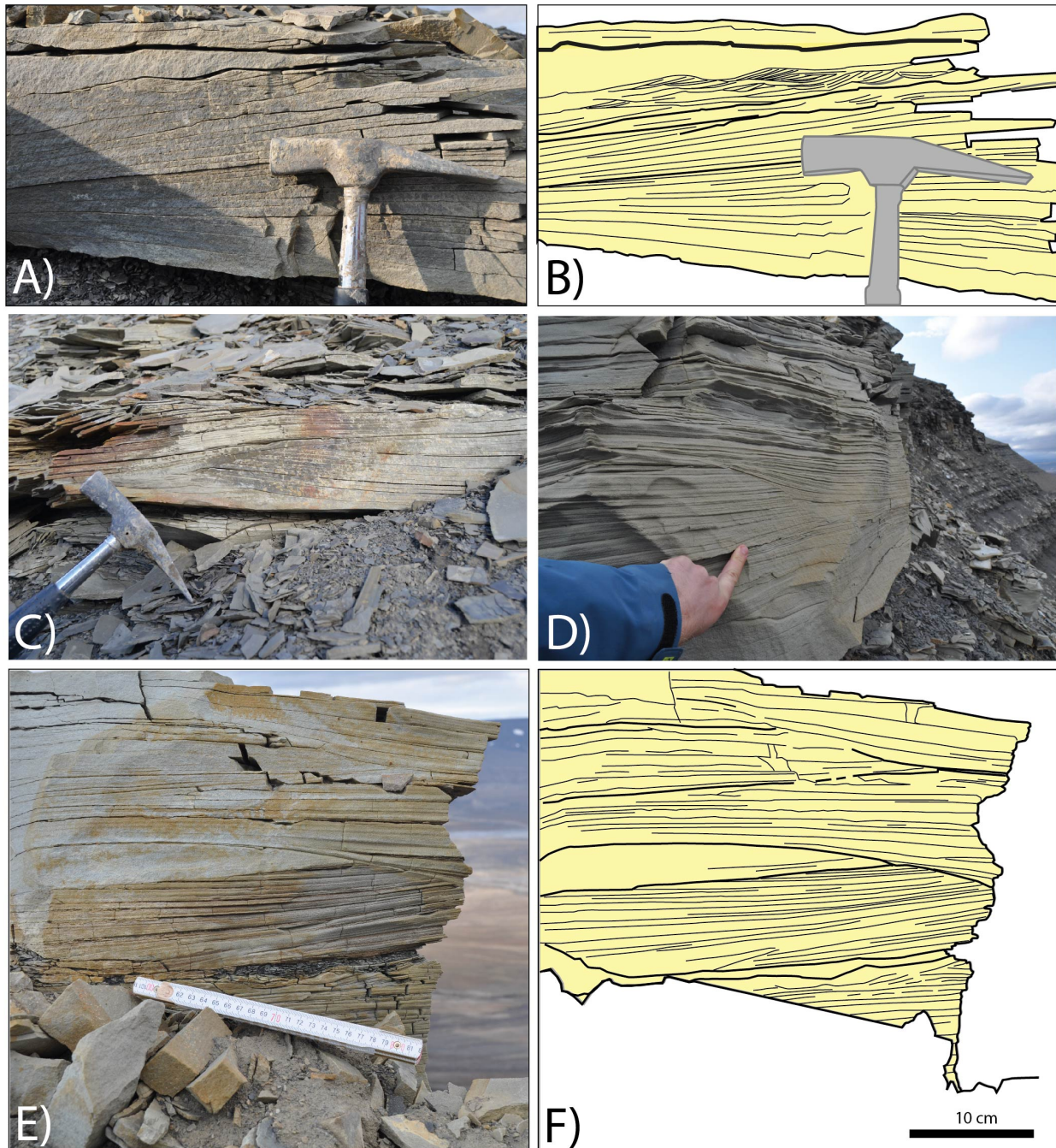


Figure 4.9: Low angle cross-stratified sandstone (facies I) in Fulmardalen. **(A)** Outcrop at Milne Edwardsfjellet. Notice ripples towards the top of the unit. **(B)** Sketch of the sandstone in A. **(C)** Outcrop at Storfjellet. **(D)** Outcrop at Milne Edwardsfjellet. **(E)** Outcrop at Milne Edwardsfjellet. **(F)** Sketch of the sandstone in E.

Facies J&K - Tabular & Trough Cross-Stratified Sandstone

In Fulmardalen, tabular and trough cross stratified sandstones (facies J and facies K) (Figure 4.10), share many of the characteristics with outcrops from elsewhere in Svalbard (Table 4.1). The two facies often occur within the same sandstone units, and most commonly tabular cross-stratified sandstones are found overlying trough cross-stratified sandstones. Minor sandstone units with facies J and K often display an erosive base and often have a laterally restricted geometry, tapering into scree. In units where tabular cross-stratification is overlying trough cross-stratified sandstones, the cross-stratification tends to get more tabular as the grain size gets finer upwards. In Fulmardalen facies J and K are also commonly observed in laterally extensive and upward coarsening sandstone units, especially in the lower part of the formation. These sandstones typically include facies E, I and H as well, and have gradual lower boundaries to a heterolithic succession (facies B). Herringbone structures are also observed at Storfjellet (Figure 4.10A). Such structures have not been frequently described from the De Geerdalen Formation, but Rød et al. (2014) describe herringbone structures from Edgeøya.

Facies L - Bioclastic Sandstone and Mudstone

In Fulmardalen bioclastic sandstones (facies L) (Figure 4.11) are only observed at Storfjellet and Ryssen in the middle to upper part of the logged sections. This is consistent with description from elsewhere on Svalbard (Table 4.1), where such beds are typically restricted to the lower part of Isfjorden Member (e.g., Mørk et al., 1999a; Haugen, 2016). Bioclastic beds are found encapsulated within mudstone and locally as accumulations in distinct layers within carbonate cemented sandstones (facies G).

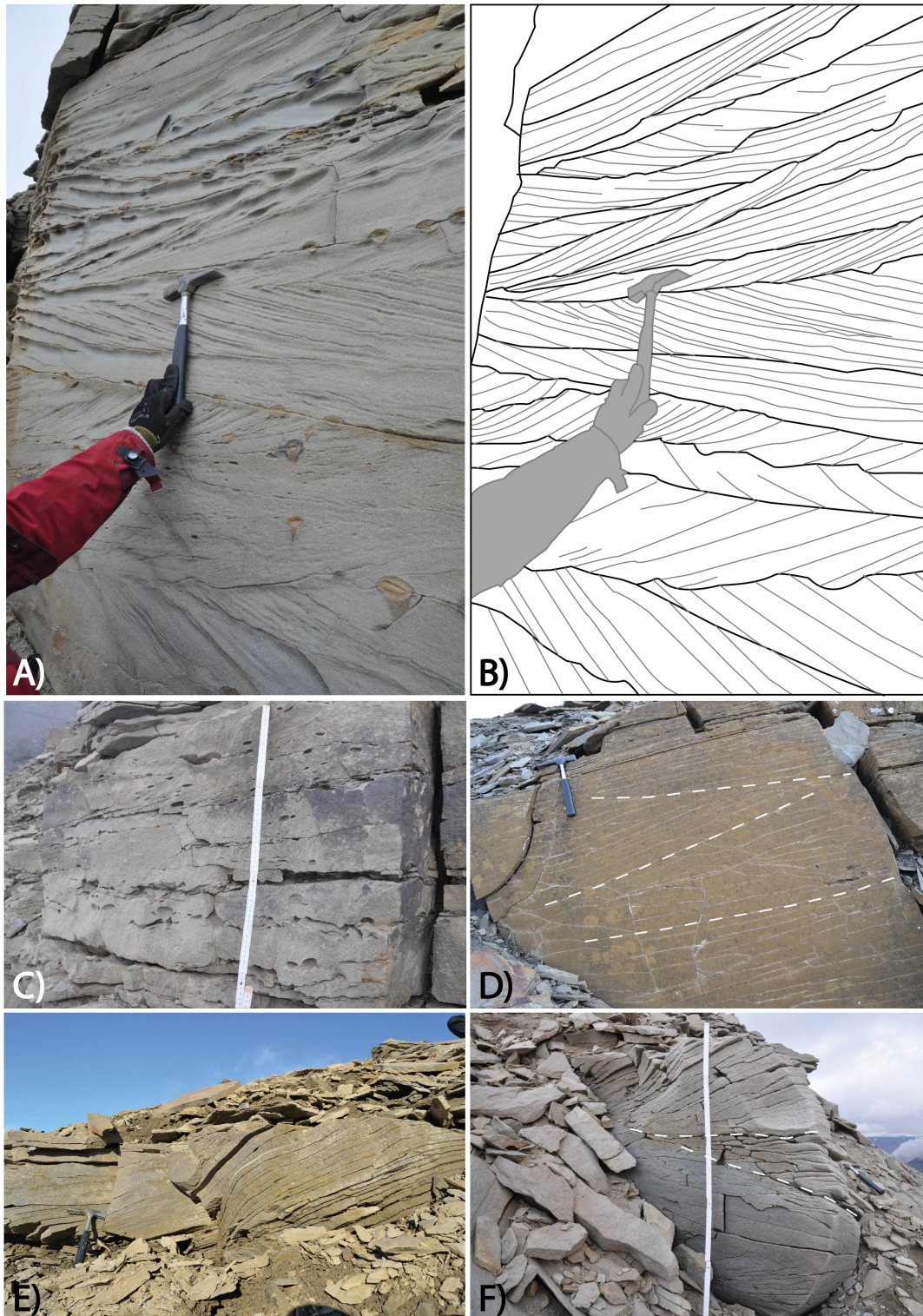


Figure 4.10: Tabular and trough cross-stratified sandstones (facies J and K) in Fulmardalen. **(A)** Bi-directional tabular to trough cross-stratified sandstone at Storfjellet. **(B)** Sketch of the sandstone in A. **(C)** Trough cross-stratified sandstone with mud clasts at Storfjellet. **(D)** Tabular cross-stratified sandstones at Wallenbergfjellet. Set boundaries are indicated by dotted lines. **(E)** Tabular cross-stratified sandstones at Wallenbergfjellet. **(F)** Trough cross-stratified sandstone at Milne Edwardsfjellet. Set boundaries are indicated by dashed lines.

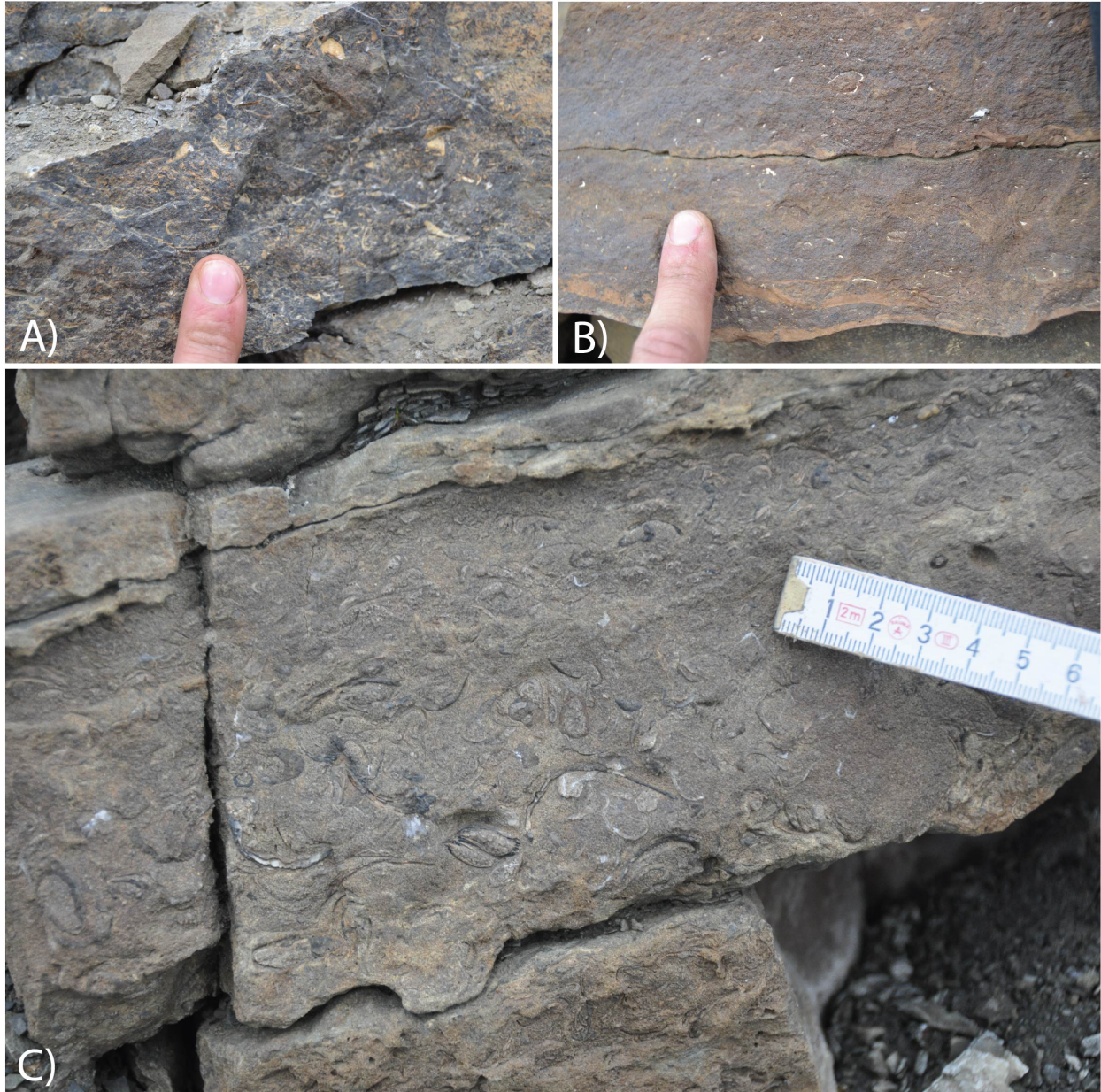


Figure 4.11: Bioclastic sandstones in Fulmardalen at (A) Ryssen, (B) Ryssen and (C) Storfjellet.

Facies M - Coal and Coal Shale

Coal shale is found only at one locality, in the upper part of Ryssen (Figure 4.12). It appears as a 5 cm thick layer and is associated with underlying paleosol and dark shale within the Isfjorden Member. The lateral continuity of the layer is uncertain due to scree cover.



Figure 4.12: Coal shale in Fulmardalen at Ryssen.

Facies N - Paleosols and Calcrete

Paleosols and calcrete (facies N) are frequently observed in the upper part of the De Geerdalen Formation, within the Isfjorden Member, in Fulmardalen ([Figure 4.13](#)).

Wood fragments are not found in this facies in Fulmardalen, which is in contrast to what has been described from other localities on Svalbard (e.g., on Wilhelmøya, [Lord et al., 2017](#)). Two different types of paleosols dominate this facies in the study area; non-calcareous red and green mudstones ([Figure 4.13A, B](#)) and carbonate soils (calcretes) ([Figure 4.13B, D](#)). The colour alternation in the mudstones is thought to be related to a change in the redox regime during formation, where red mudstone occurs in oxidising conditions and green and grey mudstone in reduced environments ([Haugen, 2016](#)). Calcrete in Fulmardalen appears as 0.5-1.5 m thick laterally extensive carbonate units, often interbedded in red and green mudstone. Calcrete

forms in semi-arid to arid climate, when CaCO_3 precipitates from oversaturated water within the soil (Wright and Tucker, 1991). Calcareous nodules (Figure 4.13C, D, E) are found within both of the soil types in Fulmardalen, and are thought to be a result of local precipitation of calcite around roots, caused by an oversaturation of calcite when water is drained from the soil.

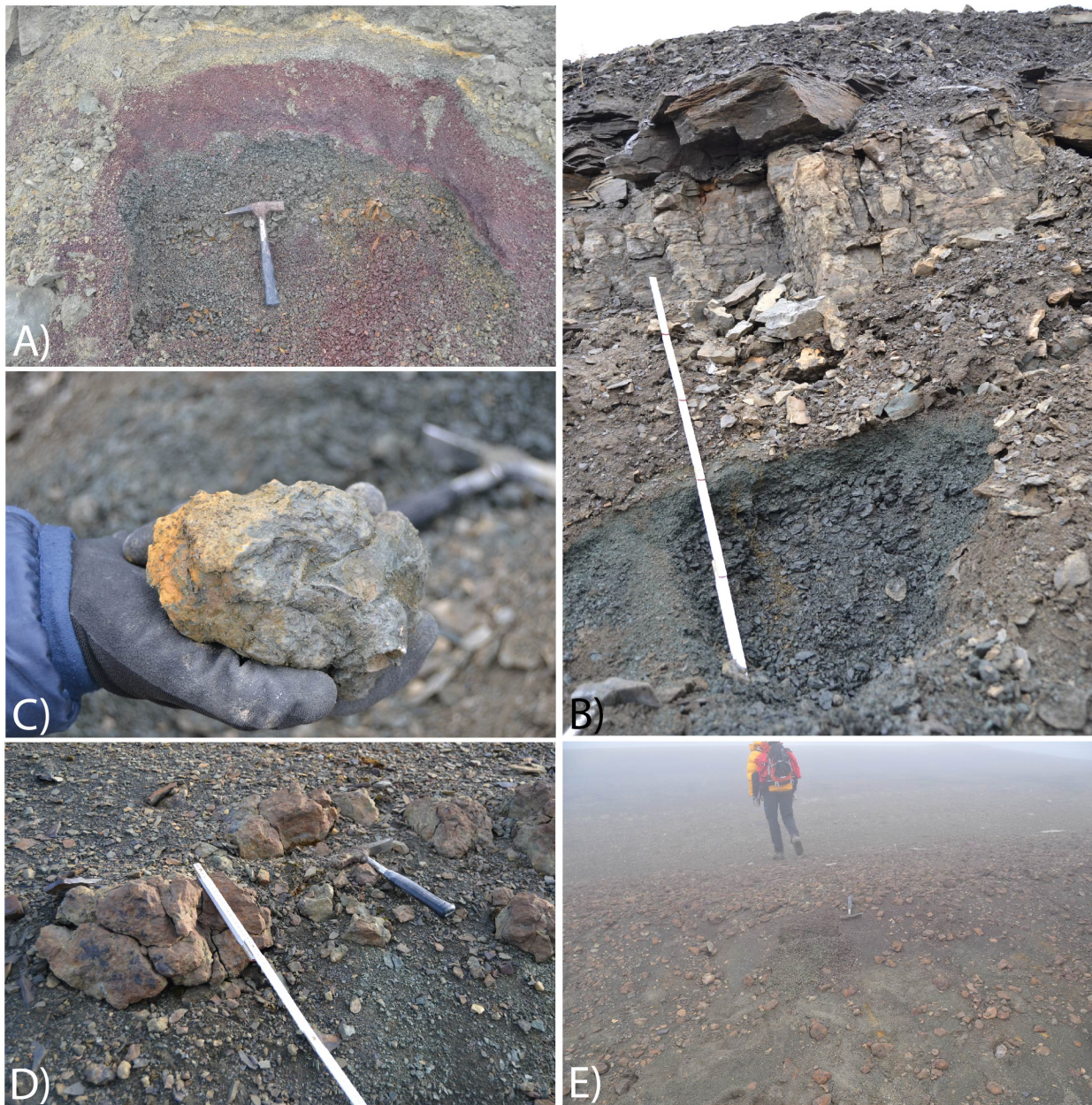


Figure 4.13: Paleosols and calcrete in Fulmardalen. (A) Red and green mudstones of the Isfjorden Member at Storffjellet. (B) Calcrete and underlying green mudstone at Dyrhø. (C) Irregular-shaped nodule found in green mudstones at Dyrhø. (D) Calcrete at Raggfjellet. Notice its irregular shape and mottled appearance. (E) Nodules that have weathered out from red mudstones at Storffjellet.

5. Logged sections from Fulmardalen

As mentioned in [Chapter 4](#), the sedimentological data from the Triassic exposures in Fulmardalen can create a link between previously collected data from central Spistbergen and eastern Svalbard. The new data may be regarded as the last missing piece of the “Triassic puzzle” in Svalbard.

The dataset from Fulmardalen consists of 6 sedimentological logs ([Figure 5.1](#)), ranging from 21 to 261 m in length. This chapter presents each mountain visited and the corresponding logged section. The logs have been sub-divided into intervals based on trends and similarities, with the purpose of making the description and interpretation of the logs easier to follow.

The logs are presented with a lithology- and grain-size column. The colours in the latter column try to illustrate the actual colour variations observed between different outcrops. A log-legend is presented in [Appendix B](#).

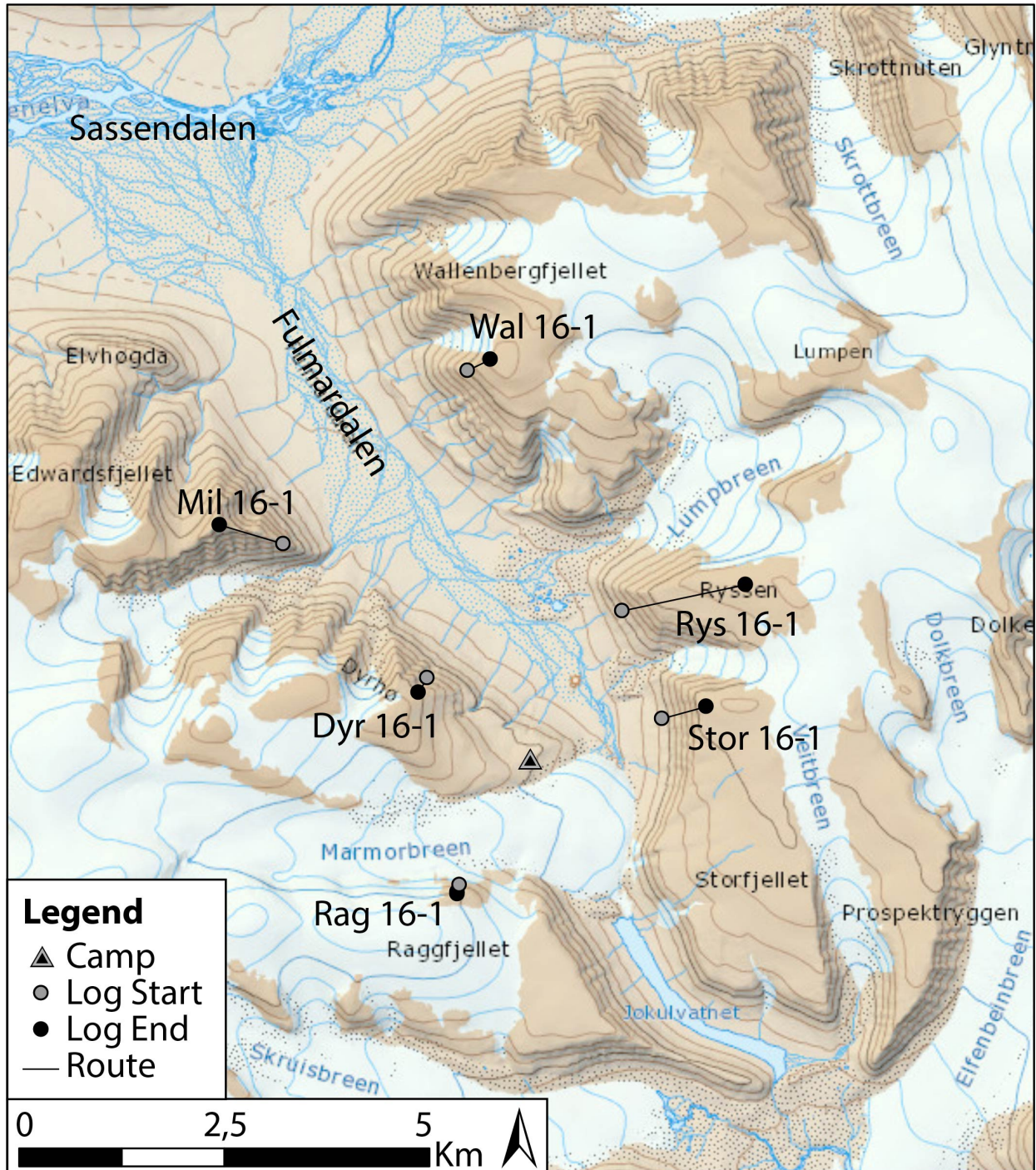


Figure 5.1: Overview map of Fulmardalen with the start and end positions of the logs indicated. Base map retrieved from Norwegian Polar Institute.

5.1 Wallenbergfjellet

Wallenbergfjellet (Figure 5.2) is a mountain on the corner between Sassendalen and Fulmardalen limited by Skrottbreen in NE, Lumpen in E and Lumpbreen in SE (Figure 5.1). The top is plateau shaped and the highest point reaches 674 masl. The south-western mountain side of Wallenbergfjellet ends in Fulmardalen and holds exposures of Vikinghøgda, Botneheia,

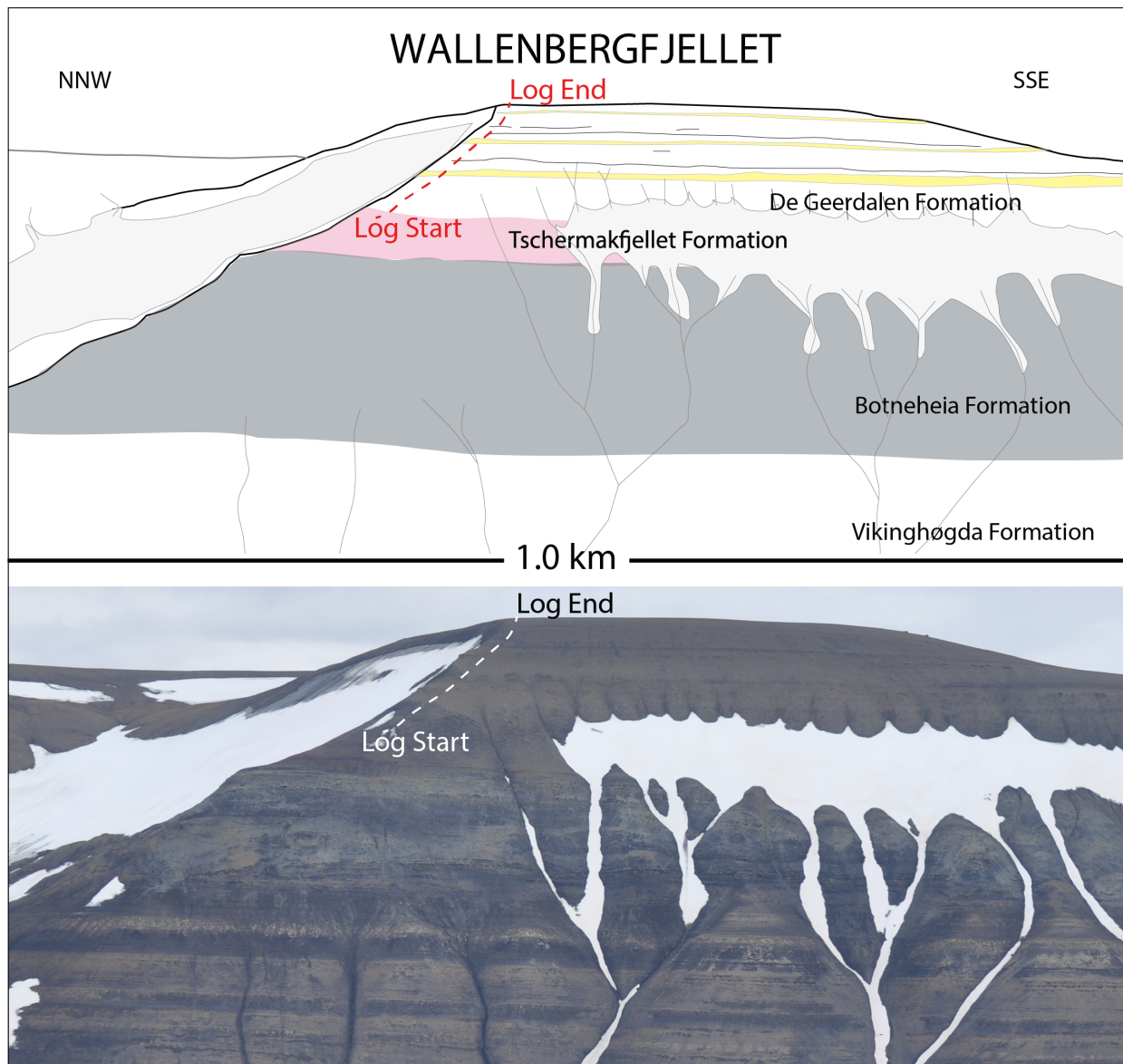


Figure 5.2: Geological sketch and corresponding overview photo of the logged section at Wallenbergfjellet. Formation names and stratigraphic boundaries have been indicated. Yellow areas within the De Geerdalen Formation mark major sandstone intervals. Log trace is indicated by a dashed line.

Tschermakfjellet and De Geerdalen formations. However, the exposures are not of the best kind. The De Geerdalen Formation, which is the target of this study, only comprises the upper part of the mountain and is relatively poorly exposed compared to most of the other mountains visited.

The logged section (Wal 16-1) (Figure 5.3) is 98 m long and is located along a ridge in the south-western slope of Wallenbergfjellet. It starts in the Tschermakfjellet Formation and continues upwards into the De Geerdalen Formation and ends on the plateau. The characteristic red and green mudstones of Isfjorden Member are not observed. Briefly described, the De Geerdalen Formation on Wallenbergfjellet consists of three major upwards coarsening units (Figure 5.4).

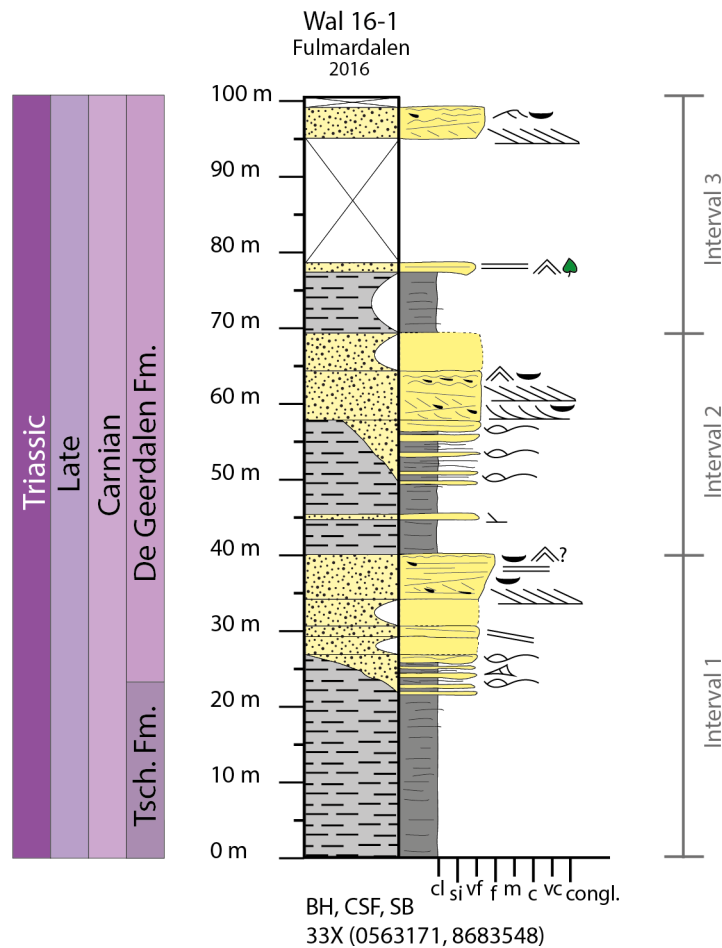


Figure 5.3: The log from the measured section at Wallenbergfjellet. Depositional age has been interpreted following Mørk et al. (1999a). Interval sub-division is indicated.

Log Wal 16-1

Interval 1 (0 – 40m)

Description: The interval can be seen as an upward coarsening sequence. The first 23 m consist of partly scree covered grey shale and siltstone beds (facies A). The next 4 m are heterolithic deposits (facies B) where decimetre thick very fine sandstones with hummocky cross-stratification (facies C) are interbedded in shales and siltstones. There is an upward coarsening partly scree covered 13 m thick very fine to fine sandstone dominated unit on top of the heterolithic package. Whether the lower boundary is sharp or gradual is difficult to say because of the scree. The lower part of the sandstone is heavily scree covered. Low angle cross-stratification is observed in the intact part further up. The upper part of the sandstone is cemented and shows a change from tabular cross-stratification (facies J) to plane parallel stratification (facies H) along with a decrease in bed thickness; from 5 cm to 1 cm. Mud flakes are found at the base of a bed. The uppermost part of the sandstone has signs of wave ripples (facies E) and is heavily fractured. The sandstone unit is laterally extensive and can be traced several hundred metres.

Interpretation: The interval is interpreted to represent a transition from a prodelta to a delta front environment. The basal 23 m of the section measured at Wallenbergfjellet is interpreted to belong to the marine pro-delta deposits of the Tschermakfjellet Formation (Mørk et al., 1982, 1999a). The hummocky cross-stratified sandstones in the overlying heterolithic package are interpreted to be storm generated beds in the offshore transition zone to lower shoreface (Reading and Collinson, 1996) and are thought to reflect the base of the De Geerdalen Formation (Mørk et al., 1999a). The sandstone at the top is thought to reflect delta front to upper shoreface sands, more specifically a barrier bar or shallow subaqueous bank deposit. A relatively thin and laterally continuous geometry is typical for such deposits (Rød et al., 2014; Lord et al., 2017a).

Interval 2 (40 – 68.5m)

Description: The following interval is an upward coarsening sequence as well. The lowermost 9 m consist of partly scree covered grey shales and siltstones (facies A) enclosing a 20 cm thick siderite cemented very fine sandstone layer. Above is 9 m of a heterolithic unit (facies B). The sandstones within the heterolithic unit are very fine with sharp bases and hummocky cross-stratification (facies C). They increase both in thickness and frequency upwards. The heterolithic unit has an upper sharp boundary to a cemented, brown, very fine sandstone dominated unit of 6 m thickness. The lower part of the sandstone unit has large scale cross bedding with mud flakes along set boundaries. The geometry of the cross beds changes from troughs (facies K) to tabular (facies J) upwards along with a decreasing bed thickness in the range of 7 to 1 cm. The upper part of the sandstone is wave rippled (facies E) and mud flakes are observed. The uppermost 4.5 m of the interval consists of sandstone scree. The sandstone unit can be laterally traced for several hundred metres.

Interpretation: The boundary to the underlying interval is interpreted to represent a relative sea level rise and a change back to an environment in the offshore transition zone to lower shoreface. Here clay is deposited from suspension during relatively calm periods, and silt and sand during periods with higher energy such as storms (Johnson and Baldwin, 1996; Bhattacharya et al., 2004). The sandstone above the heterolithic unit is believed to be delta front to shoreface sands. Its lower boundary may appear sharper than it actually is due to the contrast between its hard, cemented appearance and the easily weathered heterolithic unit below. Based on the upward coarsening nature and geometry of the sandstone unit, in addition to the sedimentological structures observed, it is likely that this is a barrier bar or subaqueous bank, similar to the sandstone in the underlying interval.

Interval 3 (68.5 – 98m)

Description: Overlying the sandstone scree there are 8.5 m of partly scree covered shales and siltstones (facies A). A very fine sandstone of 25 cm is found above the scree. It is planar stratified (facies H) and plant fragments are observed. The following 18 m are totally scree covered. A very fine sandstone of 3 m is found above the scree. It is tabular cross bedded (facies J) with mud flakes in the lower part and asymmetrical ripple laminated (facies F) in the upper part.

Interpretation: The partly covered shale is interpreted to represent deposits in the offshore transition zone to lower shoreface. The sandstones are interpreted as shoreface to delta front deposits. Tabular cross-stratification typically forms by unidirectional currents of the lower flow regime in shallow waters (Collinson et al., 2006; Boggs, 2011).

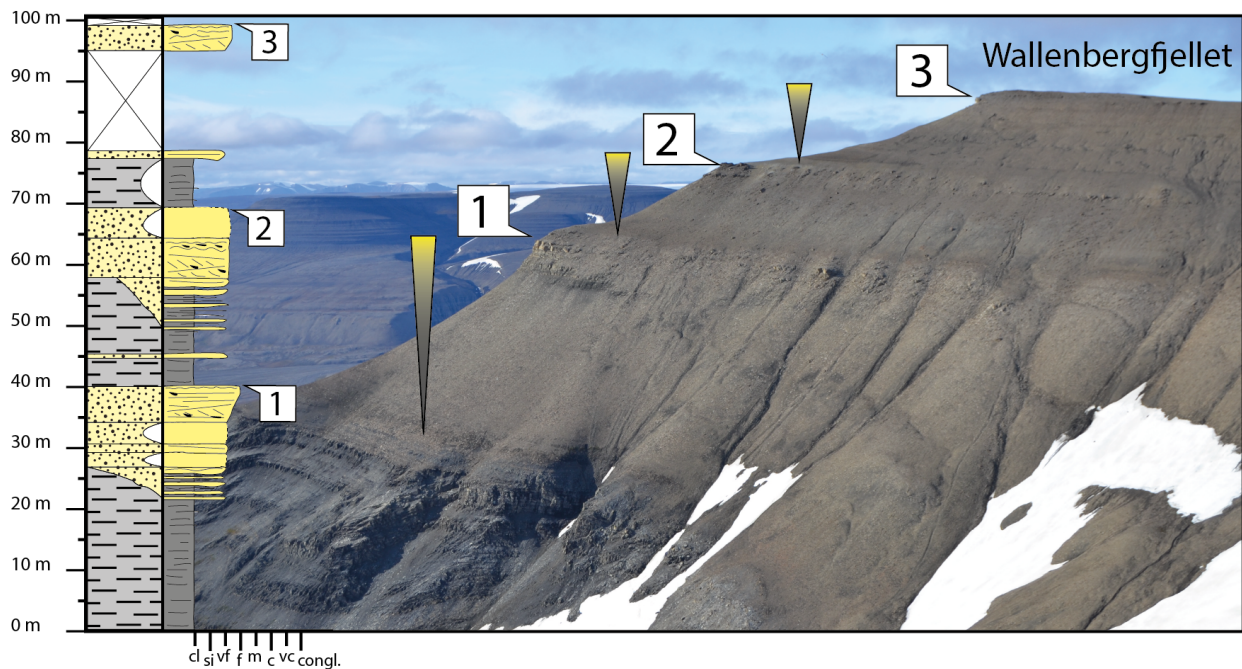


Figure 5.4: Log and picture correlation from Wallenbergfjellet. The figure shows three major coarsening upwards sequences, typical for the lower and middle part of the De Geerdalen Formation. The top of each sequence is indicated.

5.2 Dyrhø

Dyrhø (Figure 5.5) is a mountain in the south-western side of Fulmardalen (Figure 5.1). The summit of the mountain is situated at 680 masl, where the top extends out from a glacier to the west of the measured profile. The slopes facing Fulmardalen hold exposures of the Botneheia

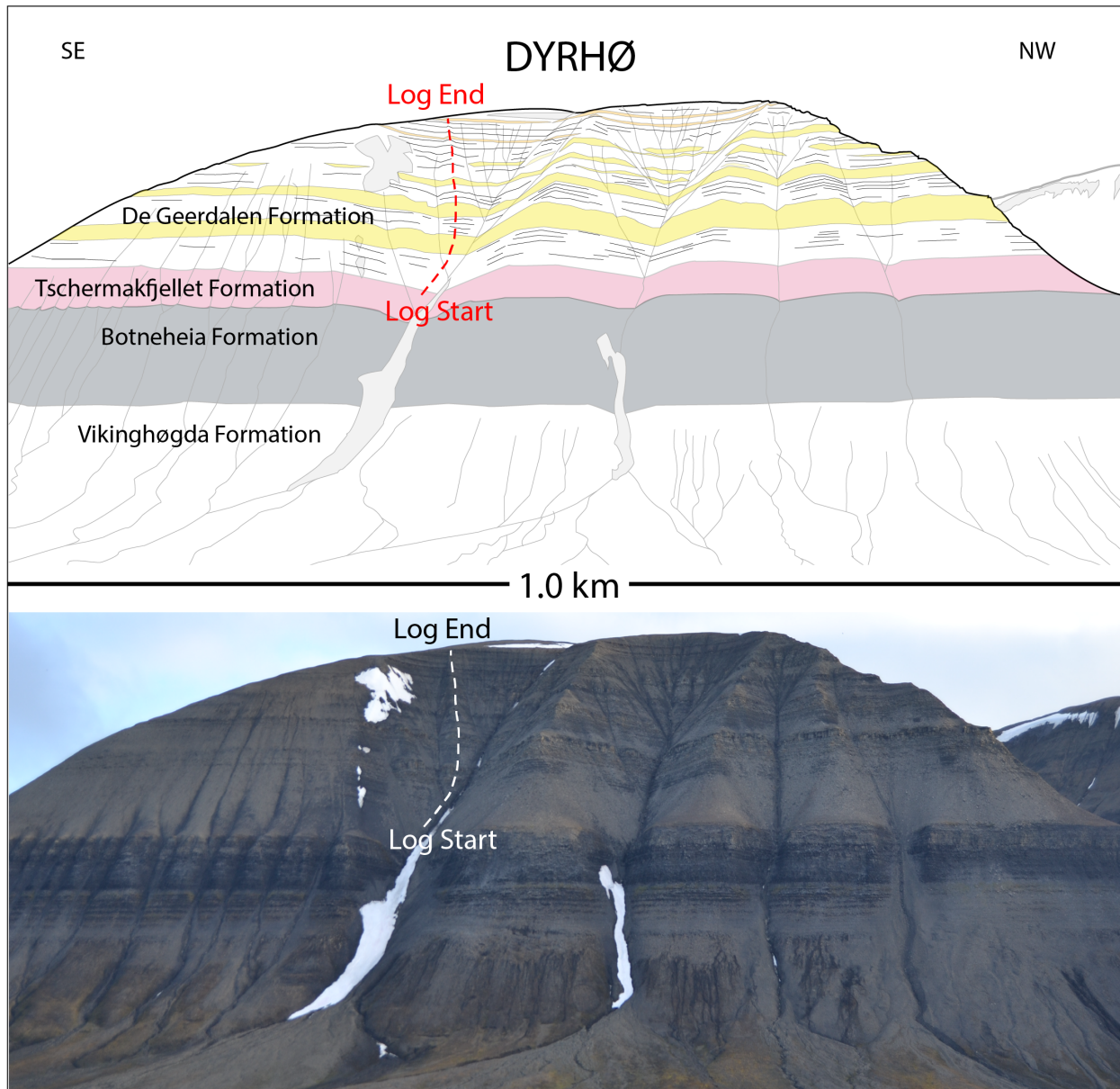


Figure 5.5: Geological sketch and corresponding overview photo of the logged section at Dyrhø. Formation names and stratigraphic boundaries have been indicated. Yellow areas within the De Geerdalen Formation mark major sandstone intervals. The Log trace is indicated by a dashed line.

Formation, the Tschermakfjellet Formation and the De Geerdalen Formation.

The section measured at Dyrhø (Dyr 16-1) (Figure 5.6) is 190 m long, and starts in the upper part of the Tschermakfjellet Formation close to the base of the De Geerdalen Formation. Characteristic features of the Isfjorden Member (e.g., Pchelina, 1983; Mørk et al., 1999a; Haugen, 2016) were found in the upper reaches of the measured slope, indicating that the log terminates somewhere in the upper parts of the De Geerdalen Formation.

The De Geerdalen Formation at Dyrhø consists of one major coarsening upwards sequence in the lower part, followed by an interval of several minor coarsening upwards sequences. The upper part of the formation is dominated by shale, interbedded with relatively thin and often carbonate cemented sandstone benches.

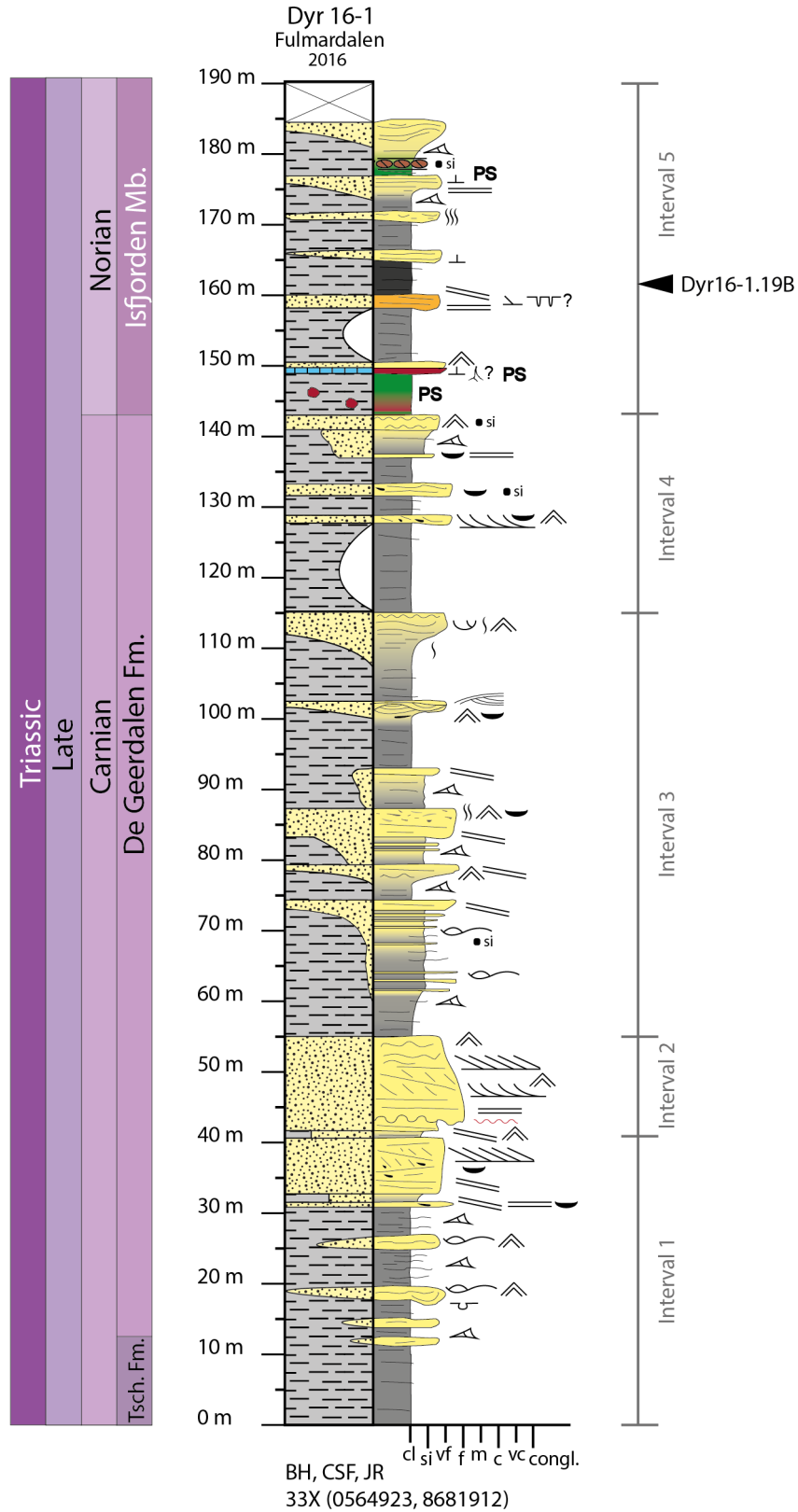


Figure 5.6: The log from the measured section at Dyrhø. Depositional age has been interpreted following [Mørk et al. \(1999a\)](#). Interval sub-division and the position of sample Dyr16-1.19B are indicated.

Log Dyr 16-1

Interval 1 (0 – 41m)

Description: The first 41 m of log Dyr 16-1 represents an upwards coarsening sequence. The lowermost 10 m consists of mudstone. The following 21 m of the interval consist of mainly heterolithic bedding (facies B) and mudstones (facies A). Minor sandstones with thicknesses ranging from 0.5-2.5 m occur within this section. The sandstones are very fine in grain size, and display hummocky cross-stratification (facies C) topped by wave ripples (facies E) and plane parallel lamination (facies H). Erosive surfaces and evidence of soft sediment deformation (facies D) are also observed. The sandstone bodies are laterally restricted, ranging from 2-20 m in width. The interval is gradually coarsening upwards into a sandstone dominated unit. The sandstone unit is very fine to fine grained with low angle cross-stratification (facies I) and large scale tabular cross-stratification (facies J). Mud flakes and thin layers of shale are present. It is laterally extensive and can be followed for several hundred metres.

Interpretation: The lower mud-dominated sequence in the basal part is interpreted as prodelta deposits, assigned to the Tschermakfjellet Formation. The base of the De Geerdalen Formation is interpreted to be the first prominent sandstone bench at the base of the heterolithic unit (Mørk et al., 1999a). The sedimentary structures within the sandstones indicate rapid deposition, potentially as storm deposits or gravity flows within a muddy environment in a prodelta setting (Reading and Collinson, 1996). The upwards coarsening, laterally extensive, low angle and tabular cross bedded sandstone unit in the upper part of the interval is interpreted as a barrier bar and correlates to the lowermost sand dominated units at the other mountains in Fulmardalen. The mud flakes herein are probably formed by tidal or wave action. Parts of semi-consolidated mud may have been ripped up by high energy currents (Dalrymple and Choi, 2007; Rød et al., 2014). The presence of thin layers of shale within the sandstone unit may indicate variations in flow velocities during deposition, potentially implying influence

from tidal activity (Dalrymple and Choi, 2007).

Interval 2 (41 – 55m)

Description: A short heterolithic unit followed by an 11 m thick, erosive based and upwards fining sandstone (Figure 5.8C) overlies the sandstone from the previous interval. The erosive surface is covered with mud flakes. The grain size changes upwards from medium to fine sand. The sandstone displays plane parallel stratification (facies H), wave ripples (facies E) and large scale trough cross-stratification (facies K). The cross-stratification gets more tabular (facies J) upwards as the grain size decreases. The sandstone is topped by wave ripples (facies E).

Interpretation: The sandstone is interpreted as a tidal inlet cutting through a barrier bar. This is supported by the upwards fining trend, the erosional base with mud flakes and the relatively coarse grain size, in addition to large scale cross-stratification. Similar tidal inlet deposits have been described from the Upper Cretaceous St. Mary River Formation in southern Alberta by Young and Reinson (1975) (Figure 5.7).

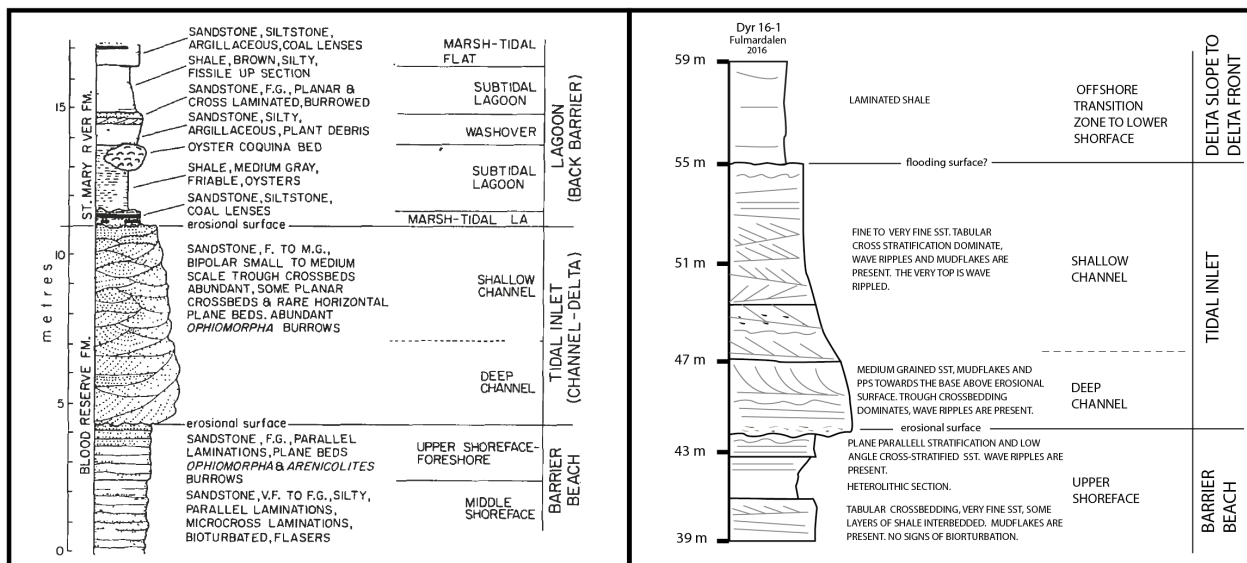


Figure 5.7: Comparison of a log through a barrier complex from the Upper Cretaceous Blood Reserve – St Mary River Formation in Southern Alberta (Young and Reinson, 1975), and a similar complex from the Upper Triassic De Geerdalen Formation at Dyrhø. The main difference between the two logs is the interpreted depositional environment of the fine grained facies towards the top.

Interval 3 (55 – 115m)

Description: The following 60 m in Dyr 16-1 are represented by series of small coarsening upwards units. Ranging from 5-19 m in length, the sequences are typically composed of shales (facies A) in the lower part, followed by a heterolithic sequence (facies B) containing thin sandstones with hummocky cross-stratification and some siderite concretions. The sandstones capping each sequence are very fine to fine in grain size, with a typical thickness between 0.5-4 m. Structures such as low angle cross-stratification (facies I) and wave ripples (facies E) are common. Mud flakes occur in several of the sandstones, and some of the units also show signs of sparse to moderate bioturbation. Large scale hummocky cross-stratification and mud-drapes are also present. The uppermost sandstone shows mud drapes in addition to wave ripples and sparse bioturbation (Figure 5.8B). The geometry of the sandstone bodies varies, with some of them being laterally extensive, stretching across the whole mountain side. Other units have a more laterally restricted appearance.

Interpretation: The contact to the underlying sandstone interval marks a change to deposition of mudstones. The contact is interpreted to represent a relative sea level rise and a change to an offshore transition zone to lower shoreface environment. Hummocky cross-stratification indicates deposition of sand in the offshore transition zone to lower shoreface setting. Wave rippled and low angle cross-stratified sandstones are interpreted as barrier bars in the delta front setting. Mud drapes and bioturbation may indicate a tidal component (Boggs, 2011) in the uppermost sandstone unit.

Interval 4 (115 – 143m)

Description: This interval has a lower part dominated by mudstone (facies A). The upper part has three relatively thin sandstone units (< 2m), in which structures like large scale trough cross-stratification (facies K), planar lamination (facies H) and wave ripples (facies E) occur, as well as features like siderite concretions and mud flakes.

Interpretation: A dominance of mud in interval 4 suggests deposition in a low energy regime. Fine grained deposits may occur in interdistributary areas which may contain tidal flats, bays, lagoons and floodplains (Rød et al., 2014). Another possibility is that the mudstones represent deposition in a lower shoreface to offshore environment. However, thin sandstones containing sedimentary structures such as trough cross-stratification and mud flakes abruptly interbedded are found within the mudstone interval. This may imply that the interval represents deposition in an interdistributary area, like a lagoon or bay with thin sandstones deposited as wash-over fans from storm episodes. Small to medium scale cross beds and low angle to planar stratification characterize the sedimentary structures in such deposits (Reinson, 1984). The sandstones could also reflect small channels on a mud dominated tidal flat (Reineck and Singh, 1980).

Interval 5 (143 - 190m)

Description: The uppermost 47 m of the measured section at Dyrhø are shale dominated (facies A), with relatively thin and carbonate cemented sandstones (facies G). The interval starts with green mudstone with nodules (facies N). Above there is a sequence of deposits that can be fully or partly recognized at Milne Edwardsfjellet, Ryssen and Storfjellet. At Dyrhø the sequence (Figure 5.8A) starts with a distinct 1 m thick carbonate rich unit with a red weathering colour containing potential root structures or vertical trace fossils. It forms a laterally extensive bench in the mountain side and is topped by a wave laminated (facies E) sandstone. The sequence continues with 10 m of grey shale followed by a 2 m thick rusty-red carbonate cemented sandstone with an overlying very dark shale. The rusty-red layer sticks out in the terrain and is laterally extensive. It shows signs of low angle and planar parallel cross-laminations, but these structures are poorly preserved due to heavy cementation. Additionally, it has lighter coloured mud laminations with possible desiccation cracks. The top of a dark shale mark the end of sequence that has also been recognized at other mountains in Fulmardalen. The uppermost 13 m of the interval consist of green mudstone (facies N) capped

by a very fine sandstone with overlying scree. A laterally continuous 20-40 cm thick layer of siderite concretions is found within the green mudstone. The concretions are 10-20 cm in diameter. A similar concretion-layer has been identified at Storfjellet.

Interpretation: The interval is interpreted to represent the Isfjorden Member, deposited in a restricted marine to lagoonal environment. Bioturbation, low angle cross-stratification and

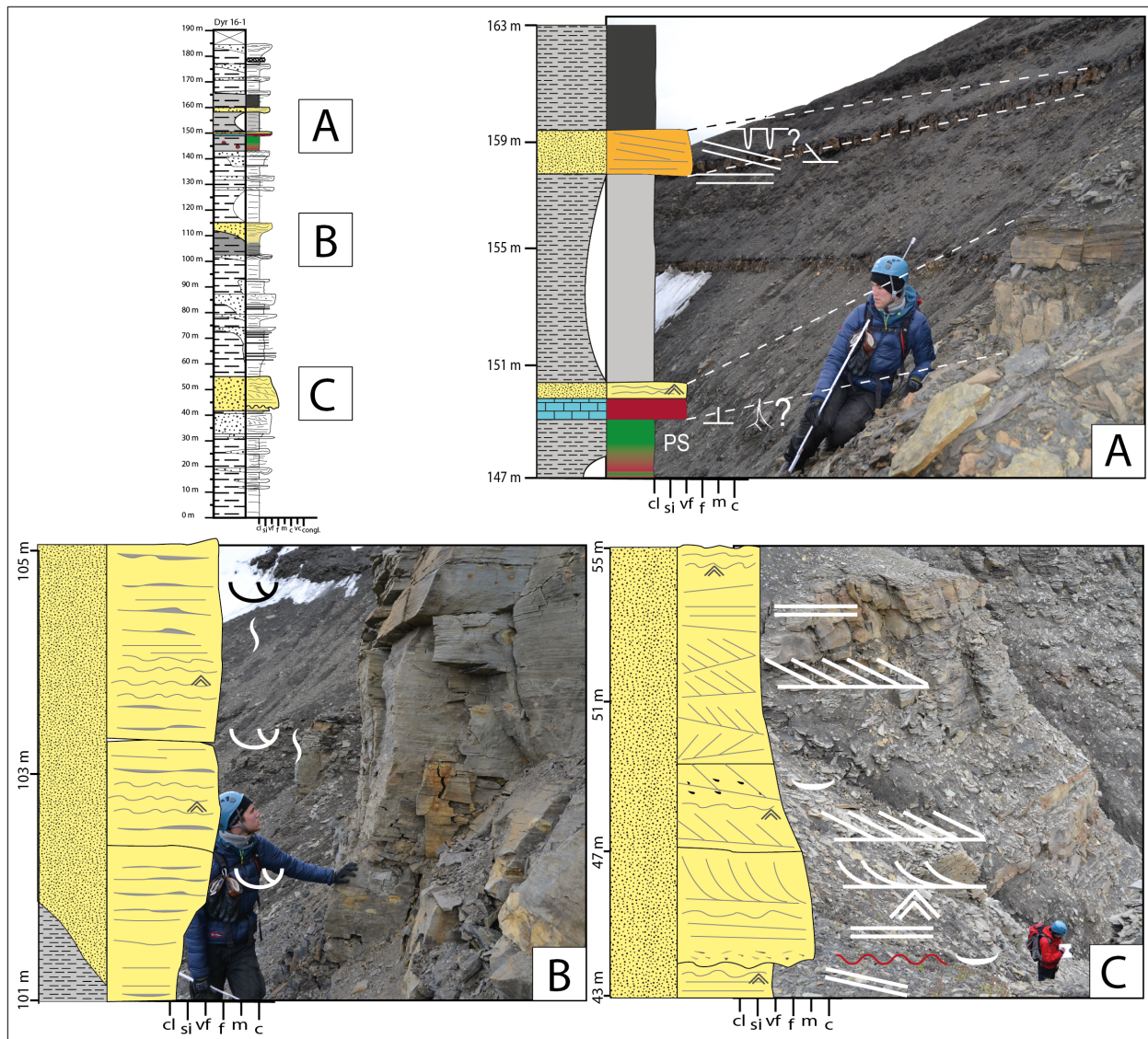


Figure 5.8: Log and picture correlation from Dyrhø. (A) A shale-dominated sequence with thin carbonate cemented sandstones, a calcrete profile, and red and green mudrocks. The deposits are typical for the Isfjorden Member. (B) Sandstone interval deposited with a tidal influence. (C) A thick sandstone interval in the lower part of the De Geerdalen Formation, interpreted as a barrier bar complex with an inlet cutting through.

carbonate cementation reflect upon a shallow marine origin. Green shales with nodules and overlying carbonate-rich deposits are interpreted as paleosols and calcrete, respectively. Such deposits are typically found in ancient delta plain environments (Enga, 2015; Haugen, 2016).

5.3 Ryssen

Ryssen (Figure 5.9) is located on the south-eastern side of Fulmardalen, with Storfjellet to the south and Wallenbergfjellet to the northwest (Figure 5.1). The mountain has a plateau-shaped top with a glacier towards the east. The highest point on the mountain is 605 masl. The slopes facing Fulmardalen holds good exposures of the upper parts of the Botneheia Formation, Tschermakfjellet Formation and probably an almost complete section of the De Geerdalen Formation.

The section measured from Ryssen (Rys 16-1) (Figure 5.10) is 261 m long and was recorded from a ridge in the middle of the slope facing Fulmardalen. Tschermakfjellet Formation constitutes the lowermost 34 m of the log, while the rest is considered belonging to the De Geerdalen Formation. Red and green mudstones characteristic for the Isfjorden Member (Pchelina, 1983; Mørk et al., 1999a; Haugen, 2016) were found close to the summit of the mountain. This means that the Wilhelmøya Subgroup is absent at Ryssen.

Broadly speaking, the lower part of the De Geerdalen Formation at Ryssen consists of two major coarsening upwards sequences from shale to fine and medium sandstone. The upper part is more complex with several smaller sequences, thinner sandstone bodies, coquina beds and orange carbonate-cemented sandstones. Most of the sandstone bodies tend to be laterally continuous and some of them can be traced to sections on the neighbouring mountains. Magmatic intrusions have affected the Triassic succession at several levels on the north-eastern side of Fulmardalen, and a dolerite sill has also intruded the middle section of the De Geerdalen Formation at Ryssen.

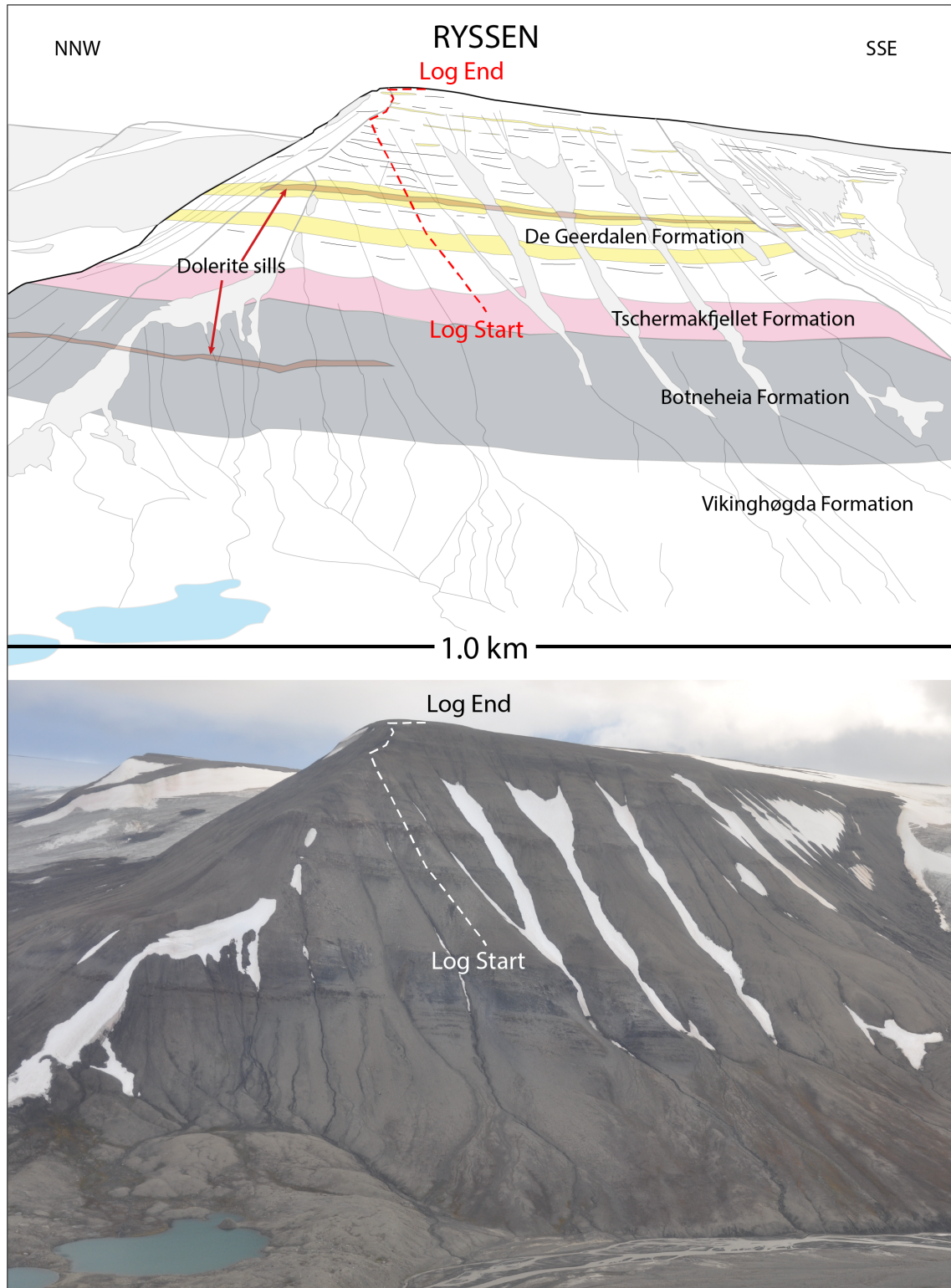


Figure 5.9: Geological sketch and corresponding overview photo of the logged section at Ryssen. Formation names and stratigraphic boundaries have been indicated. Yellow areas within the De Geerdalen Formation mark major sandstone intervals. Log trace is indicated by a dashed line. Dolerite sills of the Diabasodden Suite appears at two stratigraphic levels.

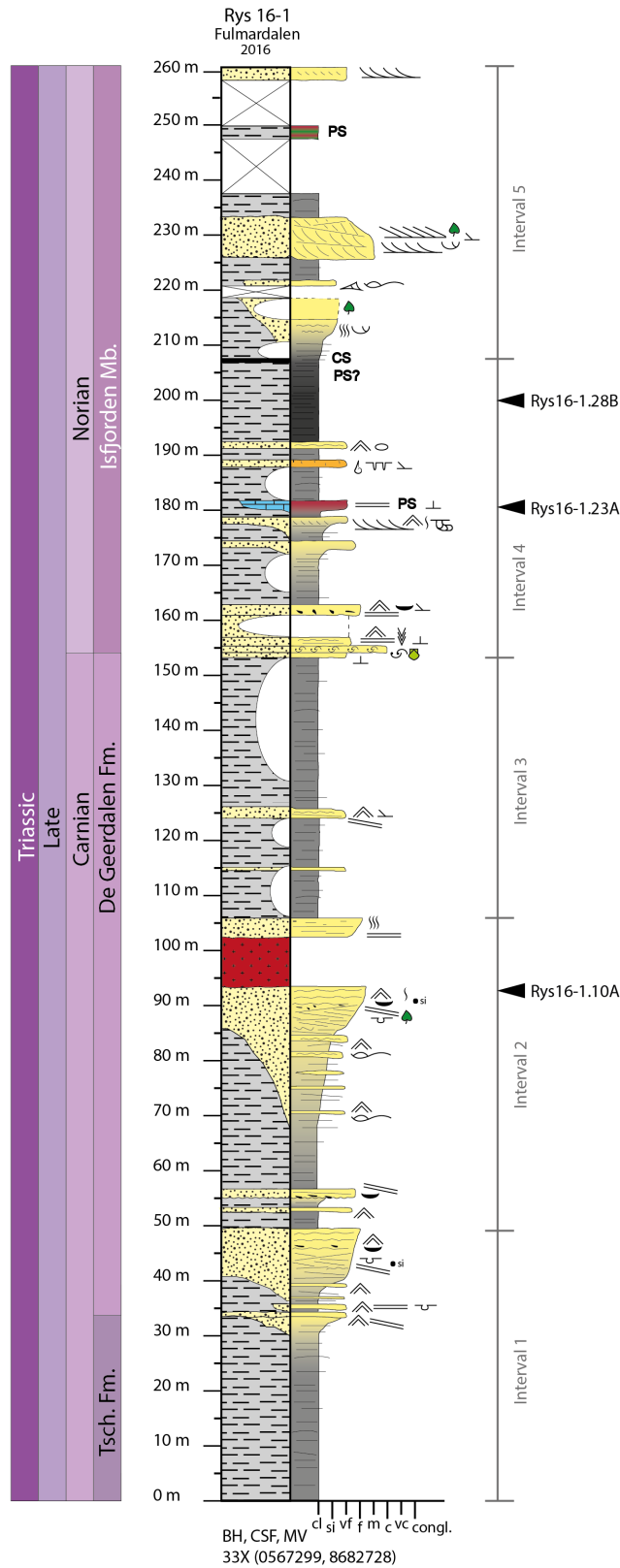


Figure 5.10: The log from the measured section at Ryssen. Depositional age has been interpreted following [Mørk et al. \(1999a\)](#). Interval sub-division and the position of samples (Rys16-1.10A, 23A, 28B) are indicated.

Log Rys 16-1

Interval 1 (0 – 50m)

Description: The interval is an upwards coarsening sequence. The lower part consists of grey shales and siltstones (facies A), which gradually coarsen upwards into a heterolithic bedding (facies B). Sandstones within the heterolithic bedding are up to a metre thick, with planar parallel stratification (facies H), mud flakes and loading structures (facies D). The heterolithic sequence coarsens upward into an 8.5 m thick very fine to fine sandstone. This is the most sand-rich interval at Ryssen, similar to that which was observed at approximately the same stratigraphic levels in the successions at Storfjellet, Milne Edwardsfjellet, Dyrhø and Wallenbergfjellet. The lower part of the sandstone is dominated by low angle cross-lamination (facies I) and wave ripples (facies E). Soft sediment deformation structures (facies D) are found within the sandstone unit in addition to mud flakes and a siderite concretion. The very top of the sandstone is wave rippled (facies E).

Interpretation: The lower grey shales and siltstones are interpreted as the prodeltaic deposits of the Tschermakfjellet Formation (Mørk et al., 1999a). Sharply based and relatively thin (<15 cm) siltstone layers are interpreted as storm deposits (Bhattacharya et al., 2004). The transition to the De Geerdalen Formation is found at the first prominent sandstone bench (Mørk et al., 1999a) at the base of a heterolithic section. This transition marks a development to a more proximal and shallow depositional environment, probably in an offshore transition zone to shoreface setting. The sand dominated unit above is interpreted as a barrier bar complex.. Soft sediment deformational structures within the sandstone could indicate rapid loading of sediment (Reineck and Singh, 1980; Bhattacharya and MacEachern, 2009). Wave ripples support a shallow marine environment.

Interval 2 (50 – 107m)

Description: The sandstone unit from the underlying interval is capped by 18 m of mudstone (facies A) which mark the onset of a new coarsening upwards sequence. Two 1 m thick sandstone beds with wave ripples (facies E), low angle cross-stratification (facies I) and mud flakes are found within the mudstone unit. The interval gets progressively sandier upwards, turning into a heterolithic section (facies B) with thin layers (< 30 cm) of very fine sandstones. These sandstones are characterized by hummocky cross-stratification (facies C) in the lower part and wave ripples (facies E) in the upper part. The heterolithic section is overlain by an upwards coarsening 9 m thick low angle cross-stratified sandstone (facies I), also with deformation structures (facies D), plant fragments, sparse bioturbation, siderite nodules and wave ripples (facies E) at the top. The following 9 m consists of a dolerite intrusion. Above the intrusion there is a 3 m thick fine sandstone unit with plane parallel stratification (facies H) at the base, a massive and structureless middle part and an intensely bioturbated upper part.

Interpretation: The transition from the underlying barrier bar complex is interpreted as a flooding surface. A similar stratigraphic surface can be observed in the logs from the other mountains in Fulmardalen. Such changes in depositional environment may be related to autogenic delta processes (Martinius et al., 2014). The interval is interpreted to reflect a transition from the offshore transition zone to a shoreface to delta front setting. The sand dominated unit in the upper part has the same characteristics as the deposits interpreted as a barrier bar from the underlying interval. The sandstone is laterally extensive and can be partly recognized in the other logs from Fulmardalen. The dolerite intrusion is interpreted to belong to the Diabasodden Suite of Late Jurassic to Early Cretaceous age (Mørk et al., 1999a).

Interval 3 (107 – 153m)

Description: Interval 3 is dominated by partly covered mudstones (facies A). The mudstones are interrupted by two thin sandstone beds, ranging from approximately 0.4-2 m in thickness.

One of the sandstones is low angle cross-stratified (facies I), wave rippled (facies E) and siderite cemented. The similar stratigraphic level at the other mountains seems to contain more sandstones than at Ryssen, especially at Storfjellet.

Interpretation: The interval is interpreted to reflect a low-energy environment. The low amount of sandstones at Ryssen in this interval compared to the other mountains at the same stratigraphic level may indicate that the deposits at Ryssen reflect a local restricted marine environment, such as a small lagoon or interdistributary bay. Bioturbation is often intense in lagoons protected by barriers (Reineck and Singh, 1980), which could explain the bioturbation in the upper part of the sandstone in the underlying interval. Thin low angle cross-stratified and wave rippled sandstone units in the lower part of the interval may represent wash-over deposits from storms. Modern studies of wash-over deposits indicate subhorizontal to planar stratification as one of the dominant sedimentary structures (Reinson, 1984).

Interval 4 (153 – 209m)

Description: The interval starts with a laterally extensive and carbonate cemented sandstone (facies G) with wave ripples, planar lamination and cone-in-cone structures. A 20 cm thick coquina bed (facies L) with fragmented shells is interbedded in the sandstone. The upper part of the sandstone is less carbonate cemented, and siderite cemented mud flakes are found at the base of a bed within the sandstone. The rest of the interval is mud dominated with a few interbedded and relatively thin sandstones. One of these sandstones has trough cross stratification (facies K), wave ripples (facies E) and the marine trace fossil *Rhizocorallium*.

A depositional sequence that can be fully or partly recognized at Milne Edwardsfjellet, Dyrhø and Storfjellet comprises the upper part of the interval. At Ryssen this sequence starts with a 0.5 m thick carbonate rich unit (calcrete) with a red weathering colour. Above there are 7 m of grey shale with a 1 m thick rusty-red carbonate cemented sandstone (facies G) on top. This sandstone is laterally extensive, has sporadic shell fragments and potential desiccation cracks observed within a lighter coloured muddy lamination. The rest of the sequence is

dominated by very dark grey shale capped by paleosol (facies N) and coal shale (facies M).

Interpretation: The interval is interpreted to display a continuation of a marginal marine to lagoonal environment. The occurrence of coquina beds, carbonate beds and red and green mudstones is typical for the Isfjorden Member (Mørk et al., 1999a; Haugen, 2016). Shell bearing organisms such as molluscs typically thrive in environments with low sedimentation rates (Eyles and Lagoe, 1989). Reinson (1984) describes coquina beds in lagoonal sediments from the Upper Cretaceous St. Mary Formation in southern Alberta. A fragmented appearance of the shells indicates that the shells may have been reworked and transported away from their original growing position (Reineck and Singh, 1980). A possible scenario is that shell fragments accumulate at or close to a beach or barrier bar. During high energy episodes these fragments, together with sand, may be transported into the lagoon as wash-over fan deposits (Boggs, 2011). *Rhizocorallium* in one of the sandstones is a marine trace fossil, belonging to the Cruziana ichnofacies, which is commonly found in lagoonal and shelf environments with medium to low energy conditions (Boggs, 2011). The high concentration of carbonate in the sandstones could originate from dissolution and reprecipitation of shell material in starved sediment conditions (Ketzer et al., 2003; Støen, 2016).

The dark shale in the upper part may reflect deposition in an interdistributary area with restricted energy conditions. Poor water circulation may have created anoxic conditions, allowing the preservation of accumulated organic material, resulting in the dark colour. Associated coal shale and paleosol support a marginal marine to delta plain depositional setting.

Interval 5 (209 – 261 m)

Description: The dark shale from the underlying interval gradually coarsens upwards into a bioturbated and mud draped siltstone to very fine sandstone unit (Figure 5.11). A plant fragment is found at the surface of a scree block. 8 m of shale (facies A) separates this lower sandstone unit from an upwards fining sandstone with trough and tabular cross-stratification

(facies K and J). The grain size in this sandstone changes from medium to very fine upwards. It is 6.5 m thick and has a laterally restricted geometry. The upper part of the interval is recorded

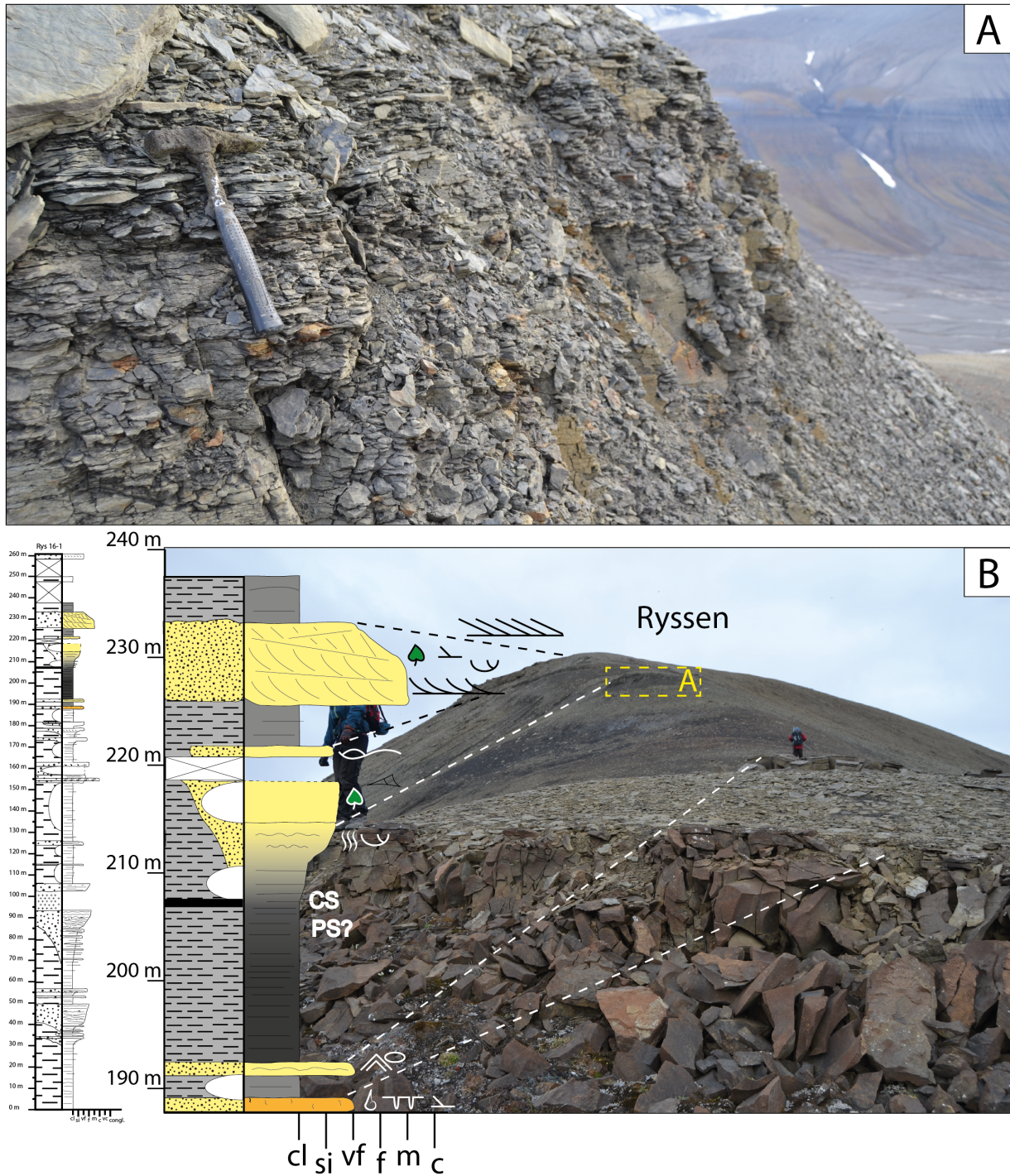


Figure 5.11: Log and picture correlation from Ryssen. (A) An intensely bioturbated and heterolithic section. (B) A rusty-red carbonate cemented bed with desiccation cracks and shell fragments. The location of (A) is indicated by a dashed square.

from a very flat and scree covered terrain with very few outcrops. However, red and green mudstones (facies N) are found after digging into the scree. The uppermost outcrop found at Ryssen is a 1.5 m thick laterally restricted very fine sandstone with trough cross-stratification (facies K).

Interpretation: The interval is interpreted to represent deposition in a marginal marine to delta plain environment. Intense bioturbation and mud-drapes in the lower siltstone unit may indicate a marine low energy environment with a potential tidal influence (e.g., [De Raaf and Boersma, 2007](#)). Mudstone intervals are interpreted as interdistributary deposits. The upwards fining and cross-stratified sandstone with mud drapes may be interpreted as a distributary channel with tidal influence ([Reading and Collinson, 1996](#)). The uppermost cross-stratified sandstone is interpreted as a small channel deposit as well. The laterally restricted geometry of the sandstones is typical for channel deposits ([Collinson, 1996](#); [Lord et al., 2014b](#)). The red and green mudstones in the upper part indicate that the deposits belong to the Isfjorden Member ([Mørk et al., 1999a](#); [Haugen, 2016](#)).

5.4 Milne Edwardsfjellet

Milne Edwardsfjellet ([Figure 5.12](#)) is a 598 m high mountain situated in the north-western corner of Fulmardalen ([Figure 5.1](#)). The slopes facing Fulmardalen are relatively steep and hold good exposures of the Botneheia, Tschermakfjellet and the De Geerdalen formations. The transition from the Tschermakfjellet Formation to the De Geerdalen Formation is well exposed at Milne Edwardsfjellet.

The log recorded from Milne Edwardsfjellet (Mil 16-1) ([Figure 5.13](#)) is 230 m long, and the log trace follows a narrow ridge at the easternmost side of the mountain. It covers the uppermost 10 m of the Botneheia Formation, the entire Tschermakfjellet Formation (24 m) and 196 m of the De Geerdalen Formation. The log ends at the summit of the mountain, somewhere in the uppermost part of the De Geerdalen Formation.

The De Geerdalen Formation on Milne Edwardsfjellet can be described as several upwards coarsening sequences, with shales coarsening up to fine and medium grained sandstones. Each of the sandstone bodies are capped by shales, marking the onset of a new coarsening upward sequence. Geometrically, the sandstone bodies are laterally continuous and relatively thin. The thickest sandstone intervals are found in the lower part of the formation.

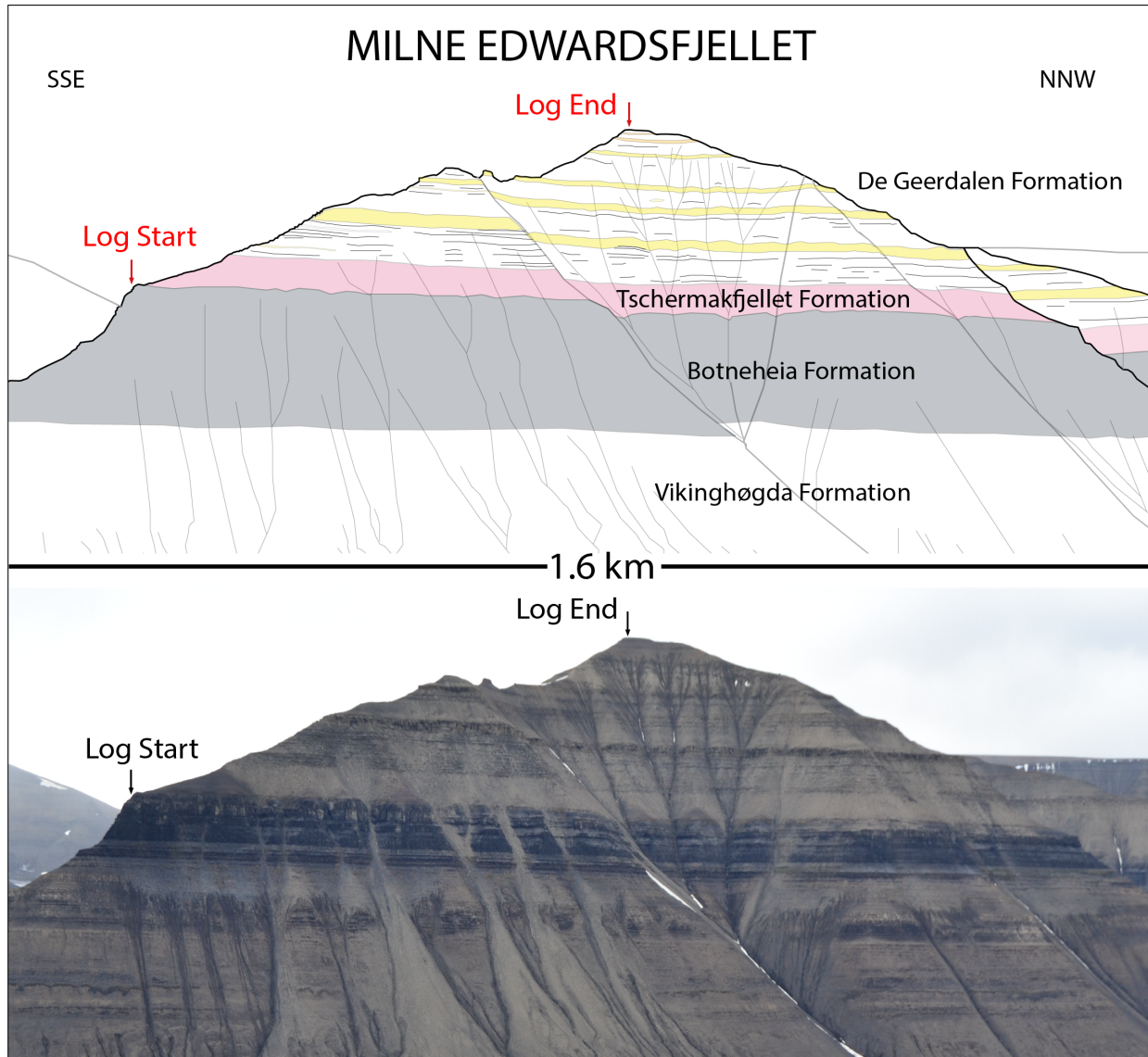


Figure 5.12: Geological sketch and corresponding overview photo of the logged section at Milne Edwardsfjellet. Formation names and stratigraphic boundaries have been indicated. Yellow areas within the De Geerdalen Formation mark major sandstone intervals. The log trace follows the ridge between the Log Start and Log End arrows.

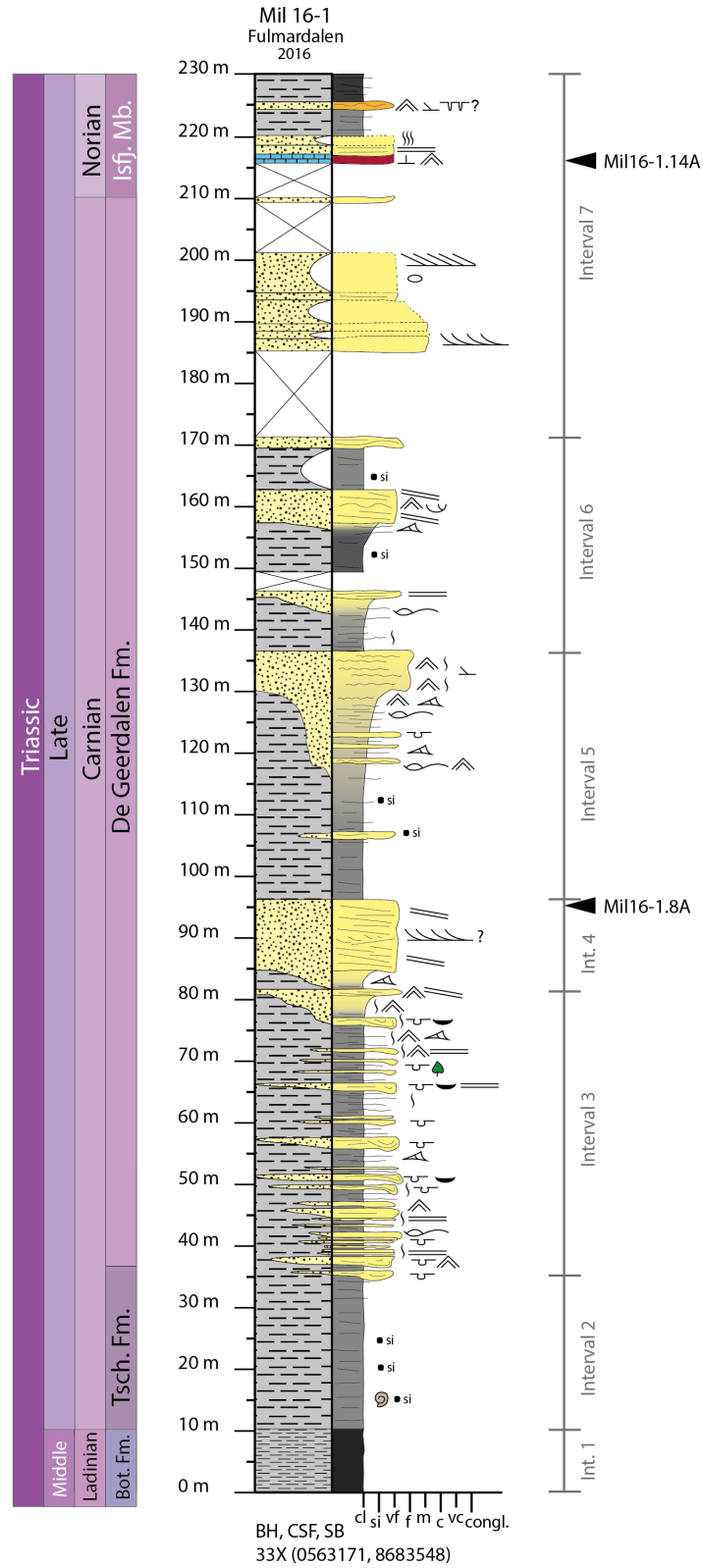


Figure 5.13: The log from the measured section at Milne Edwardsfjellet. Depositional age has been interpreted following Mørk et al. (1999a). Interval sub-division and the position of samples (Mil16-1.8A, 14A) are indicated.

Log Mil 16-1

Interval 1 (0 – 10m)

Description: Interval 1 consists of dark grey to black coloured, finely laminated paper shale. The colour is distinctly darker than the shales in the overlying intervals.

Interpretation: The dark coloured paper shale belong to the Blanknuten Member of the Botneheia Formation. This formation reflects a deltaic influenced, regressive shelf deposit with restricted water circulation conditions (Mørk et al., 1982, 1989, 1999a).

Interval 2 (10 – 34m)

Description: Interval 2 consists of grey shales (facies A) with siderite nodules and some thin (<10 cm thick) siltstone beds. The nodules weather with a distinct purple and red colour, making it possible to trace the formation laterally. Ammonoid fossil imprints are present in the siderite nodules.

Interpretation: The interval comprises the Tschermakfjellet Formation. The formation represents a shale-dominated, prodelta depositional environment (Mørk et al., 1999a). The observed imprints of ammonoid fossils support a marine origin.

Interval 3 (34 – 81m)

Description: The grey shale of the Tschermakfjellet Formation is followed by a 47 m thick heterolithic succession of alternating very fine sandstones and shales (facies B). The sandstones are characterized by soft sediment deformation structures (facies D), hummocky cross-stratification (facies C) and wave ripples (facies E). Bed thicknesses vary from 0.2-1.5 m. The deformed sandstones often hold plant fragments and mud flakes. Sparse bioturbation and wave ripples are typically found towards the top of the sandstone beds. The intensity of the bioturbation is generally sparse through the whole interval. The sandstone bodies are laterally

restricted, ranging from two to several tens of metres in width.

Interpretation: The base of the interval is interpreted to reflect the base of the De Geerdalen Formation at Milne Edwardsfjellet. The interval is interpreted to record deposition in an offshore transition and lower shoreface setting. Sandstones with erosive bases and soft sediment deformation structures are interpreted as deposits from gravitational processes such as slumping and sliding at the delta front and prodelta (Mills, 1983; Reading and Collinson, 1996). The relatively short lateral geometry of the sandstone bodies may originate from slumps and slides that moved downwards into a more muddy substrate. Plant fragments incorporated within deformed sandstones are interpreted to have been transported and deposited by mass movement processes. Hummocky cross-stratified and laminated sand- and siltstones with wave ripples and sparse bioturbation on top are interpreted to be storm-generated beds, while mudstone intervals have been deposited from suspension under fair weather conditions.

The fact that the De Geerdalen Formation at Milne Edwardsfjellet has much more sandstone bodies in the lower part with deformational structures compared to the other localities in Fulmardalen, could indicate that this locality was located in a more proximal position to a distributary channel outlet. This may have lead to a high sedimentation rate at the delta front resulting in mass movements and soft sediment failures on the prodelta slope (Reading and Collinson, 1996).

Interval 4 (81 – 96m)

Description: The heterolithic section from the underlying interval is gradually replaced by a 12 m thick very fine sandstone dominated by low angle cross-stratification (facies I) and trough cross-stratification (facies K) (Figure 5.14). The sandstone shows a weak coarsening upwards trend and is the thickest sandstone body observed at Milne Edwardsfjellet. Due to the very steep nature of this sandstone outcrop, it was not possible to carry out any detailed investigations of the middle and upper part of the unit. The sandstone body is laterally continuous and can be traced along the whole mountainside and over to the neighbouring

mountains.

Interpretation: The sandstone is interpreted to belong to the same barrier bar complex identified in the lower part of the measured sections at the other mountains in Fulmardalen.

Interval 5 (96 – 136m)

Description: Interval 5 can be considered as an upwards coarsening sequence (Figure 5.14). The lower part is dominated by mudstone (facies A) and heterolithic bedding (facies B) with very fine sandstone beds ranging from 5-50 cm in thickness. Hummocky cross-stratification (facies C), wave ripples (facies E) and deformation structures (facies D) are observed within these sandstones. The upper part consists of a 6 m thick intensely wave rippled sandstone

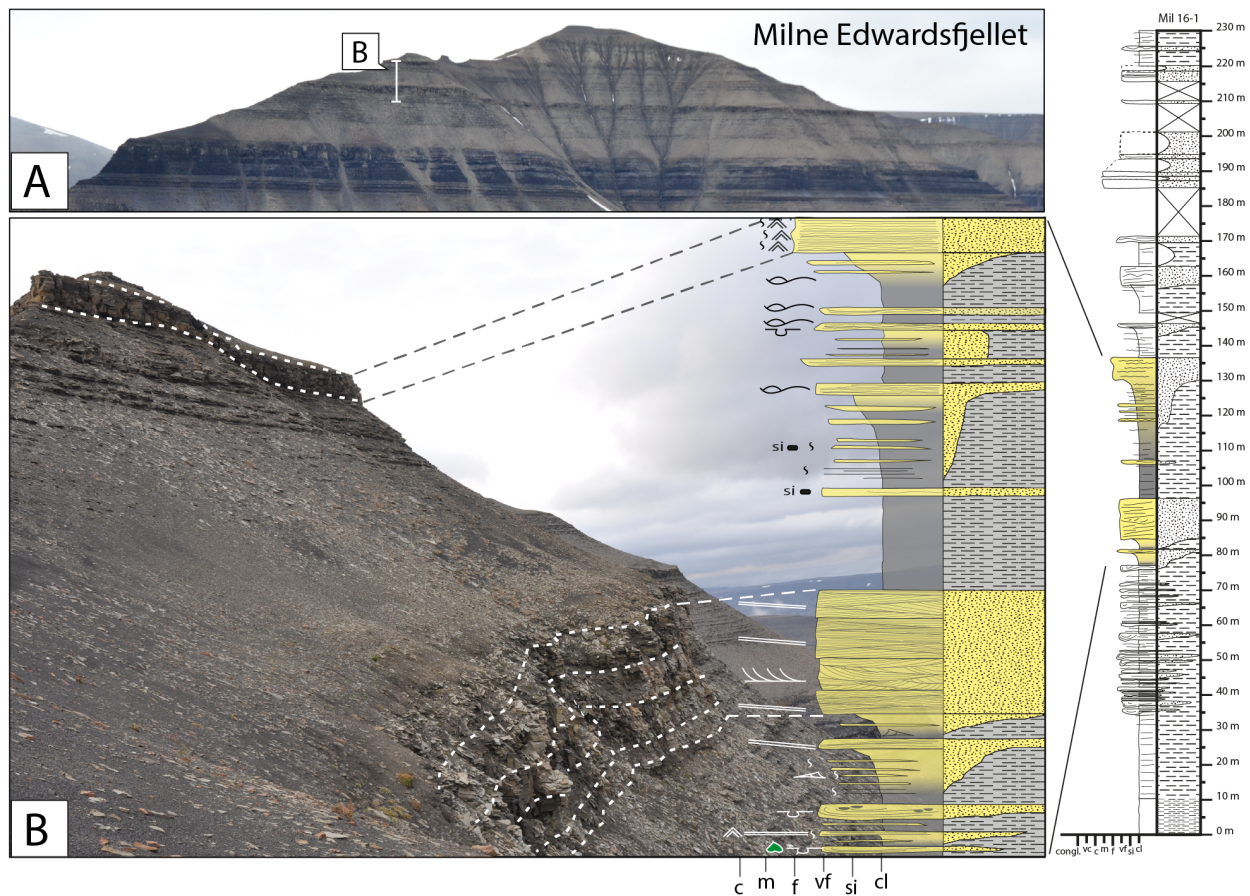


Figure 5.14: Log and picture correlation from Milne Edwardsfjellet. (A) Image of the mountain indicating the location of (B). (B) A lower sand-dominated section interpreted as a barrier bar complex, followed by an upwards coarsening unit. The uppermost sandstone has been interpreted as a shallow subaqueous bank.

(facies E) with sparse bioturbation.

Interpretation: The boundary to the underlying interval is interpreted as a flooding surface and a shift back to a lower shoreface to offshore setting. Mud is deposited in calm periods and sand during episodic storm events. The wave rippled sandstone towards the top indicates a change to a higher energy environment with time, where wave processes have reworked the sediments. It possibly reflects a proximal delta front deposit, such as a shallow subaqueous bank (Knarud, 1980). Stacked upwards coarsening sequences with relatively low bioturbation rates, like the sequences observed especially in the lower half of the De Geerdalen Formation in Fulmardalen, are typically formed in delta front settings (Hori et al., 2002).

Interval 6 (136 – 171m)

Description: Interval 6 consists of small upwards coarsening units, with mudstones (facies A) in the lower part and very fine sandstones in the upper part. There are siltstone beds displaying hummocks (facies C), whereas the sandstones are characterized by planar stratification (facies H), low angle cross-stratification (facies I) and wave ripples (facies E). Mud draped foresets are observed in addition to short intervals of flaser- and wavy bedding within the largest sandstone unit.

Interpretation: Interval 6 is interpreted to represent deposition from small migrating bars with a stronger tidal influence on the deposits compared to the underlying interval. Mud drapes, flaser- and wavy bedding are typical in tidal environments. In such settings, mud is deposited in slack-water conditions, while sand is deposited by currents created by tidal and wave energy. Alternatively, such deposits are also known to form in marine delta front environments where sediment supply and current velocities may fluctuate (Boggs, 2011).

Interval 7 (171 – 230m)

Description: The next interval consists of large sections that are totally scree-covered. Within the scree cover, there is an upwards fining sandstone unit that partly consists of unconsolidated sand. The grain size changes from medium to very fine sand. The intact parts of the sandstone show large-scale trough cross-stratification (facies K) and tabular cross-stratification (facies J). Large, grey and sandy concretions are observed within the sandstone.

The part of the interval above the scree cover consists of a sequence of deposits that can be recognized at Dyrhø, Ryssen and Storfjellet. It starts with a 2 m thick lateral continuous layer, consisting of carbonate in the lower part and a planar laminated sandstone in the upper part (facies H). The bed is topped by 2 m of an intensely bioturbated sandstone. The sandstone is capped by 4 m of shale (facies A), followed by a 1 m thick, laterally extensive and rusty-red carbonate rich sandstone (facies G) with wave ripples and potential desiccation cracks. The final 4 m consist of very dark shales (facies A).

Interpretation: The large scree-covered sections are inferred to be mud-dominated, reflecting deposition in a low-energy environment, potentially in an interdistributary area. Poorly exposed large scale trough cross bedded sandstones in the upper reaches of the interval may represent deposition in a distributary channel. The relatively thin sandstones and carbonate cemented beds alternating with muddy intervals are interpreted to represent deposition in a paralic environment from shallow marine to lower delta plain, possibly in a lagoonal setting. Desiccation cracks in one of the sandbodies indicates periods of sub-aerial exposure, while intense bioturbation in another sandstone unit may reflect upon marine influence. A very distinct, dark colour of the uppermost shale sequence may be a result of a high organic content, suggesting a low-energy, potential lagoonal, depositional environment, where organic material is allowed to accumulate. Carbonate beds and thin sand and siltstones are characteristic for the Isfjorden Member (Mørk et al., 1999a). The section is therefore interpreted to display a part of the Isfjorden Member, despite lacking the most characteristic

red and green mudstones.

5.5 Storfjellet

Storfjellet ([Figure 5.15](#)) is a mountain located in the southeastern part of Fulmardalen with Ryssen bordering to the north ([Figure 5.1](#)). The glacier, Veitbreen flows across the plateau shaped top, separating Storfjellet from the mountain ridge Prospektryggen to the east. The highest point is 556 masl and is located at the northern margin of the plateau. The slopes facing W-NW into Fulmardalen are relatively steep and hold good exposures of the De Geerdalen Formation.

The logged section at Storfjellet (Stor 16-1) ([Figure 5.16](#)) is 245 m long and is recorded in the W-NW facing slope at the northern part of the mountain. The log starts in Tschermackfjellet Formation and continues into the De Geerdalen Formation. The Isfjorden Member is found in the upper part.

[Knarud \(1980\)](#) also presents a log from Storfjellet ([Appendix C](#)), which has been recorded relatively close to the section presented herein (Atle Mørk, pers. comm., 2017).

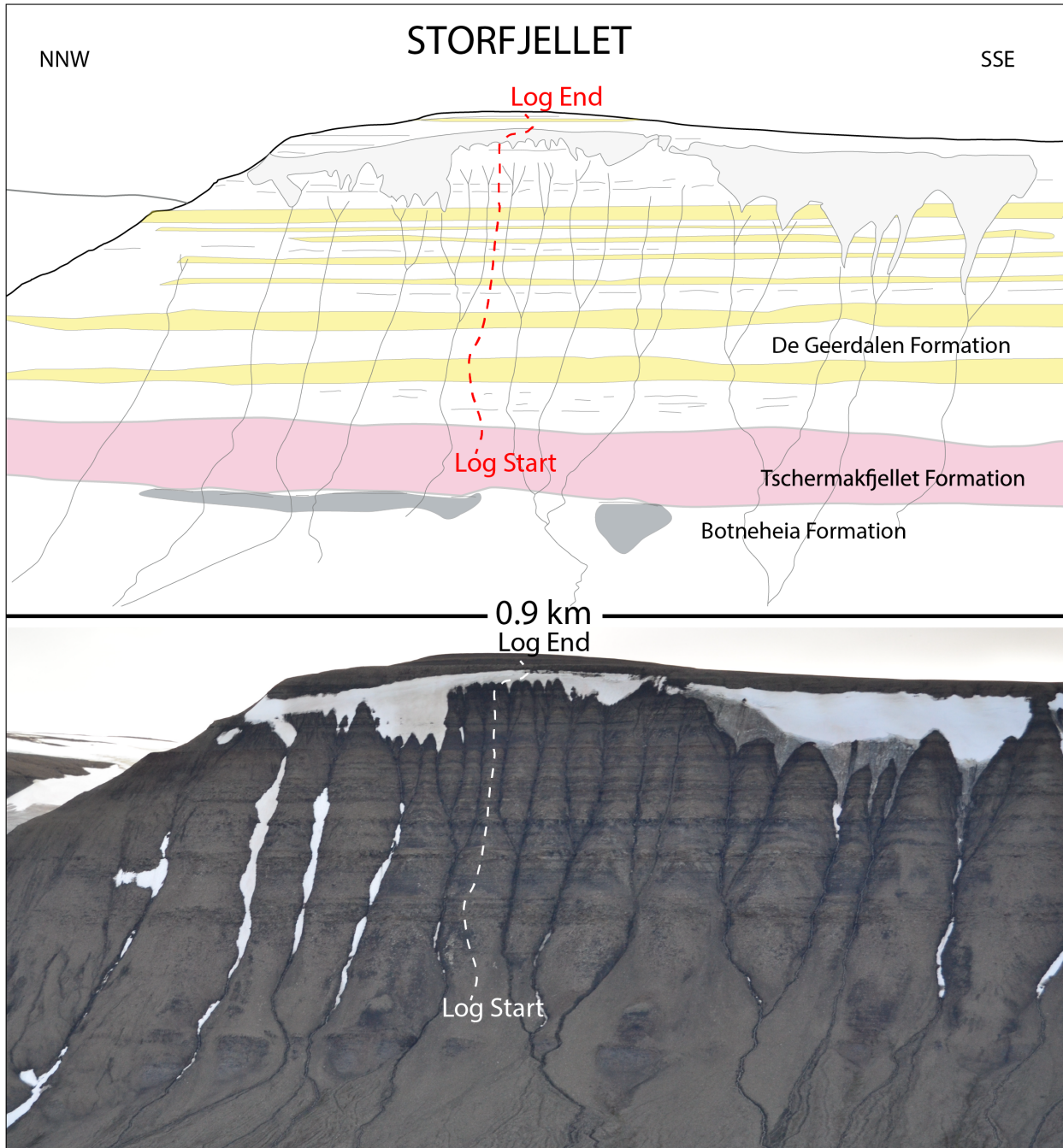


Figure 5.15: Geological sketch and corresponding overview photo of the logged section at Storfjellet. Formation names and stratigraphic boundaries have been indicated. Yellow areas within the De Geerdalen Formation mark major sandstone intervals. Log trace is indicated by a dashed line.

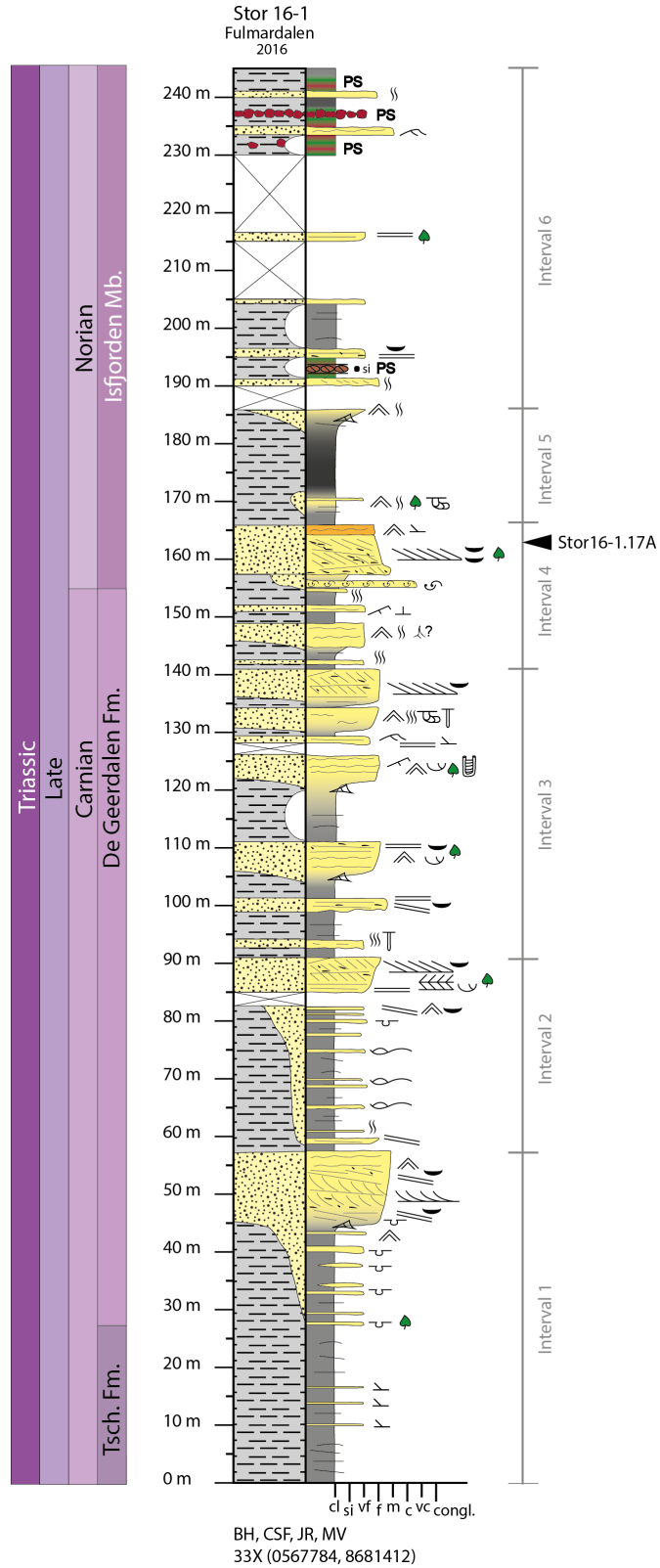


Figure 5.16: The log from the measured section at Storfjellet. Depositional age has been interpreted following Mørk et al. (1999a). Interval sub-division and the position of sample Stor16-1.17A are indicated.

Log Stor 16-1

Interval 1 (0 - 56m)

Description: The interval is an upwards coarsening unit. The lowermost 28 m of Stor 16-1 consist of grey shales (facies A) with centimetre-scale thick siltstone beds and 0.2-0.5 m thick very fine siderite cemented sandstone units. Above there is a 17 m thick heterolithic succession (facies B) with 0.5-1 m thick very fine sandstone units that become thicker in the upper part. The sandstones show soft sediment deformation structures (facies D) and are laterally restricted, varying from one m to several tens of m in width. Plant fragments are evident within these sandstones. Above the heterolithic package there is an 11 m thick, laterally continuous sandstone unit coarsening upwards from very fine to medium grained sand. Its base is gradual. Soft sediment deformation structures (facies D) are observed close to the base. The unit is mainly low angle cross-stratified (facies I), but large scale trough cross-stratification (facies K) is also observed with bed thicknesses of 10 cm. Mud flakes are observed throughout the whole sandstone unit, often at the interface between beds. Wave ripples (facies E) are only found in the upper part.

Interpretation: The lowermost part of the interval hosts the characteristics of the Tschermakfjellet Formation representing a marine pro-delta environment (Mørk et al., 1999a). The base of the De Geerdalen Formation at Storfjellet is interpreted to be at the base of the heterolithic succession. The laterally restricted sandstones with soft sediment deformation structures are interpreted to be generated from gravitational processes in an offshore transition to lower shoreface setting (e.g., Hori et al., 2002; Oliveira et al., 2011). The overlying sandstone is interpreted to represent a barrier bar deposit, possibly cut by a tidal channel, in a delta front to upper shoreface setting, similar to what has been observed at the other mountains in Fulmardalen. Knarud (1980) interprets this interval at Storfjellet as a shallow marine bank deposit, with the most important processes being controlled by marine currents, wind and

storm activity and by varying clastic input from land.

Interval 2 (56 - 91m)

Description: This interval is also an upward coarsening unit. The lowermost 25 m comprise a heterolithic package (facies B) of alternating grey shale and siltstone (facies A) and 0.2-0.5 m thick hummocky cross-stratified (facies C) very fine sandstone units. One of the sandstones show soft sediment deformation structures (facies D). The uppermost 10 m of the interval are mainly an upward coarsening sandstone unit except for some scree cover in the bottom part. The grain size changes from very fine to fine sand upwards. The lower part of the sandstone is planar parallel stratified (facies H) with mud flakes, mud drapes and plant fragments occurring between the beds, whereas the upper part is large scale tabular cross-stratified (facies J). Successive sets are occasionally bidirectional. Mud flakes are observed throughout the whole unit.

Interpretation: The contact to the underlying interval is interpreted to represent a flooding surface with marine shales, silt and sand being deposited under pulsating energy conditions in the offshore transition zone to lower shoreface (Knarud, 1980). Deformation structures in sandstone are likely due to rapid deposition of sand on a muddy substrate, as described in Section 4.2. The thick sandstone dominated unit at the top of the interval is interpreted to reflect shallow marine delta front to upper shoreface deposits. The planar stratification overlain by bidirectional cross-stratification could reflect a barrier bar cut by a tidal channel where both ebb and flow tide deposits are preserved (Boggs, 2011). Knarud (1980) interprets similar outcrops at Dalsnuten (see Figure 9.1) in central Spistbergen as point-bar deposits from a migrating tidal channel.

Interval 3 (91 - 141m)

Description: The interval consists of multiple stacked upward coarsening sequences, where shales and siltstones are gradually replaced by sandstones (Figure 5.17). The larger sandstones

display a variation between wave ripples (facies D), low angle cross-stratification (facies I), plane parallel stratification (facies H) and tabular cross-stratification (facies J). The thinner sandstones display asymmetrical ripples (facies F), planar stratification (facies H), low angle cross-stratification and some are locally intensely bioturbated. The trace fossils *Diplocraterion*, *Skolithos* and *Rhizocorallium* occur in distinct sandstone units. Mud flakes, plant fragments

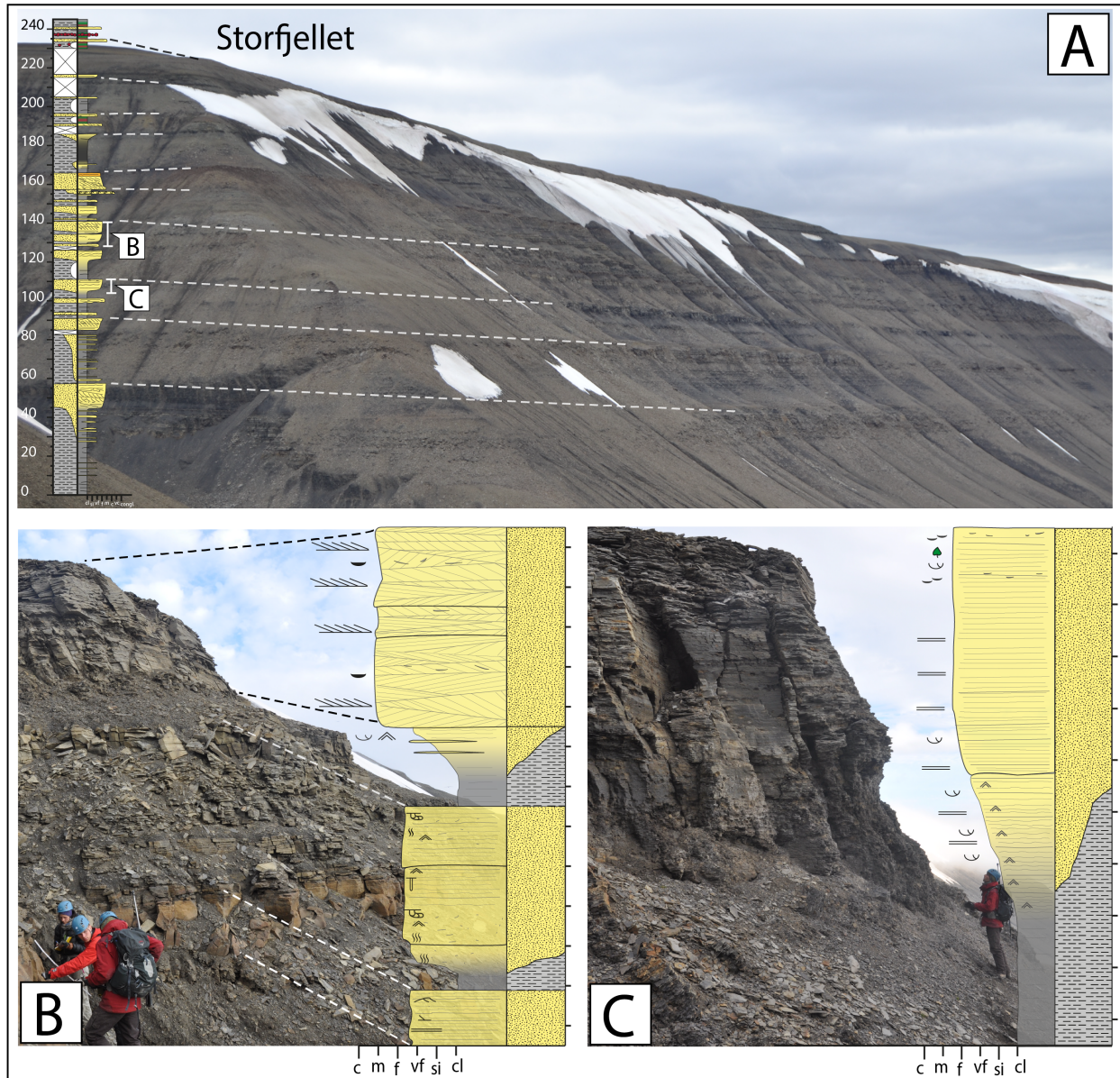


Figure 5.17: Log and picture correlation from Storfjellet. (A) Storfjellet seen from Ryssen. The top of major sandstone units has been correlated between log and picture with dashed lines. (B) Small scale upwards coarsening units within a sandstone dominated interval. (C) Upwards coarsening sequence interpreted as a shallow marine distal bar, influenced by both marine and deltaic processes.

and mud drapes are observed at several levels.

Interpretation: The main characteristic of progradational deltaic sequences is that they shallow and coarsen upwards from muds, through silts to various sand-dominated facies (Reading and Collinson, 1996). The stacked upwards coarsening sequences in this interval are interpreted as progradational subaqueous banks terminated by abandonment/flooding surfaces. The extent and nature of such surfaces depend on the process controlling relative sea-level rise. Each surface indicates a subsequent deepening, developing new accommodation space for further progradation (Reading and Collinson, 1996). The sedimentary structures observed in the sandstones typically occur in shallow marine environments. The trace fossils *Diplocraterion* and *Skolithos* indicate deposition in an upper shoreface, high energy environment, whereas the occurrence of *Rhizocorallium* points towards a medium to low energy marine environment (Boggs, 2011), indicating variable energy conditions during deposition of the sandstones. Knarud (1980) suggests that the sequences in this interval are distal shallow marine bars, in which the sediment supply is controlled by both deltaic sediment input and marine current processes. Furthermore, mud flakes within sandstones indicate that surrounding semi-consolidated muddy sediment have been ripped up by strong currents and quickly re-deposited together with sand (Spearing, 1976; Knarud, 1980).

Interval 4 (141 - 166.5m)

Description: The interval is initiated by a 15 m thick sequence of alternating sand- and mudstone units. The sandstones are very fine grained, intensely bioturbated and show signs of wave ripple lamination (facies E). The sandstones are thinner compared to those in the underlying interval. Potential rootlets are observed in the upper part of one of the sandstones. The upper part of the interval consists of a bioclastic sandstone with shell fragments (facies L) capped by an upwards fining, 8 m thick medium to fine grained sandstone with large scale tabular cross-stratification (facies J) and a high amount of rip-up clasts and mud flakes. Plant fragments are found within the sandstone and the top is intensely bioturbated. A 1.5 m thick

rusty-red, heavily cemented, carbonate rich fine sandstone with signs of ripple lamination (facies G) is overlaying the cross bedded sandstone. It is a prominent feature of the terrain and can be laterally traced to the neighbouring mountains.

Interpretation: The lower part of the interval displays features indicative of a calm and low-energy environment, interpreted as deposits in a protected shallow marine, potentially lagoonal, setting. Relatively thin and intensely bioturbated sandstones surrounded by mudstone, in addition to the presence of bioclastic sandstones, are common in such depositional settings (Reineck and Singh, 1980; Reinson, 1984; Boggs, 2011). Structures like ripples and undulating stratification in the sandstones may suggest periodically influence of higher energy processes. Roots indicate sub-aerial exposure. However, these structures could also resemble vertical trace fossils belonging to the *Skolithos* ichnofacies, and Knarud (1980) describes *Skolithos* in a sandstone at similar stratigraphic levels at Storfjellet. The cross bedded sandstone in the upper part of the interval is interpreted to represent a distributary or tidal channel. The carbonate rich sandstone at the very top is interpreted to be deposited in shallow marine water during a period of low clastic input where carbonate producing microorganisms could thrive (Knarud, 1980).

Interval 5 (166.5 - 186m)

Description: The interval consists of 14 m of dark grey shale (facies A) that gradually coarsens upwards into a 2 m thick siltstone to very fine sandstone unit. The shale has a characteristic dark colour that can easily be recognized at neighbouring mountains. The silt- to sandstone is moderately bioturbated and discontinuous wave ripple lamination (facies E) is observed. A thin sandstone layer with wave ripples (facies E), moderate bioturbation, plant fragment and the trace fossil *Rhizocorallium* is found in the lower part of the interval.

Interpretation: The interval reflects a low energy depositional environment with dominance of fine grained material settling from suspension. *Rhizocorallium* indicate a marine medium to

low energy environment, and typically occurs in lagoonal and shelf settings (Boggs, 2011). The very dark shale is interpreted as organic rich shale deposited in a lagoon or interdistributary area where water circulation was restricted. The upward coarsening sandstone is interpreted as a wash-over fan deposit into the lagoon, being reworked by organisms during calm periods.

Interval 6 (186 - 245m)

Description: The uppermost interval at Storfjellet is characterized by thin 0.5-1 m thick very fine to fine sandstones interbedded in scree or partly covered mudstones that have grey, green and red colours (facies N). Sedimentary structures observed in the sandstones are plane parallel stratification (facies H) and asymmetrical ripples (facies F) in addition to bioturbation. Plant fragments are also present. A layer of large round siderite concretions (10-30 cm in diameter) is found within red and green mudstones. A weathered carbonate rich horizon with red and green nodules that are 2-15 cm in diameter is found in the upper part. The nodules have an irregular shape.

Interpretation: The interval is thought to reflect a marginal marine, possibly lagoonal, low-energy environment belonging to the Isfjorden Member (Mørk et al., 1999a). The thin sandstones may represent small subaqueous banks or wash-over deposits. The nodule horizon is interpreted to be weathered carbonate soil (calcrete) with calcified nodules that may have formed around roots. Such nodules are commonly found in red-bed successions and especially in flood-plain deposits (Tucker, 2011). Haugen (2016) describes similar calcareous nodules in the Isfjorden Member, appearing as individual nodules within red and green mudstones, but also within calcretes from localities in Agardhdalen in eastern Svalbard and from Deltaneset in central Spistbergen (see Figure 9.1). Red and green mudstones are interpreted as paleosols as well, where the colour alternation may result from fluctuations in the groundwater table causing shifts in the redox regime (Haugen, 2016; Lord et al., 2017a). Paleosols have a high interpretative value as they indicate sub-aerial exposure (Kraus, 1999). Paleosols have been described from a variety of continental depositional settings (Kraus, 1999), but have also been

found in marginal marine environments where sea level fall has left the strata exposed (Lander et al., 1991; Webb, 1994; Wright, 1994).

5.6 Raggfjellet

Raggfjellet (Figure 5.18) is a mountain located in the southernmost part of Fulmardalen with Hellefonna located to the east and its tributary glaciers, Marmorbreen and Skruisbreen situated to the north and to the south, respectively (Figure 5.1). Raggfjellet has a plateau shaped top, similar to many of the other mountains in the area, with the highest point reaching 571 masl.

The logged section at Raggfjellet (Rag 16-1) (Figure 5.19) is only 21 m long and is recorded in the uppermost part of the slope facing north towards Marmorbreen. The lower part of the slope is extensively scree covered, and was therefore not measured. The upper part holds exposures

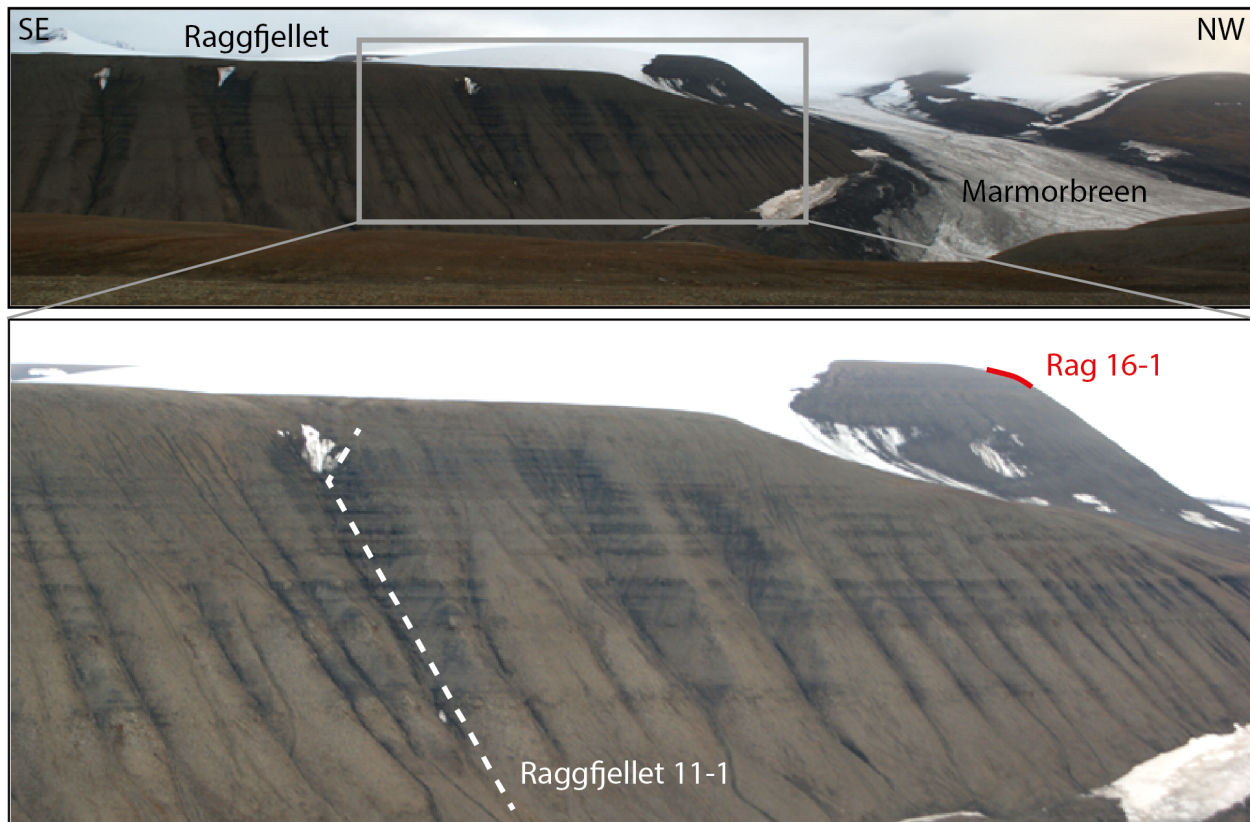


Figure 5.18: Photo of Raggfjellet captured from Storfjellet. The location of the logs Rag 16-1 and Raggfjellet 11-1 is indicated. Note the stratigraphically higher position of Rag 16-1. Photo: Gareth S. Lord

of the Isfjorden Member.

A longer sedimentological log from Raggfjellet (Raggfjellet 11-1) has been presented in [Klausen et al. \(2015\)](#) and [Lord et al. \(2017a\)](#). However, Raggfjellet 11-1 is recorded in the NE-facing slope of the mountain and is measured stratigraphically lower than Rag 16-1 ([Figure 5.18](#)). It is further discussed in [Section 9.3](#).

Rag 16-1

Description: The lower part of the log is characterized by red and green mudstones (facies N) interrupted by 0.5-1 m thick wave rippled (facies E) and bioturbated very fine sandstones. Irregular shaped and mottled nodules are found within the red mudstones in addition to a distinct carbonate layer containing similar nodules. The upper part of the log consists of grey shales (facies A) interrupted by a 60 cm thick very fine sandstone.

Interpretation: The red and green mudstones with nodules are interpreted as being paleosols belonging to the Isfjorden Member, and are interpreted to have been deposited under similar conditions to the succession in the upper part of Storfjellet. The nodular layer has been interpreted as calcrete with calcified nodules forming around roots.

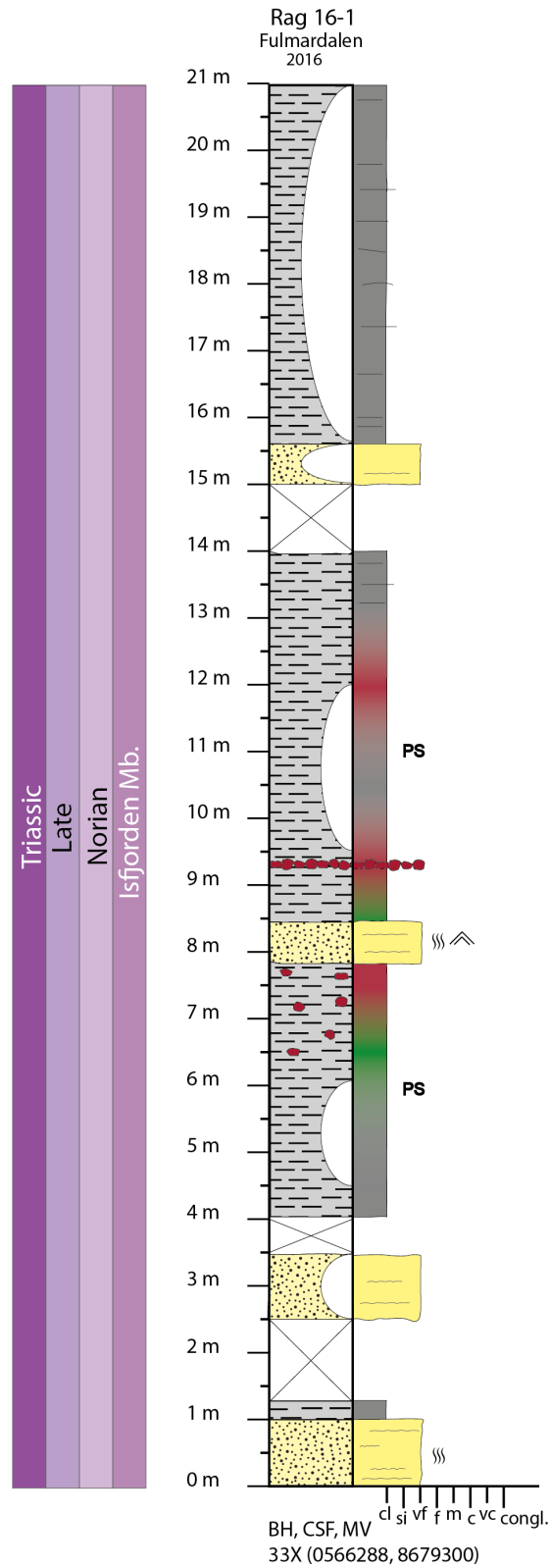


Figure 5.19: The log from the measured section at Raggfjellet. Depositional age has been interpreted following Mørk et al. (1999a). Notice that the scale is different from the other logs. Only the upper 21 m of Raggfjellet are recorded.

6. Seismic Results

The chapter will present seismic results and interpretations of channel bodies in the Snadd Formation from the ST9802 3D-seismic dataset on the Finnmark Platform (Figure 6.1). The average thickness of the Snadd Formation in the study area is 140 ms TWT (Appendix D), which corresponds to 210 m when using a seismic velocity of 3000 m/s. A similar thickness (212 m) of the formation is documented from information from well 7131/4-1.

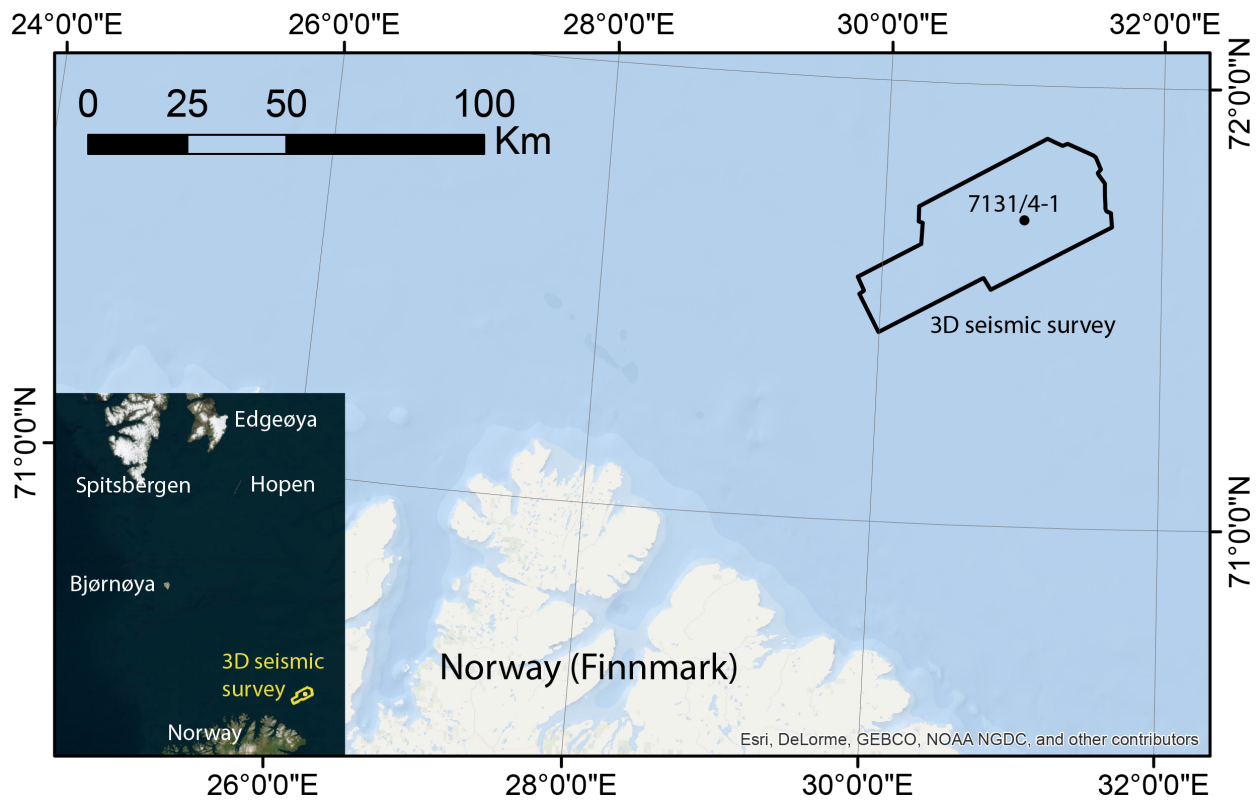


Figure 6.1: Location of the ST9802 3D-seismic dataset and the well 7131/4-1.

6.1 RMS Amplitude Maps

Three RMS amplitude maps from different intervals ([Figure 6.2](#)) within the Snadd Formation are presented and interpreted in this section. In the following explanation, + and – correspond to above and below a horizon, respectively. The lower interval (Map 1) represents a seismic window between +60 and +75 ms TWT offset from the Top Kobbe horizon. The middle interval (Map 2) represents a seismic window between -45 and -60 ms TWT offset from the Top Snadd horizon. The upper interval (Map 3) represents a seismic window between -20 and -35 ms TWT offset from the Top Snadd horizon. Two depositional environments have been interpreted from the study area; floodplain/overbank deposits and channel sandstones. Low amplitude areas are interpreted as mudstone, mainly reflecting floodplain deposits, whereas high amplitude areas are interpreted as channel sandstones.

The RMS amplitude maps display multiple channel morphologies, interpreted as meandering channel belts, braided channel belts, ribbon shaped channel fill and anastomosing channel fill, which is in accordance with observations described in [Klausen et al. \(2014\)](#) from six 3D seismic datasets located in the south-western Barents Sea. The channel fill deposits are typically narrow and relatively straight compared to the channel belt deposits which tend to be wider and having a sinuous geomorphology. Channel belt deposits show signs of lateral accretion and amalgamation, whereas channel fill deposits lack these.

There is a change from relatively large meandering and braided channel belts in the lower part (Map 1 and 2; [Figures 6.3](#) and [6.4](#)) to relatively narrow channel deposits in the upper part of the formation (Map 3; [Figure 6.5](#)). The widest channel belt in the lower part is 26.5 km, but is less than 5 km in the upper part. The observations are similar to those of [Klausen et al. \(2014\)](#). Some channels are relatively thick and can be recognized in more than one of the RMS amplitude maps presented.

According to [Klausen et al. \(2014\)](#) ribbon shaped channel fill deposits are thought to have developed from frequent avulsions preventing the channels from developing a mature

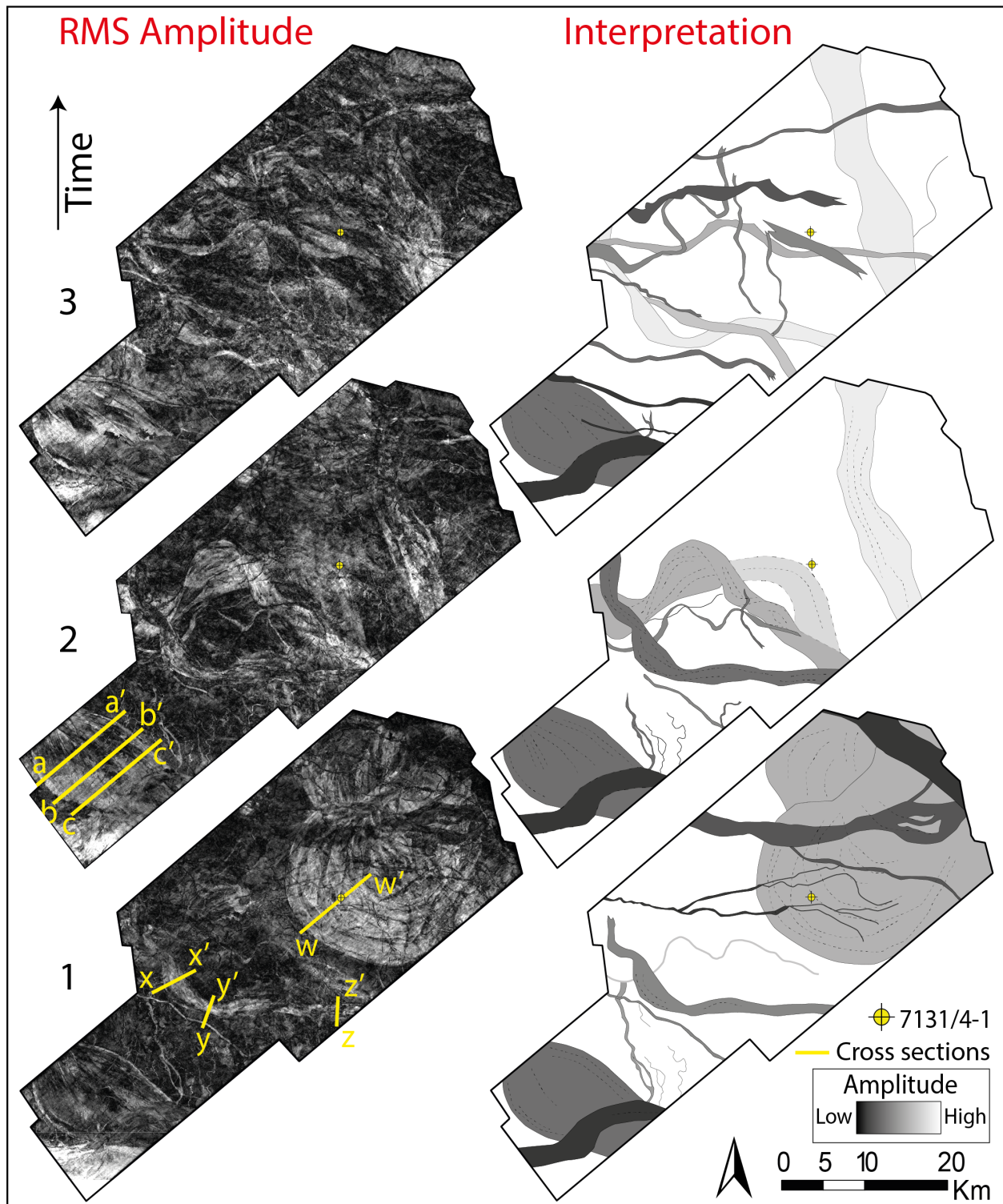


Figure 6.2: The three RMS amplitude maps with their correlative interpretation. Map 1 represents deposits located stratigraphically below map 2 which in turn is located below map 3. The location of seismic cross sections (Figures 6.6, 6.7 and 6.11) are indicated by yellow lines. The location of well 7131/4-1 is indicated by a yellow dot.

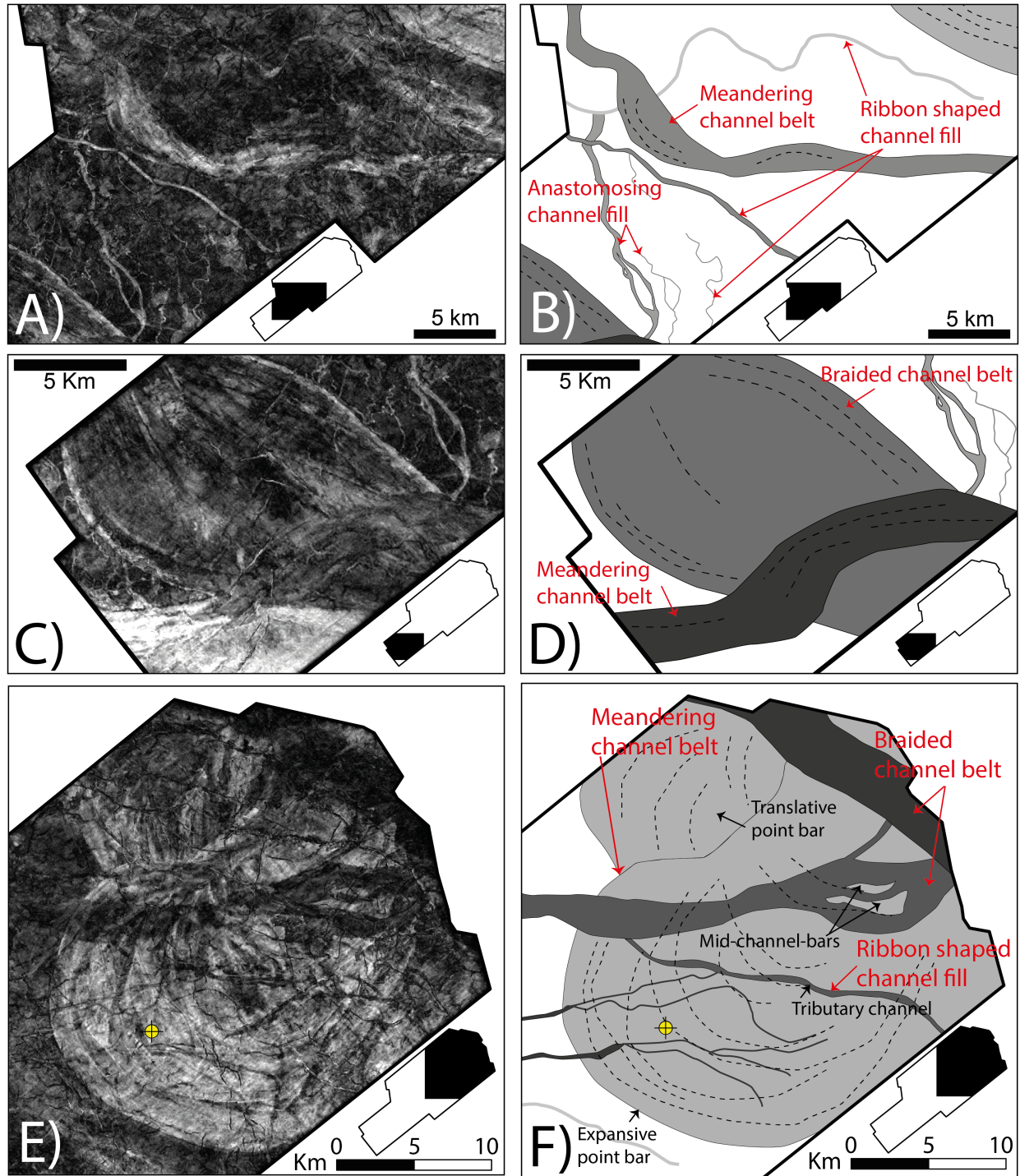


Figure 6.3: Examples of channel forms from map 1 in Figure 6.2. The position of each image within the study area is indicated. (A) RMS amplitude image and (B) the correlative interpretation of a meandering channel belt with lateral accretion surfaces (indicated by dashed lines), anastomosing channel fill and ribbon shaped channel fill.

(C) RMS amplitude image and (D) the correlative interpretation of a braided channel belt cut by a younger meandering channel belt. (E) RMS amplitude image and (F) the correlative interpretation of a large point-bar deposit (the Guovca sandstone) cut by multiple younger channels. Lateral accretion surfaces are indicated by dashed lines.

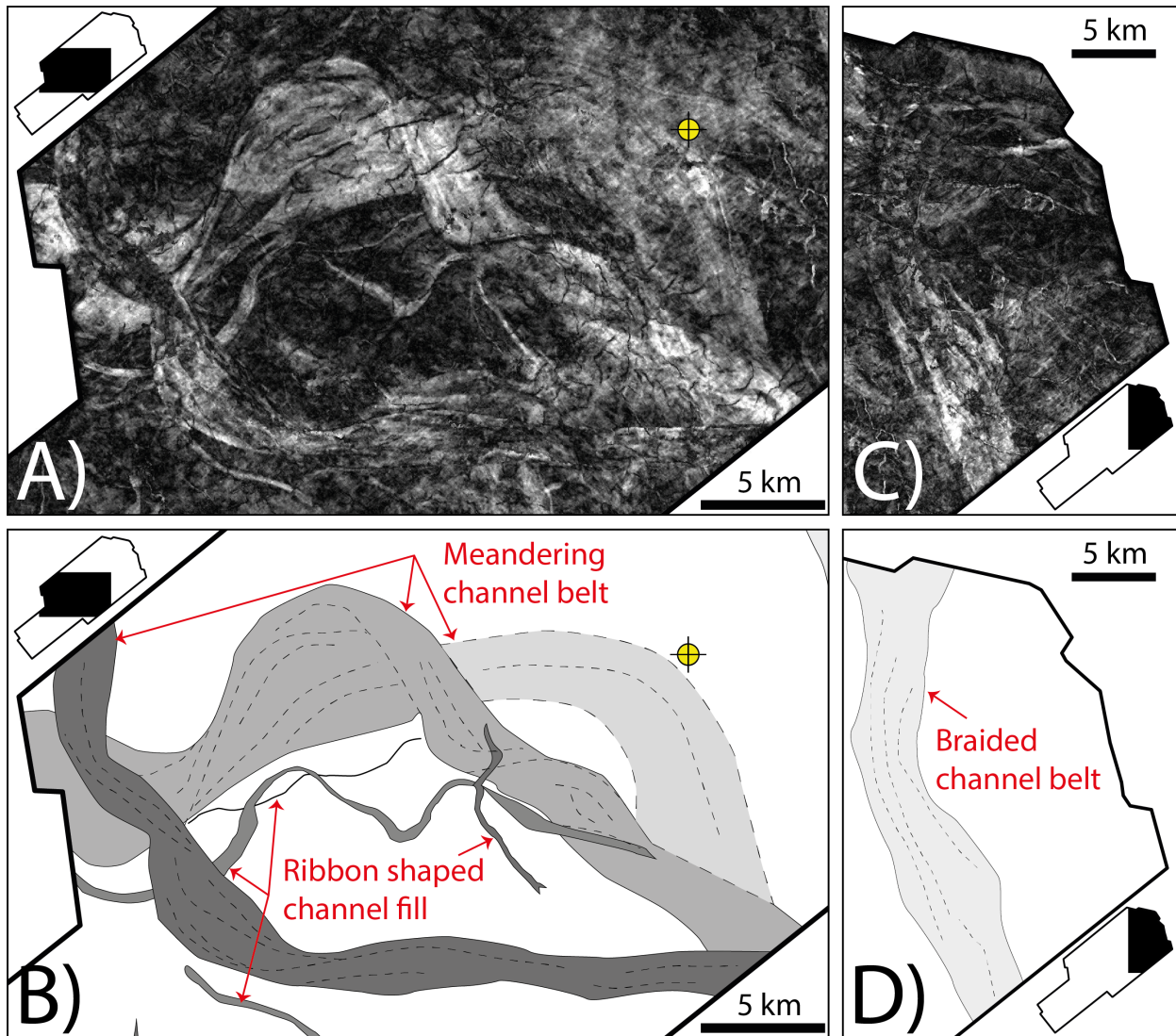


Figure 6.4: Examples of channel forms from map 2 in figure Figure 6.2. The position of each image within the study area is indicated. (A) RMS amplitude image and (B) the correlative interpretation of multiple meandering channel belts and ribbon shaped channel fill deposits. (C) RMS amplitude image and (D) the correlative interpretation of a braided channel belt.

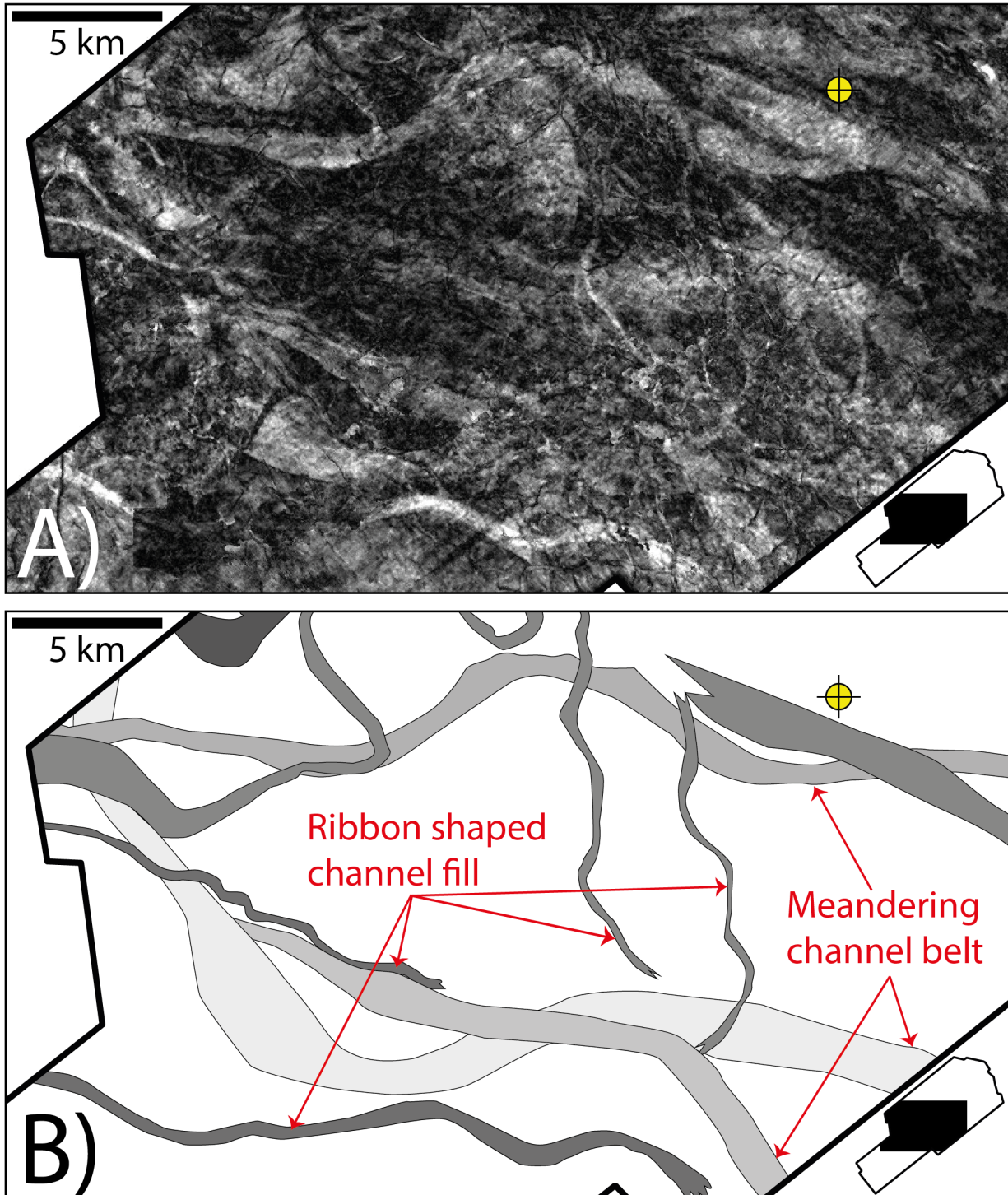


Figure 6.5: Examples of channel forms from map 3 in figure [Figure 6.2](#). The position of each image within the study area is indicated. (A) RMS amplitude image and (B) the corresponding interpretation of relatively narrow meandering channel belts and ribbon shaped channel fill deposits.

meandering shape. Both low and high amplitude ribbon shaped channels are observed (Figure 6.3A, B, E, F, Figure 6.4A, B and Figure 6.5), which may be indicative of mudstone and sandstone fill, respectively. Mudstone fill may be a result of passive infill of an abandoned channel, whereas sandstone fill may result from active lateral or vertical stacking of sand within the constraints of a single channel (Klausen et al., 2014). A few examples of channel fill deposits with an anastomosing morphology have been observed (Figure 6.3A, B). However, the key feature of such channels is that there are multiple active channels simultaneously. In ancient deposit it is impossible to confirm this, and a similar pattern may have been formed by a single channel changing position (Nichols, 2009).

6.1.1 The Guovca sandstone

Map 1 displays planform geometries resembling point-bar deposits from a large meandering channel belt, in the north-eastern part of the dataset (Figure 6.3E, F). The sandstone was the main target during hydrocarbon exploration in the so-called Guovca prospect, when well 7131/4-1 was drilled in 2005, but the well turned out to be dry (NPDFactPages). Two cores were recovered from the well during the exploration process; one from the Realgrunnen Subgroup (core 1) and one from the abovementioned channel complex called the Guovca sandstone (NPDFactPages) in the Snadd Formation (core 2). Core 2 has been analysed in Chapter 7.

Well developed lateral accretion surfaces can be observed and are helpful when interpreting the migration pattern of the point-bars. There appears to be a large expansive point-bar cutting through a translating point-bar. Both bars probably belong to the same channel system. Klausen et al. (2015) state that the channel must have formed with restricted accommodation space over a long period with multiple cut and fill cycles, with the preservation of the latest cycles only. This interpretation is supported by the fact that no significant geometrical changes of the channel deposit can be seen on RMS amplitude maps from different levels within the sandstone.

The point-bar deposits are cut by multiple younger channels, expressed as dark low

amplitude areas on the RMS amplitude map (Figure 6.3E). The amplitude contrast indicate a contrast in acoustic impedance for the different channel deposits. The younger channels may be more mud prone than the underlying point-bar. Two of the overlying channels have been interpreted as braided channel belts due to their relatively straight and sheetlike appearance in planview (Figure 6.3E, F). Lateral migration of braided rivers leaves sheetlike deposits of channels and bar complexes (Boggs, 2011). Geometries resembling mid-channel-bars can be seen in one channel (Figure 6.3E), supporting a braided river architecture. However, this morphology may also be a result of multiple channels clustering together.

6.2 Seismic Character of Channel Bodies

Seismic cross sections display channel bodies as discontinuous, high-amplitude reflectors (Figures 6.6 and 6.7). Small channels appear as bright spots (Figure 6.6B). For wide and

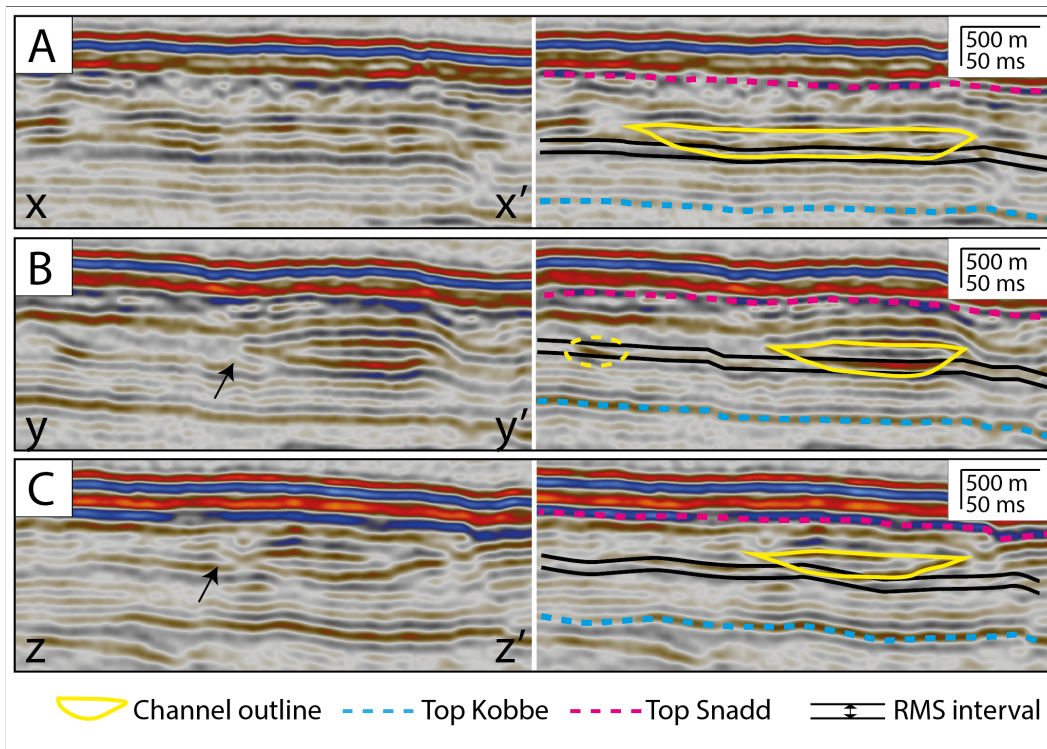


Figure 6.6: Seismic cross sections of a meandering channel belt on map 1 in Figure 6.2. The RMS interval of map 1 is indicated by black lines. Note the visible channel shape and associated terminating reflectors (indicated by arrows) from surrounding deposits along the channel boundary. (A) Cross section x-x'. (B) Cross section y-y'. A smaller ribbon shaped channel fill reflector is encircled (bright spot). (C) Cross section z-z'.

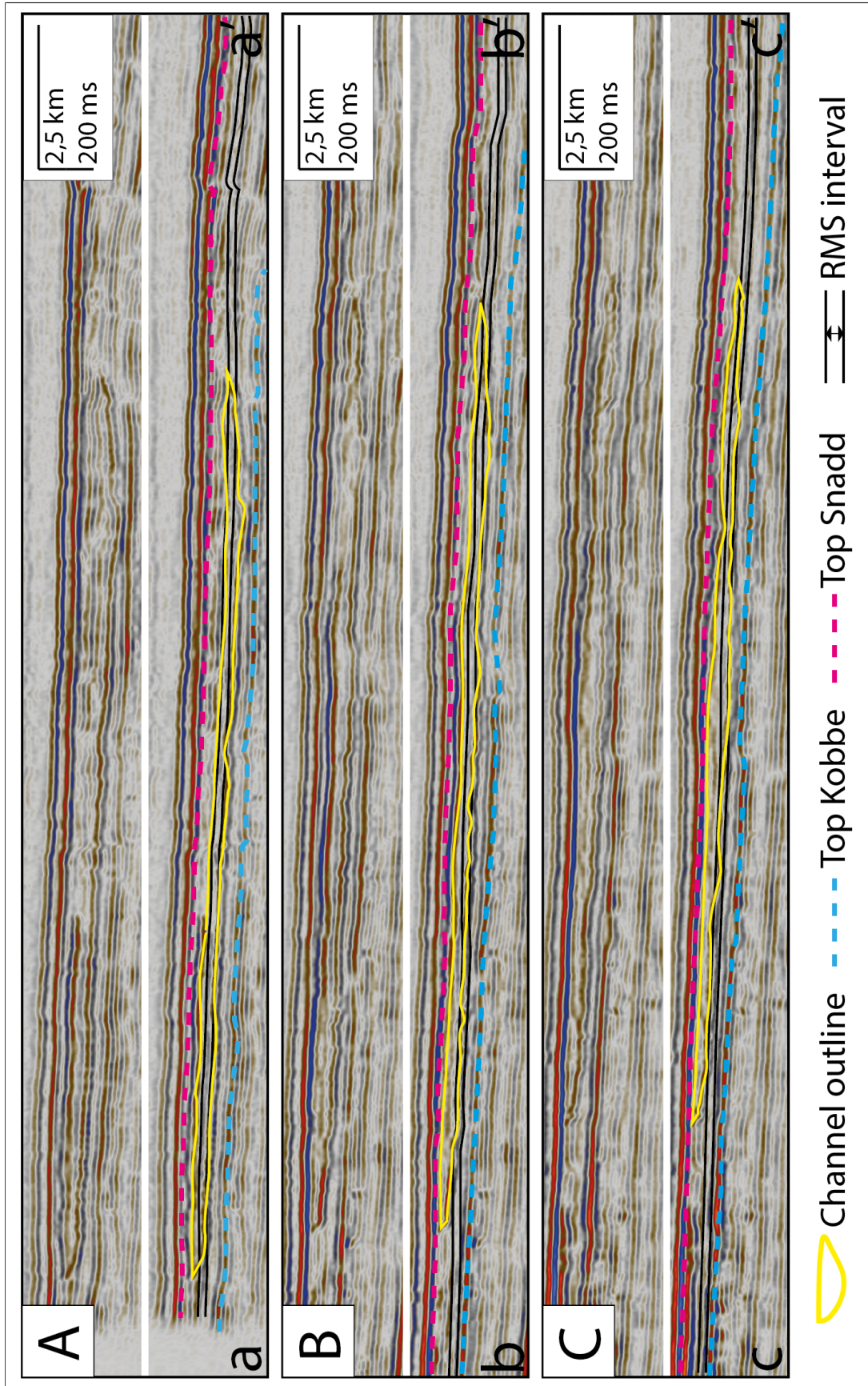


Figure 6.7: Seismic cross sections of a braided channel belt. The positions of the sections are indicated on map 2 in Figure 6.2. The RMS interval of map 2 is indicated by black lines. Note the visible channel shape and associated terminating reflectors from surrounding deposits along the channel boundary. (A) Cross section a-a'. (B) Cross section b-b'. (C) Cross section c-c'.

relatively deep channels, on the other hand, it is possible to observe cross sectional channel shapes and associated terminating reflectors representing surrounding deposits (e.g., [Figure 6.6B, C](#)).

6.3 Channel Measurements

In total 25 channels throughout the Snadd Formation have been measured with respect to their orientation, thickness and width. The channels indicate an overall WNW-ESE orientation ([Figure 6.8](#)). This trend has been interpreted to reflect the progradation of the delta system towards the west and northwest ([Figure 2.3](#)).

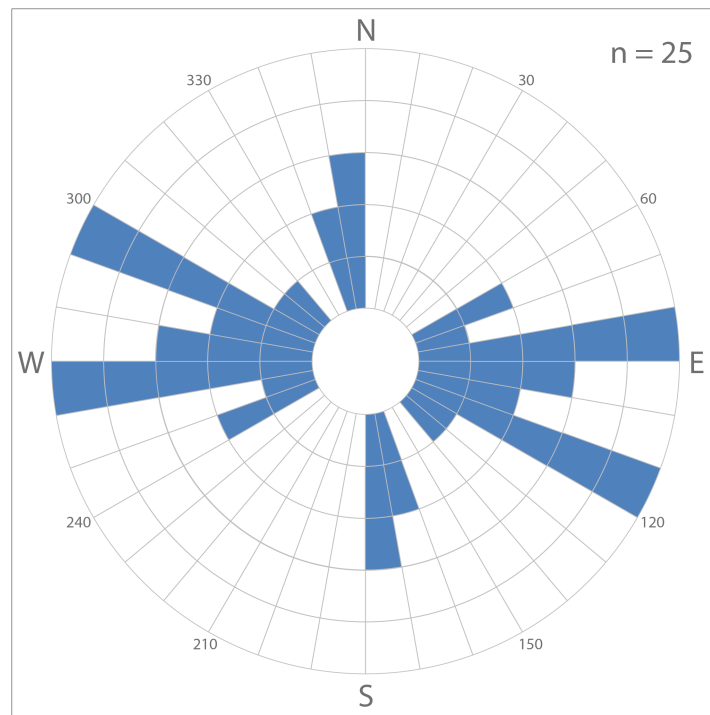


Figure 6.8: Rose diagram displaying the orientation of the measured channels in the Snadd Formation.

The width and thickness of the channels vary significantly. Width measurements vary between 100 m for channel fill deposits to 26,5 km for the widest channel belt (Guovca sandstone). Thickness measurements are limited by the vertical seismic resolution. However, the width-to-thickness plot ([Figure 6.9](#)) shows a broad correlation between width and

thickness of the channels, indicated by the coefficient of correlation ($R^2 = 0,7$) of the dataset's regression line.

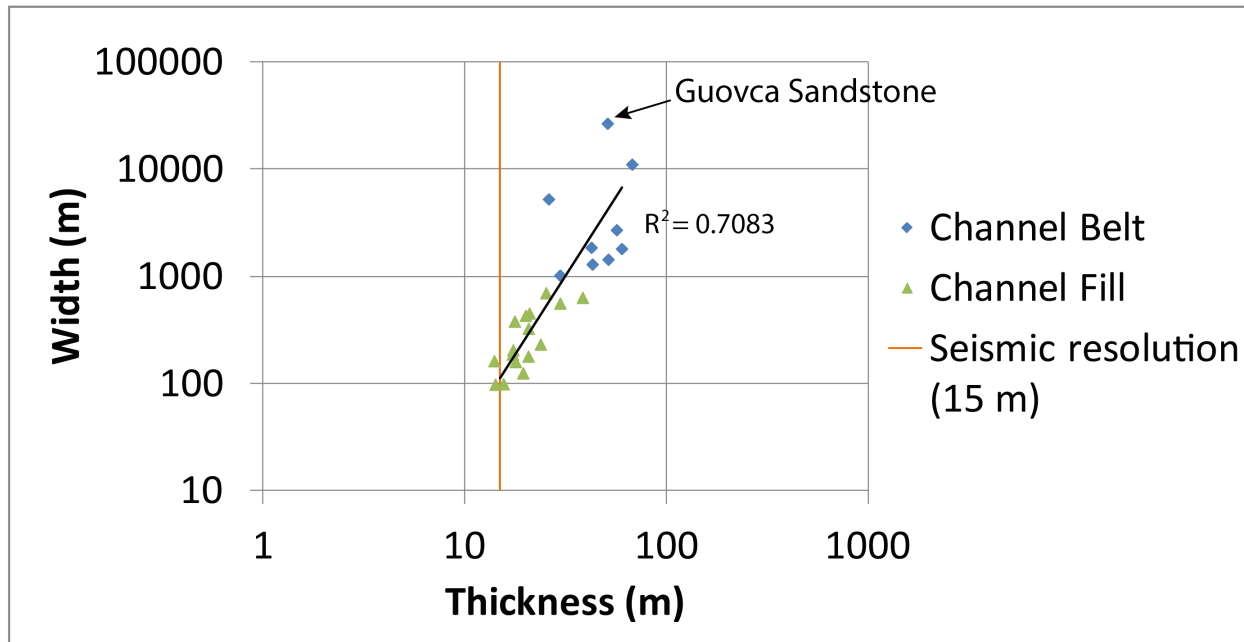


Figure 6.9: Cross plot of width vs thickness measurements of channels in the Snadd Formation. R^2 = coefficient of correlation.

6.3.1 Geometries of the Guovca sandstone

The geometries of the Guovca sandstone have been studied in more detail compared to the other channels observed (Figure 6.10). Measured geometries of the interpreted expansive point-bar are summarized in Table 6.1.

The sandstone's thickness was obtained from information from well 7131/4-1, rather than from manual measurements of seismic cross sections. The gamma-ray log of the Snadd Formation shows a rather thick interval (1036-1070 ms TWT) with values that are conspicuously lower than the rest of the formation (Figure 6.11). The seismic interval of the RMS amplitude map displaying the Guovca sandstone (Figure 6.10) coincides with the low gamma-ray value. It can therefore be concluded that the thickness of the low gamma-ray interval represents the thickness of the channel sandstone. Depth information from well 7131/4-1 indicates a thickness of 49 m for the sandstone. A conceptual sketch (Figure 6.12) of

the river that deposited the Guovca sandstone has been made based on the measured parameters in [Table 6.1](#).

Table 6.1: Measurement values of the Guovca channel-body. MBW = Meander Belt Width, BW = Bankfull Width, RL = Real Length, X = Shortest distance, RL/X = Sinuosity, SST = Sandstone Thickness.

MBW	BW	RL	X	RL/X	SST
26500 m	1500 m	59900 m	17600 m	3.4	49 m

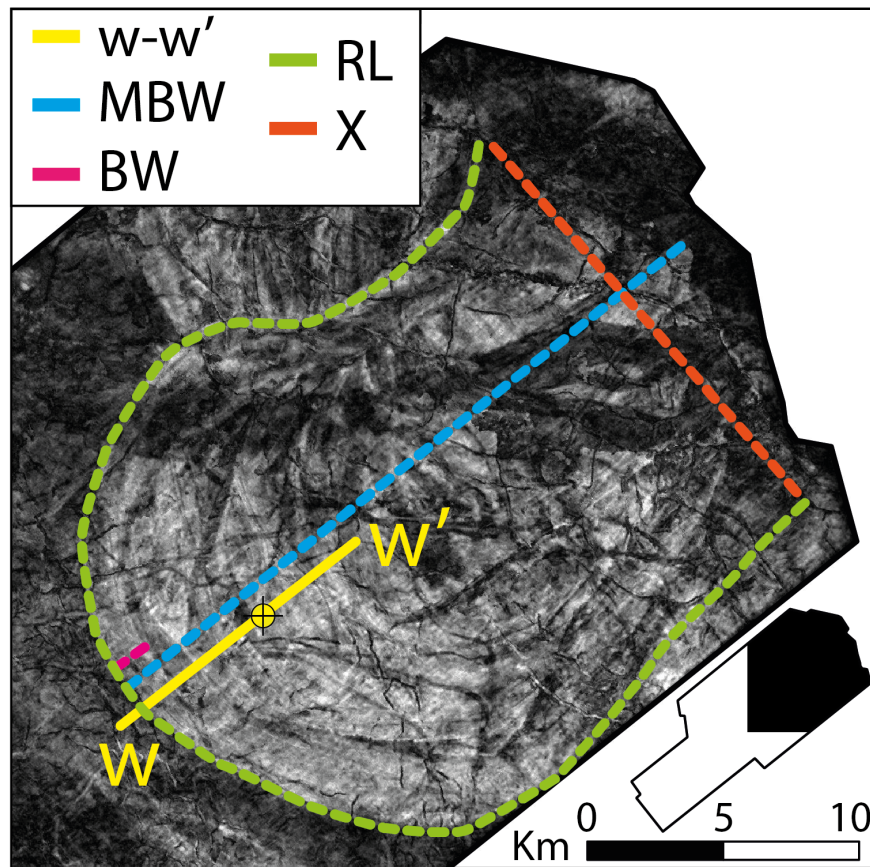


Figure 6.10: Outline of planform measurements ([Table 6.1](#)) of the Guovca channel-body. The cross section w-w' is presented in [Figure 6.11](#). MBW = Meander Belt Width, BW = Bankfull Width, RL = Real Length, X = Shortest distance.

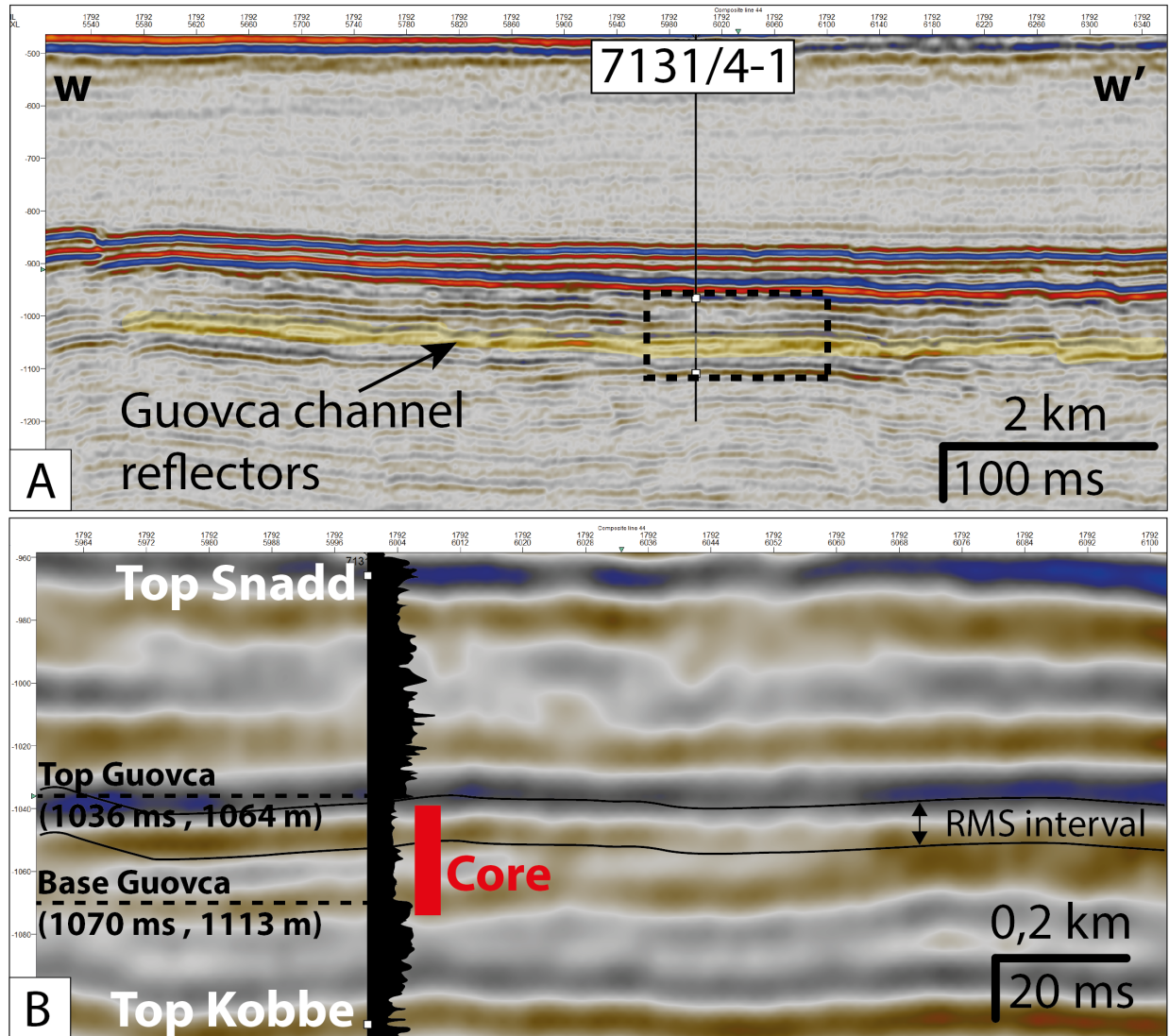


Figure 6.11: (A) The seismic cross section w-w'. Yellow area marks the Guovca channel reflectors. Well 7131/4-1 is displayed. Dashed square indicates the location of B. (B) The Snadd Formation around well 7131/4-1. The gamma-ray log is displayed indicating the location of the Guovca sandstone. Depth values, both in ms TWT and m, of the sandstone's base and top were retrieved from well information, and a thickness of 49 m was calculated. The seismic interval representing the RMS amplitude map in Figure 6.10 is indicated. The vertical position of the core presented in Chapter 7 is illustrated.

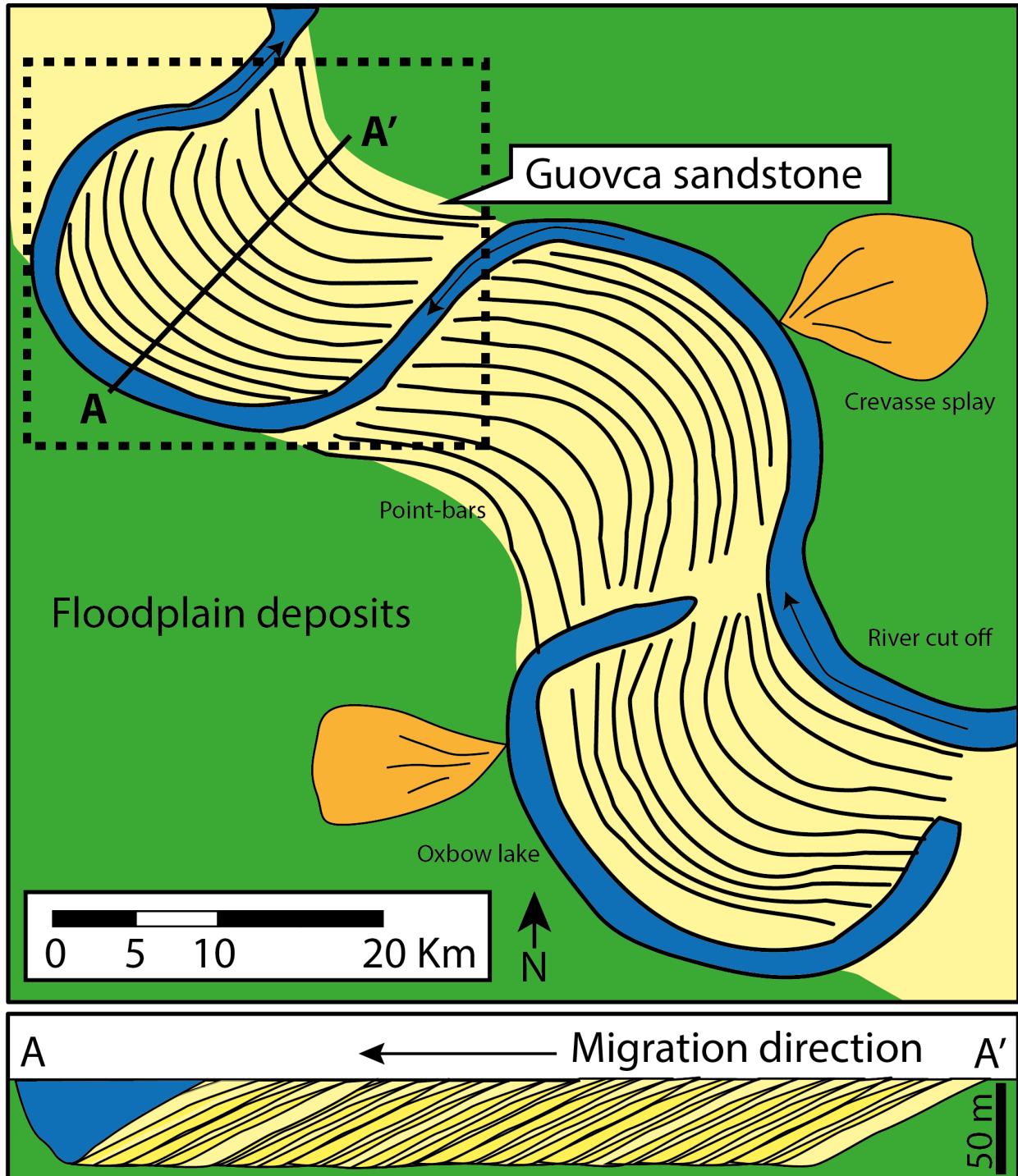


Figure 6.12: Conceptual sketch of the meandering river that deposited the Guovca sandstone. The dashed square roughly corresponds to the part of the channel deposits that is visible on RMS amplitude maps (e.g., [Figure 6.3E](#), [F](#)). The green part is floodplain deposits, whereas the yellow part is channel sands. The sandstone thickness is thought to correspond to the bankfull depth of the formative channel (discussed in [Section 9.4](#)).

7. Core Results

This chapter will present a sedimentological log of core 2 from well 7131/4-1 in addition to the corresponding gamma-ray log (Figure 7.2). The core is recovered from 1117.89 - 1070 m, from the Guovca sandstone (Figure 6.11), and has been sub-divided into intervals based on trends and similarities in order to make the description and interpretation easier to follow.

As mentioned in Section 6.1.1, the Guovca sandstone is interpreted to reflect a large point-bar deposit from a meandering river (Figures 6.12 and 7.1), which is also supported by the presence of typical fluvial facies in the presented core (Section 7.1).

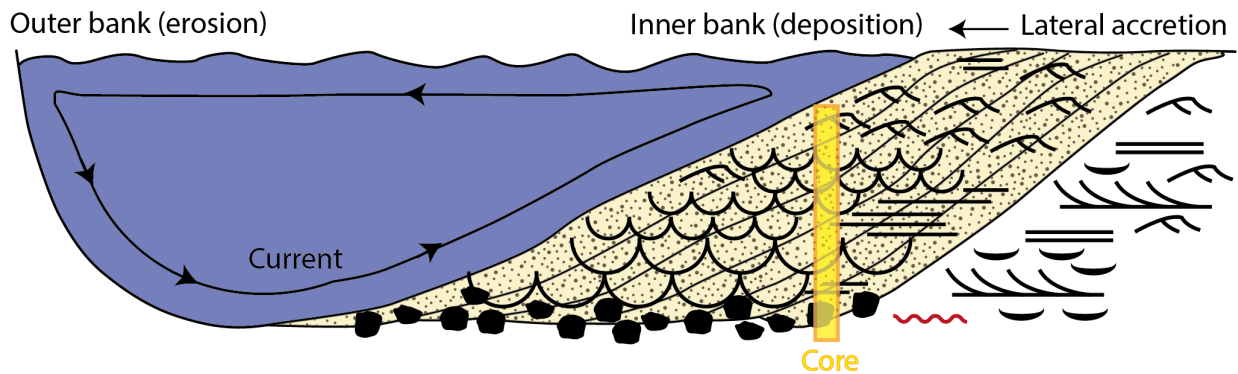


Figure 7.1: Conceptual sketch made of a point-bar deposit with a scoured base and associated sedimentary structures. The core is thought to reflect lateral accreted deposits from a meandering river as illustrated. The current is strongest when flowing down the outer bank and decreases when going up the inner bank, resulting in erosion and deposition, respectively. Legend for sedimentary structures can be found in Appendix B. The illustration is based on point-bar descriptions from Nichols (2009).

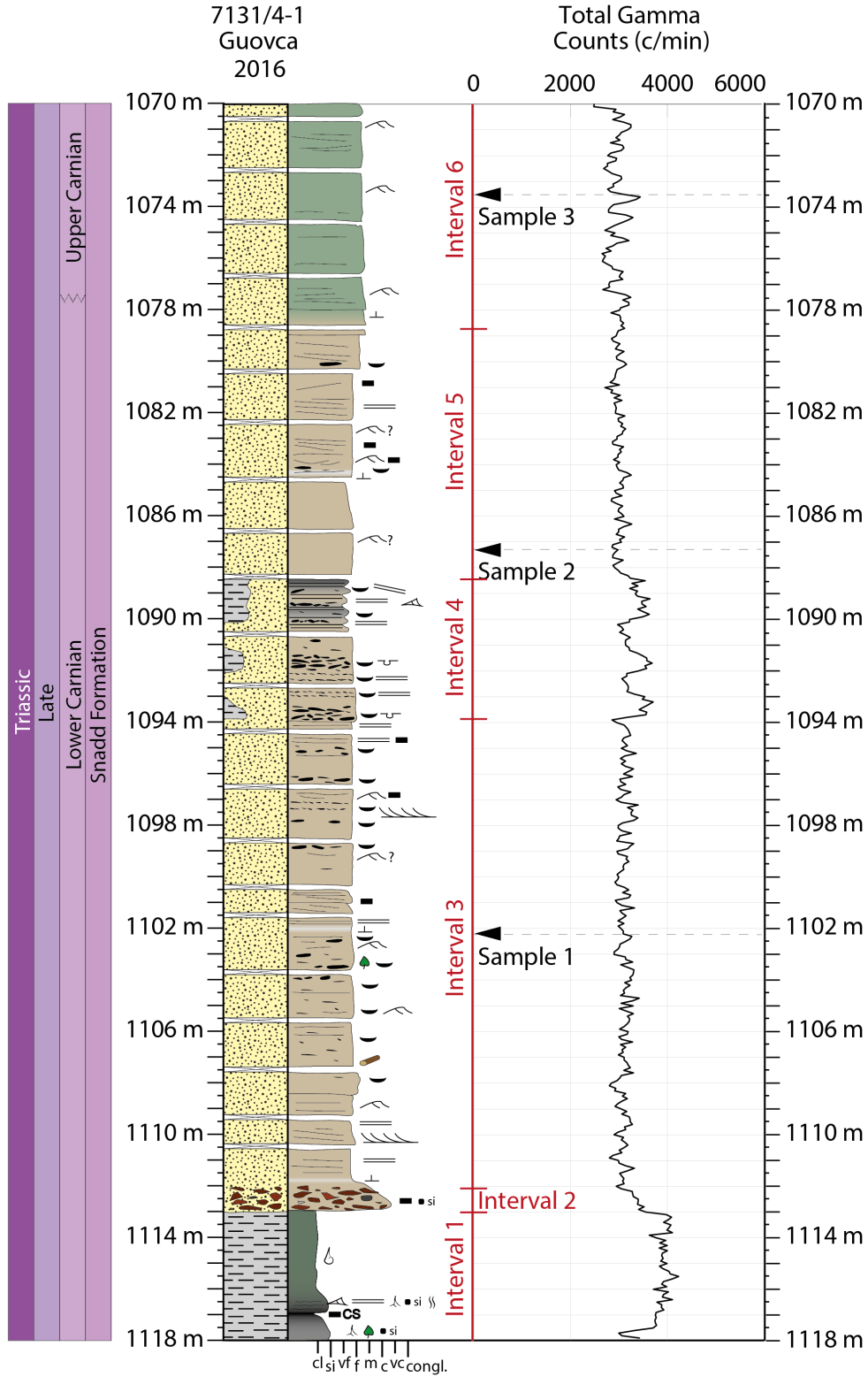


Figure 7.2: The sedimentological log of core 2 in well 7131/4-1, and the corresponding gamma-ray log. Depositional age is based on Statoil's palynological database. Interval sub-division and the position of collected samples are indicated. The colour of the grain size column try to visualize the observed colour change. A log-legend is presented in [Appendix B](#).

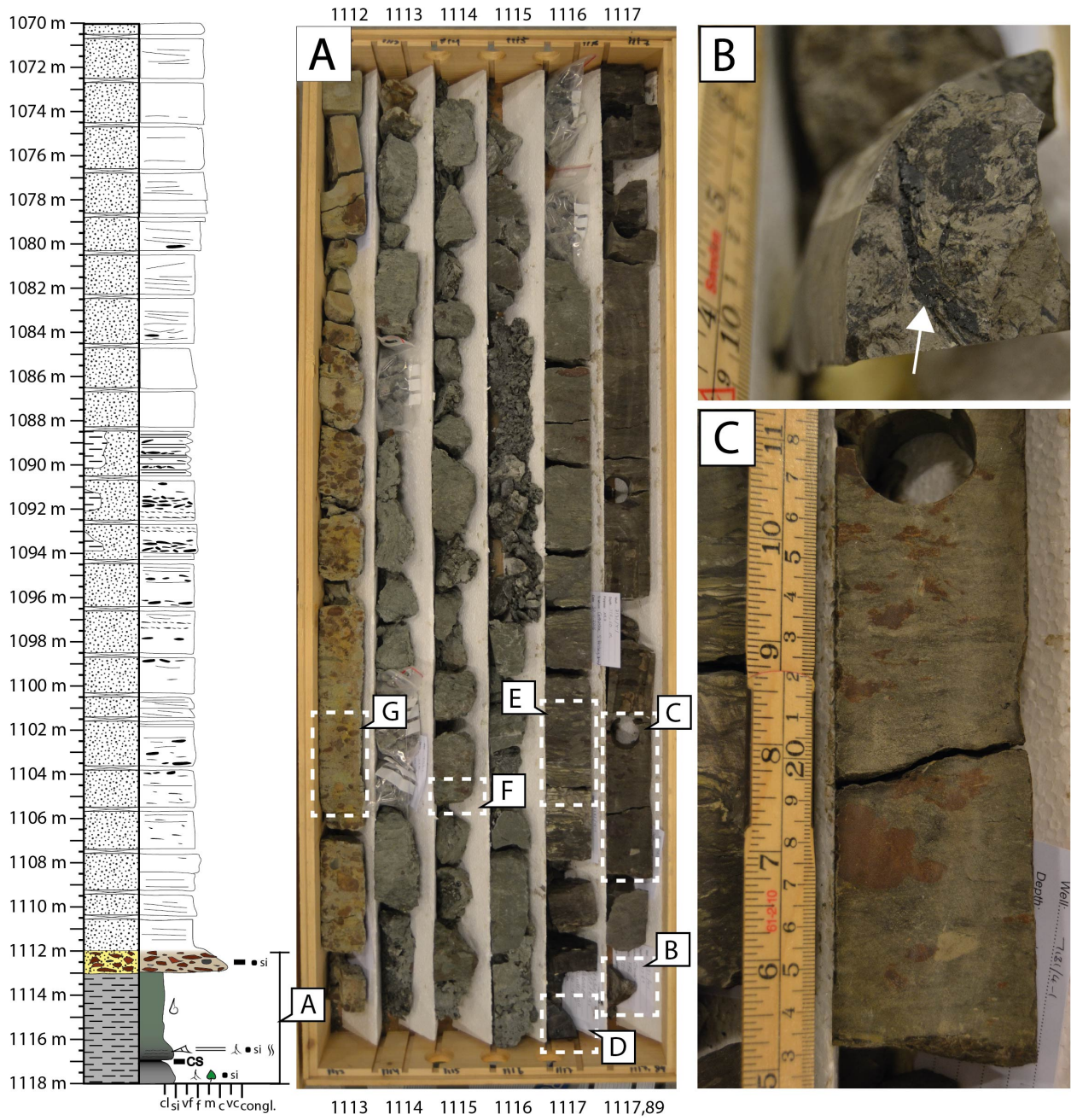
7.1 Description and Interpretation

Interval 1 (1117.89 – 1113.10m)

Description: Interval 1 (Figure 7.3) is dominated by silt- and mudstones. The lowermost metre consists of grey siltstone with no apparent sedimentary structures. Plant fragments are observed (Figure 7.3B) in addition to thin black cracks resembling rootlets and red-brown siderite mottles (Figure 7.3C). The overlying metre starts with 10 cm of black shale with coal fragments (Figure 7.3D) followed by a bioturbated, partly laminated siltstone (Figure 7.3E). The lamination is undulating. The colour of the lamination alternates between white, green and black. It is gradually replaced by a green-grey coloured, homogeneous mudstone that makes up the rest of the interval. Small white shell fragments that fizz with acid are observed in the mudstone (Figure 7.3F).

Interpretation: Interval 1 is interpreted to reflect floodplain deposits. Such deposits are typically fine-grained and bioturbated by land-dwelling organisms or plant roots, and plant fragments are common (Boggs, 2011). The association with fluvial sandstones in the overlying intervals supports the interpretation of a floodplain environment. The observed shell fragment may origin from a terrestrial shell bearing organism such as a gastropod. However, it may have a marine origin which could indicate a coastal influenced floodplain. Siderite is related to post-depositional cementation, and typically forms in organic-rich brackish to meteoric pore waters (Morad, 1998).

Gamma-ray log: The gamma-ray value for interval 1 (Figure 7.2) is relatively high (ca 4000 c/min) compared to the rest of the core. The lowermost part has a slightly lower value. The relatively high value of the gamma-ray log reflects the high content of fine-grained material. The silt content may explain the slightly higher gamma-ray value in the lower part.



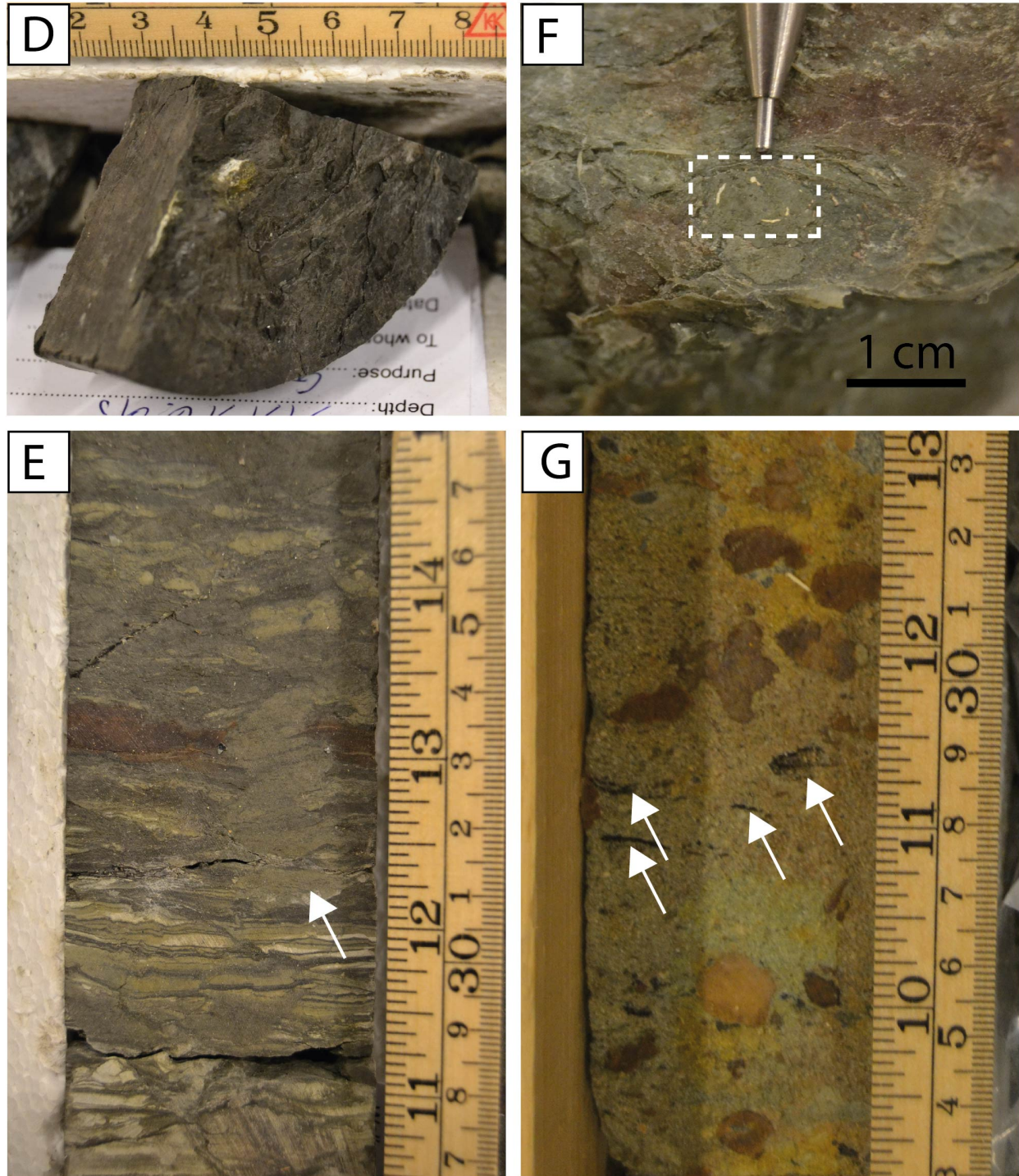


Figure 7.3: Photos and log (coloured part) of interval 1 and 2. (A) Overview of Interval 1 and 2 (1117.89 - 1112 m). Note the mud dominated character of interval 1 and the sharp erosive boundary to the conglomerate in interval 2. The position of photo B-G is indicated. (B) Coalified plant fragment indicated with an arrow. (C) Siderite mottles in siltstone. Note the lack of sedimentary structures, which could indicate intense bioturbation. (D) Coal shale. (E) Laminated siltstone that is moderately-intensely bioturbated towards the upper part. Arrow marks a vertical burrow. (F) Shell fragment in mudstone. (G) Matrix supported mud-clast conglomerate. The clasts have been sideritized. Arrows indicate coal fragments.

Interval 2 (1113.10 – 1112.10m)

Description: Overlying the mudstone is a sharp based, matrix supported conglomerate of 1 m with grey and brown coloured pebbles of mainly mudstone, but also some quartz (Figure 7.3G). Multiple mud-clasts have been siderite cemented. The pebbles vary in shape between angular and well rounded. The matrix consists of coarse to very coarse sand. There are traces of organic material within the matrix (Figure 7.3G).

Interpretation: Interval 2 is interpreted as the scoured base of the meandering channel belt that can be seen in Figure 6.10. The coarse grained material characterizing the interval probably reflects bedload carried and deposited in the deepest part of the channel where flow velocity is highest (Nichols, 2009). Remains of organic material are common in fluvial deposits (Boggs, 2011; Nichols, 2009). The inconsistent roundness of the pebbles may indicate a variable transportation time and/or distance, where round clasts have been transported further and for a longer time than angular clasts. Similar deposits to those in interval 2 were also observed during fieldwork in Fulmardalen (Figure 7.4).

Gamma-ray log: The gamma-ray response (Figure 7.2) on the transition from interval 1 to interval 2 displays a sharp boundary and a change to a lower value. The value decreases upwards throughout the whole interval. The gamma-ray log reflects a sudden change to a sand-dominated environment which commonly has a lower gamma-ray response than mud. The gradual decrease upwards is likely a consequence of a decreasing amount of mud-pebbles.

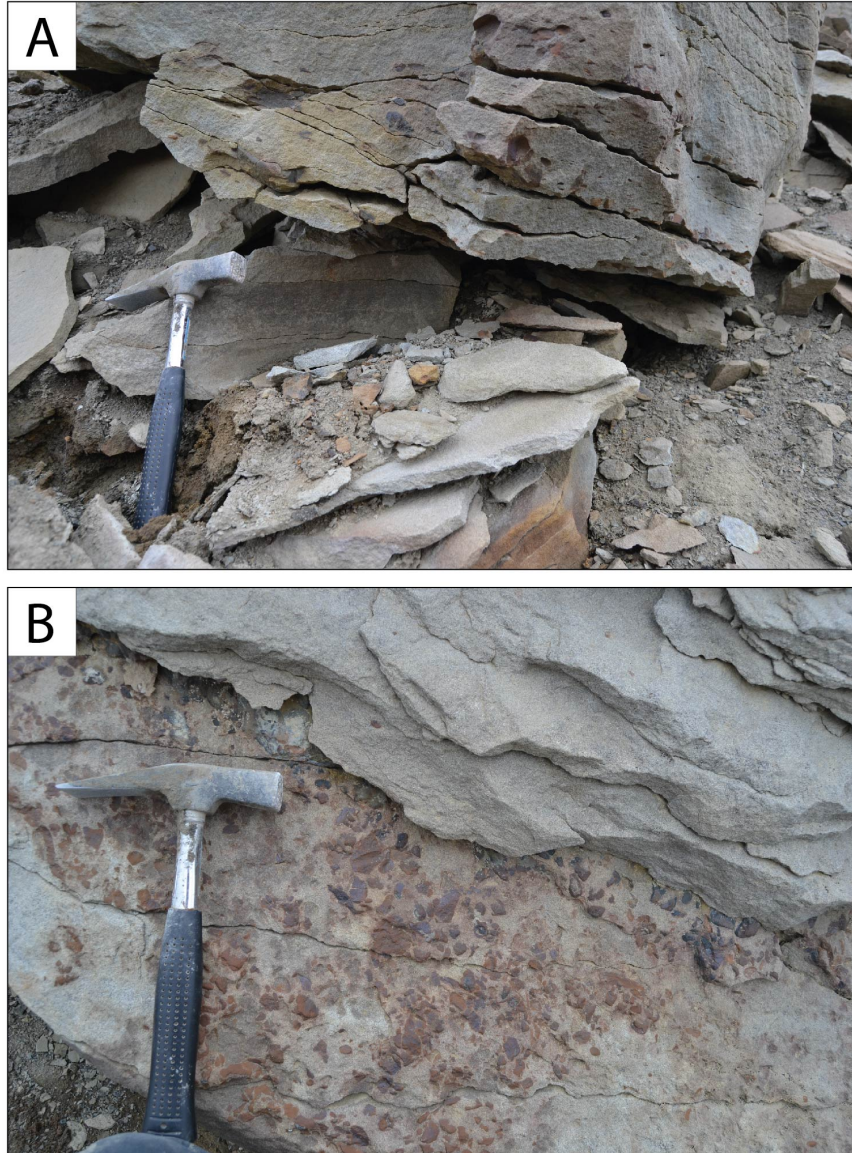


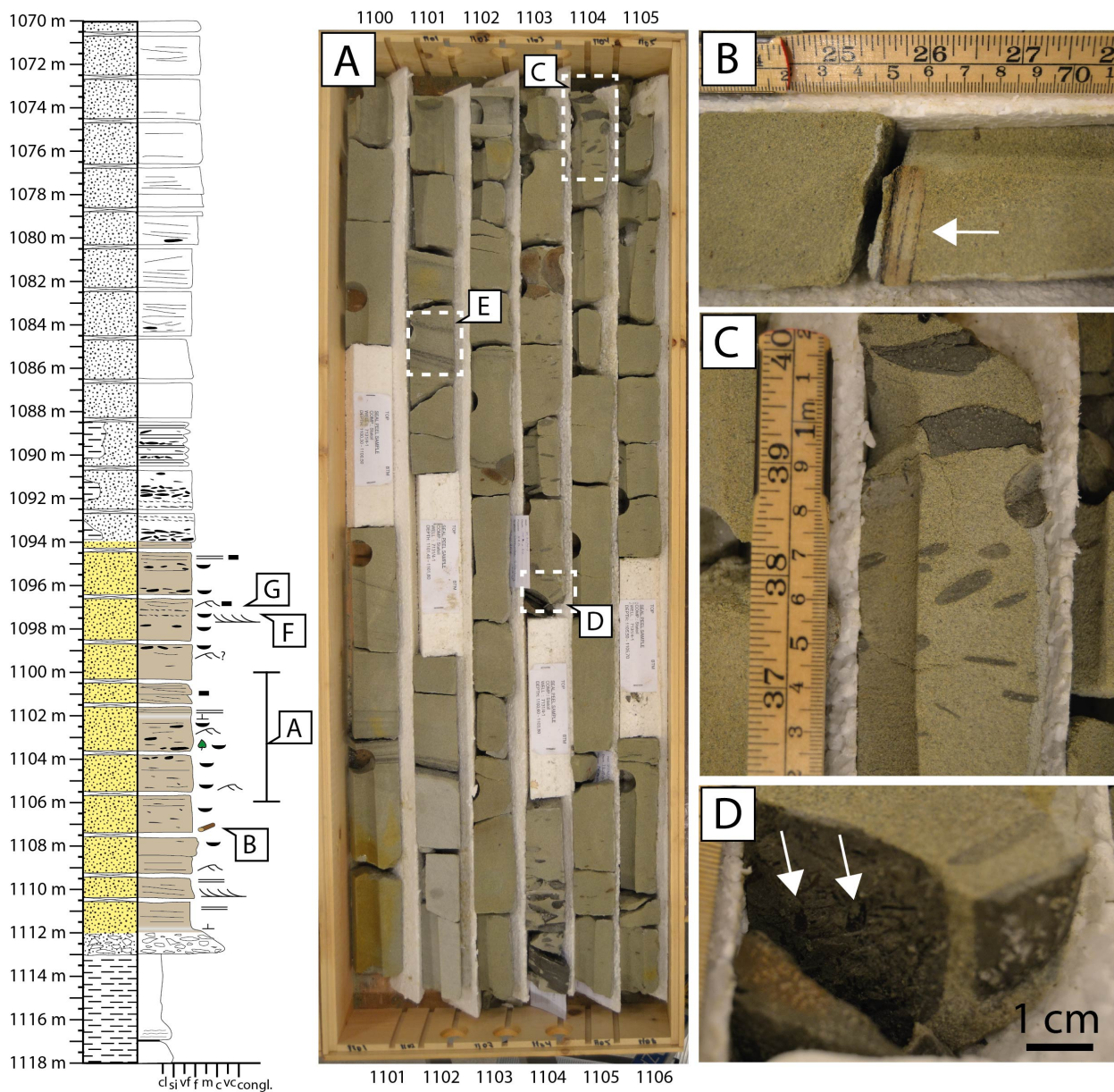
Figure 7.4: Mud clast conglomerate from Ryssen in Fulmardalen, illustrating how interval 2 in the core could look like in the field. Notice that the clasts are sideritized, similarly to the clasts in the core. (A) Side view. (B) Top view.

Interval 3 (1112.10 – 1093.90m)

Description: The conglomerate in interval 2 has a gradual upper boundary to a grey, fine grained sandstone that dominates interval 3 (Figure 7.5). The sandstone has a light grey colour at two levels, and acid reveals that these levels are carbonate cemented. When grain size variations are observed, it is within sharp based, small upwards fining sequences.

Sedimentary structures are enhanced by lamination of accumulated black coal debris and

small mud clasts (Figure 7.5E, F, G). Ripples, planar parallel lamination and trough cross-bedding are the dominating structures observed in addition to mud clasts. The mud clasts typically have an oblate shape with the longest axis being between 0.2 cm and 5 cm. Additionally, multiple clasts seem to be imbricated with the longest axis oriented sub-horizontally (Figure 7.5C). A plant fragment is observed within a mud clast at 1103.5 m (Figure 7.5D), and a wood fragment is found at 1107 m (Figure 7.5B). A sample for XRD analysis was taken from this interval at 1102.20 m and is further described in Section 8.1.



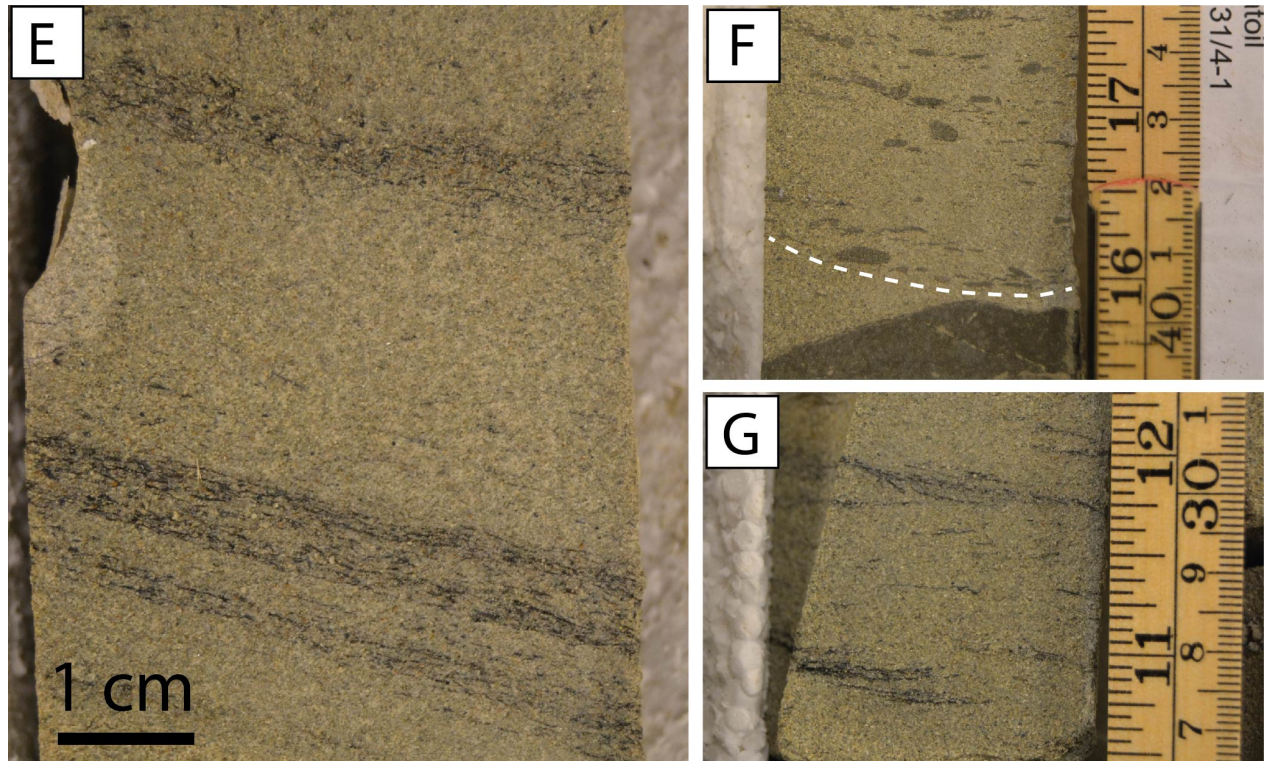


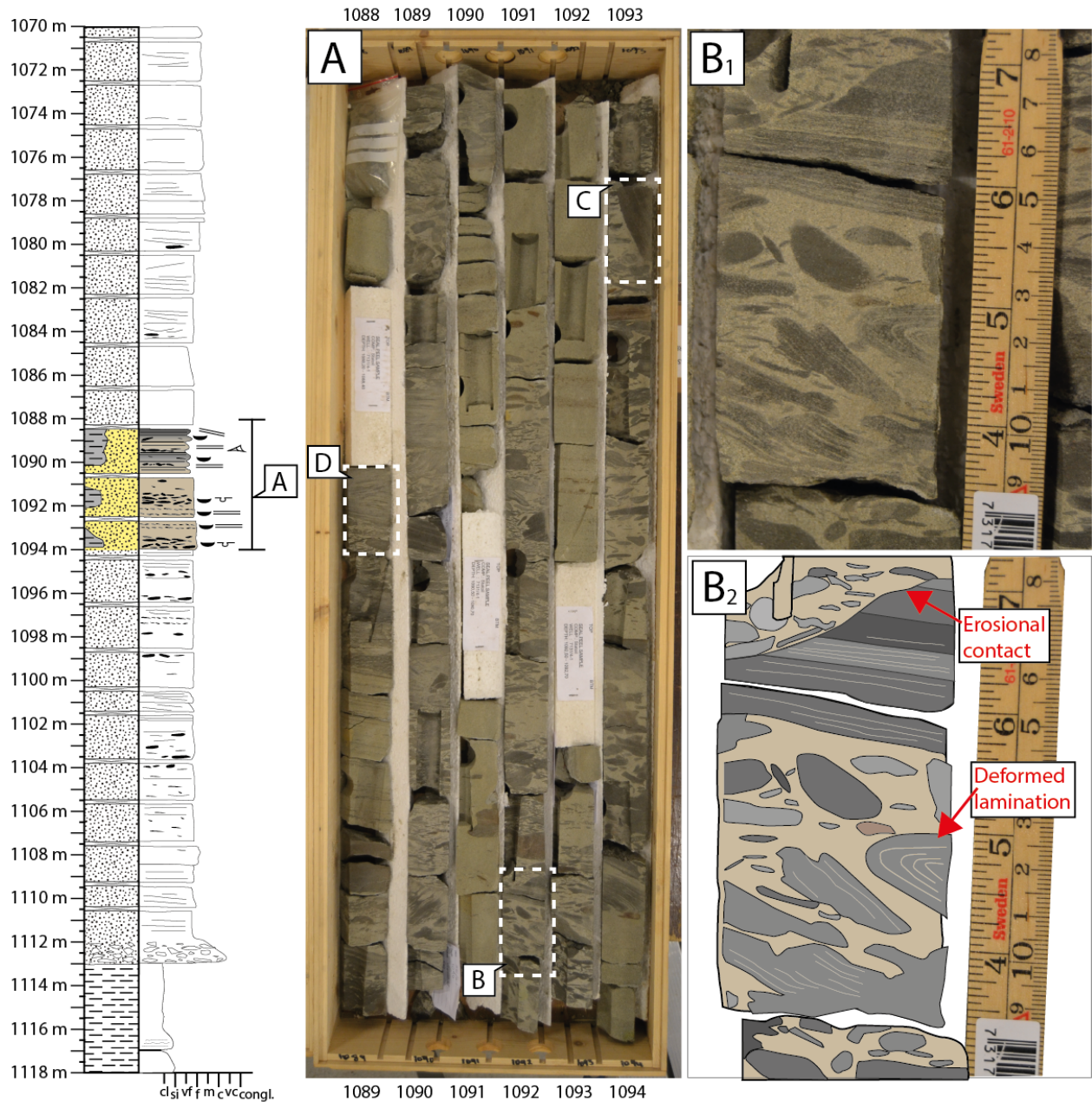
Figure 7.5: Photos and log (coloured part) of interval 3. The position of photo A-G is indicated in the log or in photo A. (A) Representative overview photo of Interval 3 (1106 - 1100 m). (B) Wood fragment indicated by an arrow. (C) Imbricated oblate mud clasts. Relatively speaking, the flow has gone from left to right. (D) Small plant fragments within a mud clast. (E) Coal debris enhancing planar parallel lamination. (F) Small mud clasts enhancing trough cross-bedding. (G) Coal debris enhancing ripple lamination.

Interpretation: Interval 3 is interpreted as sandstone deposited in a point-bar. Coarser material at the base (Interval 2), and progressively finer-grained material up the inner bank (Interval 3) is typical for a meander bend (Nichols, 2009). Moreover, laminated coal debris, wood and plant fragments, mud-clasts, imbrication, trough cross-bedding and planar-lamination interpreted as upper-flow-regime lamination, point towards a continental and fluvial origin (Nichols, 2009; Boggs, 2011; van den Berg et al., 2017).

Gamma-ray log: The gamma-ray log (Figure 7.2) of the interval displays values alternating around 3000 c/min. The relatively low value reflects the dominant sandstone content. The variation in gamma-ray log values is thought to reflect small grain size variations, where higher values may indicate higher clay-mineral content.

Interval 4 (1093.90 – 1088.40m)

Description: Interval 4 (Figure 7.6) is characterized by a mixture of fine grained grey sandstone and a high amount of dark grey and occasionally brown siderite cemented mud clasts. Heterolithic planar parallel lamination and cross-lamination are also common (Figure 7.6D), especially towards the top of the interval. The mud clasts are mostly rounded, have an oblate shape and are commonly imbricated with the longest axis oriented sub-horizontally. The clasts



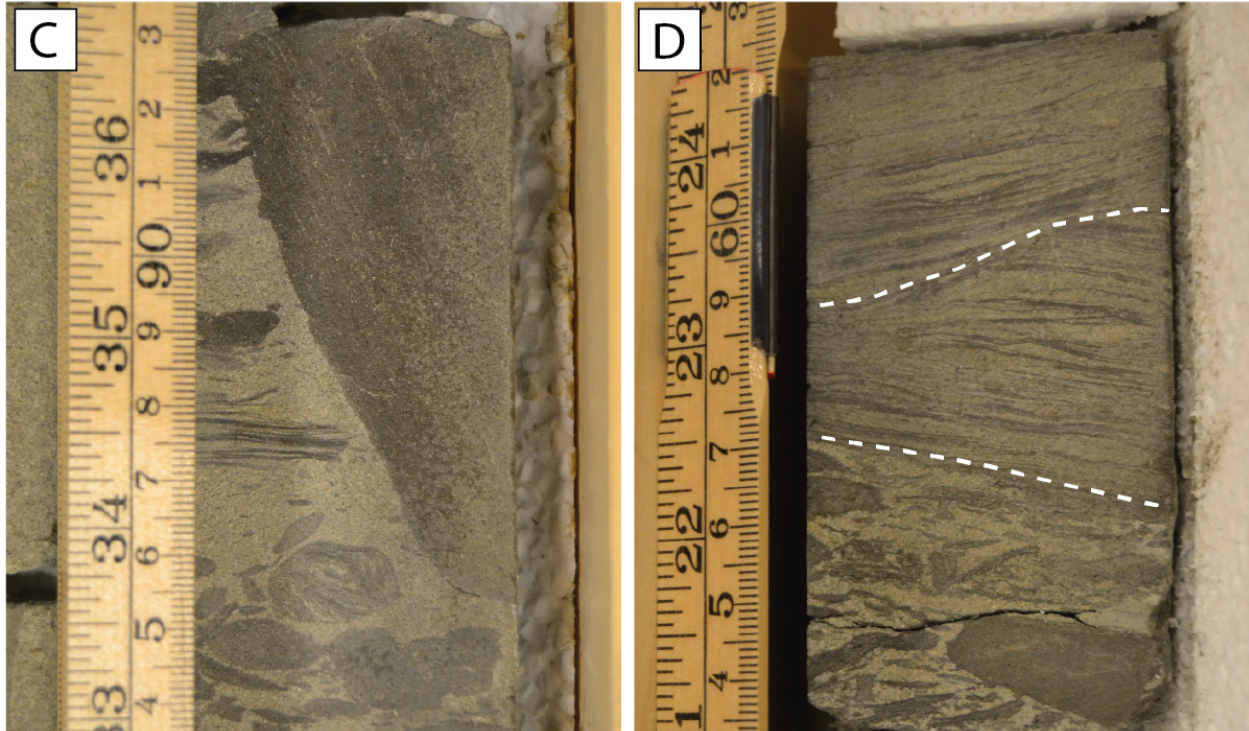


Figure 7.6: Photos and log (coloured part) of interval 4. (A) Overview photo of interval 4 (1094 - 1088 m). Note the mixture of sandstone and mudstone. The position of photo B-D is indicated. (B) Photo (1) and sketch (2) of mud-clasts and heterolithic lamination surrounded by sandstone. Note the deformed lamination within a mud-clast and the erosional contact above the heterolithic lamination. (C) A large mud-clast. (D) Cross-bedding indicated by dashed line in a heterolithic section.

often consist of deformed and folded heterolithic lamination (Figure 7.6B).

Interpretation: The high content of mud clasts within the sandstone is interpreted to be a result of an erosive current flowing over muddy material and tearing up pieces of it. Clay can be very cohesive, and as a consequence large clasts (e.g, Figure 7.6C) can be ripped up, transported and deposited when the current loses energy (Lucchi, 1995). Interval 4 may reflect repeated episodes of high discharge with enhanced erosion on the mud-dominated cut bank side of the meandering bend. Alternatively, there may have been a period of low discharge with deposition of mud and heterolithic sediments in the channel, followed by episodes of high discharge and currents tearing up the newly deposited fine-grained material. Observed heterolithic lamination associated with mud clasts with internally deformed lamination may reflect this scour and fill process (Figure 7.6B).

Gamma-ray log: The gamma-ray log (Figure 7.2) displays variable values, where high mud clast content coincides with high values, and pure sandstone coincides with low values.

Interval 5 (1088.40 – 1078.80m)

Description: Interval 5 (Figure 7.7) is dominated by fine grained grey sandstone and has the same characteristics as interval 3, but contains fewer mud clasts, in fact only two. These are relatively large (> 5 cm) and are siderite cemented (Figure 7.7B). The lower part appears very homogeneous and no clear sedimentary structures are observed. Further up, organic material is observed as single fragments and as coal debris aligned in planar parallel laminations (Figure 7.7C). A sample for XRD analysis was taken from this interval at 1087.30 m and is further described in Section 8.1.

Interpretation: The sparse mud clast content compared to the underlying intervals may indicate that the sediments are deposited in a slower flow in a shallower part of the channel. In other words, the sandstone may belong to the upper part of the point-bar deposits.

Gamma-ray log: The gamma-ray log (Figure 7.2) is similar to interval 3, with values around 3000 c/min. However, the log in interval 5 seems to be slightly more homogeneous, which could be explained by the few mud clasts.

Interval 6 (1078.80 – 1070m)

Description: Interval 6 (Figure 7.7), is characterized by a fine to medium grained sandstone with a green coloured argillaceous matrix. The colour change from grey to green sandstone is gradual (Figure 7.7A). Unlike the grey sandstone in the other intervals, the green sandstone contains neither mud clasts nor visible organic material. It appears massive with faint cross-lamination (Figure 7.7D). Ripples are also observed. A sample for XRD analysis was taken from this interval at 1073.50 m, and the results are presented in Section 8.1.

Interpretation: The sandstone is thought to reflect the same fluvial system as further down in

the core. Similar to the interpretations of interval 5, the absence of mud clasts may indicate deposition in the upper part of the point-bar. The green colour is interpreted in [Section 8.1](#).

Gamma-ray log: The transition from grey to green sandstone coincides with progressively more heterogeneous gamma-ray log values ([Figure 7.2](#)). The log is thought to reflect the relatively high clay mineral content between the sand grains.

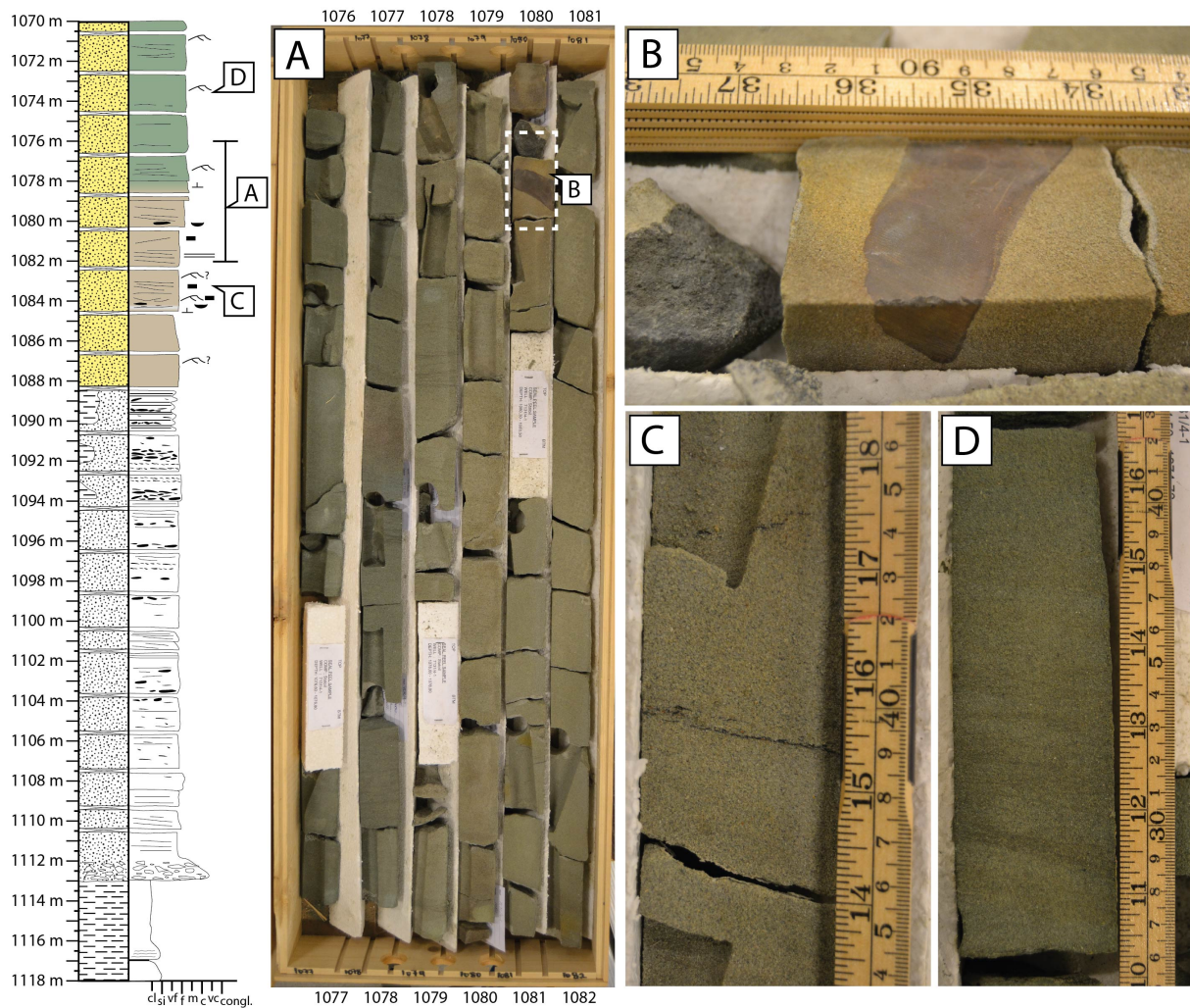


Figure 7.7: Photos and log (coloured part) of interval 5 and 6. The position of photo A-D is indicated in the log or in photo A. (A) Representative overview photo of the transition between interval 5 and 6 (1082 - 1076). Note the colour change from grey to green. (B) A large siderite cemented mud-clast in interval 5. (C) Grey sandstone belonging to interval 5 with coal debris enhancing planar parallel lamination. (D) Green sandstone with faint cross-lamination in interval 6.

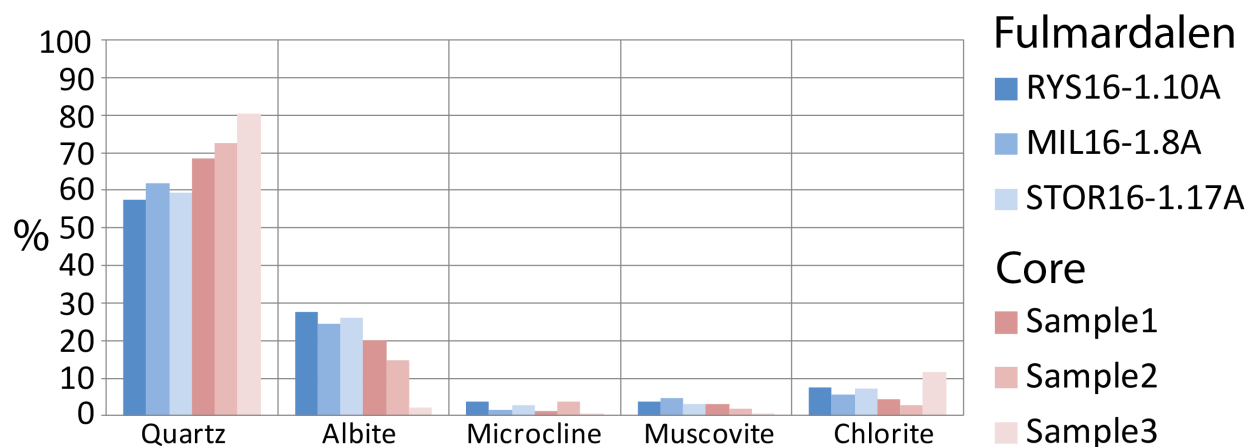
8. Laboratory Results

8.1 XRD

Table 8.1: Results of bulk (whole rock) analyses by XRD. The values represent percentage of bulk composition. The stratigraphical positions of the samples are indicated in their respective logs; Rys16-1.10A (Figure 5.10), Mil16-1.8A (Figure 5.13), Stor16-1.17A (Figure 5.16), Sample 1-3 (Figure 7.2).

	Rys16-1.10A	Mil16-1.8A	Stor16-1.17A	Sample 1	Sample 2	Sample 3
Quartz	57.54	61.74	59.21	68.49	72.66	80.24
Albite	27.48	24.53	26.16	20.11	14.84	2.06
Microcline	3.73	1.48	2.79	1.27	3.86	0.48
Muscovite	3.65	4.6	3.13	3.13	1.95	0.7
Chlorite	7.36	5.75	7.05	4.24	2.65	11.73
Calcite	0.24		0.2			
Kaolinite		1.89			1.9	
Siderite			1.46			
Halite				2.27	2.15	2.25
Hematite				0.49		2.54

Table 8.2: The table displays the percentage of the 5 most abundant minerals in the samples from Fulmardalen and the core, retrieved from XRD bulk analyses.



Observations

The XRD analyses reveal a relatively immature mineralogical composition for all the collected samples, both from the De Geerdalen Formation in Fulmardalen as well as from the Snadd Formation on the Finnmark Platform (Tables 8.1 and 8.2). The samples from Fulmardalen contain less quartz and more feldspar (albite and microcline) compared to the samples from the core, implying a slightly more mature mineralogy for the sandstone in the Snadd Formation.

The five most abundant minerals in the samples from Fulmardalen have roughly the same distribution by percentage (Table 8.2). The core samples, on the other hand, indicate a decreasing feldspar content upwards along with an increasing quartz and chlorite content. The green colour of the sandstone in the upper part of the core (Figures 7.2 and 7.7), represented by Sample 3, coincides with the relatively high content of chlorite.

Interpretations

The immature mineralogy of the samples is typical for the De Geerdalen and Snadd Formations (Bergan and Knarud, 1993; Mørk, 1999, 2013). The slightly more mature mineralogy in the core samples compared to those from Fulmardalen may reflect the energy level in the respective depositional environments. The energy level in the shallow marine shoreface environment that prevailed in Fulmardalen may have been more variable than in the fluvial channel on the Finnmark Platform, resulting in the preservation of more immature minerals, such as feldspar, muscovite and chlorite.

Diagenetic processes, such as dissolution and precipitation of minerals, may also contribute to the mineralogical differences observed. The increased chlorite content and the associated low feldspar content in the upper part of the core, is thought to be a result of precipitation from porewaters and dissolution, respectively. Chlorite is a green mineral, and the change from grey to green sandstone upwards in the core is likely a result of increasing chlorite cement. Humphreys et al. (1989) try to determine the origin of chlorite cements in

some Triassic fluvial and marginal marine sandstones in the Noth Sea. The most satisfactory explanation for the occurrence of chlorite in the fluvial sandstones is by direct precipitation from porewaters during burial with dissolution of feldspar, mica and chlorite grains supplying most of the necessary chemical components (Humphreys et al., 1989). The same process may have occurred in the fluvial sandstone in the Snadd Formation. If true, the chlorite is not constrained by the original depositional environment.

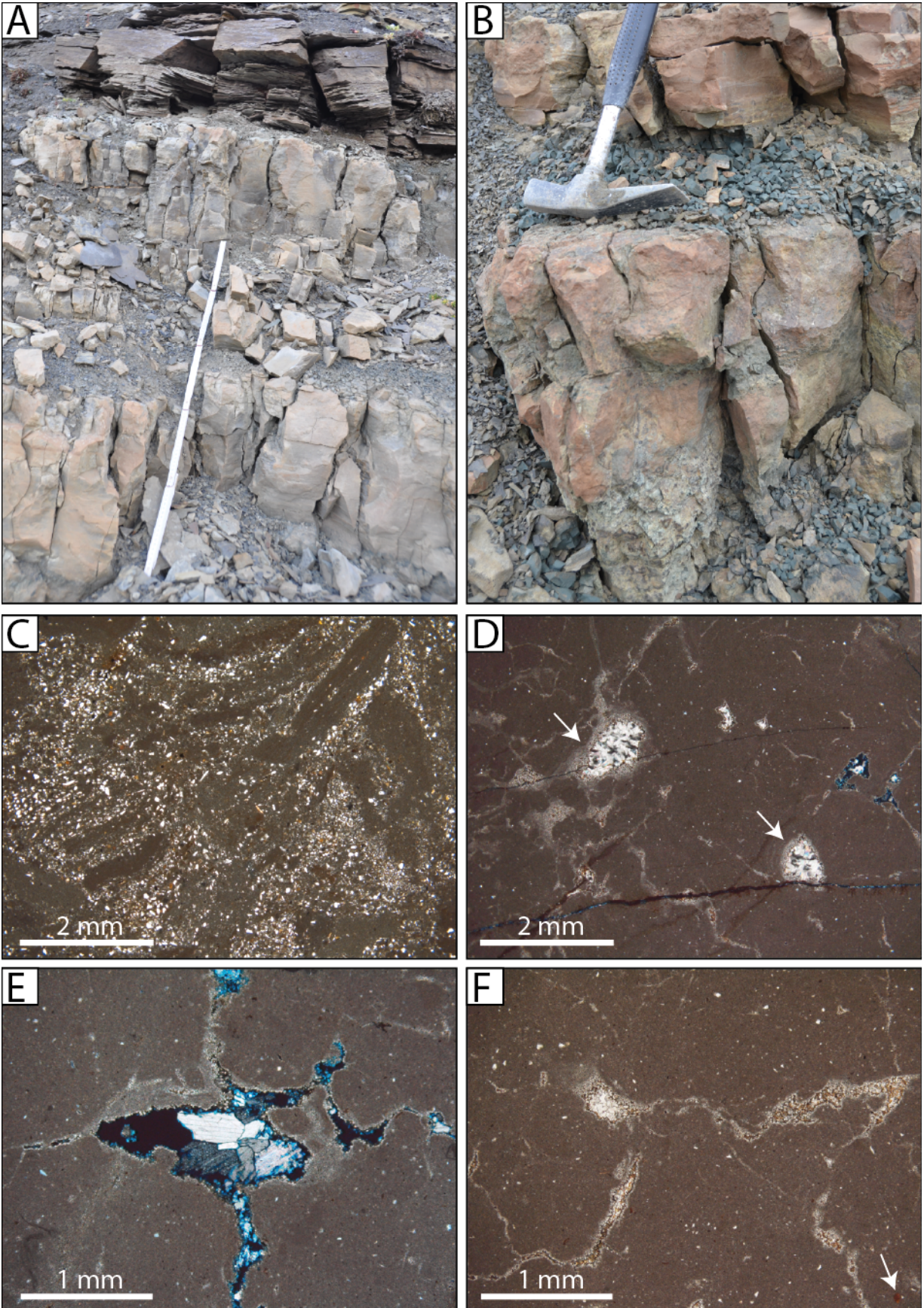
8.2 Optical microscopy

In order to investigate potential calcrete units from Fulmardalen, two petrographic thin sections were made from two separate carbonate units within the Isfjorden Member. One of the samples was collected from Milne Edwardsfjellet (Mil16-1.14A; Figure 5.13), while another was collected from Ryssen (Rys16-1.23A; Figure 5.10). Thin section analyses of calcrete units from the Isfjorden Member have also been presented in (Haugen, 2016). Typical microfeatures from calcretes have been described by (Alonso-Zarza and Wright, 2010), where the features are sub-divided into alpha- and beta microfabrics.

Alpha-microfabrics are non-biogenetic features that form in supersaturated soil solution (Haugen, 2016), and is typically expressed as a groundmass of crystalline carbonate. The fabrics are thought to form as a result of carbonate replacement, recrystallization and precipitation of carbonate in pores (Alonso-Zarza and Wright, 2010; Haugen, 2016). Beta-microfabrics are mainly formed by biogenetic processes (Alonso-Zarza and Wright, 2010).

Thin section analyses of the samples from Fulmardalen (Figure 8.1) indicate the presence of both alpha- and beta-microfabrics. All samples show a groundmass of micrite which is interpreted to be a result of the aforementioned processes forming alpha-microfabrics.

Additional beta-fabrics are thought to be present, but are less abundant. Potential alveolar structures have been interpreted in the sample from Milne Edwardsfjellet (Figure 8.1C). Such structures are mainly a product of fungal activity related to roots (Haugen, 2016). Other structures observed that may have formed by biogenic processes are coated grains. These



structures, as seen in the samples from Fulmardalen, are interpreted to have formed as a result of precipitation of micrite around an organic substrate (like a root) that was later oxidized, leaving a void where sparitic calcite could grow (Figure 8.1D, E, F).

Müller et al. (2004) studied pedogenetic (soil forming) mud aggregates from dryland river systems in the North Sea. The study distinguishes between in-situ mud aggregates formed by soil processes in paleosols and aggregates that were reworked on the floodplain. Reworked beds of floodplain mud-rocks often loose internal aggregate texture and get a more massive and structureless appearance, and a heterogeneous appearance in thin section. In-situ formed beds, on the other hand, are characterized by mudrock aggregates with the same internal texture, separated by calcite cement (Müller et al., 2004). The calcrete from Ryssen has a relatively homogeneous texture (Figure 8.1D, E, F), which may imply that it is in-situ. However, the sample from Milne Edwardsfjellet (Figure 8.1C), has a more heterogeneous texture, and could represent reworked floodplain deposits rather than alveolar structures.

Observations from thin sections and outcrops from Fulmardalen are similar to those described from previously interpreted calcrete deposits in the De Geerdalen Formation by Haugen (2016). The calcrete observations of Haugen (2016) were restricted to Spitsbergen, with the best developed calcretes found in the west (at Deltanaset, see Figure 9.1). Haugen (2016) suggests that this trend, together with more frequently observed coal seams in the east, point towards lateral semi regional variations in paleomoisture, with more arid conditions prevailing in the west. The outcrops from Fulmardalen are less developed than those described from Deltanaset, and the present study supports the interpretations of Haugen (2016) of a lateral

Figure 8.1: Calcrete from Fulmardalen. Cross-polarized light = XPL. Plan-polarized light = PPL. (A) Calcrete from Milne Edwardsfjellet where sample Mil16-1.14A was taken. (B) Calcrete from Ryssen where sample Rys16-1.23A was taken. (C) Potential alveolar structures in beta-microfabrics in Mil16-1.14A. PPL. (D) A groundmass of micrite (alpha-microfabrics) in Rys16-1.23A. Additional irregular shaped patches of slightly coarser micritic calcite are present. These may have precipitated around an organic substrate that was later oxidized, creating a void that was later filled with sparitic calcite. XPL. (E) Large calcite crystals filling a void in Rys16-1.23A. Note the micritic grain coating. XPL. (F) Micritic groundmass (alpha-microfabrics) and voids filled with sparitic calcite in Rys16-1.23A. Arrow indicates a patch of brown material interpreted as organic remains. PPL.

←

variation in the conditions controlling calcrete formation. A western uplift, causing better drainage of the soil, has been suggested as a possible explanation to the lateral trend (Haugen, 2016). Alternatively, paleotopography may have caused local variations in precipitation patterns. It could also indicate that calcretes of the Isfjorden Member on Spitsbergen were formed relatively far inland, further away from a more humid coastal climate.

8.3 Rock-Eval analysis

A relatively distinct dark shale layer can be correlated between Milne Edwardsfjellet, Dyrhø, Ryssen and Storfjellet in Fulmardalen. The shale occurs within a succession that has been interpreted to mainly display delta plain facies in the Isfjorden Member, where a lacustrine, lagoonal or marginal marine origin would be logical. However, also marine flooding surfaces are found at several levels in the De Geerdalen Formation. A Rock-Eval analysis was performed on two samples from the dark shale, at Ryssen (Rys16-1.28B; Figure 5.10) and Dyrhø (Dyr16-1.19B; Figure 5.6), with the purpose of obtaining information about the depositional environment. The results of the analysis can be found in Appendix E.

The hydrogen index (HI) and oxygen index (OI), retrieved from the Rock-Eval analysis, can be used as a measure to describe the quality of the organic matter (kerogen type) in the samples. Kerogen type I typically originates from algal material in lacustrine and lagoonal environments, type II kerogen from marine plankton, while type III is mainly derived from terrestrial woody material (Langford and Blanc-Valleron, 1990).

Plotting the derived OI and HI against each other in a van Krevelen diagram indicates a mixture of type II and III kerogen for the samples from Fulmardalen (Figure 8.2). However, both samples plot in the left corner of the diagram, close to where the van Krevelen curves converge. Moreover, the positions of the curves are approximate. The cross plots of the samples should, in other words, be treated with care and not be conclusively assigned to one kerogen type or another. The organic material in both samples has a very low OI, which is typical for algal derived material. It is possible that the samples reflect algal (kerogen I)

material with influence of terrestrial (kerogen III) material, forcing the cross plots towards the kerogen III type in the van Krevelen diagram.

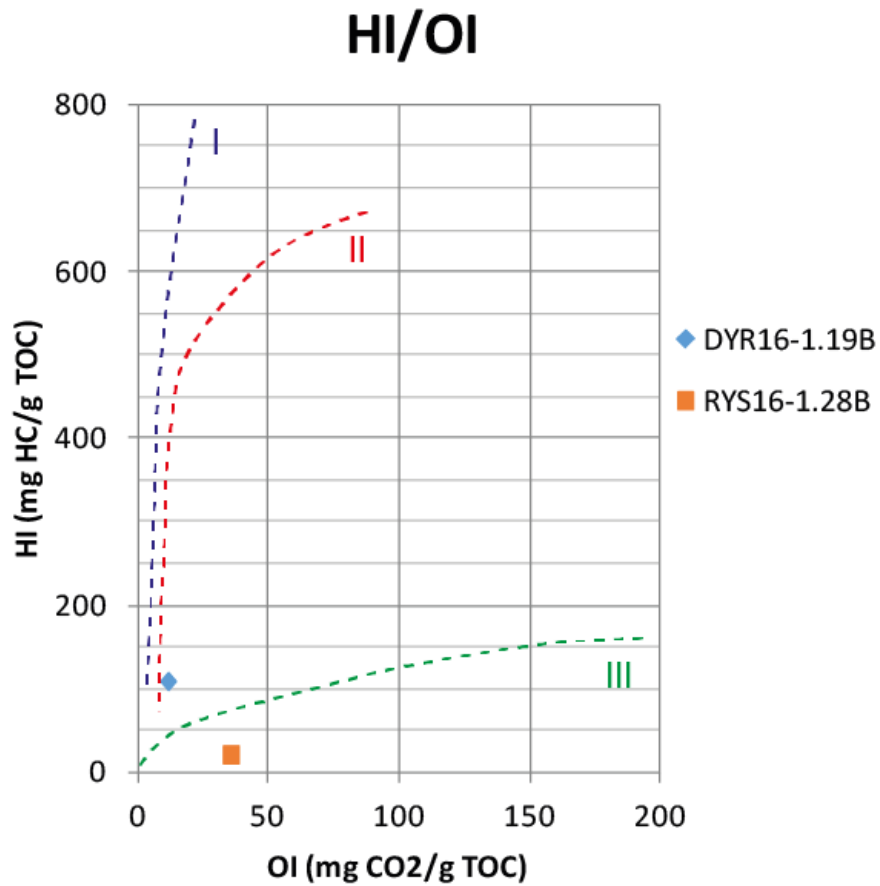


Figure 8.2: Plot of Oxygen Index (OI) vs Hydrogen Index (HI) for the samples from Fulmardalen. Van Krevelen curves have been added indicating the zones of different kerogen types (I-III).

9. Discussion

The following chapter will present a discussion on the implications of the observations from the De Geerdalen in Fulmardalen and from the Snadd Formation on the Finnmark Platform.

In [Section 9.1](#), a modern understanding of deltaic sequences and the process that control them will be discussed. [Section 9.2](#) discusses the facies distribution in Fulmardalen, whereas [Section 9.3](#) extend the discussion to a more regional context, where the findings from Fulmardalen have been attempted to be fit into the established depositional models of the De Geerdalen Formation from other areas of Svalbard ([Figures 9.1](#) and [9.2](#)). Finally, [Section 9.4](#) discusses the findings from the Snadd Formation, and the observed channels will be compared to other ancient and modern fluvial systems.

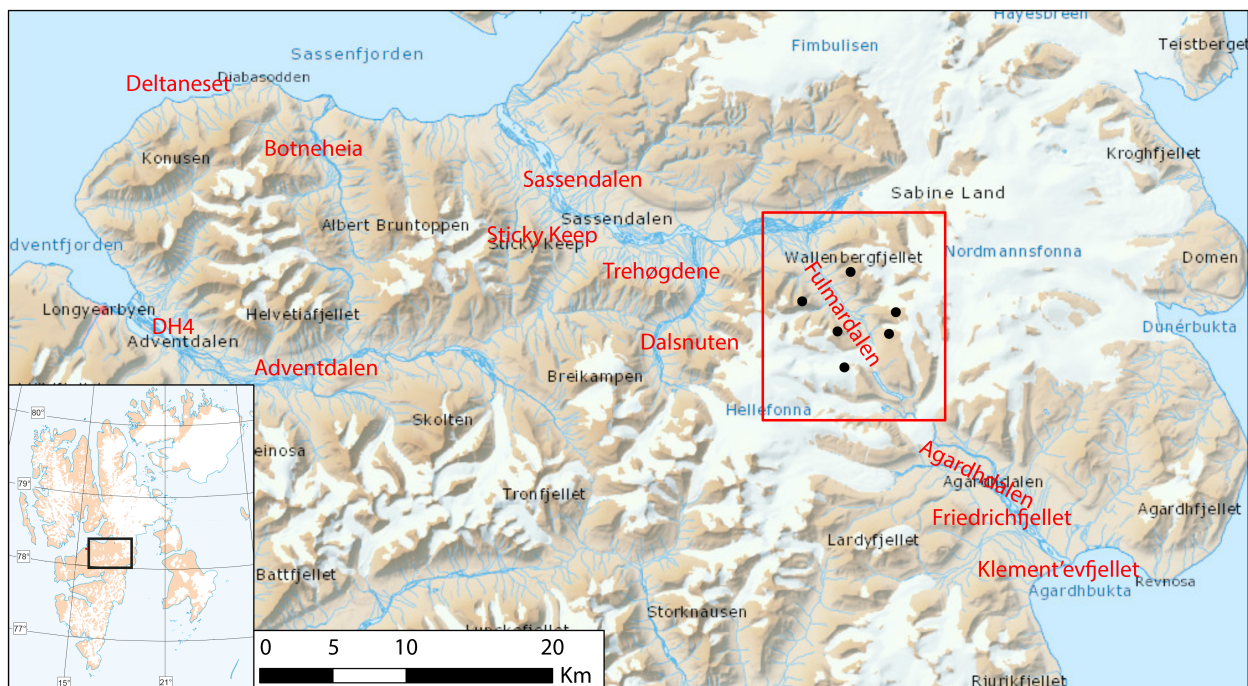


Figure 9.1: Map of central and eastern Spitsbergen. Relevant place names for the discussion are marked in red. The red square encloses Fulmardalen ([Figure 5.1](#)). Base map retrieved from Norwegian Polar Institute.

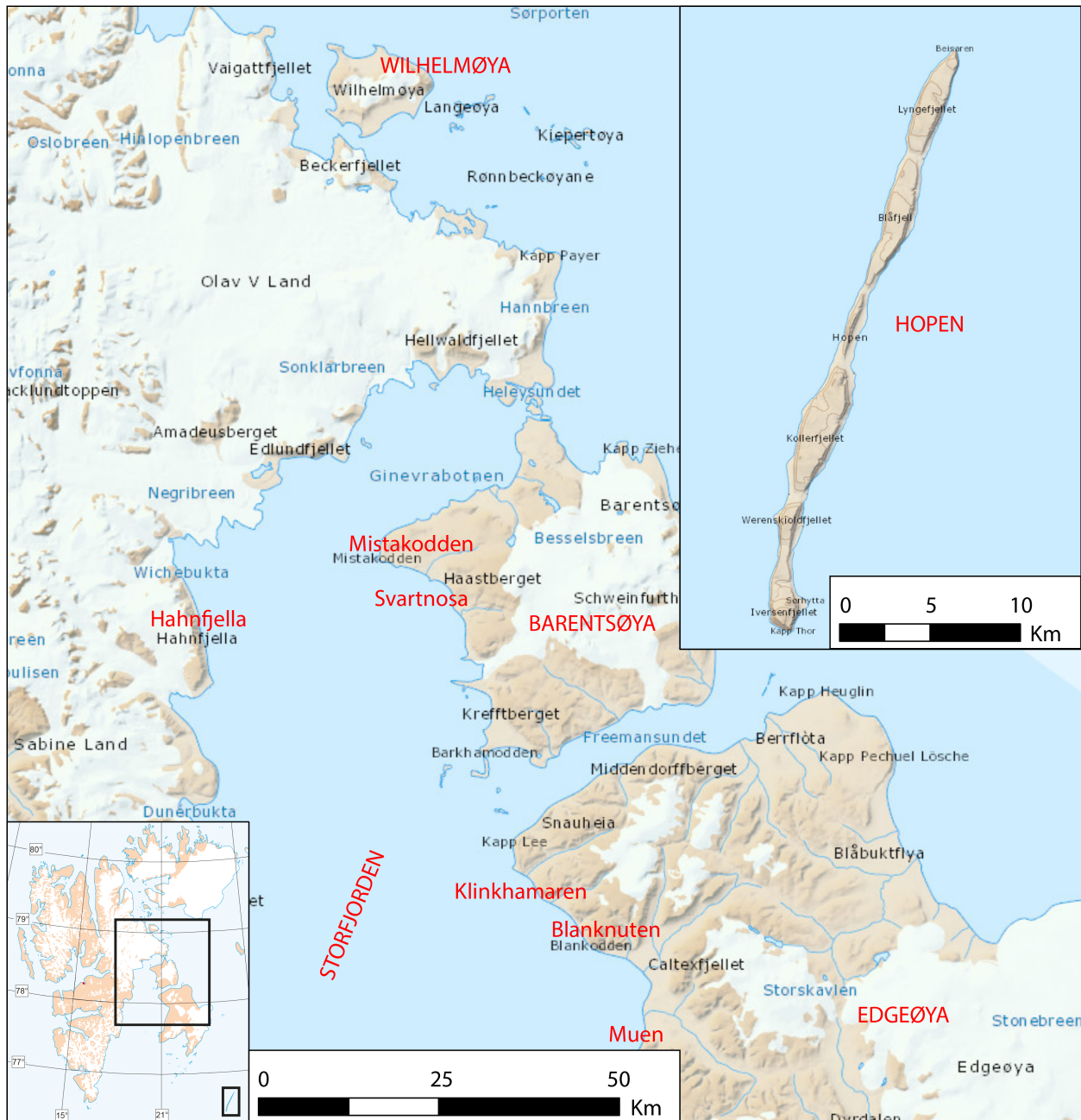


Figure 9.2: Map of selected areas from eastern Svalbard. Relevant place names for the discussion are marked in red. Base map retrieved from Norwegian Polar Institute.

9.1 Delta classification and deltaic sequences

Deltas are often regarded as the single largest repository of sediment in sedimentary basins (Miall, 2016). Delta protuberances form at shorelines where rivers enter standing bodies of water and supplies sediments at a rate that is too high for the basinal processes, such as waves and tides, to redistribute (Elliott, 1986; Bhattacharya, 2006). In that sense, all deltas may be regarded as river-dominated and regressive in nature (Dalrymple, 1999), but the morphology and facies architecture of a delta is also largely dependent on the proportion of wave, tide and river processes, depth of the sedimentary basin, salinity contrasts between the river water and the basinal water, sediment discharge and sediment grain size (Reading and Collinson, 1996; Bhattacharya, 2006).

Several classification schemes for differentiating between delta-types have been proposed. A tripartite classification scheme, which classifies deltas based on the relative importance of fluvial input, wave modulation and tidal energy, was introduced in Galloway (1975). This is at present one of the most commonly applied schemes. However, it does not come without controversy. Most deltas are influenced by each of the three processes to a varying degree, and while process dominance may be averaged over the entire delta, the dominating processes may vary over short distances (Olariu, 2014). Bhattacharya and Giosan (2003) also pointed out a general tendency of delta examples being force-fitted into the endmembers of the tripartite process scheme, despite the fact that most deltas experience a mixed influence of all endmember processes.

The De Geerdalen Formation exhibits evidence of both fluvial-, wave- and tidal influence on the deposition. The formation displays a lateral variability in how dominant each of the processes has been, where a fluvial dominance has been interpreted from the eastern islands of Svalbard, opposed to a more wave and tidally influenced deposition on Spitsbergen (Knarud, 1980; Rød et al., 2014; Lord et al., 2017a). Rød et al. (2014) suggested that this pattern reflected upon changes in the proximity to the source, differences in accommodation space, varying

degree of sedimentation rates, wave- and tide modulation. [Bhattacharya and Giosan \(2003\)](#) pointed out that significant differences in the dominating deposition processes may occur between different deltaic lobes within the same deltaic system. Portions of large deltas may comprise several elements indicative of different dominating depositional processes. Such elements may be tidal estuaries, beach-ridge strandplains, wave-formed shorefaces, barrier-islands and lagoons, offshore bars, as well as distributary mouth bars ([Reading and Collinson, 1996](#); [Bhattacharya, 2006](#)). The De Geerdalen Formation comprises several of these elements, and represents an example of the difficulty in trying to classify ancient deltas as either fluvial-, wave- or tidally dominated. The problem with such classifications, lies largely with the scale that is under consideration and the objective of the study ([Reading and Collinson, 1996](#); [Bhattacharya, 2006](#)).

[Orton and Reading \(1993\)](#) extended the process-based classification scheme by adding the dominant grain size as an important factor as to how deltas develop. Generally speaking, river deltas are characterized by an input of mud, silt and sand deposited with low and moderate gradients, which allow for basinal processes to affect the sedimentation ([Reading and Collinson, 1996](#)). The geometry of the basins that receive sediments and the proximity to the shelf edge have an influence on the morphology and facies architecture of the delta ([Bhattacharya, 2006](#)). The De Geerdalen Formation reflects upon a relatively fine-grained system, with a general grain size variation between clay and medium sand. The formation has been interpreted to represent the distal part of a large deltaic systems that filled a relatively shallow (less than 500 m deep) Barents Sea Basin during the Triassic ([Klausen et al., 2015](#)).

Another issue with delta classification has been the eagerness of finding suitable modern analogues to ancient deltas inferred from deltaic sequences. Important controls on the deposition, such as the mean sea-level at the time of deposition, are fundamental to how deltas develop. Such controls change with time, and add controversy to correlations with modern examples, that were mainly formed under high eustatic sea level conditions during the Holocene ([Clifton, 2006](#)). In other words, large modern delta systems, for example the

Mississippi-Atchafalaya delta, the Ganges-Brahmaputra delta, the Nile delta, the Amazon delta and the Niger delta, prograde into much deeper waters compared to that of the Triassic. The Triassic deltaic system that created the deposits of the Snadd and the De Geerdalen formations must represent a very large regressive system, as it filled the entire Barents Sea shelf over a course of approximately 50 million years. There are few if any modern deltas with a similar extent, and representative modern analogues may thus not exist.

Sequences formed due to deltaic progradation, are characterized by an upward coarsening facies succession, with sandy delta front facies building over more fine grained deeper water facies (Bhattacharya, 2006). Repetitive or cyclic successions created as a result of repeated progradation and abandonment of deltaic lobes or of the entire delta, are typical for ancient deltaic deposits (Reading and Collinson, 1996). Facies sequences within deltaic deposits may occur on different scales. Large allocyclic sequences represent the development of the entire delta, and may be caused by tectonics, climatic changes, major river avulsions and eustatic sea-level changes (Reading and Collinson, 1996). Medium-scale sequences are mainly a result of delta lobes switching within the same deltaic system, while small-scale sequences may result from more restricted factors, such as differential subsidence on delta plains, lacustrine delta formation, crevassing of distributary channels and migration of tidal channels (Reading and Collinson, 1996). The De Geerdalen Formation comprises facies sequences at all three scales. The whole formation itself represents one large upwards shallowing unit, while medium-scale and small-scale sequences occur at all levels of the formation. In all modern deltas, the delta grades up from marine to non-marine facies following the principles of Walter's Law, but in low accommodation space settings the upper delta plain facies are often eroded and removed by wave and tidal activity during transgression (Bhattacharya, 2006). In general, the inter-fingering facies elements and cyclic facies architecture of deltaic deposits reflect upon the dynamic nature of deltaic environments, where waves, rivers and tides continuously interact to form complex sequences (Bhattacharya and Giosan, 2003). Thus, local variations occur both laterally and vertically over short distances. Differences between river-, wave- and

tidal-dominated deltas are most visible in the delta front facies association. Here, the interplay between fluvial and basinal processes is recorded (Reading and Collinson, 1996). Dependent on the portion and efficiency of each process, the delta front may hold facies of sub-environments such as distributary mouth bars, barrier bars, subaqueous levees, beach ridges, beach spits, tidal channels, ebb and flood tidal deltas (Reading and Collinson, 1996).

Sedimentation styles on deltaic coastlines are largely governed by depositional regressions and transgressions. The transgressive parts of deltaic systems will normally experience a large degree of subsidence and marine reworking, while regressive parts are characterised by a large fluvial sediment supply (Bhattacharya, 2006). Switching between transgressive stages and regressive stages causes cyclic deposition patterns, patterns that are typical but not exclusive to deltaic sequences. Sequences that form as a result of repeated deltaic progradations are often referred to as parasequences. The concept of parasequences originates back to the work of Van Wagoner et al. (1988, 1990), in which parasequences were defined as a succession of beds that recorded upwards shallowing and were bound by marine flooding surfaces. Following this definition, a single parasequence may include several minor upwards coarsening and fining units, also called sub-sequences. Both parasequences and sub-sequences are characteristic for the De Geerdalen Formation, recently quantified by Lord et al. (2017b). A pattern of stacked upwards shallowing units, or parasequences, are characteristic for the De Geerdalen Formation, as well as for the Snadd Formation in the Barents Sea (Klausen et al., 2015), and have been interpreted as a result of auto-cyclic switching of delta lobes within a major deltaic system (Knarud, 1980; Riis et al., 2008).

9.2 Facies distribution in Fulmardalen

The dataset that was collected from Fulmardalen represents a fairly narrow spaced dataset, with only a couple kilometres between the logged sections. While previous sedimentological studies of the De Geerdalen Formation (e.g., Lord et al., 2017a), have presented correlations between localities sometimes spaced by several tens of kilometres, a denser spacing in the dataset from

Fulmardalen enables a more detailed study of local vertical and lateral depositional variations within the formation.

The facies distribution in Fulmardalen reflects an overall shallowing upwards depositional environment (DE), with open marine shelf and prodelta (DE 1) deposits in the lower part (belonging to the Botneheia and Tschermakfjellet Formations), shallow marine (DE 2) and delta front (DE 3) deposits in the middle part and delta plain (DE 4) deposits in the upper part, reflecting an overall change from a distal to proximal deltaic setting. This shallowing upwards trend is concordant with previous studies of the De Geerdalen Formation (e.g., [Knarud, 1980](#); [Mørk et al., 1982](#); [Riis et al., 2008](#); [Høy and Lundschieen, 2011](#); [Lundschieen et al., 2014](#); [Rød et al., 2014](#); [Lord et al., 2017a](#)).

Each depositional environment represents a group of facies associations ([Table 9.1](#) and [Figure 9.3](#)). For simplicity, the classification of depositional environments has been used to correlate the logs in the study area ([Figure 9.4](#)). Due to the paralic nature of the De Geerdalen Formation, individual facies associations may be difficult to correlate laterally ([Lord et al., 2017a](#)). The lower half of the De Geerdalen Formation in Fulmardalen (DE 2-3) consists of laterally extensive, stacked upwards coarsening units which have been interpreted as parasequences, reflecting repeated switching between regressive and transgressive phases within an overall prograding deltaic system. Many of the sandstones in the upper part of the parasequences are thought to reflect ancient barrier bar complexes or shallow subaqueous bank deposits. Traditionally, barrier bars are associated with transgressive phases of a delta complex, when the regressive phase reaches a state of over-extension, leading to abandonment and reworking of sediments ([Boyd and Penland, 1988](#); [Bhattacharya, 2006](#)). However, [Bhattacharya and Giosan \(2003\)](#) show that barrier bars/islands may form naturally in modern prograding wave-influenced deltaic systems. In other words, the barrier bars interpreted in the De Geerdalen Formation are not necessarily associated with transgressive phases. The deposits witness a depositional environment considerably influenced by marine processes (and to some extent by tidal processes) which is concordant with previous studies from Spitsbergen (e.g.,

Knarud, 1980; Rød et al., 2014; Lord et al., 2017a).

Table 9.1: An overview of facies associations (FA) interpreted from the De Geerdalen Formation and facies incorporated therein. The facies associations have also been linked with their gross depositional environments (DE). From Lord et al. (2017a).

DE	Facies Associations (FA)	Facies Incorporated	Description	Geometry/Forms
DE 1 – Open Marine Shelf & Prodelta	FA 1 – Open Marine Shelf Deposits	A	Pelagic, organic rich shales and marine shale deposits. Abundant fossils and bone fragments and thin interlaminae of silt.	Extensive in thickness and areal extent. Forms major units.
	FA 2 – Prodelta Slope Deposits	A, B, C & H	Marine shales and siltstones, minor sand and bioturbation. Tempestites may be present with minor hummocky cross-stratification and ripples.	Areally extensive throughout Svalbard. Forms stratigraphic unit with variable thickness (10-130m).
DE 2 – Shallow Marine	FA 3 – Offshore Deposits	A, I & J	Mud and silt dominated distal deltaic sediments. Forms dark mudstone and heterolithic bedded units with minor storm induced sandstones and thin offshore bars.	1-10's of metres thick. Laterally extensive and grade into offshore transition or lower shoreface deposits.
	FA 4 – Offshore Transition Deposits	A, B, C & E	Thin beds of hummocky cross-stratified sandstone in fine-grained shale and siltstones. Wave and symmetrical ripples common. Bioturbation and shell fragments also present.	1-10 m thick, laterally extensive for 100's m. Grades laterally into offshore or lower shoreface deposits.
	FA 5 – Lower Shoreface Deposits	A, B, C, E, G & H	Below normal wave base deposits dominated by mudstone and siltstone, with storm induced sandstone beds. Wave rippled, carbonate cemented or plane parallel laminated sandstone beds are common.	1-5 m thick and laterally extensive. Grades laterally into upper shoreface deposits of fluvial distributary deposits.
DE 3 – Delta Front	FA 6 – Upper Shoreface Deposits	C, E, F, I & K (also G & L)	Sandstone and siltstone, showing re-working of sediment in a turbulent environment. Wave structures indicate marine processes. Mud drapes suggest tidal influence. Forms prominent sandstone benches.	1-5 m thick and laterally extensive. Overlies lower shoreface or offshore transition deposits.
	FA 7 – Distributary Mouth Bar Deposits	D, F, H, I, J & M	Soft sediment deformed sandstone with trough, low-angle and tabular cross stratified sandstones. Erosive base indicates rapid deposition. Reworking of sediment by wave or tide processes evident. Also amalgamated.	Laterally extensive sheets for 100's of m. Thickness varies but is in the order of 1-4 m. Grades into distributary facies.
	FA 8 – Barrier Bar Deposits	E, F, H, I & K	Upwards coarsening facies, with trough or low angle cross-stratified sandstone, with current or wave-rippled sandstone. Tidal indicators and bioturbation suggest a marine origin.	Laterally extensive. Thickness ca. 1-2 m. Grades laterally into shoreface or inter distributary deposits.
DE 4 – Delta Plain	FA 9 – Distributary Channel Deposits	F, H, J, K, M & N	Sharp erosive base, contains trough and tabular cross-stratified sandstone facies. Mud-flakes are common in this association. Often underlies palaeosol facies. Can also form lateral sheets with amalgamated channels.	Extensive sandstone bodies. Often less than 10 m in thickness. Grades laterally into floodplain deposits.
	FA 10 – Floodplain Deposits	A, E, F, J, M & N	Fine-grained floodplain deposits, or overbank fines. Silt with sandstone laminae common. Coal, coal-shale and palaeosols present in this FA.	Laterally extensive with variable thickness, ca. 0.2-1.5 m. Overlies or incised by fluvial distributary deposits.
	FA 11 – Inter-distributary Areas	A, L, M & N (with E, F, & H)	Fine-grained facies. Some rare sandstone incursions with hummocks or ripples may be present, facies generally suggest a low energy marine or lacustrine environment. Bioturbation and palaeosols common.	1-10's of metres thick, laterally extensive, grading laterally into shoreface or barrier bar deposits.

The deposits from Fulmardalen fit well into the description of ancient wave-dominated deltas (e.g., [Reading and Collinson, 1996](#)). Laterally extensive coarsening upward sequences characterized by wave- and storm-dominated facies typically comprise the shallow marine to delta front environment in such deltas. Furthermore, typical delta plain elements in wave-dominated deltas include distributary channels, interdistributary lagoonal facies with minor bars and lagoonal beach deposits ([Reading and Collinson, 1996](#)), which is exactly what has been interpreted in the upper part (DE 4) of the measured sections in Fulmardalen, in the Isfjorden Member. In fact, the type locality of the Isfjorden Member is in Fulmardalen ([Mørk et al., 1999a](#)), and issues related to the definition of its base are discussed in [Section 9.2.1](#). It is important to remember that the deposits in Fulmardalen only represent a small portion of a large complex delta system which, depending on location, shows different dominating depositional processes. A more regional facies distribution discussion will be given in [Section 9.3](#), putting the deposits from Fulmardalen into a larger scale context.

9.2.1 The base of the Isfjorden Member

[Mørk et al. \(1999a\)](#) suggest Storfjellet to be the type locality of the Isfjorden Member, where the lower boundary is defined by a bivalve coquina bed which occurs above a thick cross-bedded sandstone unit. This definition was based on the log from Storfjellet that was presented in [Knarud \(1980\)](#) ([Appendix C](#)). The rusty-red carbonate rich sandstone overlying a cross-bedded sandstone observed during fieldwork in 2016 (at 165 m in log Stor16-1), is probably the same layer described as the coquina bed by [Knarud \(1980\)](#). Local accumulations and/or dissolution of shell fragments may have caused variable observations within short distances, and may explain the differences between Knarud's log and Stor16-1. This statement is supported by the fact that the correlative rusty-red layer observed at Ryssen (at 188 m in log Rys16-1) contains shell fragments ([Figure 9.5](#)). However, at Ryssen the coquina bed does not have any underlying cross-bedded sandstone, which makes the definition of the base of the Isfjorden Member questionable. Additionally, the 2016 field campaign observed a coquina bed that has not been

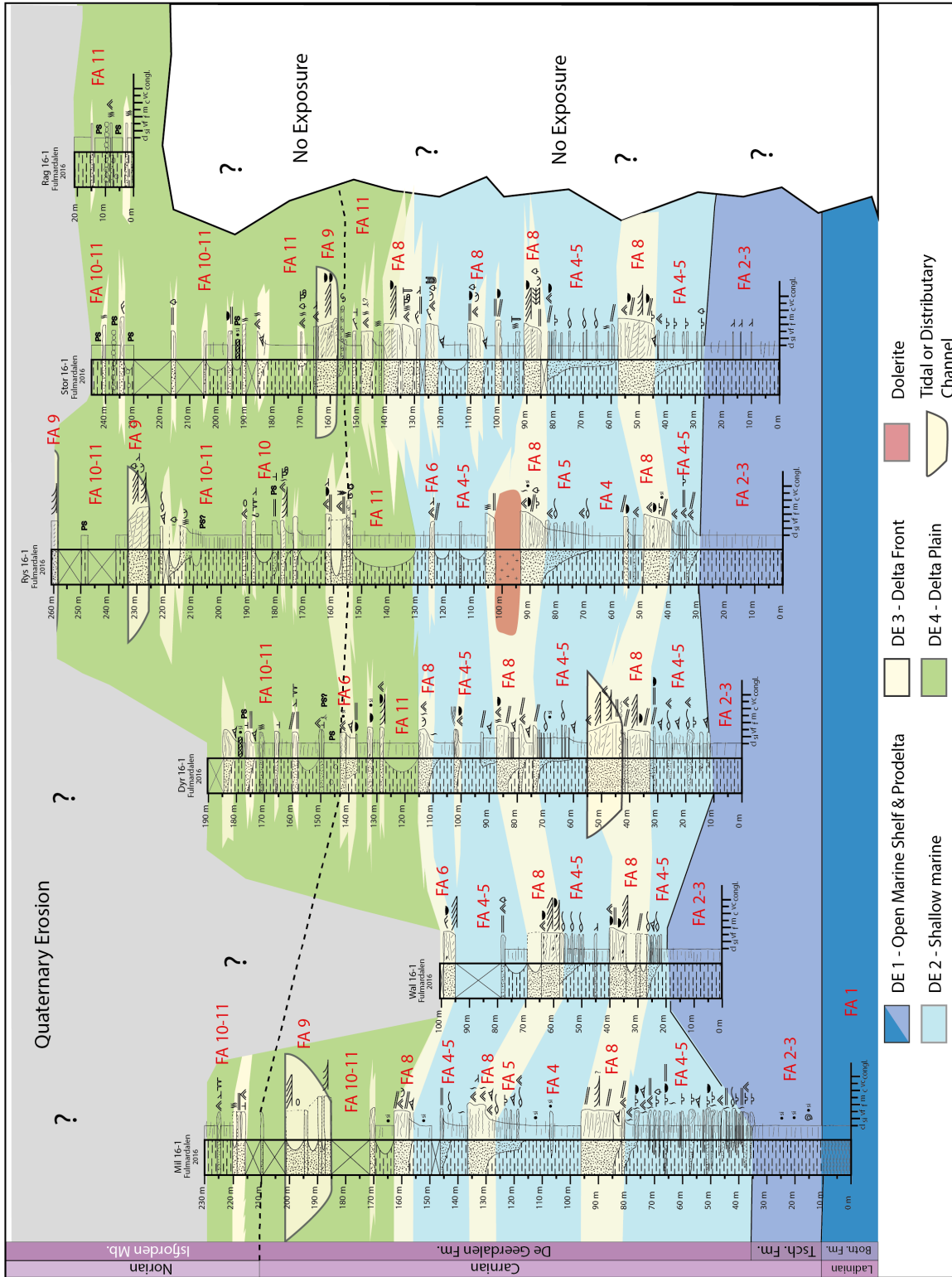


Figure 9.4: Log correlations for sections measured in Fulmardalen. Positions of the individual logs are indicated in Figure 5.1. Depositional environments have been suggested based on facies and the interpreted facies associations.

described by [Knarud \(1980\)](#) below the aforementioned cross-bedded sandstone at Storffjellet. A coquina bed was also observed at Ryssen at a lower stratigraphic layer relative to the correlative layer defined as the base of the Isfjorden Member. [Haugen \(2016\)](#) studied the Isfjorden Member in eastern Svalbard and states that coquina beds are considered diagnostic features of the member. Furthermore, [Haugen \(2016\)](#) concludes that the lower boundary of the Isfjorden Member differs depending on facies associations and locality. This study is in accordance with those conclusions and suggests that the definition of the lower boundary of the Isfjorden Member following [Mørk et al. \(1999a\)](#) should be revised. Knarud's section from 1980 was not logged with the purpose of being a type section, a definition was later created by [Mørk et al. \(1999a\)](#) based on re-interpretation of the original log (Atle Mørk, pers. comm., 2017). The fact that the defined lower boundary cannot be recognized even within the type locality area shows the necessity of a revision, and the definition proposed by [Haugen \(2016\)](#) seems more applicable.

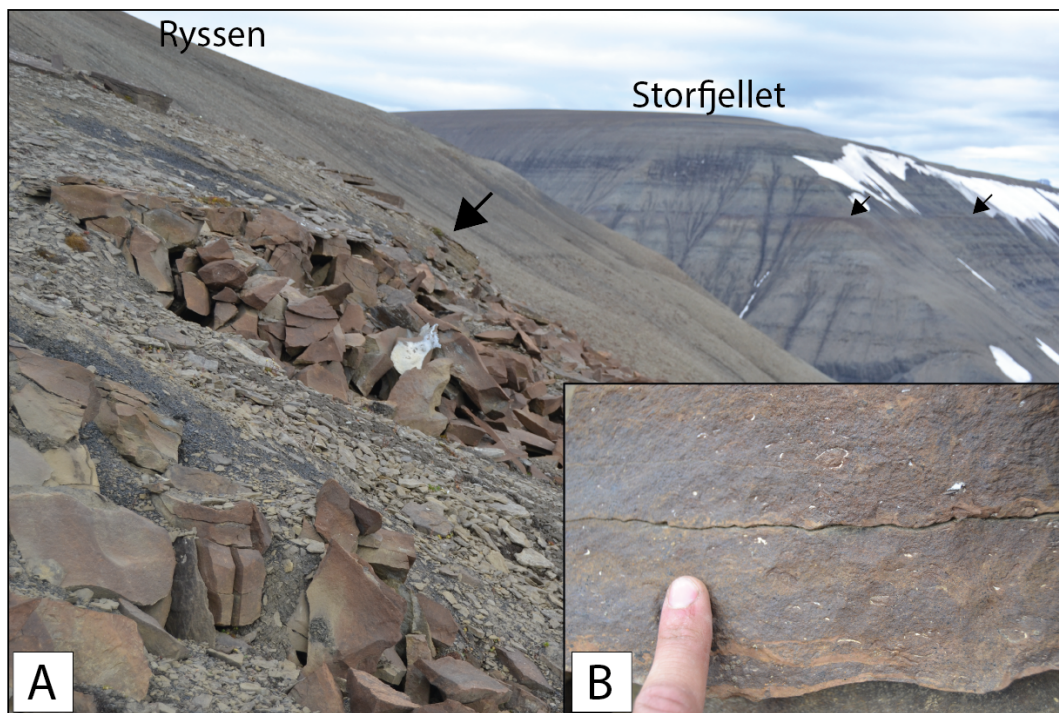


Figure 9.5: (A) The rusty-red carbonate cemented sandstone at Ryssen can be laterally traced to Storffjellet (indicated by arrows). The layer occurs above a cross bedded sandstone at Storffjellet where it defines the base of the Isfjorden Member according to the definition in [Mørk et al. \(1999a\)](#). (B) Shell fragments in the rusty-red layer at Ryssen.

9.3 Regional facies distribution

9.3.1 Spitsbergen

The new data presented from Fulmardalen provides important infill to previous work on the De Geerdalen Formation on Svalbard, and allows for data-comparison on a regional scale. A selection of representative logs from adjacent datasets from Botneheia, Sticky Keep and Trehøgdene on central Spitsbergen and from Klement'evfjellet and Friedrichfjellet in Agardhdalen, presented in [Rød et al. \(2014\)](#) and [Lord et al. \(2017a\)](#) respectively, have been correlated and compared to the new data from Fulmardalen ([Figure 9.6](#))

The logs presented in the correlation panel are located on a NW-SE trending transect across Spitsbergen ([Figure 9.7](#)). Fulmardalen represents a transition area that connects the observations from more westerly located areas on central Spitsbergen to Agardhdalen on eastern Spitsbergen. [Rød et al. \(2014\)](#) found that the De Geerdalen Formation in central Spitsbergen was characterized by laterally continuous, blocky sandstone and siltstone layers interbedded with shale. The most adjacent log to Fulmardalen that was collected by [Rød et al. \(2014\)](#) on central Spitsbergen was measured from Trehøgdene ([Figure 9.7](#)). In this section low angle cross-stratified sandstone units have been interpreted as barrier bar complexes in the lower part of the formation. This interpretation is consistent with the interpretation of barrier complexes occurring at similar stratigraphic levels in Fulmardalen. At Botneheia, which is located to the NW of Trehøgdene, the barrier complexes become absent or less prominent, but such deposits have been interpreted from the cores of well DH4 in Adventdalen ([Rød et al., 2014](#)), which is located west of Fulmardalen ([Figure 9.1](#)).

In general, exposures of the De Geerdalen Formation NW of Fulmardalen shows a tendency of being very fine grained, with a relatively low content of sand. The barriers and subaqueous banks that have been interpreted from the middle part of the De Geerdalen Formation in Fulmardalen seem to be less prominent at similar stratigraphic levels further northwest. On

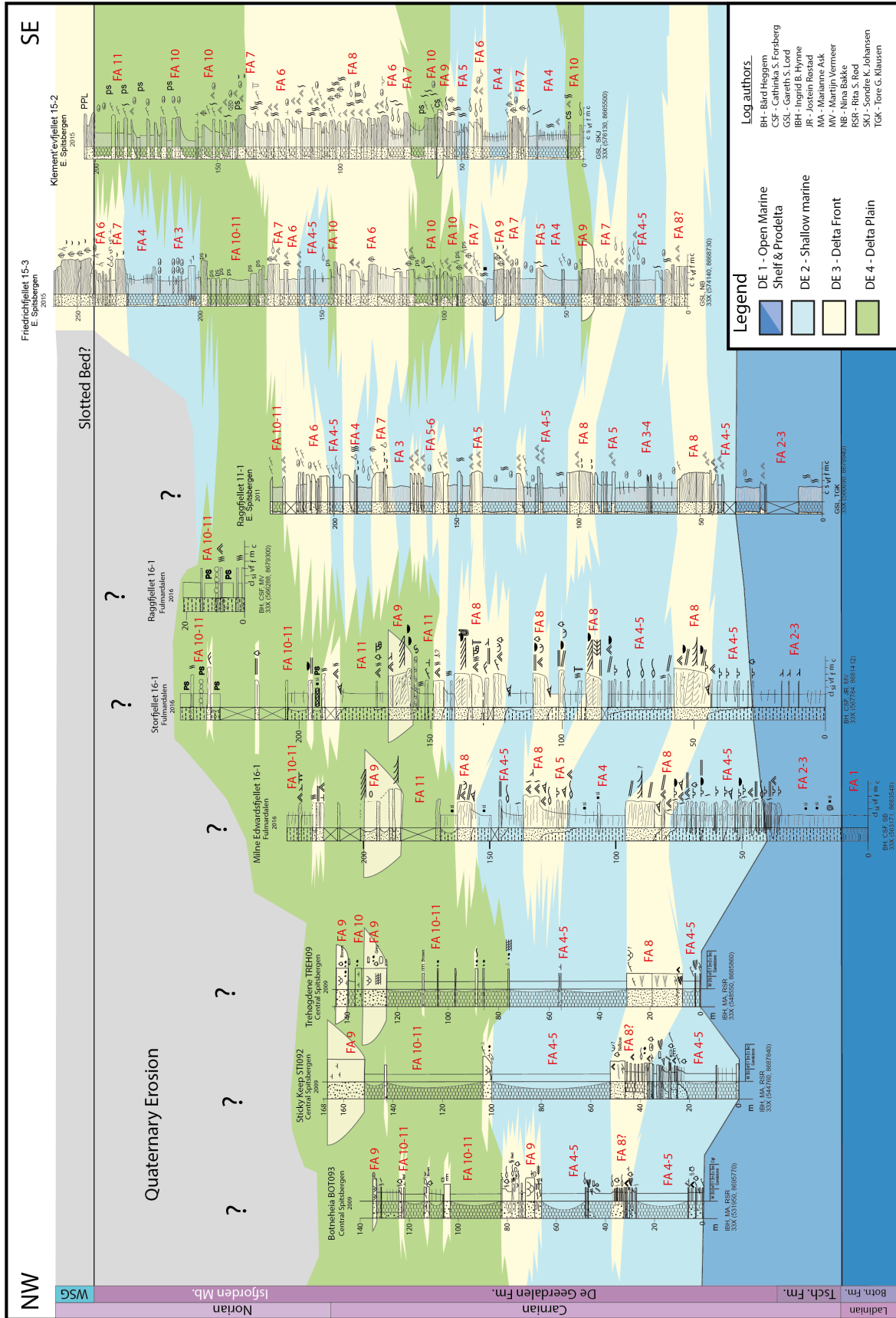


Figure 9.6: Log correlations for sections measured in central Spitsbergen (Rød et al., 2014), Fulmardalen and Agardhdalen (Lord et al., 2017a). Positions of the individual logs are indicated in Figure 9.7. Depositional environments have been suggested based on facies and the interpreted facies associations.

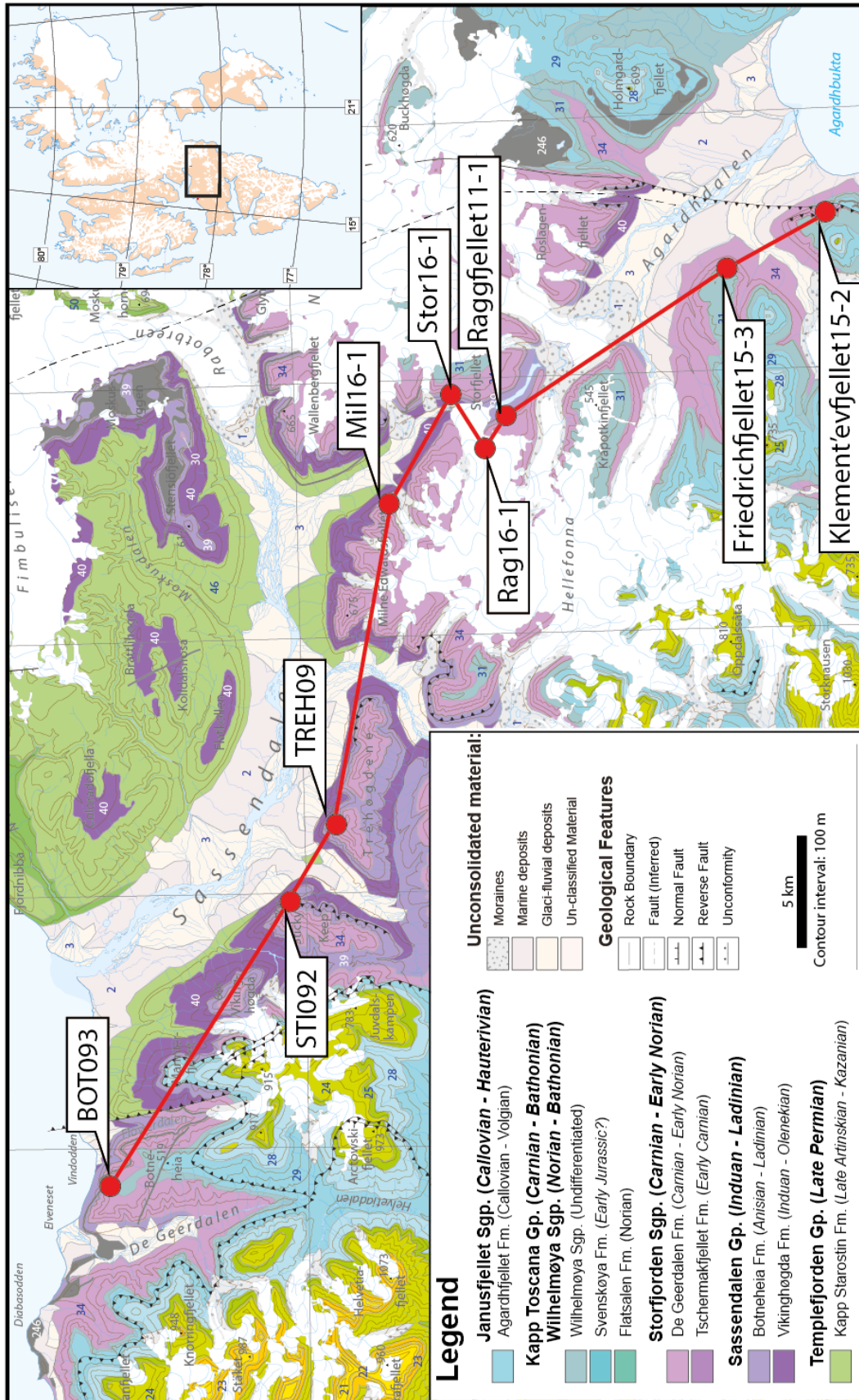


Figure 9.7: Transect across Spitsbergen through Agardhdalen, Fulmardalen and Sassendalen. The positions of the logs from the correlation panel in Figure 9.6 have been marked. Geological map retrieved from Dallmann (2015).

central Spitsbergen the middle part of the De Geerdalen Formation is generally characterised by thinner sandstone beds and a domination of shale, which could imply a more distal facies expression than displayed in the deposits in Fulmardalen. However, the differences between the deposits in the two areas are mainly related to the relative portion of sand and shale, and sandy units from both areas are characterized by the same structures and facies types. This suggests a similar depositional regime for both Fulmardalen and the areas further west on central Spitsbergen. [Rød et al. \(2014\)](#) argue that the sediments in central Spitsbergen were deposited in a setting with strong modulation from wave-energy, as well as with tidal influence. It seems likely that reworking and redistribution of sediments by basinal processes, especially wave activity, also played a major role in the depositional environment in Fulmardalen.

In Agardhdalen to the SE of Fulmardalen, the facies assemblages of the De Geerdalen Formation display a somewhat different trend compared to on central Spitsbergen. Here, the formation is dominated by more sandy intervals. The basal parts of the De Geerdalen Formation in this area are generally poorly exposed, but the deposits from the middle part of the succession and upwards have been interpreted to reflect upon a paralic nearshore setting dominated by delta front and shallow marine facies ([Lord et al., 2017a](#)). The sandstone geometries from the measured sections in Agardhdalen are described as thin and laterally continuous ([Johansen, 2016](#)), similar to sandstone bodies described from Fulmardalen and central Spitsbergen. Delta plain deposits in Agardhdalen include distributary channel facies, often associated with overlying paleosols, coal and coaly shales ([Lord et al., 2017a](#)). Indications of a more developed delta plain depositional environment are stronger in Agardhdalen than in Fulmardalen, where comparatively few distributary channels, paleosols and coal shale horizons have been interpreted. Fossil fragments of plants appear to be less abundant in Fulmardalen compared to in Agardhdalen. Although plant debris may be transported relatively far away from growth position, more frequent occurrences of fossilized plant debris in Agardhdalen may indicate a more proximal facies expression towards the SE. [Lord et al. \(2017a\)](#) suggest that a more developed delta plain environment, with paleosols, coal and coaly shales,

requires time to develop in a relatively stable environment. This could imply more stable conditions on the delta plain in Agardhdalen compared to in the Fulmardalen area. Additionally, higher bioturbation rates in Agardhdalen compared to in Fulmardalen may indicate a higher energy regime influencing the deposition in Fulmardalen causing more restricted and harsher living-conditions.

Generally, the facies development found along the SE-NW directed transect (Figure 9.7) shows a development from a relatively proximal to distal facies expression. Johansen (2016) points out a more proximal expression in Agardhdalen compared to the observations of Rød et al. (2014) on central Spitsbergen, and base the interpretation on a higher amount of sand-rich facies in Agardhdalen. Fulmardalen represents a transition zone between these areas, both geographically and with regards to the facies expression. However, a relatively high sand content is present in the De Geerdalen Formation in the Festningen section (Vigran et al., 2014), which represents the westernmost exposure of the formation in Svalbard. This adds complexity to the sand distribution pattern, and may suggest that the aforementioned east-west decreasing trend in sand content does not occur all over Svalbard.

Thickness trends have often been used as a parameter for understanding the evolution of a deltaic system, where thick and thin deposits are associated with proximal and distal positions to the source area, respectively. However, variations in accommodation space and paleotopography are also factors controlling the basin fill patterns. Interpretations of the delta evolution based on thickness variations should therefore be treated with care, and should not conclusively be associated with the source proximity. Previous work has shown that the De Geerdalen Formation has a relatively uniform thickness across central Spitsbergen (e.g., Vigran et al., 2014; Lord et al., 2017b). Comparing thickness measurements between localities on Svalbard is challenging due to the fact that none of the areas display a complete succession of the formation. While the lower boundary of the formation is not exposed in Agardhdalen, the upper boundary is missing in both Fulmardalen and on central Spitsbergen. This makes direct and quantitative thickness comparisons controversial and speculative at best, and other

parameters, such as facies analysis, are needed in order to understand the deltaic evolution of the De Geerdalen Formation across Spitsbergen.

The Isfjorden Member is exposed both in Agardhdalen and in Fulmardalen, but has not been described from central Spitsbergen where it may have been eroded or not been recognized (Rød et al., 2014). Lord et al. (2017a) recognise facies that indicate a marine incursion in the upper parts of the De Geerdalen Formation in Agardhdalen. This marine interval is not recognised in Fulmardalen, where it may have been subjected to Quaternary erosion. Alternatively, the incursion may represent a local phenomenon such as an interdistributary lobe bay area.

9.3.2 Edgeøya, Barentsøya, Wilhelmøya and Hopen

The De Geerdalen Formation on the islands Edgeøya, Wilhelmøya and Hopen, reflects a paralic deltaic environment with a generally stronger fluvial signature compared to observations from Fulmardalen and elsewhere on Spitsbergen (Rød et al., 2014; Klausen and Mørk, 2014; Lord et al., 2014a,b, 2017a).

Rød et al. (2014) describe thick ellipsoid shaped sandstone bodies at Blanknuten on Edgeøya (Figure 9.2), typical for fluvial dominated delta fronts. Similar deposits are described from Svartnosa at Barentsøya (Lord et al., 2017a). The relatively thick sandstones are interpreted as being amalgamated mouth bars deposited in a delta lobe and may represent the eastern and more proximal equivalent to the relatively thin and laterally extensive shoreface deposits observed in Agardhdalen, Fulmardalen and on central Spitsbergen (Rød et al., 2014; Lord et al., 2017a). Available accommodation space has been suggested as being the most likely reason for the geometrical differences, with the formation of thick and thin sandstone bodies forming in areas of high and low accommodation space, respectively. The fluvial signatures on the deposits are thought to decrease with less accommodation space, which allows basinal processes, such as wave activity, to rework and redistribute the sediment (Rød et al., 2014; Lord et al., 2017a). Furthermore, growth faults are described from the western side of Edgeøya on Klinkhamaren (Edwards, 1976; Anell et al., 2013; Osmundsen et al., 2014; Rød et al., 2014)

(Figure 9.2). Such faults are typically associated with delta progradations with high rates of deposition (Edwards, 1976).

The northernmost localities presented in Lord et al. (2017a) are located on Wilhelmøya. Here, a complete succession of the De Geerdalen Formation is exposed and is characterized by units of paralic, delta front and delta plain deposits with abundant coal layers in the lower part (Haugen, 2016; Lord et al., 2017a). The upper part consists of delta plain deposits with well-developed paleosols, interpreted to belong to the Isfjorden Member (Haugen, 2016; Lord et al., 2017a). The lower part has been interpreted as being deposited in a minor delta lobe system with fluvial distributary channels flowing in a coastal setting (Lord et al., 2017a). Both the paleosols and the coal deposits are better developed here compared to on Spitsbergen. The paleosols in the Isfjorden Member may have developed as a result of a delta lobe abandonment resulting in local subaerial unconformities and a change to a more stable environment with lower volumes of deltaic deposits (Lord et al., 2017a). Haugen (2016) suggests a slightly more proximal and terrestrial setting of the Isfjorden Member on Wilhelmøya compared to elsewhere on Svalbard.

The island of Hopen in south eastern Svalbard is the most proximal locality with respect to the proposed Uralian source areas, where outcrops of the De Geerdalen Formation can be studied. Only the upper part of the formation, composed of paralic delta plain sediments with minor marine incursions, is exposed (Klausen and Mørk, 2014; Lord et al., 2014a,b) and is late Carnian in age (Paterson and Mangerud, 2015; Paterson et al., 2016a). The island holds exposures of multiple fluvial trunk and distributary channel deposits (Klausen and Mørk, 2014; Lord et al., 2014b). Channel bodies occur more frequently on Hopen, and are significantly larger in size compared to the channels observed in Spitsbergen. Evidence of coal formation (Klausen and Mørk, 2014; Lord et al., 2014b) indicates an environment where organic material was allowed to accumulate, and Paterson et al. (2016a) suggest wet and humid conditions to have prevailed at that time. The presence of large tree remains in addition to a large volume of plant materials seen in sandstone units, witness of a well vegetated landscape in the late

Carnian (Lord et al., 2014a, 2017a). The channel deposits on Hopen are further discussed in Section 9.4.

There is a significant thinning of the late Triassic succession across Svalbard from southeast to northwest (Anell et al., 2014a,b; Lord et al., 2017a,b). A well from Hopen shows the composite thickness of the Tschermakfjellet and the De Geerdalen Formation to be 1100 m (Anell et al., 2014a), whereas in Spitsbergen the equivalent thickness is approximately 300 m (Vigran et al., 2014). At Wilhelmøya, the De Geerdalen Formation alone is some 350-400 m (Lord et al., 2017a). The equivalent Snadd Formation in the Barents Sea reaches a thickness up to 1500 m (Klausen et al., 2014). This northwestward thinning is according to Anell et al. (2014a,b) related to the progression of the Carnian deltaic system on to the Svalbard Platform and an associated decreased accommodation space, similar to the interpretations of Rød et al. (2014). The overall paralic deltaic setting of the De Geerdalen Formation, with laterally discontinuous facies and depositional environments, reflects upon a low progradation angle of the system, easily influenced by changes in the delta or sea level (Lord et al., 2017a). The new dataset from Fulmardalen is, as discussed above, in accordance with this existing model.

9.4 Channels in the Snadd Formation

As discussed in previous sections, the Triassic delta deposits on Svalbard, belonging to the De Geerdalen Formation, experienced a mixture of wave-, tidal- and fluvial processes, and which of these three processes that dominated varied laterally, often over short distances. A stronger fluvial influence on the deposits has been interpreted on the eastern islands compared to on Spitsbergen, where wave- and tidal processes have been more important. The equivalent delta deposits on the Finnmark Platform studied herein, belonging to the Snadd Formation, indicate that fluvial processes have prevailed in the respective area during the Triassic (Figure 2.3).

This section will discuss possible mechanisms behind the changes observed in channel morphology upwards in the formation (Section 9.4.1), from relatively large channel belts in the lower part towards narrow channel bodies in the upper part. Furthermore, the channels in the

Snadd Formation will be compared to other studies of both ancient and modern fluvial systems (Section 9.4.2).

9.4.1 A change in channel morphology

A general trend in fluvial systems is a reduction of gradient and discharge downstream. These factors affect the flow velocity, which in turn controls the ability of the river to erode and carry material (Nichols, 2009). Coarse grained braided morphologies typically develop in proximal positions of river profiles, whereas a meandering pattern tends to develop where the gradient is very gentle in more distal positions, with the deposition of finer grained material (Nichols, 2009) (Figure 9.8). A bifurcating pattern of smaller distributary channels typically develop in the most distal parts of the river profile (Nichols, 2009). A change in base-level will make the fluvial system to “reorganize”, and the river will try to adapt to the new conditions. The different channel morphologies seen in the Snadd Formation may be related to sea-level fluctuations and associated base-level changes. Large meandering and braided channel bodies in the lower part of the formation may have developed in relatively proximal areas on the delta plain, whereas smaller channels in the upper part of the formation may represent more distally developed channels. Distal deposits overlaying proximal deposits indicate a net-transgressive succession and a relative sea-level rise. An intra-Carnian marine flooding surface has been reported to the west of the study area (Klausen et al., 2014), and it is possible that this event may have triggered more frequent avulsions influencing the channel morphologies. However, data from the western and northern part of the Barents Sea (e.g., Glørstad-Clark et al., 2010; Høy and Lundschieen, 2011; Lundschieen et al., 2014) indicate a progradational development in the upper part of the Snadd Formation, which is inconsistent with the abovementioned interpretation of a net-transgressive system. An alternative interpretation may be related to tectonic activity. Nichols (2009) states that avulsion is frequent in rivers located in areas that are tectonically active. The Late Triassic Novaya Zemlya phase of the Uralian Orogeny (O’leary et al., 2004; Stoupakova et al., 2011) may represent such a tectonic event, resulting in changes

in the hinterland and associated changes in sediment dispersal, depositional styles and river morphologies (Klausen et al., 2014).

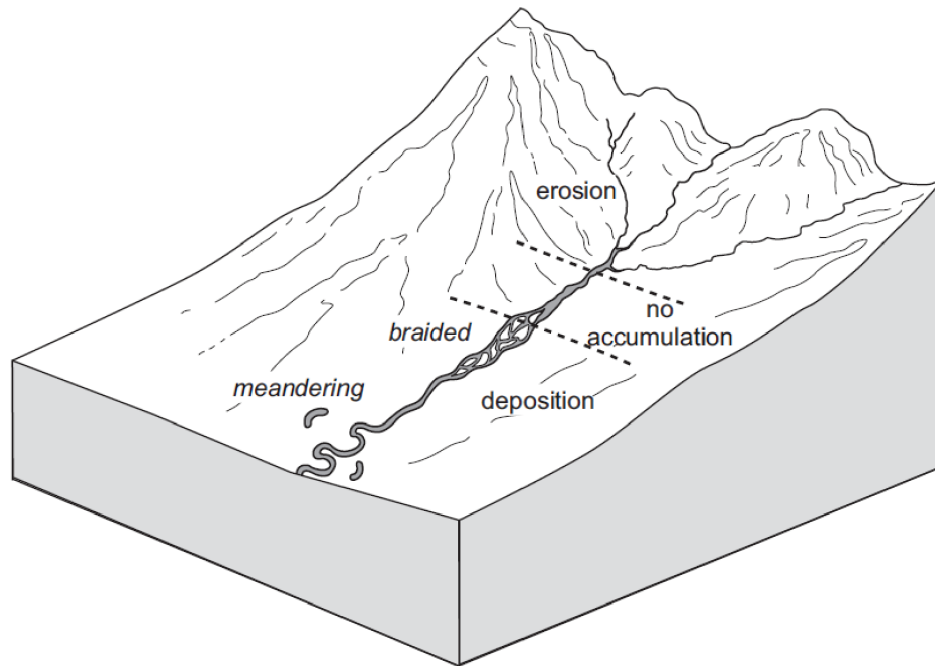


Figure 9.8: Braided rivers commonly occur in more proximal areas and meandering rivers occur further downstream. From Nichols (2009).

9.4.2 Comparison to ancient and modern fluvial systems

Klausen et al. (2014) present measurements of channels in the Snadd Formation from six 3D seismic surveys in the south-western Barents Sea, within which the ST9802 survey is included. Most width-to-thickness measurements from the present study fall within two envelopes confining the cross plots of Klausen et al. (2014) (Figure 9.9). The two envelopes represent in total 714 measurements of channel belt and channel fill deposits from all the six 3D seismic surveys. The relatively large scatter of these measurements compared to the present study is most likely explained by the large difference in the number of measured channels. The fact that some measurements from this study fall outside the envelopes of Klausen et al. (2014) is probably a result of different interpretations and methods used when measuring the channel geometries.

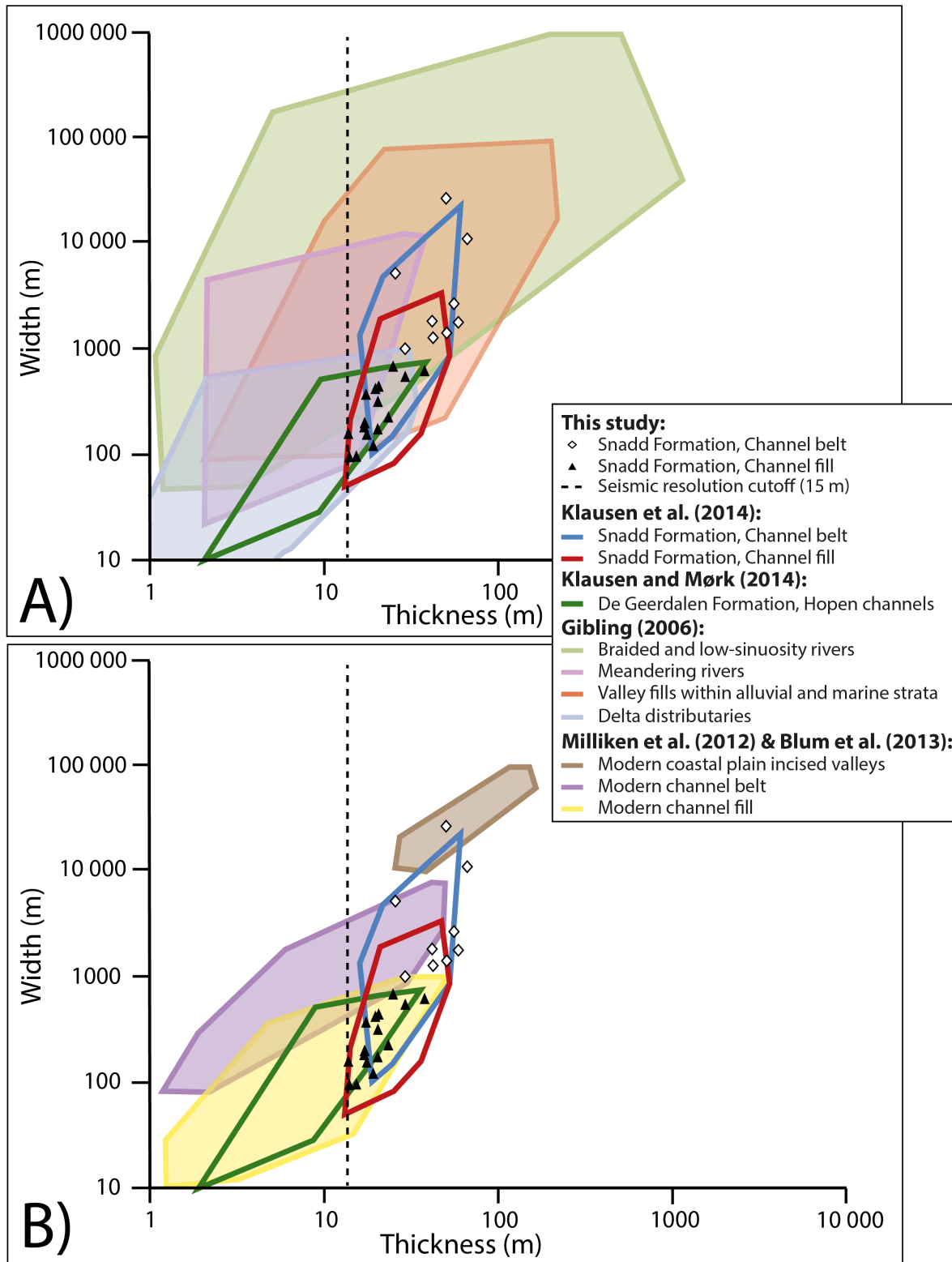


Figure 9.9: Width-to-thickness plots of measured channels in the Snadd Formation from the present study and from Klausen et al. (2014) and of measured channels in the De geerdalen Formation on Hopen by Klausen and Mørk (2014) are compared to (A) ancient fluvial systems in Gibling (2006) and to (B) modern fluvial systems in Blum et al. (2013) and Milliken et al. (2012)

Comparison of the data from the Snadd Formation to width-to-thickness cross plots of ancient fluvial systems in [Gibling \(2006\)](#) ([Figure 9.9A](#)) and of modern fluvial systems in [Blum et al. \(2013\)](#) and [Milliken et al. \(2012\)](#) ([Figure 9.9B](#)), show that the channels in the Snadd Formation seem to plot within or slightly above the examples to which they are compared. [Klausen et al. \(2014\)](#) argue that this may result from the nature of the seismic dataset used to estimate the thickness values, and it is likely that this is the case for the measured channels in the present study as well. As explained in [Section 3.2.1](#), channels as thin as 2 m may be detected, but their seismic reflector will appear no thinner than the vertical seismic resolution which is ca 15 m when using an optimistic frequency value of plus two standard deviations from the mean ($\mu + 2\sigma$) ([Table 3.2](#)). Even the Guovca channel sandstone, which is thicker than the vertical seismic resolution, appears thicker (in the scale of tens of metres) in seismic sections compared to thickness values indicated from well logs, implying that also relatively thick channel bodies may be thinner than presented herein. Alternatively, assuming that the measurements are correct, the depositional environment may have developed thicker channel deposits in the Snadd Formation than those that have been reported in the respective studies ([Klausen et al., 2014](#)).

The channel fill deposits in the Snadd Formation seem to correspond to distributary channels following the classification of [Gibling \(2006\)](#) ([Figure 9.9A](#)). The channel belts, on the other hand, may correspond to meandering rivers, braided and low-sinuosity rivers and valley fills, which fit well with the interpretation of channel types from RMS amplitude maps in [Chapter 6](#). However, there seems to be a stronger correlation to the envelope representing meandering rivers when taking the data of [Klausen et al. \(2014\)](#) into account. The two other categories show a very wide scatter compared to the values from the Snadd Formation, which may indicate a weaker link to the respective categories ([Klausen et al., 2014](#)).

Comparison of the Snadd channels to the envelopes of modern fluvial systems presented in [Milliken et al. \(2012\)](#) and [Blum et al. \(2013\)](#) ([Figure 9.9B](#)), indicates a better correlation with respect to [Gibling \(2006\)](#). Moreover, the channel measurements from the present study seem to

have a better correlation to the width-value distribution of modern fluvial systems than the study of [Klausen et al. \(2014\)](#). [Klausen et al. \(2014\)](#) explain the much wider width-value distribution in the Snadd Formation as a result of potentially too widely defined criteria used when identifying channel belts, and that some of these measurements may belong to the channel fill category instead. Some of the widest channel belt measurements, for example the Guovca channel complex, compare to modern valley fills, but the absence of deep incision makes this interpretation less likely. [Klausen et al. \(2014\)](#) suggest that these deposits instead reflect trunk rivers located close to the delta plain-paleovalley transition.

[Klausen and Mørk \(2014\)](#) present width-to-thickness measurements of channel deposits from the De Geerdalen Formation on Hopen. These channels seem to represent distributary channels and channel fills, following the classification of [Gibling \(2006\)](#) and [Blum et al. \(2013\)](#), respectively, even though there are examples of channels which compare to meandering rivers and channel belts as well ([Figure 9.9](#)). The Hopen channels are generally smaller than those observed on seismic attribute maps in the Snadd Formation. They are thought to reflect a more distal and paralic position, where avulsion frequencies are assumed to be higher than in more proximal positions ([Klausen and Mørk, 2014](#)), preventing mature meandering profiles to develop. Paleocurrent measurements of the Hopen channels indicate transport to the northwest ([Klausen and Mørk, 2014](#)), which correlates to the orientation of the channels measured in this study ([Figure 6.8](#)), reflecting the overall progradational direction of the delta system. Furthermore, outcrop observations of the sedimentary structures in the fluvial channels on Hopen ([Klausen and Mørk, 2014](#); [Lord et al., 2014b](#)) are comparable to the observations made from the core presented in this study, including an erosive base, rip-up mud clasts, trough cross-bedding, current ripple cross-lamination and plant fragments.

The channel measurements from the present study, particularly those of the Guovca sandstone, have also been compared to the study of [Fielding and Crane \(1987\)](#), where a compilation of 45 published sources of modern and ancient fluvial channel belt widths to channel depths for various channel morphologies is presented ([Figure 9.10](#)). The thickness

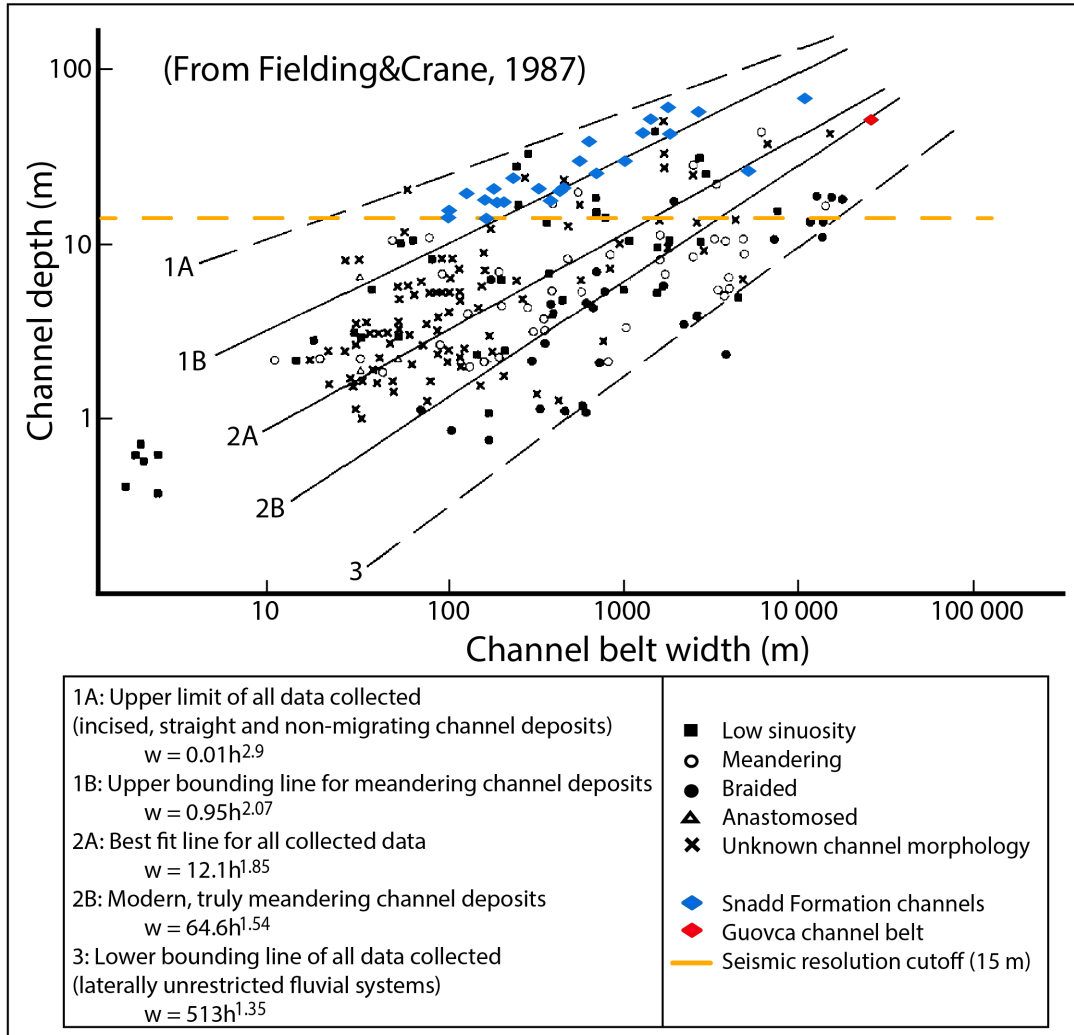


Figure 9.10: Cross plots of modern and ancient fluvial channel belt widths vs channel depths for various channel morphologies, from [Fielding and Crane \(1987\)](#). The Snadd Formation channels seem to cluster around case 1B. The cross plot of the Guovca channel belt deposit falls on the line defining case 2B.

values of the channel bodies in the Snadd Formation are, in other words, in this comparison, assumed to correspond to the depth of the channels within which deposition took place. Most ancient fluvial deposits, however, accrete vertically and laterally with time ([Fielding and Crane, 1987](#)), and using a 1:1 relationship between preserved thickness and channel depth may be rather oversimplified. When that is said, most of the Snadd channels seem to cluster around case 1B in [Figure 9.10](#), which represent the upper bounding line for meandering channel deposits, but also channels that have not been allowed to migrate laterally (low sinuosity channels), excluding vertically accreted types that are narrow and highly incised. This

description fits well with the channel morphologies described from the Snadd Formation, where meandering channel belts and smaller ribbon shaped channel fills are most common.

The cross plot of the Guovca channel belt deposit falls more or less on top of the line defining case 2B in [Figure 9.10](#). Case 2B describes the relationship of modern, truly meandering river deposits, supporting the interpretation of the Guovca sandstone being a large point-bar deposit from a meandering river. Furthermore, the concurrence implies that the sandstone thickness corresponds to the bankfull depth of the formative channel. In other words, the channel may have laterally migrated without any significant vertical accretion as illustrated in [Figure 6.12](#). This is also supported by the fact that no significant geometrical changes of the channel deposit can be seen on RMS amplitude maps from different levels within the sandstone. Using the measured sandstone thickness of the Guovca deposit ([Table 6.1](#)) in the equation defining case 2B ([Figure 9.10](#)) result in a calculated channel belt width of ca 25900 m, which is very close to the measured channel belt width value of 26500 m ([Table 6.1](#)).

The thickness of the Guovca sandstone, likely corresponding to the bankfull depth of a migrating channel as indicated above, can be used to calculate the bankfull width of the channel. [Leeder \(1973\)](#) presents a relation between bankfull width and bankfull depth of modern meandering rivers with sinuosity > 1.7 ([Figure 9.11](#)). The measured sinuosity of the Guovca channel is 3.4 ([Table 6.1](#)), and a comparison to [Leeder \(1973\)](#) is therefore realistic. The calculated bankfull width for the channel assumed to have deposited the Guovca sandstone is 2700 m using the measured sandstone thickness ([Table 6.1](#)) as bankfull depth in the equation representing the best fit line in [Figure 9.11](#). The actual measured bankfull width value is 1500 m ([Table 6.1](#)). However, it cannot be excluded that the measured bankfull width value is inaccurate or has been misinterpreted from RMS amplitude maps. Nevertheless, the cross plot of the respective measured parameters of the Guovca sandstone in the diagram of [Leeder \(1973\)](#), falls relatively close to the best fit line, indicating that the measurements may be correct.

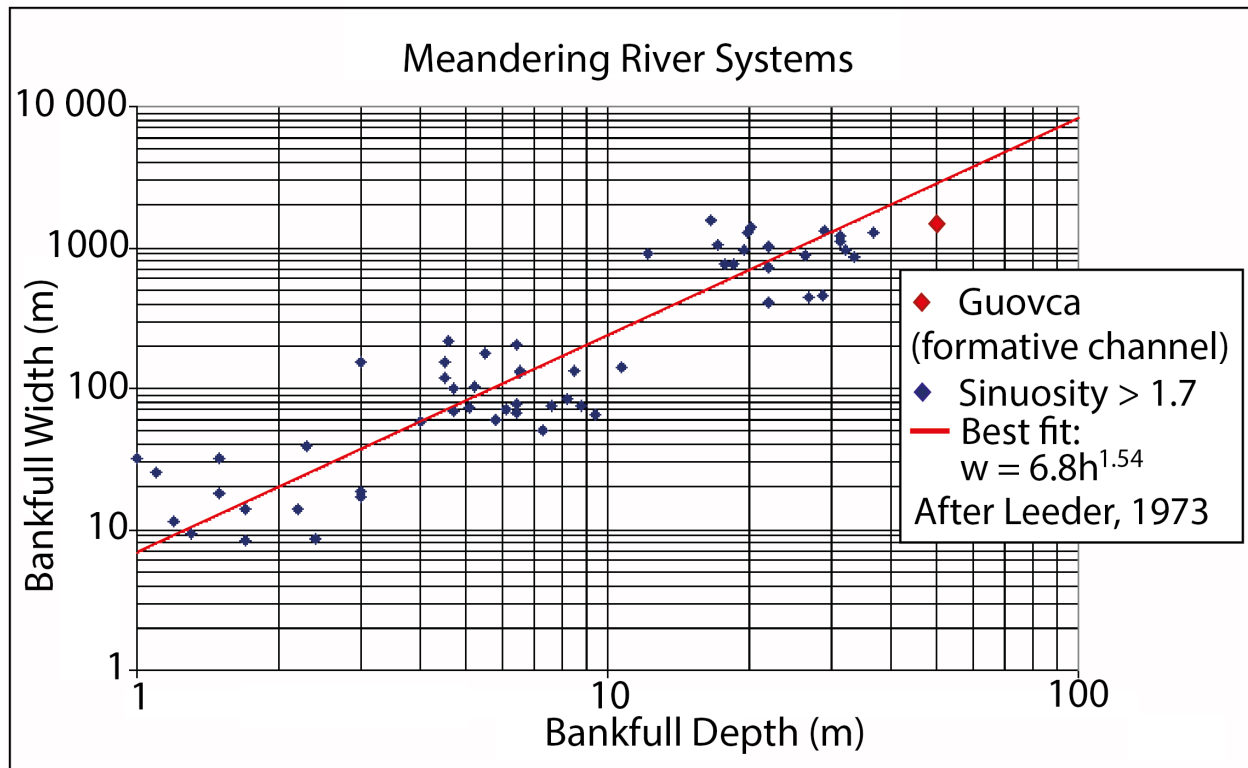


Figure 9.11: Bankfull width (w) plotted against bankfull depth (h) for modern meandering rivers with sinuosity > 1.7. The cross plot of the interpreted formative channel of the Guovca sandstone falls relatively close to the best fit line. After [Leeder \(1973\)](#).

10. Conclusions

- The De Geerdalen Formation on Svalbard and the Snadd Formation in the Barents Sea reflect deposits from a large-scale delta complex that evolved during the Triassic, mainly sourced from east and south-east by the erosional products of the Uralian Mountains.
- The facies distribution in Fulmardalen reflects an overall shallowing upwards depositional environment, with open marine shelf and prodelta deposits in the lower part (the Botneheia and Tschermakfjellet formations), shallow marine and delta front deposits in the middle part (the De Geerdalen Formation), and delta plain deposits in the upper part (the Isfjorden Member), reflecting the progradation of the delta with a development from distal to more proximal facies associations with time. This shallowing upwards trend is concordant with previous studies of the Upper Triassic succession on Svalbard ([Rød et al., 2014](#); [Lord et al., 2017a](#)).
- The De Geerdalen Formation in Fulmardalen consists of multiple stacked upwards shallowing parasequences, and may record repeated delta lobe switches and associated shoreline progradations.
- Laterally extensive and upwards coarsening sandstone units with sedimentary structures typically associated with wave- and tidal activity, characterize the shallow marine and delta front deposits in Fulmardalen. These units have been interpreted as barrier bars, forming as a result of low accommodation space allowing for basinal processes to rework the sediment. The deposits compare well to the description of ancient wave-dominated deltas. Previous studies of the De Geerdalen Formation report of a stronger fluvial influence on the deposits on the eastern islands compared to Spitsbergen.

- The equivalent Snadd Formation on the Finnmark Platform record a much more fluvial dominated depositional environment compared to the De Geerdalen Formation in Fulmardalen. Fluvial seismic geomorphological features include point-bar deposits from large meandering rivers, braided river morphologies with mid-channel-bars and ribbon shaped channel bodies.
- The study of a sediment core from a large point-bar complex shows characteristics typical of fluvial deposits. These include an erosional base, trough cross-stratification, current-ripple cross-lamination, rip-up clasts (often imbricated), plant/coal debris, internal scours and small upwards-fining units.
- Orientation measurements of selected channel bodies in the Snadd Formation support the interpreted progradation direction of the delta towards west and north-west. Width-to-thickness plots of channels compare well to plots of mainly meandering rivers and distributaries from ancient and modern fluvial systems. Moreover, channel bodies in the lower part appear larger than channels further up in the formation. This may be related to tectonic changes in the hinterland.

Bibliography

- Alonso-Zarza, A. M. and Wright, V. (2010). Calcretes. *Developments in Sedimentology*, 61:225–267.
- Anell, I., Braathen, A., and Olaussen, S. (2014a). The Triassic–Early Jurassic of the northern Barents Shelf: a regional understanding of the Longyearbyen CO 2 reservoir. *Norwegian Journal of Geology/Norsk Geologisk Forening*, 94.
- Anell, I., Braathen, A., Olaussen, S., and Osmundsen, P. (2013). Evidence of faulting contradicts a quiescent northern Barents Shelf during the Triassic. *first break*, 31(6):67–76.
- Anell, I., Midtkandal, I., and Braathen, A. (2014b). Trajectory analysis and inferences on geometric relationships of an Early Triassic prograding clinoform succession on the northern Barents Shelf. *Marine and Petroleum Geology*, 54:167–179.
- Bergan, M. and Knarud, R. (1993). Apparent changes in clastic mineralogy of the Triassic–Jurassic succession, Norwegian Barents Sea: possible implications for palaeodrainage and subsidence. *Arctic Geology and Petroleum Potential, Norwegian Petroleum Society (NPF), Special Publication*, 2:481–493.
- Bergh, S. G., Braathen, A., and Andresen, A. (1997). Interaction of basement-involved and thin-skinned tectonism in the Tertiary fold-thrust belt of central Spitsbergen, Svalbard. *AAPG bulletin*, 81(4):637–661.
- Bhattacharya, H., Bhattacharya, B., Chakraborty, I., and Chakraborty, A. (2004). Sole marks in storm event beds in the Permo-Carboniferous Talchir Formation, Raniganj basin, India. *Sedimentary Geology*, 166(3):209–222.
- Bhattacharya, J. P. (1992). Deltas. *In: Facies models: response to sea level change (Ed. by R. G. Walker & N. P. James): Geological Association of Canada*, pages 157–177.
- Bhattacharya, J. P. (2006). Deltas. *Special Publication-SEPM*, 84:237–292.
- Bhattacharya, J. P. and Giosan, L. (2003). Wave-influenced deltas: Geomorphological implications for facies reconstruction. *Sedimentology*, 50(1):187–210.
- Bhattacharya, J. P. and MacEachern, J. A. (2009). Hyperpycnal rivers and prodeltaic shelves in the Cretaceous seaway of North America. *Journal of Sedimentary Research*, 79(4):184–209.
- Blakey, R. Paleogeography library. *Colorado Plateau Geosystems*. Available at: <http://cpgeosystems.com/paleomaps.html/> (accessed 2013).
- Blomeier, D. (2015). Chapter 6.6: Historical geology-Permian. *Geoscience Atlas of Svalbard. In: Dallmann, W.(Ed.): Geoscience Atlas of Svalbard. Norwegian Polar Institute Report Series*, (148):110–113.

- Blum, M., Martin, J., Milliken, K., and Garvin, M. (2013). Paleovalley systems: insights from Quaternary analogs and experiments. *Earth-Science Reviews*, 116:128–169.
- Boggs, S. (2009). *Petrology of sedimentary rocks*. Cambridge University Press.
- Boggs, S. (2011). *Principles of sedimentology and stratigraphy*. Pearson Prentice Hall.
- Boyd, R. and Penland, S. (1988). A geomorphologic model for Mississippi Delta evolution.
- Braathen, A., Bælum, K., Maher Jr, H., and Buckley, S. J. (2011). Growth of extensional faults and folds during deposition of an evaporite-dominated half-graben basin; the carboniferous billefjorden trough, svalbard. *Norwegian Journal of Geology/Norsk Geologisk Forening*, 91(3).
- Braathen, A., Bergh, S. G., and Maher, H. D. (1999). Application of a critical wedge taper model to the Tertiary transpressional fold-thrust belt on Spitsbergen, Svalbard. *Geological Society of America Bulletin*, 111(10):1468–1485.
- Brown, A. R. (2011). *Interpretation of three-dimensional seismic data*. Society of Exploration Geophysicists and American Association of Petroleum Geologists.
- Buchan, S., Challinor, A., Harland, W., and Parker, J. (1965). The Triassic stratigraphy of Svalbard.
- Buiter, S. J. and Torsvik, T. H. (2007). Horizontal movements in the eastern Barents Sea constrained by numerical models and plate reconstructions. *Geophysical Journal International*, 171(3):1376–1389.
- Clifton, H. (2006). A reexamination of facies models for clastic shorelines. *SEPM - Special Publication*, 84:293.
- Collinson, J. (1996). Alluvial sediments. *Sedimentary environments: processes, facies and stratigraphy*, 3:37–82.
- Collinson, J., Mountney, N., and Thompson, D. (2006). *Sedimentary Structures*. Terra Publishing, London, third edition edition.
- Daber, R., Aqrabi, A., and Limited, S. (2010). *Petrel 2010: Interpreter's Guide to Seismic Attributes*. Houston Schlumberger.
- Dallmann, W. (2015). Geoscience Atlas of Svalbard. *Norwegian Polar Institute Report Series*, (148):292.
- Dalrymple, R. (1999). Tide-dominated deltas: do they exist or are they all estuaries. In *American Association of Petroleum Geologists Annual Meeting, Official Program, San Antonio*, pages A29–A30.
- Dalrymple, R. (2010). Interpreting sedimentary successions: facies, facies analysis and facies models. *Facies models*, 4(2):3–18.
- Dalrymple, R. W. and Choi, K. (2007). Morphologic and facies trends through the fluvial–marine transition in tide-dominated depositional systems: a schematic framework for environmental and sequence-stratigraphic interpretation. *Earth-Science Reviews*, 81(3):135–174.

- Davis Jr, R. A. (2012). Tidal signatures and their preservation potential in stratigraphic sequences. In *Principles of tidal sedimentology*, pages 35–55. Springer.
- De Raaf, J. and Boersma, J. (2007). Tidal deposits and their sedimentary structures (seven examples from Western Europe). *Netherlands Journal of Geosciences/Geologie en Mijnbouw*, (Classic Papers).
- Dumas, S. and Arnott, R. (2006). Origin of hummocky and swaley cross-stratification—the controlling influence of unidirectional current strength and aggradation rate. *Geology*, 34(12):1073–1076.
- Edwards, M. B. (1976). Growth faults in Upper Triassic deltaic sediments, Svalbard. *AAPG Bulletin*, 60(3):341–355.
- Elliott, T. (1986). Deltas. *Sedimentary environments and facies*, 2:113–154.
- Elvevold, S., Dallmann, W., and Blomeier, D. (2007). Svalbards geologi.
- Enga, J. (2015). Paleosols in the Triassic De Geerdalen and Snadd Formations. Master's thesis, NTNU.
- Eyles, N. and Lagoe, M. B. (1989). Sedimentology of shell-rich deposits (coquinas) in the glaciomarine upper Cenozoic Yakataga Formation, Middleton Island, Alaska. *Geological Society of America Bulletin*, 101(1):129–142.
- Faleide, J. I., Tsikalas, F., Breivik, A. J., Mjelde, R., Ritzmann, O., Engen, O., Wilson, J., and Eldholm, O. (2008). Structure and evolution of the continental margin off Norway and the Barents Sea. *Episodes*, 31(1):82–91.
- Fielding, C. R. and Crane, R. C. (1987). An application of statistical modelling to the prediction of hydrocarbon recovery factors in fluvial reservoir sequences.
- Galloway, W. E. (1975). Process framework for describing the morphologic and stratigraphic evolution of deltaic depositional systems.
- Gibling, M. R. (2006). Width and thickness of fluvial channel bodies and valley fills in the geological record: a literature compilation and classification. *Journal of sedimentary Research*, 76(5):731–770.
- Glørstad-Clark, E., Birkeland, E., Nystuen, J., Faleide, J., and Midtkandal, I. (2011). Triassic platform-margin deltas in the western Barents Sea. *Marine and Petroleum Geology*, 28(7):1294–1314.
- Glørstad-Clark, E., Faleide, J. I., Lundschie, B. A., and Nystuen, J. P. (2010). Triassic seismic sequence stratigraphy and paleogeography of the western Barents Sea area. *Marine and Petroleum Geology*, 27(7):1448–1475.
- Gressly, A. (1838). Observations géologiques sur le Jura soleurois (vol. 2). *Neuchâtel: Nouveaux mémoires de la Société Helvétique des Sciences Naturelles*.

- Harland, W. B., Cutbill, J., Friend, P. F., Gobbett, D. J., Holliday, D., Maton, P., Parker, J., and Wallis, R. H. (1974). The Billefjorden Fault Zone, Spitsbergen: the long history of a major tectonic lineament.
- Haugen, T. (2016). A Sedimentological Study of the De Geerdalen Formation with Focus on the Isfjorden Member and Palaeosols. Master's thesis, NTNU.
- Henriksen, E., Ryseth, A., Larssen, G., Heide, T., Rønning, K., Sollid, K., and Stoupakova, A. (2011). Tectonostratigraphy of the greater Barents Sea: implications for petroleum systems. *Geological Society, London, Memoirs*, 35(1):163–195.
- Hofmann, H. (1973). Stromatolites: characteristics and utility. *Earth-Science Reviews*, 9(4):339–373.
- Hori, K., Saito, Y., Zhao, Q., and Wang, P. (2002). Evolution of the coastal depositional systems of the Changjiang (Yangtze) River in response to late Pleistocene-Holocene sea-level changes. *Journal of Sedimentary Research*, 72(6):884–897.
- Howell, J. A., Skorstad, A., MacDonald, A., Fordham, A., Flint, S., Fjellvoll, B., and Manzocchi, T. (2008). Sedimentological parameterization of shallow-marine reservoirs. *Petroleum Geoscience*, 14(1):17–34.
- Høy, T. and Lundschieen, B. (2011). Triassic deltaic sequences in the northern Barents Sea. *Geological Society, London, Memoirs*, 35(1):249–260.
- Humphreys, B., Smith, S., and Strong, G. (1989). Authigenic Chlorite in Late Triassic Sandstones from the Central Graben, North Sea. *Clay Minerals*, 24:427–444.
- Hynne, I. B. (2010). Depositional environment on eastern Svalbard and central Spitsbergen during Carnian time (Late Triassic): A sedimentological investigation of the De Geerdalen Formation. Master's thesis, NTNU.
- Johansen, S. K. (2016). Sedimentology and facies distribution of the Upper Triassic De Geerdalen Formation in the Storfjorden area and Wilhelmøya, eastern Svalbard. Master's thesis, NTNU.
- Johnson, H. and Baldwin, C. (1996). Shallow clastic seas. *Sedimentary environments: processes, facies and stratigraphy*, pages 232–280.
- Ketzer, J. M., Holz, M., Morad, S., and Al-Aasm, I. (2003). Sequence stratigraphic distribution of diagenetic alterations in coal-bearing, paralic sandstones: evidence from the Rio Bonito Formation (early Permian), southern Brazil. *Sedimentology*, 50(5):855–877.
- Klausen, T. and Mørk, A. (2014). The Upper Triassic paralic deposits of the De Geerdalen Formation on Hopen: outcrop analog to the subsurface Snadd Formation in the Barents Sea. *AAPG Bulletin*, 98(10):1911–1941.
- Klausen, T. G., Ryseth, A. E., Helland-Hansen, W., Gawthorpe, R., and Laursen, I. (2014). Spatial and temporal changes in geometries of fluvial channel bodies from the triassic snadd formation of offshore Norway. *Journal of Sedimentary Research*, 84(7):567–585.

- Klausen, T. G., Ryseth, A. E., Helland-Hansen, W., Gawthorpe, R., and Laursen, I. (2015). Regional development and sequence stratigraphy of the middle to late triassic snadd formation, norwegian barents sea. *Marine and Petroleum Geology*, 62:102–122.
- Knarud, R. (1980). En sedimentologisk og diagenetisk undersøkelse av kapp toscana formasjonens sedimenter på svalbard.(a sedimentological and diagenetic study of the sediments of the kapp toscana formation in svalbard). *University of Oslo*.
- Krajewski, K. P. (2008). The Botneheia Formation (Middle Triassic) in Edgeøya and Barentsøya, Svalbard: lithostratigraphy, facies, phosphogenesis, paleoenvironment. *Polish Polar Research*, 29(4):319–364.
- Kraus, M. J. (1999). Paleosols in clastic sedimentary rocks: their geologic applications. *Earth-Science Reviews*, 47(1):41–70.
- Lander, R., Bloch, S., Mehta, S., and Atkinson, C. (1991). Burial diagenesis of paleosols in the Giant Yacheng gas field, People's Republic of China: bearing on Illite reaction pathways. *Journal of Sedimentary Research*, 61(2).
- Langford, F. and Blanc-Valleron, M.-M. (1990). Interpreting Rock-Eval pyrolysis data using graphs of pyrolizable hydrocarbons vs. total organic carbon (1). *AAPG Bulletin*, 74(6):799–804.
- Leeder, M. (1973). Fluvial fining-upwards cycles and the magnitude of palaeochannels. *Geological Magazine*, 110(03):265–276.
- López, G. I. (2015). Walther's Law of Facies. *Encyclopedia of Scientific Dating Methods*, pages 957–958.
- Lord, G. S., Johansen, S. K., Støen, S. J., and Mørk, A. (2017a). Facies development of the Upper Triassic succession on Barentsøya, Wilhelmøya and NE Spitsbergen, Svalbard. *Norwegian Journal of Geology*, 97:33–62.
- Lord, G. S., Mørk, A., and Høy, T. (2017b). Sequence patterns in the Triassic succession of Svalbard and the Northern Barents Sea. In Lord, G. S.: *Sequence stratigraphy and facies development of the Triassic succession in Svalbard and the Northern Barents Sea*. Phd thesis, NTNU, 200 pages.
- Lord, G. S., Mørk, M. B. E., Mørk, A., and Olaussen, S. (2017c). The Svenskøya Formation on Hopen: An analogue to sandstone reservoirs in the Realgrunnen Subgroup. In Lord, G. S.: *Sequence stratigraphy and facies development of the Triassic succession in Svalbard and the Northern Barents Sea*. Phd thesis, NTNU, 200 pages.
- Lord, G. S., Solvi, K. H., Ask, M., Mørk, A., Hounslow, M. W., and Paterson, N. W. (2014a). The Hopen Member: A new member of the Triassic De Geerdalen Formation, Svalbard. *Norwegian Petroleum Directorate Bulletin*, 11(1):81–96.
- Lord, G. S., Solvi, K. H., Klausen, T. G., and Mørk, A. (2014b). Triassic channel bodies on Hopen, Svalbard: Their facies, stratigraphical significance and spatial distribution. *Norwegian Petroleum Directorate Bulletin*, 11:41–59.

- Lucchi, F. R. (1995). *Sedimentographica: Photographic atlas of sedimentary structures*. Columbia University Press.
- Lundschieen, B. A., Høy, T., and Mørk, A. (2014). Triassic hydrocarbon potential in the northern barents sea; integrating svalbard and stratigraphic core data. *Norwegian Petroleum Directorate Bulletin*, 11:3–20.
- Lyberis, N. and Manby, G. (1993). The origin of the West Spitsbergen Fold Belt from geological constraints and plate kinematics: implications for the Arctic. *Tectonophysics*, 224(4):371–391.
- Mangerud, J., Jansen, E., and Landvik, J. Y. (1996). Late Cenozoic history of the Scandinavian and Barents Sea ice sheets. *Global and Planetary Change*, 12(1-4):11–26.
- Martinius, A. W., Howell, J., Steel, R., Wonham, J., et al. (2014). *From Depositional Systems to Sedimentary Successions on the Norwegian Continental Margin (Special Publication 46 of the IAS)*. John Wiley & Sons.
- Miall, A. D. (2016). Facies Models. In *Stratigraphy: A Modern Synthesis*, pages 161–214. Springer.
- Middleton, G. V. (1973). Johannes Walther's law of the correlation of facies. *Geological Society of America Bulletin*, 84(3):979–988.
- Midtgaard, H. H. (1996). Inner-shelf to lower-shoreface hummocky sandstone bodies with evidence for geostrophic influenced combined flow, Lower Cretaceous, West Greenland. *Journal of Sedimentary Research*, 66(2).
- Milliken, K., Blum, M., and Martin, J. (2012). Scaling relationships for channel fills, channel belts and incised valleys: insights from Quaternary systems: American Association of Petroleum Geologists, Annual Conference and Exhibition, Long Beach, California.
- Mills, P. C. (1983). Genesis and diagnostic value of soft-sediment deformation structures — a review. *Sedimentary Geology*, 35(2):83–104.
- Morad, S. (1998). Carbonate cementation in sandstones: distribution patterns and geochemical evolution. In Morad, S., editor, *Carbonate cementation in sandstones*, volume 26, pages 1 – 26. International Association of Sedimentologists Special Publication.
- Mørk, A. and Bjorøy, M. (1984). Mesozoic source rocks on Svalbard. In *Petroleum geology of the North European margin*, pages 371–382. Springer.
- Mørk, A. and Bromley, R. G. (2008). Ichnology of a marine regressive systems tract: the Middle Triassic of Svalbard. *Polar Research*, 27(3):339–359.
- Müller, R., Nystuen, J. P., and Wright, V. P. (2004). Pedogenic mud aggregates and paleosol development in ancient dryland river systems: criteria for interpreting alluvial mudrock origin and floodplain dynamics. *Journal of Sedimentary Research*, 74(4):537–551.

- Mørk, A., Dallmann, W., Dypvik, H., Johannessen, E., Larssen, G., Nagy, J., Nøttvedt, A., Olaussen, S., Pchelina, T., and Worsley, D. (1999a). Mesozoic lithostratigraphy. *Lithostratigraphic lexicon of Svalbard. Upper Palaeozoic to Quaternary bedrock. Review and recommendations for nomenclature use*, pages 127–214.
- Mørk, A., Elvebakk, G., Forsberg, A. W., VIGRAN, J. O., WEITSCHAT, W., et al. (1999b). The type section of the Vikinghogda Formation: a new Lower Triassic unit in central and eastern Svalbard. *Polar Research*, 18(1):51–82.
- Mørk, A., Embry, A. E., and Weitschat, W. (1989). Triassic transgressive-regressive cycles in the Sverdrup Basin, Svalbard and the Barents Shelf. In *Correlation in hydrocarbon exploration*, pages 113–130. Springer.
- Mørk, A., Knarud, R., and Worsley, D. (1982). Depositional and diagenetic environments of the Triassic and Lower Jurassic succession of Svalbard.
- Mørk, M. B. E. (1999). Compositional variations and provenance of Triassic sandstones from the Barents Shelf. *Journal of Sedimentary Research*, 69(3):690–710.
- Mørk, M. B. E. (2013). Diagenesis and quartz cement distribution of low-permeability Upper Triassic–Middle Jurassic reservoir sandstones, Longyearbyen CO2 lab well site in Svalbard, Norway. *AAPG bulletin*, 97(4):577–596.
- Nichols, G. (2009). *Sedimentology and stratigraphy*. John Wiley & Sons.
- Nøttvedt, A. and Kreisa, R. (1987). Model for the combined-flow origin of hummocky cross-stratification. *Geology*, 15(4):357–361.
- NPDFactPages. Wellbore/exploration/(7131/4-1).
Available at: <http://factpages.npd.no/factpages/> (accessed 2017).
- Olariu, C. (2014). Autogenic process change in modern deltas. *From Depositional Systems to Sedimentary Successions on the Norwegian Continental Margin*, pages 149–166.
- O’leary, N., White, N., Tull, S., Bashilov, V., Kuprin, V., Natapov, L., and Macdonald, D. (2004). Evolution of the timan–pechora and south barents sea basins. *Geological Magazine*, 141(02):141–160.
- Oliveira, C. M., Hodgson, D. M., and Flint, S. S. (2011). Distribution of soft-sediment deformation structures in clinoform successions of the Permian Ecca Group, Karoo Basin, South Africa. *Sedimentary Geology*, 235(3):314–330.
- Orton, G. and Reading, H. (1993). Variability of deltaic processes in terms of sediment supply, with particular emphasis on grain size. *Sedimentology*, 40(3):475–512.
- Osmundsen, P. T., Braathen, A., Rød, R. S., and Hynne, I. B. (2014). Styles of normal faulting and fault-controlled sedimentation in the Triassic deposits of Eastern Svalbard. *Norwegian Petroleum Directorate Bulletin*, 11:61–79.

- Paterson, N. W. and Mangerud, G. (2015). Late Triassic (Carnian–Rhaetian) palynology of Hopen, Svalbard. *Review of Palaeobotany and Palynology*, 220:98–119.
- Paterson, N. W., Mangerud, G., Cetean, C. G., Mørk, A., Lord, G. S., Klausen, T. G., and Mørkved, P. T. (2016a). A multidisciplinary biofacies characterisation of the Late Triassic (late Carnian–Rhaetian) Kapp Toscana Group on Hopen, Arctic Norway. *Palaeogeography, Palaeoclimatology, Palaeoecology*, 464:16–42.
- Paterson, N. W., Mangerud, G., and Mørk, A. (2016b). Late Triassic (early Carnian) palynology of shallow stratigraphical core 7830/5-U-1, offshore Kong Karls Land, Norwegian Arctic. *Palynology*, pages 1–25.
- Pchelina, T. (1983). Novye dannye po stratigrafii mezozoja arkipelaga spitsbergen (new evidence on mesozoic stratigraphy of the spitsbergen archipelago). *Geologija Spicbergena*, pages 121–141.
- Pettijohn, F., Potter, P., and Siever, R. (1987). *Sand and Sandstone*. Springer-Verlag, New York, 2nd edition.
- Rafaelsen, B. (2006). Seismic resolution and frequency filtering. *Univ. Tromso Lecture Series, Tromso, Norway*.
- Reading, H. and Collinson, J. (1996). Clastic coasts. *Sedimentary environments: processes, facies and stratigraphy*, 3:154–231.
- Reading, H. and Levell, B. (1996). Controls on the sedimentary rock record. *Sedimentary environments: processes, facies and stratigraphy*, pages 5–36.
- Reineck, H. and Singh, I. (1980). Depositional Sedimentary Environments.
- Reinson, G. E. (1984). Barrier-Island and Associated Strand-Plain Systems. In: Walker, R.G (Ed.). In *Facies models*, volume 1, pages 119–140. Geoscience Canada.
- Reinson, G. E. (1992). Transgressive barrier island and estuarine systems. In: *Facies models: response to sea level change (Ed. by R. G. Walker & N. P. James): Geological Association of Canada*, pages 179–194.
- Retallack, G. (1991). Untangling the effects of burial alteration and ancient soil formation. *Annual Review of Earth and Planetary Sciences*, 19(1):183–206.
- Riis, F., Lundschieen, B. A., Høy, T., Mørk, A., and Mørk, M. B. E. (2008). Evolution of the Triassic shelf in the northern Barents Sea region. *Polar Research*, 27(3):318–338.
- Rød, R. S. (2011). Spatial occurrences of selected sandstone bodies in the De Geerdalen Formation, Svalbard, and their relation to depositional facies. Master's thesis, NTNU.
- Rød, R. S., Hynne, I. B., and Mørk, A. (2014). Depositional environment of the Upper Triassic De Geerdalen Formation—an EW transect from Edgeøya to Central Spitsbergen, Svalbard. *Norwegian Petroleum Directorate Bulletin*, 11:21–40.

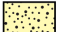







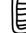





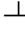

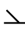


- Sheriff, R. (2006). Encyclopedic dictionary of applied geophysics. *Society of Exploration Geophysicists, Tulsa*.
- Spearing, D. R. (1976). Upper Cretaceous Shannon Sandstone: an offshore, shallow-marine sand body.
- Steno, N. (1916). 1669: De solido intra solidum naturaliter contento dissertationis prodromus. *Florence, 78p*.
- Støen, S. J. (2016). Late Triassic sedimentology and diagenesis of Barentsøya, Wilhelmøya and eastern Spitsbergen. Master's thesis, NTNU.
- Stoupakova, A., Henriksen, E., Burlin, Y. K., Larsen, G., Milne, J., Kiryukhina, T., Golynchik, P., Bordunov, S., Ogarkova, M., and Suslova, A. (2011). The geological evolution and hydrocarbon potential of the Barents and Kara shelves. *Geological Society, London, Memoirs*, 35(1):325–344.
- Syssemmannen (2012). Geology. Available at: <http://www.syssemmannen.no/en/Toppmeny/About-Svalbard/Geology/> (accessed 14.03.2017).
- Teichert, C. (1958). Concepts of facies. *AAPG Bulletin*, 42(11):2718–2744.
- Tucker, M. E. (2011). *Sedimentary rocks in the field: A practical guide*, volume 38. John Wiley & Sons.
- Tugarova, M. A. and Fedyaevsky, A. G. (2014). Calcareous microbialites in the Upper Triassic succession of Eastern Svalbard. *Norwegian Petroleum Directorate Bulletin*, 11:137–52.
- van den Berg, J., Martinius, A., and Houthuys, R. (2017). Breaching-related turbidites in fluvial and estuarine channels: Examples from outcrop and core and implications to reservoir models. *Marine and Petroleum Geology*, 82:178–205.
- Van Wagoner, J., Posamentier, H., Mitchum, R., Vail, P., Sarg, J., Loutit, T., and Hardenbol, J. (1988). An overview of the fundamentals of sequence stratigraphy and key definitions.
- Van Wagoner, J. C., Mitchum, R., Campion, K., and Rahmanian, V. (1990). Siliciclastic sequence stratigraphy in well logs, cores, and outcrops: concepts for high-resolution correlation of time and facies.
- Vigran, J. O., Mangerud, G., Mørk, A., Worsley, D., and Hochuli, P. A. (2014). Palynology and geology of the Triassic succession of Svalbard and the Barents Sea. *Geological Survey of Norway Special Publication*, 14:270 pp.
- Vigran, J. O., Mørk, A., Forsberg, A. W., Weiss, H. M., and Weitschat, W. (2008). Tasmanites algae—contributors to the Middle Triassic hydrocarbon source rocks of Svalbard and the Barents Shelf. *Polar Research*, 27(3):360–371.
- Walker, R. (2006). Facies models revisited: Introduction. *SPECIAL PUBLICATION-SEPM*, 84:1.
- Walther, J. (1894). *Einleitung in die Geologie als historische Wissenschaft: Beobachtungen über die Bildung der Gesteine und ihrer organischen Einschlüsse*. G. Fischer.

- Webb, G. E. (1994). Paleokarst, paleosol, and rocky-shore deposits at the Mississippian-Pennsylvanian unconformity, northwestern Arkansas. *Geological Society of America Bulletin*, 106(5):634–648.
- Worsley, D. (2008). The post-Caledonian development of Svalbard and the western Barents Sea. *Polar Research*, 27(3):298–317.
- Wright, V. and Tucker, M. (1991). Calcretes. the international association of sedimentologists. *Blackwell Scientific Publications, Oxford, Reprint Ser*, 2:380.
- Wright, V. P. (1994). Paleosols in shallow marine carbonate sequences. *Earth-Science Reviews*, 35(4):367–395.
- Yang, B., Dalrymple, R. W., and Chun, S. (2006). The significance of hummocky cross-stratification (hcs) wavelengths: evidence from an open-coast tidal flat, south korea. *Journal of Sedimentary Research*, 76(1):2–8.
- Young, F. and Reinson, G. (1975). Sedimentology of Blood Reserve and adjacent formations (Upper Cretaceous), St. Mary River, southern Alberta. In *Guidebook to selected sedimentary environments In southwestern Alberta, Canada: Canadian Society of Petroleum Geologists, Field Conference*, pages 10–20.














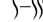








A. UTM coordinates of measured sections from Fulmardalen

Name of mountain	Name of log	UTM Start (Zone , E, N)	UTM End (Zone, E, N)
Wallenbergfjellet	Wal 16-1	33X, 0565413, 8685660	33X, 0565693, 8685796
Dyrhø	Dyr 16-1	33X, 0564923, 8681912	33X, 0564813, 8681730
Ryssen	Rys 16-1	33X, 0567299, 8682728	33X, 0568800, 8683050
Milne Edwardsfjellet	Mil 16-1	33X, 0563171, 8683548	33X, 0562392, 8683776
Storfjellet	Stor 16-1	33X, 0567784, 8681412	33X, 0568321, 8681562
Raggfjellet	Rag 16-1	33X, 0565288, 8679300	33X, 0565286, 8679272



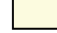

B. Legend for measured sections

Lithology	Fossils	Trace fossils
 Sandstone	 Ammonoids	 <i>Skolithos</i> (<i>Sk</i>)
 Mud - and siltstone	 Bivalves	 <i>Rhizocorallium</i> (<i>Rh</i>)
 Limestone	 Unidentified fossil fragment	 <i>Diplocraterion</i> (<i>Di</i>)
 Coal	Cements	Concretions/nodules
 Covered / partly covered	 Dolomite cementation	 Calcareous nodules
 Dolerite	 Calcite cementation	 Siderite concretion layer
PS Paleosol/Calcrete	 Siderite cementation	 ● si Siderite concretion/mottles
CS Coal Shale	 Unspecified cementation	

Sedimentary structures

 Planar parallel lamination / stratification (PPL / PPS)	 Loading/deformation structure
 Low-angle cross-bedding	 Mud drapes
 Wave ripples	 Mud flakes
 Current ripples	 Desiccation cracks
 Ripple lamination (undifferentiated)	 Coquina
 Heterolithic lamination (alternating sand/mud)	 Cone-in-cone
 Hummocky crossbedding	 Bioturbation (sparse - intense)
 Herringbone cross-stratification	 Roots
 Planar / angular cross-stratification	 Coal fragment
 Trough cross-stratification	 Plant fragment
 Erosional surface	 Wood fragment

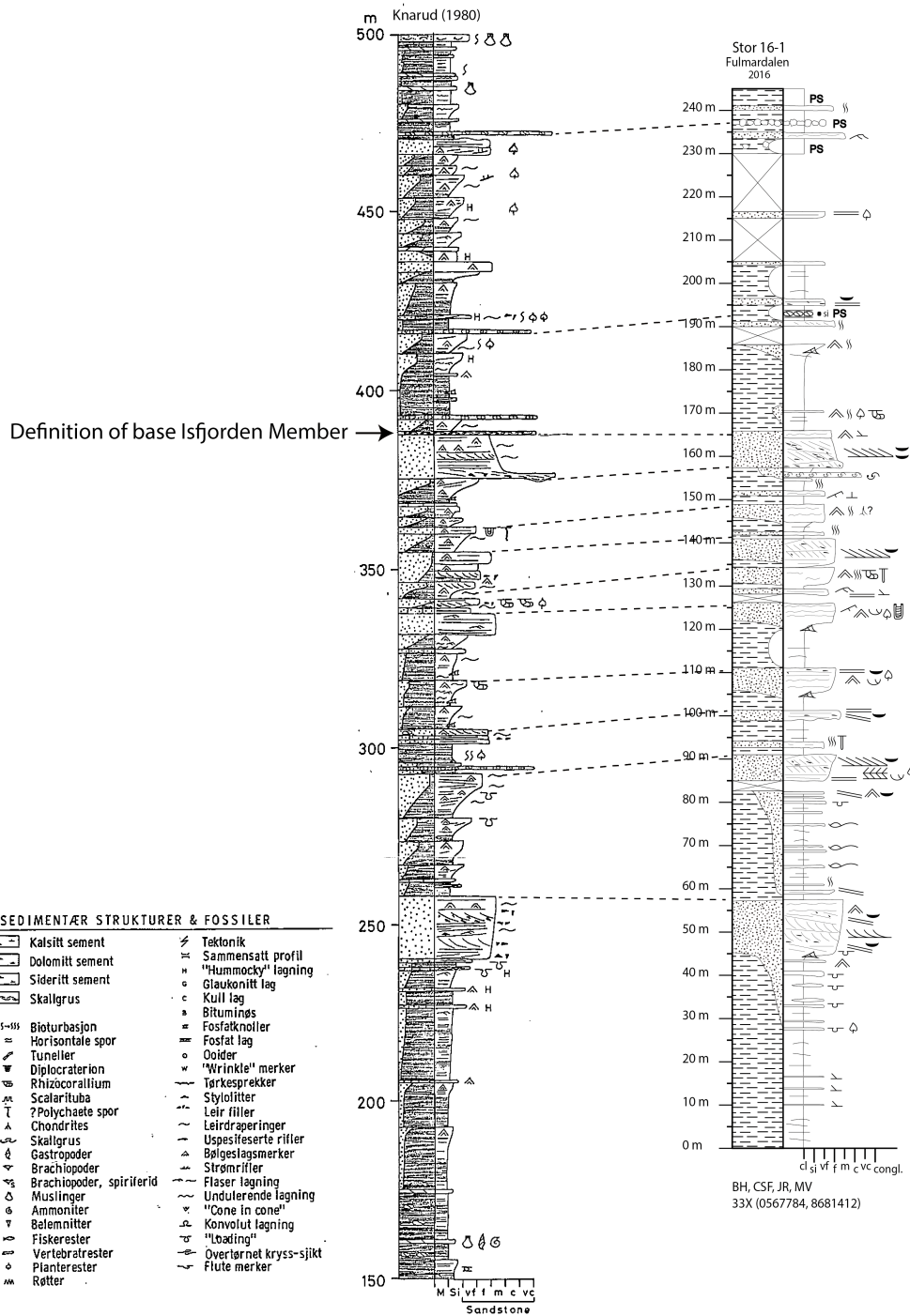
Depositional Environment

 DE 1 - Open Marine Shelf & Prodelta
 DE 2 - Shallow marine
 DE 3 - Delta front
 DE 4 - Delta plain

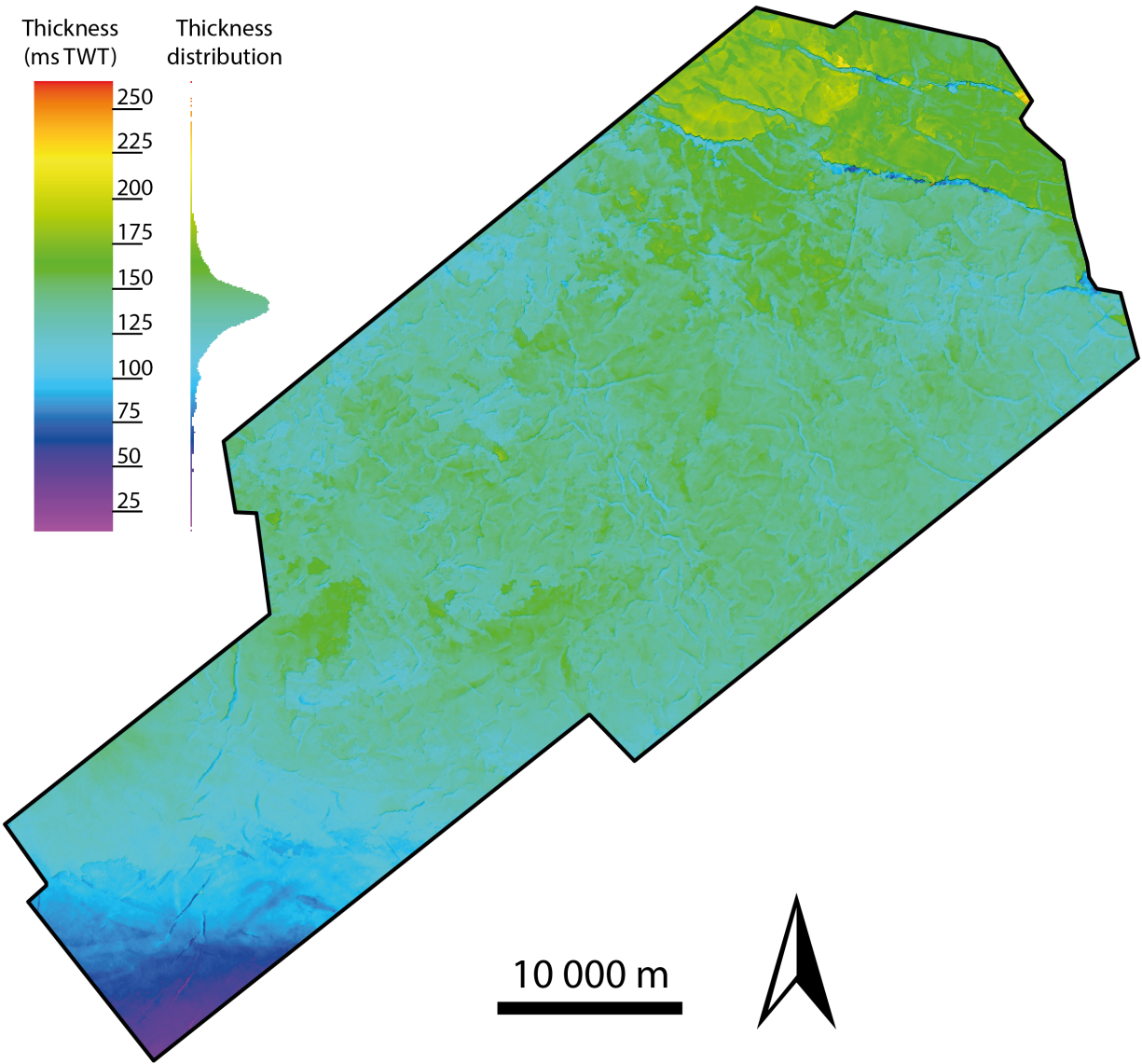
Log authors

BH - Bård Heggem	MA - Marianne Ask
CSF - Cathinka S. Forsberg	MV - Martijn Vermeer
GSL - Gareth S. Lord	NB - Nina Bakke
IBH - Ingrid B. Hynne	RSR - Rita S. Rød
JR - Jostein Røstad	SKJ - Sondre K. Johansen
	TGK - Tore G. Klausen

C. Storfjellet (Knarud, 1980) correlated to Stor 16-1



D. Thickness map of the Snadd Formation in ST9802



E. Rock-Eval Analysis

Table E.1: Measured values from Rock-Eval analysis.

	Dyr16-1.19B	Rys16-1.28B
S1 (mg/g)	0.13	0.01
S2 (mg/g)	2.55	0.47
S3 (mg/g)	0.26	0.32
Tmax (C)	446	449
HI (mg HC/g TOC)	109	51
OI (mg CO ₂ /g TOC)	11	35
TOC (%)	2.35	0.92

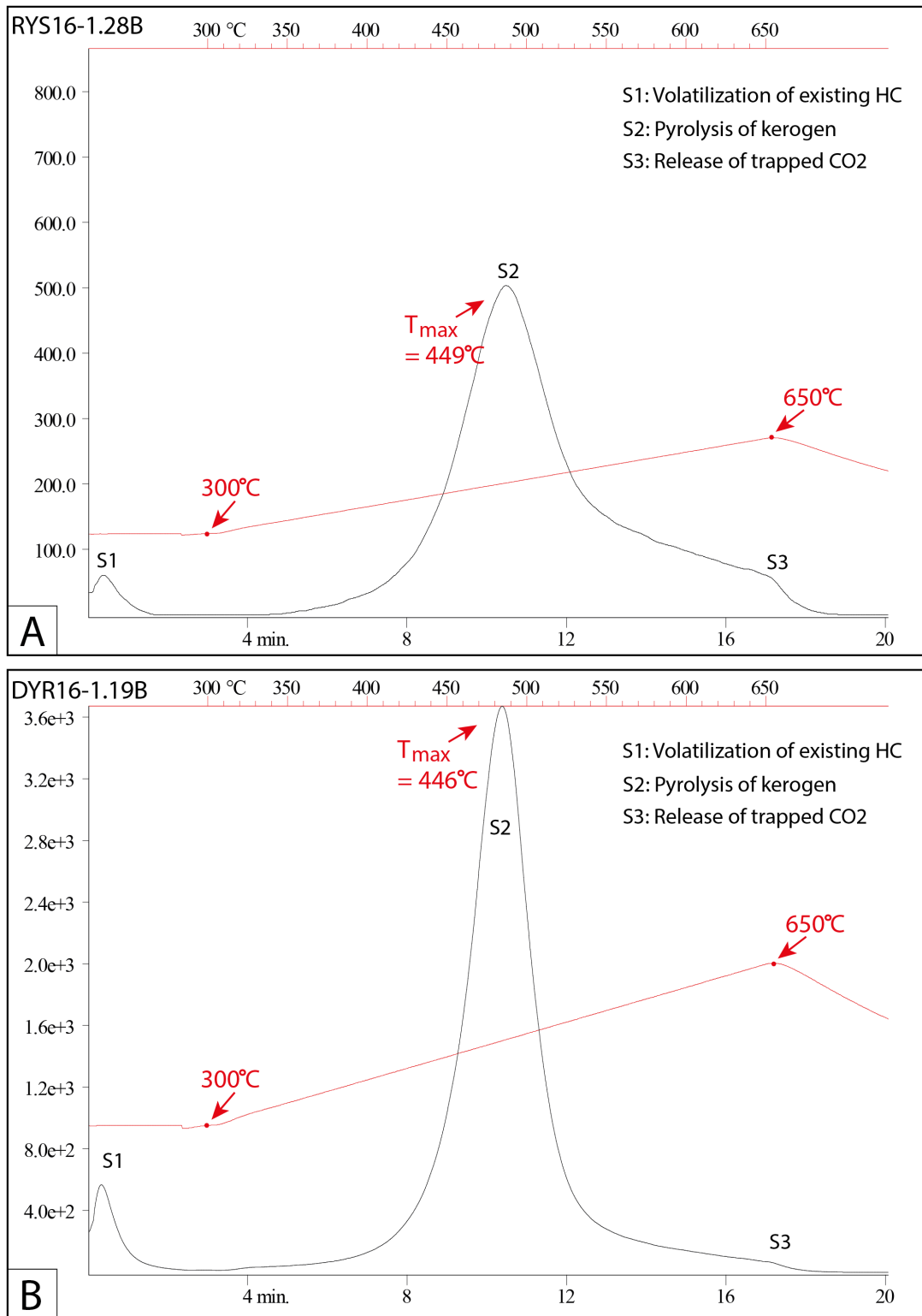


Figure E.1: Resulting chromatograms from pyrolysis of (A) Rys16-1.28B and (B) Dyr16-1.19B